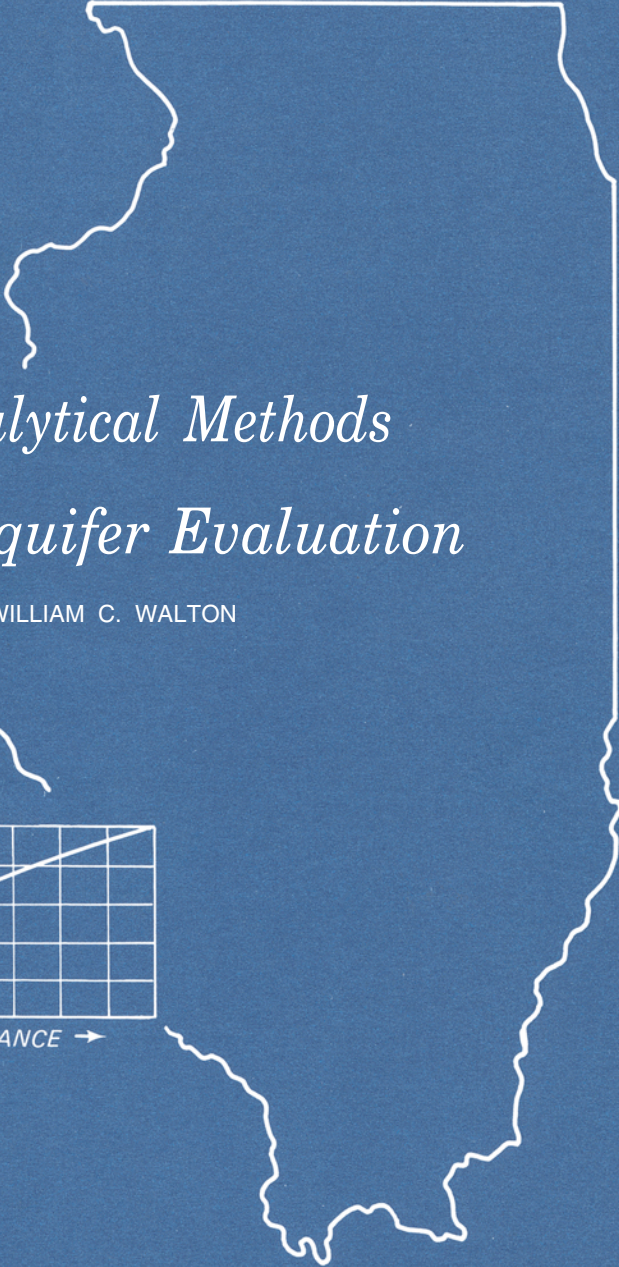


BULLETIN 49

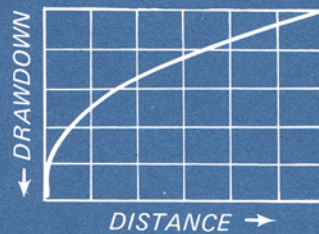
STATE OF ILLINOIS

DEPARTMENT OF REGISTRATION AND EDUCATION



*Selected Analytical Methods  
for Well and Aquifer Evaluation*

by WILLIAM C. WALTON



ILLINOIS STATE WATER SURVEY

URBANA

1962

STATE OF ILLINOIS  
HON. OTTO KERNER, *Governor*  
DEPARTMENT OF REGISTRATION AND EDUCATION  
WILLIAM SYLVESTER WHITE, *Director*

BOARD OF NATURAL RESOURCES AND CONSERVATION

WILLIAM SYLVESTER WHITE, *Chairman*  
ROGER ADAMS, Ph.D., D.Sc., LL.D., *Chemistry*  
ROBERT H. ANDERSON, B.S., *Engineering*  
THOMAS PARK, Ph.D., *Biology*  
WALTER H. NEWHOUSE, Ph.D., *Geology*  
CHARLES E. OLMSTED, Ph.D., *Botany*  
WILLIAM L. EVERITT, E.E., Ph.D.,  
*University of Illinois*  
DELYTE W. MORRIS, Ph.D.,  
*President, Southern Illinois University*

Funds derived from University of Illinois administered grants and contracts were used to produce this report.

STATE WATER SURVEY DIVISION  
WILLIAM C. ACKERMANN, *Chief*

URBANA

1962

Second Printing 1967  
Third Printing 1969  
Fourth Printing 1977  
Fifth Printing 1983  
(Sixth Printing 12-90-500)

# Contents

PAGE

Abstract .....	1
Introduction .....	1
Part 1. Analysis of geohydrologic parameters .....	3
Hydraulic properties .....	3
Aquifer tests .....	3
Drawdown .....	3
Leaky artesian formula .....	4
Nonleaky artesian formula .....	6
Water-table conditions .....	6
Partial penetration .....	7
Modified nonleaky artesian formula .....	8
Leaky artesian constant-drawdown formula .....	10
Nonleaky artesian drain formula .....	10
Specific-capacity data .....	12
Statistical analysis .....	13
Flow-net analysis .....	14
Geohydrologic boundaries .....	15
Image-well theory .....	15
Barrier boundary .....	15
Law of times .....	16
Aquifer-test data .....	16
Recharge boundary .....	17
Aquifer-test data .....	18
Percentage of water diverted from source of recharge .....	19
Time required to reach equilibrium .....	19
Multiple boundary systems .....	20
Primary and secondary image wells .....	20
Recharge .....	21
Flow-net analysis .....	21
Ground-water and hydrologic budgets .....	22
Part 2. Analysis of yields of wells and aquifers .....	24
Model aquifers and mathematical models .....	24
Records of past pumpage and water levels .....	24
Computation by electronic digital computer .....	25
Well characteristics .....	26
Well loss .....	27
Collector wells .....	27
Well design criteria .....	28
Screened wells .....	28
Spacing of wells .....	29
Part 3. Illustrative examples of analyses .....	31
Barometric efficiency of a well .....	31
Aquifer-test data under leaky artesian conditions .....	31
Aquifer-test data under nonleaky artesian conditions .....	33
Aquifer-test data under water-table conditions .....	34
Specific-capacity data .....	38
Statistical analysis .....	38
Yields of deep sandstone wells and the effects of shooting .....	40
Effects of acid treatment .....	43
Flow-net studies .....	43
Coefficient of transmissibility .....	45
Coefficient of vertical permeability .....	45
Aquifer-test data under boundary conditions .....	47
Barrier boundaries .....	47
Recharge boundary .....	48
Recharge rates .....	51
Area of influence of pumping .....	51
Flow-net analysis .....	52
Leakage through confining beds .....	53
Ground-water and hydrologic budgets .....	53

	PAGE
Model aquifer and mathematical model for Arcola area .....	55
Evaluation of several aquifers in Illinois .....	59
Chicago region .....	59
Taylorville area .....	59
Tallula area .....	61
Assumption area .....	61
Pekin area .....	63
Well loss .....	63
Sand and gravel well .....	63
Bedrock wells .....	64
Collector well data .....	66
Design of sand and gravel well .....	67
Conclusions .....	69
Acknowledgments .....	69
Selected references .....	70
Appendix A. Values of $W(u, r/B)$ .....	73
Appendix B. Values of $K_o(r/B)$ .....	76
Appendix C. Values of $W(u)$ .....	78
Appendix D. Values of $G(\lambda, r_w/B)$ .....	79
Appendix E. Values of $D(u)q$ .....	80
Appendix F. Selected conversion constants and factors .....	81

## Illustrations

FIGURE		PAGE
1	Nonleaky artesian drain type curve .....	11
2	Graphs of specific capacity versus coefficient of transmissibility for a pumping period of 2 minutes .....	12
3	Graphs of specific capacity versus coefficient of transmissibility for a pumping period of 10 minutes .....	12
4	Graphs of specific capacity versus coefficient of transmissibility for a pumping period of 60 minutes .....	12
5	Graphs of specific capacity versus coefficient of transmissibility for a pumping period of 8 hours .....	13
6	Graphs of specific capacity versus coefficient of transmissibility for a pumping period of 24 hours .....	13
7	Graphs of specific capacity versus coefficient of transmissibility for a pumping period of 180 days .....	13
8	Graphs of specific capacity versus well radius (A) and pumping period (B) .....	13
9	Diagrammatic representation of the image-well theory as applied to a barrier boundary .....	15
10	Generalized flow net showing flow lines and potential lines in the vicinity of a discharging well near a barrier boundary. ....	16
11	Diagrammatic representation of the image well theory as applied to a recharge boundary .....	17
12	Generalized flow net showing flow lines and potential lines in the vicinity of a discharging well near a recharge boundary .....	17
13	Graph for determination of percentage of pumped water being diverted from a source of recharge .....	19
14	Plans of image-well systems for several wedge shaped aquifers .....	21
15	Plans of image-well systems for selected parallel boundary situations. ....	21
16	Plan of image-well system for a rectangular aquifer .....	21
17	Illustrative data input format for digital computer analysis of a mathematical model .....	25
18	Abbreviated flow diagram for digital computer analysis of a mathematical model .....	26
19	Effect of atmospheric pressure fluctuations on the water level in a well at Savoy. ....	31
20	Map showing location of wells used in test near Dieterich .....	31
21	Generalized graphic logs of wells used in test near Dieterich .....	32

FIGURE	PAGE
22 Time-drawdown graph for well 19 near Dieterich .....	32
23 Distance-drawdown graph for test near Dieterich .....	32
24 Map showing location of wells used in test at Gridley .....	33
25 Generalized graphic logs of wells used in test at Gridley .....	33
26 Time-drawdown graph for well 3 at Gridley .....	33
27 Time-drawdown graph for well 1 at Gridley .....	33
28 Map showing location of wells used in test near Mossville .....	34
29 Generalized graphic logs of wells used in test near Mossville .....	34
30 Time-drawdown graph for well 15 near Mossville .....	35
31 Distance-drawdown graph for test near Mossville .....	35
32 Areal geology of the bedrock surface in DuPage County .....	36
33 Thickness of dolomite of Silurian age in DuPage County .....	37
34 Specific capacity frequency graphs for dolomite wells in DuPage County .....	38
35 Specific capacity frequency graphs for the units penetrated by dolomite wells in DuPage County .....	39
36 Estimated specific capacities of dolomite wells in DuPage County .....	39
37 Specific capacity frequency graphs for dolomite wells in northeastern Illinois .....	39
38 Specific capacities of wells uncased in the Glenwood-St. Peter Sandstone (A) and the Prairie du Chien Series, Trempealeau Dolomite, and Franconia Formation (B) in northeastern Illinois .....	40
39 Specific capacities of wells uncased in the Cambrian-Ordovician Aquifer, theoretical (A) and actual (B) in northeastern Illinois .....	40
40 Relation between the specific capacity of a well and the uncased thickness of the Glenwood-St. Peter Sandstone (A) and the uncased thickness of the Mt. Simon Aquifer (B) .....	41
41 Thickness of the Glenwood-St. Peter Sandstone in northeastern Illinois .....	41
42 Step-drawdown test data showing the results of acid treatment of dolomite wells in DuPage County .....	43
43 Cross sections of the structure and stratigraphy of the bedrock and piezometric profiles of the Cambrian-Ordovician Aquifer in northeastern Illinois. ....	44
44 Piezometric surface of Cambrian-Ordovician Aquifer in northeastern Illinois in 1958 .....	45
45 Thickness of the Maquoketa Formation in northeastern Illinois.....	46
46 Piezometric surface of Cambrian-Ordovician Aquifer in northern Illinois, about 1864 (A); and decline in artesian pressure in Cambrian-Ordovician Aquifer, 1864-1958 (B) .....	46
47 Map showing location of wells used in test near St. David .....	47
48 Generalized graphic logs of wells used in test near St. David .....	47
49 Time-drawdown graph for well 1-60 near St. David. ....	47
50 Time-drawdown graph for well 2-60 near St. David. ....	47
51 Map showing location of wells used in test at Zion .....	48
52 Generalized graphic logs of wells used in test at Zion .....	49
53 Lake stage and water levels in wells during test at Zion .....	49
54 Distance-drawdown graphs for test at Zion .....	49
55 Piezometric surface of the Silurian dolomite aquifer in DuPage County .....	50
56 Areas influenced by withdrawals from wells in the Silurian dolomite aquifer in selected parts of DuPage County .....	51
57 Estimated recharge rates for the Silurian dolomite aquifer in DuPage County .....	52
58 Flow-net analysis of the piezometric surface of the Cambrian-Ordovician Aquifer in northeastern Illinois in 1958 .....	52
59 Mean daily ground-water stage in Panther Creek basin, 1952 .....	53
60 Mean daily streamflow in Panther Creek basin, 1952 .....	53
61 Mean daily precipitation in Panther Creek basin, 1952 .....	53
62 Rating curves of mean ground-water stage versus ground-water runoff for gaging station in Panther Creek basin .....	54
63 Graph showing relation of gravity yield and average period of drainage for Panther Creek basin .....	55
64 Map and geologic cross section showing thickness and areal extent of aquifer at Arcola .....	56

FIGURE		PAGE
65	Model aquifers and mathematical models for Arcola area (A and B) and Chicago region (C and D) .....	58
66	Model aquifers and mathematical models for Taylorville (A and B) and Tallula (C and D) areas .....	60
67	Model aquifers and mathematical models for Assumption (A and B) and Pekin (C and D) areas .....	62
68	Time-drawdown graph for well near Granite City. ....	64
69	Generalized graphic logs of wells used in test at Iuka .....	64
70	Map showing location of wells used in test at Iuka. ....	65
71	Time-drawdown graph for well 3 at Iuka. ....	65
72	Time-drawdown graphs for wells 2 and 4 at Iuka. ....	65
73	Well-loss constant versus specific capacity, pumping levels are above the top of the Silurian dolomite aquifer in DuPage County. ....	66
74	Well-loss constant versus specific capacity, pumping levels are below top of the Silurian dolomite aquifer in DuPage County .....	66
75	Mechanical analyses of samples of an aquifer at Woodstock. ....	67
76	Mechanical analyses of samples of an aquifer near Mossville. ....	67

PLATE		IN POCKET
1	Nonsteady-state leaky artesian type curves	
2	Steady-state leaky artesian type curve	
3	Nonleaky artesian type curve	
4	Nonsteady-state leaky artesian, constant drawdown, variable discharge type curves	

## Tables

TABLE		PAGE
1	Values of partial penetration constant for observation well .....	8
2	Values of partial penetration constant for pumped well .....	8
3	Effective radii of collector wells. ....	28
4	Optimum screen entrance velocities .....	29
5	Time-drawdown data for well 19 near Dieterich .....	32
6	Distance-drawdown data for test near Dieterich .....	32
7	Time-drawdown data for well 1 at Gridley .....	34
8	Time-drawdown data for well 3 at Gridley .....	34
9	Time-drawdown data for well 15 near Mossville .....	35
10	Distance-drawdown data for test near Mossville .....	35
11	Results of shooting deep sandstone wells in northern Illinois .....	41
12	Results of acid treatment of dolomite wells in DuPage County .....	42
13	Coefficients of transmissibility computed from aquifer-test data for the Joliet area .....	45
14	Time-drawdown data for test at St. David. ....	47
15	Distance-drawdown data for test at Zion .....	49
16	Recharge rates for the Silurian dolomite aquifer in DuPage County .....	51
17	Results of flow-net analysis for area west of Joliet .....	52
18	Monthly and annual streamflow, ground-water runoff, and surface runoff in inches, 1951, 1952, and 1956, Panther Creek basin.....	54
19	Monthly and annual ground-water evapotranspiration in inches, 1951, 1952, and 1956, Panther Creek basin.....	54
20	Results of gravity yield analysis for Panther Creek basin.....	54
21	Monthly and annual ground-water recharge and changes in storage in inches, 1951, 1952, and 1956, Panther Creek basin .....	55
22	Log of well near Granite City .....	63
23	Data for step-drawdown test near Granite City.....	64
24	Drawdowns and pumping rates for well 1 near Granite City.....	64
25	Time-drawdown data for test at Iuka.....	65

# *Selected Analytical Methods for Well and Aquifer Evaluation*

by William C. Walton

## **Abstract**

The practical application of selected analytical methods to well and aquifer evaluation problems in Illinois is described in this report. The subject matter includes formulas and methods used to quantitatively appraise the geohydrologic parameters affecting the water-yielding capacity of wells and aquifers and formulas and methods used to quantitatively appraise the response of wells and aquifers to heavy pumping. Numerous illustrative examples of analyses based on actual field data are presented.

The aquifer test is one of the most useful tools available to hydrologists. Analysis of aquifer-test data to determine the hydraulic properties of aquifers and confining beds under nonleaky artesian, leaky artesian, water table, partial penetration, and geohydrologic boundary conditions is discussed and limitations of various methods of analysis are reviewed. Hydraulic properties are also estimated with specific-capacity data and maps of the water table or piezometric surface. The role of individual units of multiunit aquifers is appraised by statistical analysis of specific-capacity data.

The influence of geohydrologic boundaries on the yields of wells and aquifers is determined by means of the image-well theory. The image-well theory is applied to multiple boundary conditions by taking into consideration successive reflections on the boundaries.

Several methods for evaluating recharge rates involving flow-net analysis and hydrologic and ground-water budgets are described in detail. Well loss in production wells is appraised with step-drawdown test data, and well screens and artificial packs are designed based on the mechanical analysis of the aquifer. Optimum well spacings are estimated taking into consideration aquifer characteristics and economics.

Emphasis is placed on the quantitative evaluation of the practical sustained yields of wells and aquifers by available analytical methods. The actual ground-water condition is simulated by a model aquifer having straight-line boundaries, an effective width, length, and thickness, and sometimes a confining bed with an effective thickness. The hydraulic properties of the model aquifer and its confining bed, if present, the image-well theory, and appropriate ground-water formulas are used to construct a mathematical model which provides a means of evaluating the performance of wells and aquifers. Records of past pumpage and water levels establish the validity of this mechanism as a model of the response of an aquifer to heavy pumping.

## **Introduction**

During the last few years it has been more fully realized that refined quantitative answers are needed concerning available ground-water resources and their management. Utilization of aquifers continues to accelerate to meet the needs of irrigation, industrial, urban, and suburban expansion. As ground-water development intensifies, well owners become more interested in the response of aquifers to heavy pumping whereas initially they were concerned largely with the delineation and exploration of aquifers. Competition for available sources has brought about an awareness that one of the principal problems confronting hydrologists is resource management. Before ground-water resources can be managed they must be quantitatively appraised.

In ever increasing numbers engineers and geologists are being called upon to estimate how much ground water is

available for development and what will be the consequences of exploitation. Ground-water users are continually asking for suggestions as to how available resources can be properly managed. The advice of hydrologists concerning proper well design is often sought.

The development of ground-water resources has reached a stage wherein it is highly desirable that the voluminous material in the well and aquifer evaluation field be assembled and briefed in order that engineers and geologists actively engaged in quantitative studies can have available a ready reference. This report is concerned primarily with a brief description of the analytical methods presently used by the Illinois State Water Survey in evaluating wells and aquifers and supersedes Report of Investigation 25. The principles set forth will be applicable, with slight modifica-

tion, to many parts of the United States and the world. This report is by no means a substitute for the many exhaustive treatises on ground-water hydrology but rather is intended to be a handbook describing formulas and methods commonly used by hydrologists. A comprehensive bibliography is presented containing references to the literature germane to ground-water resource evaluation that may be used to expand the reader's understanding of subject matter.

The formulas and analytical methods available to hydrologists are almost unlimited in number, and the discussion of all of them would necessitate several volumes and unwarranted duplications. A selection has therefore been made to include formulas and analytical methods most frequently applied to actual field problems in Illinois.

The derivations and proofs of formulas have been elim-

inated, and formulas are presented in their developed form. The application and limitations of formulas and methods are discussed in detail. A consistent nomenclature has been adopted with clarity and general usage as criteria.

This report will find its field of greatest use in aiding the systematic appraisal of ground-water resource problems by professional and practicing engineers, geologists, and well contractors. The subject matter has been arranged in three major parts: 1) formulas and methods used to quantitatively appraise the geologic and hydrologic parameters affecting the water-yielding capacity of wells and aquifers, 2) formulas and methods used to quantitatively appraise the response of wells and aquifers to heavy pumping, and 3) illustrative examples of analyses based on actual field data collected by the Illinois State Water Survey.

## Part 1. Analysis of Geohydrologic Parameters

*This section describes methods used to evaluate hydraulic properties of aquifers and confining beds, the influence of geohydrologic boundaries on drawdowns in wells, and recharge to aquifers. Analyses of aquifer-test data, specific-capacity data, flow-net data, and hydrologic and ground-water budget data are discussed.*

### Hydraulic Properties

The coefficients of permeability or transmissibility, storage, and vertical permeability are the major hydraulic properties of aquifers and confining beds upon which the foundation of quantitative ground-water studies is based.

The rate of flow of ground water in response to a given hydraulic gradient is dependent upon the permeability of the aquifer. The field coefficient of permeability  $P$  is defined as the rate of flow of water, in gallons per day, through a cross-sectional area of 1 square foot of the aquifer under a hydraulic gradient of 1 foot per foot at the prevailing temperature of the water. A related term, the coefficient of transmissibility  $T$ , indicates the capacity of an aquifer as a whole to transmit water and is equal to the coefficient of permeability multiplied by the saturated thickness of the aquifer  $m$ , in feet. The coefficient of transmissibility is defined as the rate of flow of water, in gallons per day, through a vertical strip of the aquifer 1 foot wide and extending the full saturated thickness under a hydraulic gradient of 1 foot per foot at the prevailing temperature of the water.

The rate of vertical leakage of ground water through a confining bed in response to a given vertical hydraulic gradient is dependent upon the vertical permeability of the confining bed. The field coefficient of vertical permeability  $P'$  is defined as the rate of vertical flow of water, in gallons per day, through a horizontal cross-sectional area of 1 square foot of the confining bed under a hydraulic gradient of 1 foot per foot at the prevailing temperature of the water.

The storage properties of an aquifer are expressed by its coefficient of storage  $S$ , which is defined as the volume of water the aquifer releases from or takes into storage per unit surface area of the aquifer per unit change in the component of head normal to that surface. Under artesian conditions, when the piezometric surface is lowered by pumping, water is derived from storage by the compaction of the aquifer and its associated beds and by expansion of the water itself, while the interstices remain saturated. Under water-table conditions, when the water table is lowered by pumping, ground water is derived from storage mainly by the gravity drainage of the interstices in the portion of the aquifer unwatered by the pumping.

Under artesian conditions and for granular or loosely cemented aquifers reasonably free from clay beds, the coefficient of storage is a function of the elasticity of water and the aquifer skeleton, as expressed in the following equation (see Jacob, 1950):

$$S = (\rho\gamma m\beta/144) [1 + (\phi/p\beta)] \quad (1)$$

where:

$S$  = coefficient of storage, fraction

$p$  = porosity, fraction

$m$  = saturated thickness of aquifer, in ft

$\beta$  = reciprocal of the bulk modulus of elasticity of water, in sq in./lb

$\phi$  = reciprocal of the bulk modulus of elasticity of aquifer skeleton, in sq in./lb

$\gamma$  = specific weight of water, in lb/cu ft

Recognizing that for practical purposes  $\gamma = 62.4$  lb/cu ft and  $\beta = 3.3 \times 10^{-6}$  sq in./lb, the fraction of storage attributable to expansibility of the water  $S_w$  is given by the following equation:

$$S_w = 1.4 \times 10^{-6} (pm) \quad (2)$$

### Aquifer Tests

The hydraulic properties of aquifers and confining beds may be determined by means of aquifer tests, wherein the effect of pumping a well at a known constant rate is measured in the pumped well and in observation wells penetrating the aquifer. Graphs of drawdown versus time after pumping started, and/or of drawdown versus distance from the pumped well, are used to solve formulas which express the relation between the hydraulic properties of an aquifer and its confining bed, if present, and the lowering of water levels in the vicinity of a pumped well.

### Drawdown

To determine drawdown, the water-level trend before pumping started is extrapolated through the pumping period, and differences between extrapolated stages of the water level that would have been observed if the well had not been pumped and water levels measured during the pumping period are computed. Drawdown is not determined from the water level that was measured just prior to the start of the aquifer test. Before water-level data are

used to determine hydraulic properties they must be adjusted for any pumping-rate changes in nearby production wells.

Water levels in wells in artesian aquifers are affected by fluctuations in atmospheric pressure. As the atmospheric pressure increases the water level falls, and as the atmospheric pressure decreases the water level rises. The ratio of the change in water level in a well to the change in atmospheric pressure is known as the barometric efficiency of the well and is usually expressed as a percentage.

Barometers are generally calibrated in inches of mercury and changes in atmospheric pressure must be converted from inches of mercury to feet of water before the barometric efficiency of a well can be computed. The conversion is readily expressed as:

$$\text{inches of mercury} \times 1.13 = \text{feet of water}$$

Equations for the barometric efficiency of a well and for the change in water level in response to an atmospheric-pressure change are as follows:

$$B.E. = (\Delta W/\Delta B) 100 \quad (3)$$

$$\Delta W = [B.E. (\Delta B)]/100 \quad (4)$$

where:

$B.E.$  = barometric efficiency, in per cent

$\Delta W$  = change in water level resulting from a change in atmospheric pressure, in ft

$\Delta B$  = change in atmospheric pressure, in ft of water

Drawdown data must be adjusted for atmospheric-pressure changes before they are used to determine hydraulic properties. Changes in the time-rate of drawdown due to atmospheric-pressure fluctuations may be mistaken for evidence of geohydrologic boundary conditions. A time interval during which water levels are not affected by pumping changes is selected. Barometer readings, converted to feet of water, are inverted and plotted on plain coordinate paper, together with water-level data for the pumped and observation wells. Prominent barometric fluctuations are used to compare changes in water level caused by changes in atmospheric pressure. The amount of rise in water level as a result of a decrease in atmospheric pressure and the amount of decline in water level as a result of an increase in atmospheric pressure are calculated. The barometric efficiency can then be computed with equation 3. Drawdown data are adjusted for atmospheric-pressure changes occurring during an aquifer test by obtaining a record of atmospheric-pressure fluctuations and using equation 4.

Water levels in wells near surface bodies of water are often affected by surface-water stage fluctuations either because of a loading effect or a hydraulic connection between the surface-water body and the aquifer. As the surface-water stage rises the water level rises, and as the surface-water stage declines the water level falls. The ratio of the change in the water level in a well to the change in surface-water stage in the case of a loading effect is known as the tidal efficiency, and the ratio of the change in the water level in a well to the change in surface-water stage in the

case where a hydraulic connection exists between the surface-water body and the aquifer is known as the river efficiency.

Equations for the tidal and river efficiencies of a well and for the change in water level in response to a surface-water stage change are as follows:

$$T.E. = (\Delta W/\Delta R) 100 \quad (5) \quad \Delta W = [T.E. (\Delta R)]/100 \quad (6)$$

$$R.E. = (\Delta W/\Delta R) 100 \quad (7) \quad \Delta W = [R.E. (\Delta R)]/100 \quad (8)$$

where:

$T.E.$  = tidal efficiency, in per cent

$R.E.$  = river efficiency, in per cent

$\Delta W$  = change in water level resulting from a change in surface-water stage, in ft

$\Delta R$  = change in surface-water stage, in ft

The tidal or river efficiency can be computed and drawdown data can be adjusted for surface-water stage changes occurring during an aquifer test by obtaining a record of surface-water stage fluctuations during the test and using equations 5 and 6 or 7 and 8.

The application or the removal of heavy loads in the vicinity of some artesian wells causes changes in their water levels. Fluctuations in water levels (Roberts and Romine, 1947) sometimes occur when railroad trains or trucks pass aquifer test sites. Drawdown data must be adjusted for these changes in loading before they are used to determine the hydraulic properties of aquifers and confining beds.

### Leaky Artesian Formula

The data collected during aquifer tests may be analyzed by means of the leaky artesian formula (Hantush and Jacob, 1955a). The leaky artesian formula may be written as:

$$s = (114.6Q/T) W(u, r/B) \quad (9)$$

where:

$$u = 2693r^2S/Tt \quad (10)$$

and

$$r/B = r/\sqrt{T/(P'/m')} \quad (11)$$

$s$  = drawdown in observation well, in ft

$r$  = distance from pumped well to observation well, in ft

$Q$  = discharge, in gallons per minute (gpm)

$t$  = time after pumping started, in minutes (min)

$T$  = coefficient of transmissibility, in gallons per day per foot (gpd/ft)

$S$  = coefficient of storage of aquifer, fraction

$P'$  = coefficient of vertical permeability of confining bed, in gallons per day per square foot (gpd/sq ft)

$m'$  = thickness of confining bed through which leakage occurs, in ft

$W(u, r/B)$  is read as the "well function for leaky artesian

aquifers" (Hantush, 1956) and is defined by the following equation:

$$W(u, r/B) = \int_u^{\infty} (1/u) \exp(-u - r^2/4B^2u) du$$

or, evaluating the integral,

$$\begin{aligned} W(u, r/B) = & 2K_0(r/B) - I_0(r/B) \left[ -Ei\left(-\frac{r^2}{4B^2u}\right) \right] \\ & + \left[ \exp\left(-\frac{r^2}{4B^2u}\right) \right] \left\{ 0.5772 + \ln u + [-Ei(-u)] \right. \\ & - u + u [I_0(r/B) - 1] / \frac{r^2}{4B^2} \\ & \left. - u^2 \sum_{n=1}^{\infty} \sum_{m=1}^n \frac{(-1)^{n+m} (n-m+1)!}{(n+2)!} \left(\frac{r^2}{4B^2}\right)^m u^{n-m} \right\} \end{aligned}$$

where:

$K_0(r/B)$  = modified Bessel function of the second kind and zero order and  $I_0(r/B)$  = modified Bessel function of the first kind and zero order.

The leaky artesian formula was developed on the basis of the following assumptions: that the aquifer is infinite in areal extent and is of the same thickness throughout; that it is homogeneous and isotropic; that it is confined between an impermeable bed and a bed through which leakage can occur; that the coefficient of storage is constant; that water is released from storage instantaneously with a decline in head; that the well has an infinitesimal diameter and penetrates the entire thickness of the formation; that leakage through the confining bed into the aquifer is vertical and proportional to the drawdown; that the hydraulic head in the deposits supplying leakage remains more or less uniform; that the flow is vertical in the confining bed and horizontal in the aquifer; and that the storage in the confining bed is neglected.

In cases where leakage is derived in part by the reduction in storage in the confining bed, aquifer-test data can be analyzed with formulas derived by Hantush (1960).

The leaky artesian formula may be solved by the following method (Walton, 1960a) which is a modification of the type curve graphical method devised by Theis and described by Jacob (1940). Values of  $W(u, r/B)$  in terms of the practical range of  $u$  and  $r/B$  were given by Hantush (1956) and are presented in tabular form in appendix A of this report. Values of  $W(u, r/B)$  are plotted against values of  $l/u$  on logarithmic paper and a family of leaky artesian type curves is constructed as shown in plate 1. Values of  $s$  plotted on logarithmic paper of the same scale as the type curves against values of  $t$  describe a time-drawdown field data curve that is analogous to one of the family of leaky artesian type curves.

The time-drawdown field data curve is superposed on the family of leaky artesian type curves, keeping the  $W(u, r/B)$  axis parallel with the  $s$  axis and the  $l/u$  axis parallel with the  $t$  axis. In the matched position a point at the intersection of the major axes of the leaky artesian type curve is selected and marked on the time-drawdown field data curve (the point also may be selected anywhere on the type curve). The coordinates of this common point (match point)  $W(u, r/B)$ ,  $l/u$ ,  $s$ , and  $t$  are substituted into equa-

tions 9, 10, and 11 to determine the hydraulic properties of the aquifer and confining bed.  $T$  is calculated using equation 9 with the  $W(u, r/B)$  and  $s$  coordinates.  $S$  is determined using equation 10, the calculated value of  $T$ , and the  $l/u$  and  $t$  coordinates of the match point. The coefficient of storage must exceed  $S_w$  in equation 2 or the analysis is incorrect. The value of  $r/B$  used to construct the particular leaky artesian type curve found to be analogous to the time-drawdown field data curve is substituted in equation 11 to determine  $P'$ .

Interpretations of aquifer-test data based solely on time drawdown graphs are weak. Distance-drawdown data complement time-drawdown data, and the hydraulic properties of the aquifer and confining bed can be determined from distance-drawdown field data curves (radial profiles of cones of depression). Values of  $W(u, r/B)$  are plotted against values of  $r/B$  on logarithmic paper and a family of leaky artesian type curves is constructed. Values of  $s$  plotted against values of  $r$  on logarithmic paper of the same scale as the type curves describe a distance-drawdown field data curve that is analogous to one of the family of leaky artesian type curves. The distance-drawdown field data curve is superposed on the family of leaky artesian type curves, keeping the  $W(u, r/B)$  axis parallel with the  $s$  axis and the  $r/B$  axis parallel with the  $r$  axis. The distance-drawdown field data curve is matched to one of the family of leaky artesian type curves. In the matched position a point at the intersection of the major axes of the leaky artesian type curve is selected and marked on the distance-drawdown field data curve. Match-point coordinates  $W(u, r/B)$ ,  $r/B$ ,  $s$ , and  $r$  are substituted in equations 9 and 11 to determine the coefficients of transmissibility and vertical permeability. The value of  $u/r^2$  used to construct the particular leaky artesian type curve found to be analogous to the distance-drawdown field data curve is substituted in equation 10 to compute  $S$ .

Under steady-state leaky artesian conditions, that is when time-drawdown data fall on the flat portions of the family of leaky artesian type curves indicating that discharge is balanced by leakage, the cone of depression is described by the following formula (see Jacob, 1946a):

$$s = [229QK_0(r/B)]/T \quad (12)$$

where:

$$r/B = r/\sqrt{T/(P'm')} \quad (13)$$

$s$  = drawdown in observation well, in ft

$r$  = distance from pumped well to observation well, in ft

$Q$  = discharge, in gpm

$T$  = coefficient of transmissibility, in gpd/ft

$P'$  = coefficient of vertical permeability of confining bed, in gpd/sq ft

$m'$  = thickness of confining bed through which leakage occurs, in ft

$K_0(r/B)$  = modified Bessel function of the second kind and zero order

Jacob (1946a) devised the following graphical method

for determining values of the parameters  $T$  and  $P'$  under steady-state leaky artesian conditions. A steady-state leaky artesian type curve is prepared by plotting values of  $K_o(r/B)$  against values of  $r/B$  on logarithmic paper as shown in plate 2. Values of  $K_o(r/B)$  in terms of the practical range of  $r/B$  are given in appendix B. Aquifer-test data collected under steady-state conditions are plotted on logarithmic paper of the same scale as the type curve with  $r$  as the abscissa and  $s$  as the ordinate to describe a distance-drawdown field data curve. A match of the two curves is obtained by superposing the distance-drawdown field data curve over the steady-state leaky artesian type curve, keeping the axes of the two graphs parallel. In the matched position a point at the intersection of the major axes of the steady-state leaky artesian type curve is selected and marked on the distance-drawdown field data curve. Match-point coordinates  $K_o(r/B)$ ,  $r/B$ ,  $s$ , and  $r$  are substituted into equations 12 and 13 to determine  $T$  and  $P'$ . The coefficient of storage cannot be computed by use of the steady-state leaky artesian type curve because, under such conditions of flow, the entire yield of the well is derived from leakage sources only.

### Nonleaky Artesian Formula

If leakage through the confining bed into the aquifer is not measurable or the confining bed is missing, equation 9 becomes

$$s = (114.6Q/T) W(u) \quad (14)$$

where:

$$W(u) = \int_u^{\infty} e^{-u}/u \, du = -0.5772 - \ln u + u - (u^2/2.2!) + (u^3/3.3!) - (u^4/4.4!) \dots$$

and

$$u = 2693r^2S/Tt \quad (15)$$

$s$  = drawdown in observation well, in ft

$Q$  = discharge, in gpm

$T$  = coefficient of transmissibility, in gpd/ft

$r$  = distance from observation well to pumped well, in ft

$S$  = coefficient of storage, fraction

$t$  = time after pumping started, in min

Equation 14 is the nonequilibrium formula introduced by Theis (1935) and will be referred to hereafter as the nonleaky artesian formula.  $W(u)$  is the "well function for nonleaky artesian aquifers" (see Wenzel, 1942).

If leakage is not measurable during the aquifer test or the confining bed is missing, the time-drawdown field data curve will be analogous to the nonleaky artesian type curve which is shown in plate 1 as the outside curve of the family of leaky artesian type curves. The time-drawdown field data curve and the nonleaky artesian type curve are matched and match point coordinates  $W(u)$ ,  $1/u$ ,  $s$ , and  $t$  are substituted into equations 14 and 15 to determine  $T$  and  $S$ .

The coefficients of transmissibility and storage can also be computed with distance-drawdown data under non-

leaky artesian conditions. Values of  $W(u)$ , given by Wenzel (1942) and presented in tabular form in appendix C, were plotted against values of  $u$  on logarithmic paper to obtain the nonleaky artesian type curve in plate 3. Values of  $s$  measured at the same time in several wells at various distances from the pumped well are plotted against the squares of the respective distances on logarithmic paper of the same scale as the type curve to obtain a distance-drawdown field data curve. The distance-drawdown field data curve is superposed on the nonleaky artesian type curve keeping the axes of the two graphs parallel. In the matched position a point at the intersection of the major axes of the nonleaky artesian type curve is selected and marked on the distance-drawdown field data curve. Match-point coordinates  $W(u)$ ,  $u$ ,  $s$ , and  $r^2$  are substituted into equations 14 and 15 to determine  $T$  and  $S$ .

### Water-Table Conditions

The methods described in preceding paragraphs pertain to leaky artesian and nonleaky artesian conditions. The nonleaky artesian formula can be applied to the results of aquifer tests made with wells in water-table aquifers under certain limiting conditions. The nonleaky artesian formula was developed in part on the basis of the following assumptions: that the coefficient of storage is constant and that water is released from storage instantaneously with a decline in head. Under water-table conditions, water is derived largely from storage by the gravity drainage of the interstices in the portion of the aquifer unwatered by the pumping. The gravity drainage of water through stratified sediments is not immediate and the nonsteady flow of water towards a well in an unconfined aquifer is characterized by slow drainage of interstices. Thus, the coefficient of storage varies and increases at a diminishing rate with the time of pumping. The important effects of gravity drainage are not considered in the nonleaky artesian formula and that formula does not describe completely the drawdown in wells especially during short periods of pumping. With long periods of pumping the effects of gravity drainage become small and time-drawdown and distance-drawdown curves conform closely to the nonleaky artesian type curve.

According to Boulton (1954a) whether or not the nonleaky artesian formula gives a good approximation of the drawdown in a well under water-table conditions depends on the distance of the observation well from the pumped well  $r$ , the hydraulic properties of the aquifer, the saturated thickness of the aquifer  $m$ , and a dimensionless "time factor." He further implies that the nonleaky artesian formula describes the drawdown in wells with sufficient accuracy for practical purposes when the time factor is greater than 5 and  $r$  is between about 0.2  $m$  and 6  $m$ . By substituting a numerical value equal to 5 for Boulton's time factor, the following equation can be derived:

$$t_{wt} = 37.4S_y m/P \quad (16)$$

where:

$t_{wt}$  = approximate time after pumping starts when the

application of the nonleaky artesian formula to the results of aquifer tests under water-table conditions is justified, in days

$S_y$  = specific yield, fraction

$P$  = coefficient of permeability, in gpd/sq ft

$m$  = saturated thickness of aquifer, in ft

The above equation is not valid when  $r$  is less than about 0.2  $m$  or greater than about 6  $m$ . For observation wells at great distances from the pumped well,  $t_{wr}$  must be something greater than that given by equation 16 before the nonleaky artesian formula can be applied to aquifer-test data. It is evident that  $t_{wr}$  is small if an aquifer is thin and very permeable. For example,  $t_{wr}$  is about 1 hour if an observation well is close to a pumped well and penetrates an aquifer 30 feet thick with a coefficient of permeability of 5000 gpd/sq ft. In contrast, substituting the data for a thick aquifer of low permeability ( $m = 200$  feet and  $P = 1000$  gpd/sq ft) in equation 16 results in a  $t_{wr}$  of about 1.5 days.

Gravity drainage of interstices decreases the saturated thickness and therefore the coefficient of transmissibility of the aquifer. Under water-table conditions, observed values of drawdown must be compensated for the decrease in saturated thickness before the data can be used to determine the hydraulic properties of the aquifer. The following equation derived by Jacob (1944) is used to adjust drawdown data for decrease in the coefficient of transmissibility:

$$s' = s - (s^2/2m) \quad (17)$$

where:

$s'$  = drawdown that would occur in an equivalent nonleaky artesian aquifer, in ft

$s$  = observed drawdown under water-table conditions, in ft

$m$  = initial saturated thickness of aquifer, in ft

Under water-table conditions values of drawdown adjusted for decreases in saturated thickness are plotted against the logarithms of values of  $t$  to describe a time-drawdown field data curve. The time-drawdown field data curve is superposed on the nonleaky artesian type curve, keeping the axes of the two curves parallel. The time-drawdown field data curve is matched to the nonleaky artesian type curve. Emphasis is placed on late time-drawdown data (usually after several minutes or hours of pumping) because early time-drawdown data are affected by gravity drainage. Match-point coordinates  $W(u)$ ,  $1/u$ ,  $s$ , and  $t$  are substituted into equations 14 and 15 to determine  $T$  and  $S$ . After tentative values of  $T$  and  $S$  have been calculated,  $t_{wr}$  is computed from equation 16. The time  $t_{wr}$  is compared with the early portion of data ignored in matching curves. If the type curve is matched to drawdown data for values of time equal to and greater than  $t_{wr}$  then the solution is judged to be valid. If the type curve is matched to drawdown data for values of time earlier than  $t_{wr}$  then the solution is not correct and the time-drawdown field data curve is re-

matched to the nonleaky artesian type curve and the procedures mentioned earlier are repeated until a valid solution is obtained.

Gravity drainage is far from complete during the average period (8 to 24 hours) of aquifer tests; therefore, the coefficient of storage computed with data collected under water-table conditions will generally be less than the specific yield of the aquifer and it cannot be used to predict long-term effects of pumping. It should be recognized that the coefficient of storage computed from test results applies largely to the part of the aquifer unwatered by pumping and it may not be representative of the aquifer at lower depths.

### Partial Penetration

Production and observation wells often do not completely penetrate aquifers. The partial penetration of a pumping well influences the distribution of head in its vicinity, affecting the drawdowns in nearby observation wells. The approximate distance  $r_{pp}$  from the pumped well beyond which the effects of partial penetration are negligible is given by the following equation (see Butler, 1957):

$$r_{pp} = 2m\sqrt{P_h/P_v} \quad (18)$$

where:

$m$  = saturated thickness of aquifer, in ft

$P_h$  = horizontal permeability of aquifer, in gpd/sq ft

$P_v$  = vertical permeability of aquifer, in gpd/sq ft

According to Hantush (1961), the effects of partial penetration closely resemble the effects of leakage through a confining bed, the effects of a recharge boundary, the effects of a sloping water-table aquifer, and the effects of an aquifer of nonuniform thickness. He outlines methods for analysis of time-drawdown data affected by partial penetration under nonsteady state, nonleaky artesian conditions.

In many cases distance-drawdown data can be adjusted for partial penetration according to methods described by Butler (1957). If the pumped well only partially penetrates an aquifer, the cone of depression is distorted and observed drawdowns in observation wells differ from theoretical drawdowns for a fully penetrating well according to the vertical position of the observation well. If the pumped and observation wells are both open in either the top or the bottom portion of the aquifer, the observed drawdown in the observation well is greater than for fully penetrating conditions. If the pumped well is open to the top of the aquifer and the observation well is open to the bottom of the aquifer, or vice versa, the observed drawdown in the observation well is smaller than for fully penetrating conditions.

In the case where both the pumped and observation wells are open in the same zone of the aquifer, the following equation (see Butler, 1957) can be used to adjust observed drawdowns in observation wells for the effects of partial penetration:

$$s = C_{po}s_{pp} \quad (19)$$

where:

- $s$  = drawdown in observation well for fully penetrating conditions, in ft
- $C_{po}$  = partial penetration constant for observation well, fraction
- $s_{pp}$  = observed drawdown for partial penetrating conditions, in ft

**Table 1. Values of partial penetration constant for observation well**

$r/m \sqrt{P_v/P_h}$	$\alpha$		
	0.3	0.5	0.7
Values of $C_{po}$ for $r_e/m = 3$			
0.318	0.621	0.768	0.882
0.40	0.716	0.817	0.905
0.50	0.792	0.860	0.927
0.60	0.848	0.897	0.943
0.80	0.918	0.941	0.966
1.00	0.954	0.967	0.980
1.40	0.984	0.988	0.993
2.23	0.998	0.999	0.999
Values of $C_{po}$ for $r_e/m = 5$			
0.318	0.691	0.811	0.904
0.40	0.774	0.854	0.925
0.50	0.837	0.891	0.943
0.60	0.884	0.921	0.957
0.80	0.940	0.957	0.975
1.00	0.969	0.976	0.986
1.40	0.991	0.993	0.996
2.23	0.999	0.999	1.000
Values of $C_{po}$ for $r_e/m = 10$			
0.318	0.753	0.848	0.923
0.40	0.823	0.884	0.941
0.50	0.874	0.917	0.956
0.60	0.913	0.940	0.968
0.80	0.957	0.968	0.983
1.00	0.978	0.983	0.989
1.40	0.993	0.994	0.998
2.23	0.999	0.999	1.000
Values of $C_{po}$ for $r_e/m = 100$			
0.318	0.853	0.909	0.954
0.40	0.897	0.933	0.966
0.50	0.929	0.953	0.976
0.60	0.953	0.968	0.983
0.80	0.978	0.984	0.990
1.00	0.990	0.993	0.996
1.40	0.997	0.998	0.999
2.23	1.000	1.000	1.000

From Butler (1957); adapted from Jacob (1945)

Values of  $C_{po}$  can be obtained from table 1. In table 1,  $r$  = distance from pumped well to observation well, in feet;  $m$  = saturated thickness of aquifer, in feet;  $\alpha$  = fractional penetration;  $P_h$  = horizontal permeability of aquifer, in gpd/sq ft;  $P_v$  = vertical permeability of aquifer, in gpd/sq ft; and  $r_e$  = virtual radius of cone of depression, assumed to be 10,000 feet for artesian conditions and 1000 feet for water-table conditions.

In the case where the pumped well penetrates the top of the aquifer and the observation well penetrates the bottom of the aquifer, or vice versa, the following equation (see

Butler, 1957) can be used to adjust observed drawdowns for the effects of partial penetration:

$$s = [C_{po} / (2C_{po} - 1)] s_{pp} \quad (20)$$

The following equation (see Butler, 1957) can be used to adjust the observed drawdown in a pumped well for the effects of partial penetration:

$$s = C_{pp} s_{pp} \quad (21)$$

where:

- $s$  = drawdown for pumped well for fully penetrating conditions, in ft
- $C_{pp}$  = partial penetration constant for pumped well, fraction
- $s_{pp}$  = observed drawdown for partial penetration conditions, in ft

**Table 2. Values of partial penetration constant for pumped well**

$r_w/m \sqrt{P_v/P_h}$	$\alpha$			
	0.2	0.3	0.5	0.7
Values of $C_{pp}$				
0.0000	0.200	0.300	0.500	0.700
0.0001	0.221	0.324	0.525	0.719
0.0003	0.236	0.342	0.543	0.732
0.0010	0.266	0.376	0.578	0.759
0.002	0.294	0.408	0.611	0.783
0.003	0.315	0.432	0.636	0.803
0.006	0.363	0.487	0.642	0.846
0.010	0.410	0.541	0.748	0.888

From Butler (1957); based on equation derived by Kozeny (1933)

Values of  $C_{pp}$  are given in table 2 where  $r_w$  = nominal radius of well, in feet.

Equations 19 through 21 assume steady-state conditions which are not always attained during actual periods of aquifer tests. Tests one day or more in duration are generally long enough to establish steady-state flow in the vicinity of the pumped well and observation wells within the area affected by partial penetration. Equations 19 through 21 give fair results even though steady-state conditions are not attained especially when the aquifer penetrated is of small and known thickness. At best, adjustments for partial penetration by any method can be considered only approximate because the ratio  $P_v/P_h$  is never precisely known.

To determine the hydraulic properties of an aquifer with aquifer-test data affected by partial penetration, drawdowns computed with equation 19 or 20 are plotted against the squares of the respective distances to obtain a distance-drawdown field data curve. The distance-drawdown field data curve is superposed on the appropriate type curve (either plate 2 or 3). The two curves are matched and match-point coordinates are substituted into appropriate equations for computation of the hydraulic properties of the aquifer and confining bed, if present.

### Modified Nonleaky Artesian Formula

Jacob (1946b) recognized that when  $u$  becomes small (less than, say, 0.01) the sum of the terms in  $W(u)$  be-

yond  $\ln u$  becomes insignificant. When the pumping period becomes large or when the distance  $r$  is small, values of  $u$  will be small.

When  $u \leq 0.01$   
 then  $W(u) = (-0.5772 - \ln u)$   
 and  $s = (114.6Q/T) (-0.5772 - \ln u)$  (22)

Equation 22 is the modified nonleaky artesian formula and can be solved graphically (Cooper and Jacob, 1946). Drawdowns in an observation or pumped well are adjusted, if needed, for effects of atmospheric-pressure changes, surface-water stage changes, dewatering, and partial penetration. Values of adjusted drawdown are plotted against the logarithms of time after pumping started on semilogarithmic paper. The time-drawdown field data graph will yield a straight-line graph in the region where  $u \leq 0.01$ . The straight-line portion of the time-drawdown field data graph is extrapolated to its intersection with the zero-drawdown axis. The slope of the straight line is used to determine the coefficient of the transmissibility, and the zero-drawdown intercept is used to calculate the coefficient of storage. Expressions for the computations are:

$$T = 264Q/\Delta s \quad (23)$$

$$S = Tt_o/4790r^2 \quad (24)$$

where:

- $T$  = coefficient of transmissibility, in gpd/ft
- $S$  = coefficient of storage, fraction
- $Q$  = discharge, in gpm
- $\Delta s$  = drawdown difference per log cycle, in ft
- $r$  = distance from pumped well to observation well, in ft
- $t_o$  = intersection of straight-line slope with zero-drawdown axis, in min

The coefficient of storage cannot be determined with any degree of accuracy from data for the pumped well because the effective radius of the pumped well is seldom known and drawdowns in the pumped well are often affected by well losses which cannot be determined precisely.

Drawdowns observed at the end of a particular pumping period in two or more observation wells at different distances from the pumped well can be plotted against the logarithms of the respective distances on semilogarithmic paper. The distance-drawdown field data graph will yield a straight-line graph in the region where  $u \leq 0.01$ . The straight-line portion of the distance-drawdown graph is extrapolated to its intersection with the zero-drawdown axis. The slope of the straight line is used to determine the coefficient of transmissibility, and the zero-drawdown intercept is used to calculate the coefficient of storage. Expressions for the computations are:

$$T = 528Q/\Delta s \quad (25)$$

$$S = Tt/4790r_o^2 \quad (26)$$

where:

- $T$  = coefficient of transmissibility, in gpd/ft
- $S$  = coefficient of storage, fraction
- $Q$  = discharge, in gpm

- $\Delta s$  = drawdown difference per log cycle, in ft
- $r_o$  = intersection of straight-line slope with zero-drawdown axis, in ft
- $t$  = time after pumping started, in min

The straight-line method based on the modified nonleaky artesian formula is popular largely because of its simplicity of application and interpretation; however, as pointed out by Cooper and Jacob (1946), "the method is not applicable in some cases and it supplements, rather than supersedes, the type curve method." They state further, "the method is designed especially for artesian conditions, but it may be applied successfully to tests of non-artesian aquifers under favorable circumstances."

The straight-line method is based on the fact that when  $u$  becomes small a plot of drawdown against the logarithm of time after pumping started or distance from the pumped well describes a straight line. A semilogarithmic graph of values of  $W(u)$  and  $u$  does not describe a straight line until  $u \leq 0.01$ . Deviation from a straight line becomes appreciable when  $u$  exceeds about 0.02. Therefore, a plot of drawdown against the logarithm of time after pumping started or the logarithm of distance from the pumped well cannot describe a straight line until  $u$  becomes small (say less than 0.02).

Scattered drawdown data are often interpreted as describing a straight line when actually they plot as a gentle curve. After tentative values of  $T$  and  $S$  have been calculated, the region of the data where  $u \leq 0.02$  should be calculated and compared with the region of data through which the straight line was drawn. The time that must elapse before the straight-line method can be applied to aquifer test data is readily determined from the following equation:

$$t_{sl} = 1.35 \times 10^5 r^2 S / T \quad (27)$$

where:

- $t_{sl}$  = time after pumping starts before a semilog time-drawdown or distance-drawdown plot will yield a straight-line graph, in min
- $r$  = distance from pumped well to observation well, in ft
- $T$  = coefficient of transmissibility, in gpd/ft
- $S$  = coefficient of storage, fraction

Inserting the data for an artesian aquifer ( $S = 0.0001$ ,  $T = 17,000$  gpd/ft, and  $r = 100$  feet) in equation 27 results in a  $t_{sl}$  of about 8 minutes. In contrast,  $t_{sl}$  is about 2 days for a water-table aquifer ( $S = 0.2$ ,  $T = 100,000$  gpd/ft, and  $r = 100$  feet). Although the values of  $t_{sl}$  given above apply only to the particular assumptions made, they do point out that the straight-line method should be used with caution particularly in the water-table aquifer situation.

The determination of the storage coefficient by the straight-line method may involve appreciable error. The zero-drawdown intercept is poorly defined where the slope of the semilog plot is small. Intercepts often occur at points where the values of time are very small and minor deviations in extrapolating the straight line will result in large variations in computed values of the coefficient of storage.

## Leaky Artesian Constant-Drawdown Formula

In the usual aquifer test the discharge rate of the pumped well is held constant and the drawdown varies with time. Hantush (1959b) derived an equation for determining the hydraulic properties of an aquifer and confining bed from an aquifer test in which the discharge varies with time and the drawdown remains constant. The formula describing leaky artesian constant-drawdown variable discharge conditions may be written as:

$$s_w = 229Q/[G(\lambda, r_w/B)T] \quad (28)$$

$$\lambda = 9.29 \times 10^{-5} T t / r_w^2 S \quad (29)$$

$$r_w/B = r_w / \sqrt{T/(P'/m')} \quad (30)$$

where:

$$G(\lambda, r_w/B) = (r_w/B) [K_1(r_w/B)/K_0(r_w/B)] + (4/p^2) \exp[-\lambda(r_w/B)^2]$$

$$\int_0^{\infty} \frac{u \exp(-\lambda u^2)}{J_0^2(u) + Y_0^2(u)} \cdot \frac{du}{u^2 + (r_w/B)^2}$$

$$u = r_w \sqrt{1/\exp(i\pi)} B^2$$

$T$  = coefficient of transmissibility, in gpd/ft

$S$  = coefficient of storage, fraction

$Q$  = discharge, in gpm

$r_w$  = nominal radius of pumped well, in ft

$s_w$  = drawdown in pumped well, in ft

$t$  = time after discharge started, in min

$P'$  = coefficient of vertical permeability of confining bed, in gpd/sq ft

$m'$  = thickness of confining bed through which leakage occurs, in ft

$K_1(r_w/B)$  = first-order modified Bessel function of the second kind

$K_0(r_w/B)$  = zero-order modified Bessel function of the second kind

$J_0(u)$  = zero-order Bessel function of the first kind

$Y_0(u)$  = zero-order Bessel function of the second kind

The equation is based on the same assumptions as those for the leaky artesian equation except that the drawdown is constant and the discharge is variable.  $G(\lambda, r_w/B)$  is the "well function for leaky artesian aquifers and constant drawdown."

Hantush (1959b) gave values of  $G(\lambda, r_w/B)$  in the practical range of  $\lambda$  and  $r/B$ . Values of  $G(\lambda, r_w/B)$  given in appendix D were plotted against values of  $\lambda$  on logarithmic paper and a family of leaky artesian constant-drawdown type curves was constructed as shown in plate 4. Values of discharge plotted against values of time on logarithmic paper of the same scale as the type curves describe a time-discharge field data curve that is analogous to one of the family of type curves.

The time-discharge field data curve is superposed on the

family of type curves, keeping the  $G(\lambda, r_w/B)$  axis parallel with the  $Q$  axis and the  $\lambda$  axis parallel with the  $t$  axis. The time-discharge field data curve is matched to one of the type curves and a point at the intersection of the major axes of the type curve is selected and marked on the time-discharge field data curve. The coordinates of the match point  $G(\lambda, r_w/B)$ ,  $\lambda$ ,  $Q$ , and  $t$  are substituted in equations 28 and 29 to determine  $T$  and  $S$ .  $T$  is calculated using equation 28 with the  $G(\lambda, r_w/B)$  and  $Q$  match-point coordinates.  $S$  is determined using equation 29, the calculated value to  $T$ , and the  $\lambda$  and  $t$  coordinates of the match point. The value of  $r/B$  used to construct the particular type curve found to be analogous to the time-discharge field data curve is substituted in equation 30 to compute  $P'$ .

## Nonleaky Artesian Drain Formula

In 1938 Theis (in Wenzel and Sand, 1942) developed a formula for determining the hydraulic properties of a nonleaky artesian aquifer with data on the decline in artesian head at any distance from a drain discharging water at a uniform rate. The formula is based on most of the assumptions used to derive the nonleaky artesian formula. In addition, it is assumed that the drain completely penetrates the aquifer and discharges water at a constant rate. The drain formula may be written (Knowles, 1955) as:

$$s = (720Q_b X/T) D(u)_q \quad (31)$$

where:

$$D(u)_q = [(e^{-u^2}/u\sqrt{\pi}) - 1 + (2/\sqrt{\pi})] \int_0^{X/2\sqrt{Tt/S}} e^{-u^2} du$$

and

$$u^2 = 2693 X^2 S / T t \quad (32)$$

$s$  = drawdown at any point in the vicinity of the drain, in ft

$Q_b$  = constant discharge (base flow) of the drain, in gpm per lineal foot of drain

$X$  = distance from drain to point of observation, in ft

$t$  = time after drain started discharging, in min

$T$  = coefficient of transmissibility, in gpd/ft

$S$  = coefficient of storage, fraction

Knowles (1955) gave values of  $D(u)_q$  for the practical range of values for  $u$  (see appendix E). The nonleaky artesian drain type curve in figure 1 was constructed by plotting values of  $1/u^2$  against values of  $D(u)_q$  on logarithmic graph paper.  $D(u)_q$  is read as the "drain function for nonleaky artesian aquifers."

Values of drawdown are plotted versus values of time on logarithmic paper having the same log scale as that used to construct the nonleaky artesian drain type curve. The time-drawdown field data curve is superposed over the nonleaky artesian drain type curve, the two curves are matched, and a match point is selected. The coordinates of the match

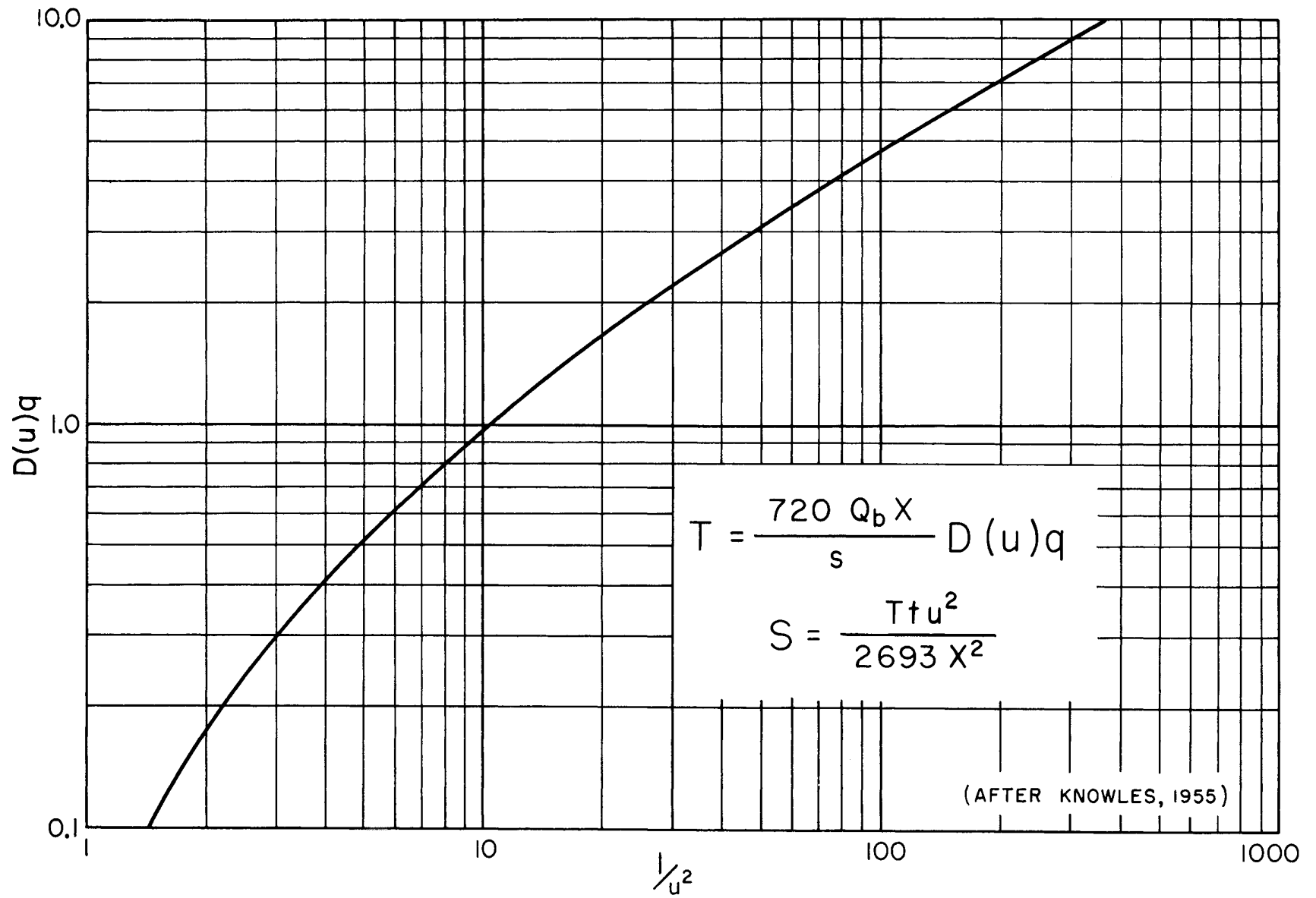


Figure 1. Nonleaky artesian drain type curve

point  $D(u)_q$ ,  $1/u^2$ ,  $s$ , and  $t$  are substituted into equations 31 and 32 for computation of  $T$  and  $S$ .

### Specific-Capacity Data

In many cases, especially in reconnaissance ground-water investigations, the hydraulic properties of an aquifer must be estimated based on well-log, water-level, and specific-capacity data. High specific capacities generally indicate a high coefficient of transmissibility, and low specific capacities generally indicate low coefficients of transmissibility.

The specific capacity of a well cannot be an exact criterion of the coefficient of transmissibility because specific capacity is often affected by partial penetration, well loss, and geohydrologic boundaries. In most cases these factors adversely affect specific capacity and the actual coefficient of transmissibility is greater than the coefficient of transmissibility computed from specific-capacity data. Because of the usefulness of rough estimates of  $T$ , an examination of the relation between the coefficient of transmissibility and specific capacity is useful.

The theoretical specific capacity of a well discharging at a constant rate in a homogeneous, isotropic, nonleaky artesian aquifer infinite in areal extent is from the modified nonleaky artesian formula given by the following equation:

$$Q/s = T/[264 \log (Tt/2693r_w^2S) - 65.5] \quad (33)$$

where:

- $Q/s$  = specific capacity, in gpm/ft
- $Q$  = discharge in gpm
- $s$  = drawdown, in ft
- $T$  = coefficient of transmissibility, in gpd/ft
- $S$  = coefficient of storage, fraction
- $r_w$  = nominal radius of well, in ft
- $t$  = time after pumping started, in min

The equation assumes that: 1) the well penetrates and is uncased through the total saturated thickness of the aquifer, 2) well loss is negligible, and 3) the effective radius of the well has not been affected by the drilling and development of the well and is equal to the nominal radius of the well.

The coefficient of storage of an aquifer can usually be estimated with well-log and water-level data. Because specific capacity varies with the logarithm of  $1/S$ , large errors in estimated coefficients of storage result in comparatively small errors in coefficients of transmissibility estimated with specific-capacity data.

The relationships between the specific capacity and the coefficient of transmissibility for artesian and water-table conditions are shown in figures 2 through 7. Pumping periods of 2 minutes, 10 minutes, 60 minutes, 8 hours, 24 hours, and 180 days; a radius of 6 inches; and storage coefficients of 0.0001 and 0.02 were assumed in constructing the graphs. These graphs may be used to obtain rough estimates of the coefficients of transmissibility from specific-capacity data. The coefficient of storage is estimated from well-log and water-level data, and a line based on the estimated  $S$  is drawn parallel to the lines on one of figures

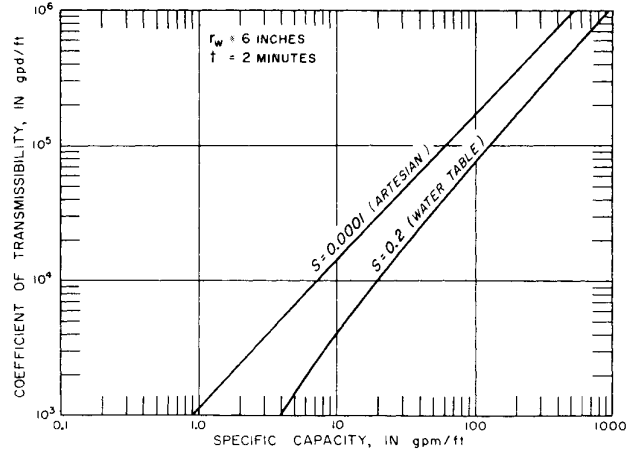


Figure 2. Graphs of specific capacity versus coefficient of transmissibility for a pumping period of 2 minutes

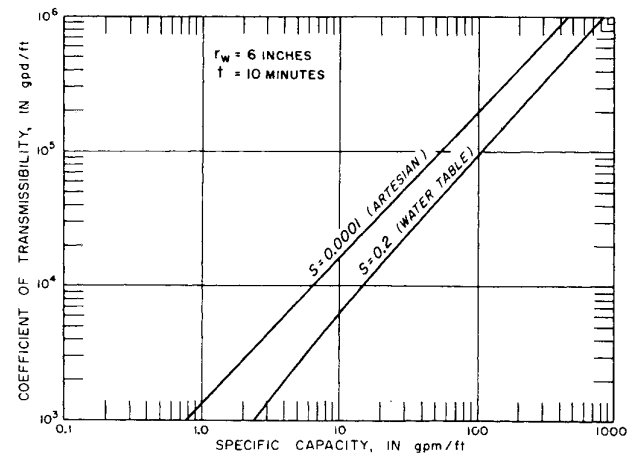


Figure 3. Graphs of specific capacity versus coefficient of transmissibility for a pumping period of 10 minutes

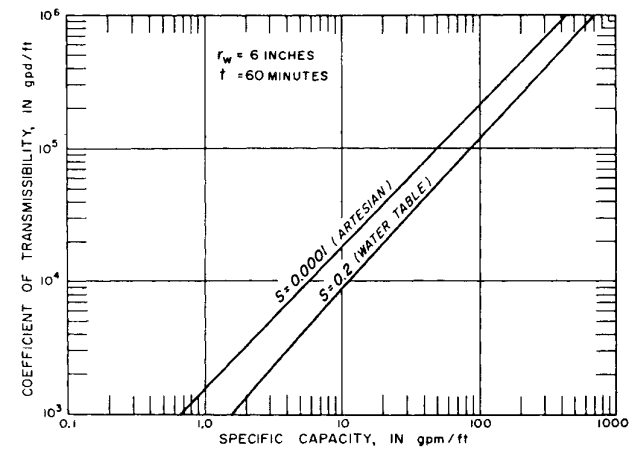


Figure 4. Graphs of specific capacity versus coefficient of transmissibility for a pumping period of 60 minutes

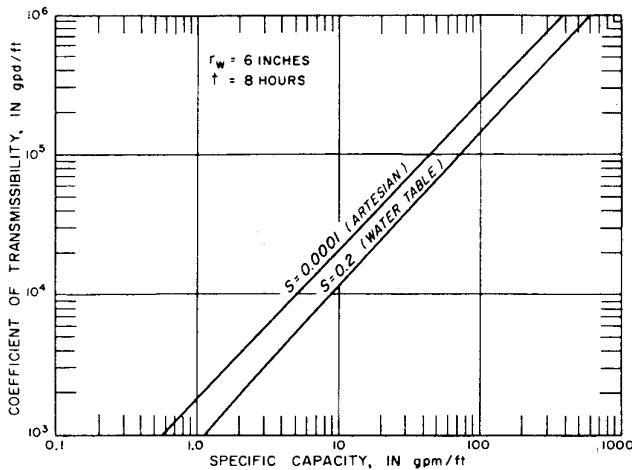


Figure 5. Graphs of specific capacity versus coefficient of transmissibility for a pumping period of 8 hours

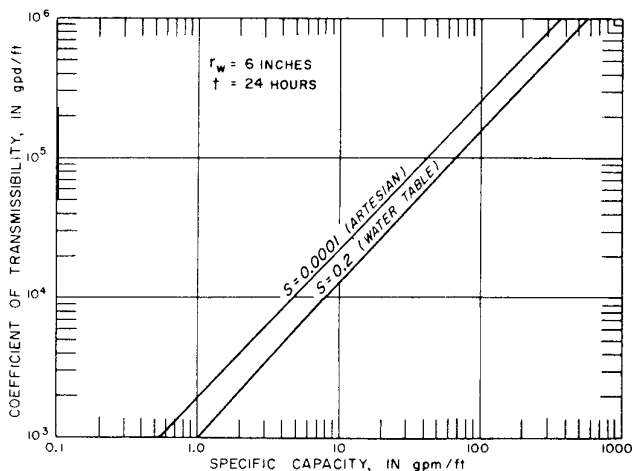


Figure 6. Graphs of specific capacity versus coefficient of transmissibility for a pumping period of 24 hours

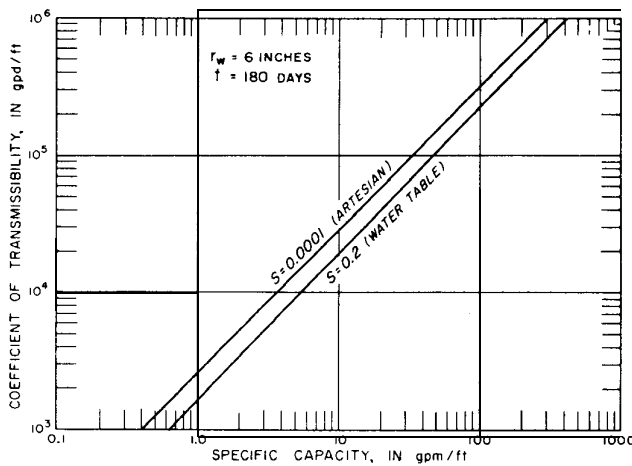


Figure 7. Graphs of specific capacity versus coefficient of transmissibility for a pumping period of 180 days

2 through 7, depending upon the pumping period. The coefficient of transmissibility is selected from the point of intersection of the  $S$  line and the known specific capacity.

As shown by equation 33, the specific capacity varies with the logarithm of  $1/r_w^2$ . Large increases in the radius of a well result in comparatively small changes in  $Q/s$ . The relationship between specific capacity and the radius of a well assuming  $T = 17,000$  gpd/ft,  $S = 0.0004$ , and  $t = 1$  day is shown in figure 8A. A 30-inch-diameter well has a specific capacity about 8 per cent more than that of a 16-inch-diameter well; a 16-inch-diameter well has a specific capacity about 3 per cent more than that of a 12-inch-diameter well.

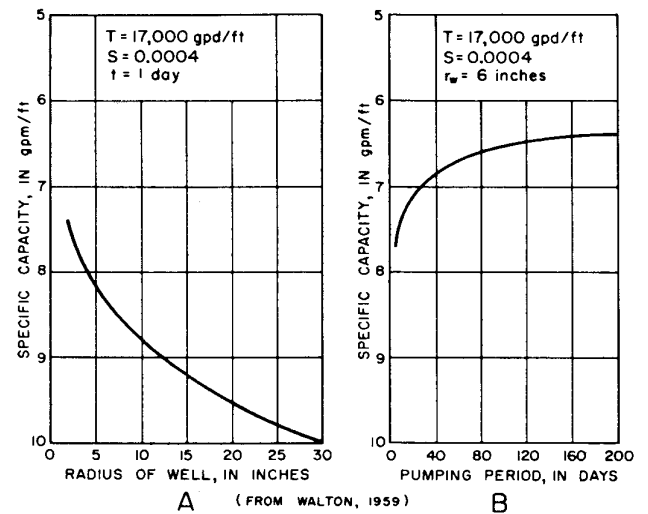


Figure 8. Graphs of specific capacity versus well radius (A) and pumping period (B)

Specific capacity decreases with the period of pumping as shown in figure 8B, because the drawdown continually increases with time as the cone of influence of the well expands. For this reason, it is important to state the duration of the pumping period for which a particular value of specific capacity is computed. The graph of specific capacity versus pumping period in figure 8B was constructed by assuming  $T = 17,000$  gpd/ft,  $S = 0.0004$ , and  $r_w = 6$  inches.

### Statistical Analysis

The methods of statistical analysis can be of great help in appraising the role of individual units of multiunit aquifers as contributors of water. The productivity of some bedrock aquifers, especially dolomite aquifers, is inconsistent and it is impossible to predict with a high degree of accuracy the specific capacity of a well before drilling at any location. However, the probable range of specific capacities of wells can often be estimated based on frequency graphs.

Suppose that specific-capacity data are available for wells penetrating one or several units of a multiunit aquifer and

it is required to estimate the range in productivity and relative consistency in productivity of the three units. Specific capacities are divided by the total depths of penetration to obtain specific capacities per foot of penetration. Wells are segregated into categories depending upon the units penetrated by wells. Specific capacities per foot of penetration for wells in each category are tabulated in order of magnitude, and frequencies are computed with the following equation derived by Kimball (1946):

$$F = [m_o / (n_w + 1)] 100 \quad (34)$$

where:

$m_o$  = the order number

$n_w$  = total number of wells

$F$  = percentage of wells whose specific capacities are equal to, or greater than, the specific capacity of order number  $m_o$

Values of specific capacity per foot of penetration are then plotted against the percentage of wells on logarithmic probability paper. Straight lines are fitted to the data.

If specific capacities per foot of penetration decrease as the depth of wells and number of units penetrated increase, the upper units are more productive than the lower units.

Unit-frequency graphs can be constructed from the category-frequency graphs by the process of subtraction, taking into consideration uneven distribution of wells in the categories. The slope of a unit-frequency graph varies with the inconsistency of production, a steeper line indicating a greater range in productivity.

### Flow-Net Analysis

Contour maps of the water table or piezometric surface together with flow lines are useful for determining the hydraulic properties of aquifers and confining beds and estimating the velocity of flow of ground water. Flow lines, paths followed by particles of water as they move through an aquifer in the direction of decreasing head, are drawn at right angles to piezometric surface or water-table contours. If the quantity of water percolating through a given cross section (flow channel) of an aquifer delimited by two flow lines and two piezometric surface or water-table contours is known, the coefficient of transmissibility can be estimated from the following modified form of the Darcy equation:

$$T = Q / IL \quad (35)$$

where:

$Q$  = discharge, in gpd

$T$  = coefficient of transmissibility, in gpd/ft

$I$  = hydraulic gradient, in feet per mile (ft/mi)

$L$  = average width of flow channel, in miles (mi)

$L$  is obtained from the piezometric surface or water-table map with a map measurer. The hydraulic gradient can be calculated by using the following formula (see Foley, Walton, and Drescher, 1953):

$$I = c / W_a \quad (36)$$

where:

$I$  = hydraulic gradient, in ft/mi

$c$  = contour interval of piezometric surface or water-table map, in ft

and

$$W_a = A' / L \quad (37)$$

in which  $A'$  is the area, in square miles, between two limiting flow lines and piezometric surface or water-table contours; and  $L$  is the average length, in miles, of the piezometric surface or water-table contours between the two limiting flow lines.

If the quantity of leakage through a confining bed into an aquifer, the thickness of the confining bed, area of confining bed through which leakage occurs, and the difference between the head in the aquifer and in the source bed above the confining bed are known, the coefficient of vertical permeability can be computed from the following modified form of the Darcy equation:

$$P' = Q_c m' / \Delta h A_c \quad (38)$$

where:

$P'$  = coefficient of vertical permeability of confining bed, in gpd/sq ft

$Q_c$  = leakage through confining bed, in gpd

$m'$  = thickness of confining bed through which leakage occurs, in ft

$A_c$  = area of confining bed through which leakage occurs, in sq ft

$\Delta h$  = difference between the head in the aquifer and in the source bed above the confining bed, in ft

The velocity of the flow of ground water can be calculated from the equation of continuity, as follows:

$$V = Q / 7.48 S_y A \quad (39)$$

where:

$V$  = velocity, in feet per day (fpd)

$Q$  = discharge, in gpd

$A$  = cross-sectional area of the aquifer, in sq ft

$S_y$  = specific yield of aquifer, fraction

The specific yield converts the total cross-sectional area of the aquifer to the effective area of the pore openings through which flow actually occurs.

The discharge  $Q$  can be calculated from Darcy's equation as the product of the coefficient of permeability, hydraulic gradient, and cross-sectional area of aquifer or:

$$Q = P I A \quad (40)$$

Substitution of equation 40 in equation 39 results in the expression (see Butler, 1957):

$$V = P I / 7.48 S_y \quad (41)$$

where:

$V$  = velocity of flow of ground water, in fpd

$P$  = coefficient of permeability, in gpd/sq ft

$I$  = hydraulic gradient, in ft/ft

$S_y$  = specific yield, fraction

The range in ground-water velocities is great. Under heavy pumping conditions, except in the immediate vicinity of a pumped well, velocities are generally less than 100 feet

per day. Under natural conditions, rates of more than a few feet per day or less than a few feet per year are exceptional (Meinzer, 1942).

### Geohydrologic Boundaries

The equations used to determine the hydraulic properties of aquifers and confining beds assume an aquifer infinite in areal extent. The existence of geohydrologic boundaries serves to limit the continuity of most aquifers in one or more directions to distances from a few hundred feet or less to a few miles or more. Geohydrologic boundaries may be divided into two types, barrier and recharge. Barrier boundaries are lines across which there is no flow and they may consist of folds, faults, or relatively impervious deposits (aquiclude) such as shale or clay. Recharge boundaries are lines along which there is no drawdown and they may consist of rivers, lakes, and other bodies of surface water hydraulically connected to aquifers. Barrier boundaries are treated mathematically as flow lines and recharge boundaries are considered as equipotential surfaces. The effect of a recharge boundary is to decrease the drawdown in a well; the effect of a barrier boundary is to increase the drawdown in a well. Geohydrologic boundaries distort cones of depression and affect the time-rate of drawdown.

Most geohydrologic boundaries are not clear-cut straight-line features but are irregular in shape and extent. However, because the areas of most aquifer test sites are relatively small compared to the areal extent of aquifers, it is generally permissible to treat geohydrologic boundaries as straight-line demarcations. Where this can be done, boundary problems can be solved by the substitution of a hypothetical hydraulic system that satisfies the geohydrologic boundary conditions,

### Image-Well Theory

The influence of geohydrologic boundaries on the response of an aquifer to pumping can be determined by means of the image-well theory described by Ferris (1959). The image-well theory as applied to ground-water hydrology may be stated as follows: the effect of a barrier boundary on the drawdown in a well, as a result of pumping from another well, is the same as though the aquifer were infinite and a like discharging well were located across the real boundary on a perpendicular thereto and at the same distance from the boundary as the real pumping well. For a recharge boundary the principle is the same except that the image well is assumed to be recharging the aquifer instead of pumping from it.

Thus, the effects of geohydrologic boundaries on the drawdown in a well can be simulated by use of hypothetical image wells. Geohydrologic boundaries are replaced for analytical purposes by imaginary wells which produce the same disturbing effects as the boundaries. Boundary problems are thereby simplified to consideration of an infinite

aquifer in which real and image wells operate simultaneously.

### Barrier Boundary

For a demonstration of the image-well theory, consider an aquifer bounded on one side by an impervious formation. The impervious formation cannot contribute water to the pumped well. Water cannot flow across a line that defines the effective limit of the aquifer. The problem is to create a hypothetical infinite hydraulic system that will satisfy the boundary conditions dictated by the finite aquifer system.

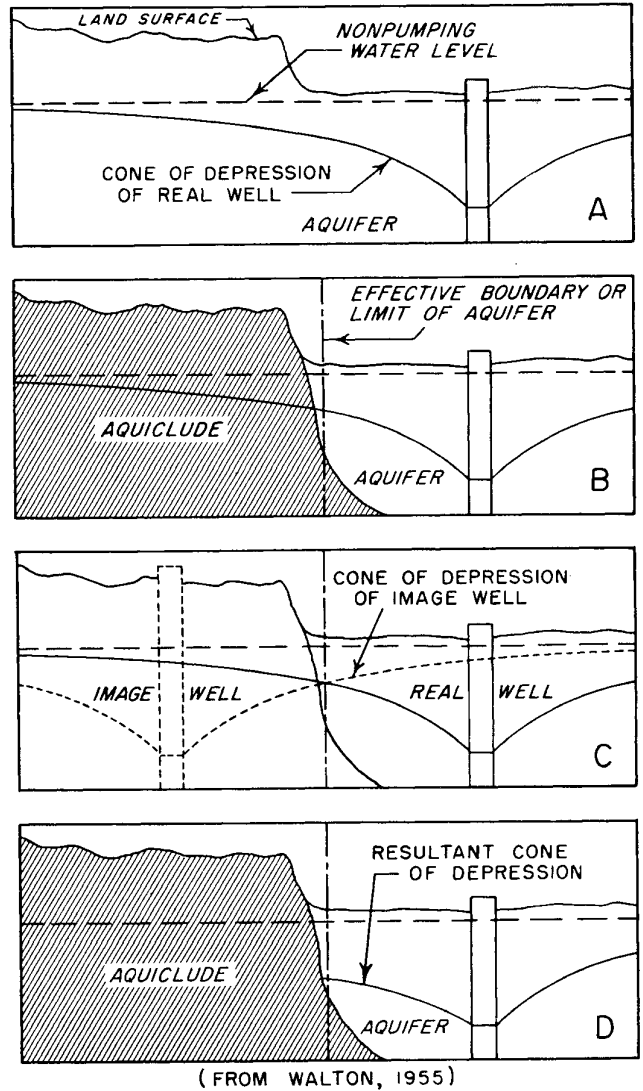


Figure 9. Diagrammatic representation of the image-well theory as applied to a barrier boundary

Consider the cone of depression that would exist if the geologic boundary was not present, as shown by diagram A in figure 9. If a boundary is placed across the cone of depression, as shown by diagram B, the hydraulic gradient cannot

remain as it was because it would cause flow across the boundary. An imaginary discharging well placed across the boundary perpendicular to and equidistant from the boundary would produce a hydraulic gradient from the boundary to the image well equal to the hydraulic gradient from the boundary to the pumped well. A ground-water divide would exist at the boundary as shown by diagram C, and this would be true everywhere along the boundary. The condition of no flow across the boundary line has been fulfilled. Therefore, the imaginary hydraulic system of a well and its image counterpart in an infinite aquifer satisfies the boundary conditions dictated by the field geology of this problem. The resultant real cone of depression is the summation of the components of both the real and image well depression cones as shown by diagram D in figure 9. The resultant profile of the cone of depression is flatter on the side of the real well toward the boundary and steeper on the opposite side away from the boundary than it would be if no boundary was present. A generalized plan view of the flow net in the vicinity of a discharging well near a barrier boundary is shown in figure 10.

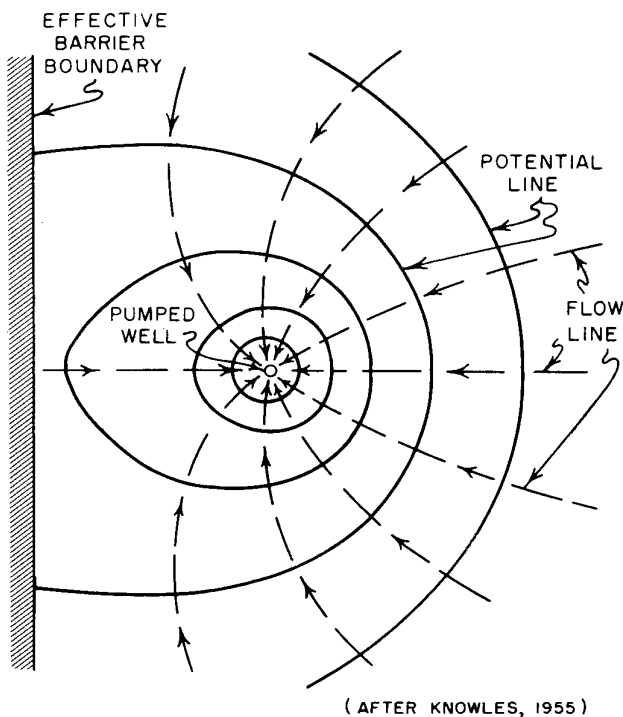


Figure 10. Generalized flow net showing flow lines and potential lines in the vicinity of a discharging well near a barrier boundary

Under barrier-boundary conditions, water levels in wells will decline at an initial rate under the influence of the pumped well only. When the cone of depression of the image well reaches the real well, the time-rate of drawdown will change. It will be increased in this instance because the total rate of withdrawal from the aquifer is now equal to that of the pumped well plus that of the discharging

image well. Thus, the drawdown curve of the real well is deflected downward.

If an aquifer test is conducted without prior knowledge of the existence of a barrier boundary, it may be possible to locate the boundary by determining the position of the discharging image well associated with the boundary (Ferris, 1948). The image well can be located by using data on the deflection of the time-drawdown curve under the influence of the discharging image well and the law of times.

### Law of Times

For a given aquifer the times of occurrence of equal drawdown vary directly as the squares of the distances from an observation well to pumping wells of equal discharge. This principle is analogous to the law of times defined by Ingersoll, Zobel, and Ingersoll (1948). The law of times is:

$$t_1/r_1^2 = t_2/r_2^2 \dots t_n/r_n^2$$

It follows that, if the time intercept of a given drawdown in an observation well caused by pumping a well at a given distance is known, and if the time intercept of an equal amount of divergence of the time-drawdown curve caused by the effect of the image well is also known, it is possible to determine the distance from the observation well to the image well using the following formula which expresses the law of times:

$$r_i = r_p \sqrt{t_i/t_p} \quad (42)$$

where:

- $r_i$  = distance from image well to observation well, in ft
- $r_p$  = distance from pumped well to observation well, in ft
- $t_p$  = time after pumping started, before the boundary becomes effective, for a particular drawdown to be observed, in min
- $t_i$  = time after pumping started, after the boundary becomes effective, when the divergence of the time-drawdown curve from the type curve, under the influence of the image well, is equal to the particular value of drawdown at  $t_p$ , in min

### Aquifer-Test Data

Values of drawdown  $s$  are plotted on logarithmic paper against values of time  $t$ . The proper type curve is matched to the early portion of the time-drawdown field data curve unaffected by the barrier boundary. Hydraulic properties are calculated using either the leaky artesian or nonleaky artesian formula.

The type curve is again matched to later time-drawdown data, this time over the portion affected by the barrier boundary. The divergence of the two type-curve traces at a convenient time  $t_i$  is determined. The time  $t_p$  at which the first type-curve trace intersects an  $s$  value equal to the divergence at  $t_i$  is also noted. The distance  $r_i$  can now be calculated with equation 42.

The correctness of the match position of the type curve over later time-drawdown data can be judged by noting the

$s$  and  $W(u)$  or  $W(u,r/B)$  match-point coordinates. For a particular value of  $W(u)$  or  $W(u,r/B)$ , the  $s$  match-point coordinate for later time-drawdown data should be twice the  $s$  match-point coordinate for early time-drawdown data. The value of  $T$  obtained from data of a match of the type curve over the later time-drawdown data will be half the value obtained from data of a match of the type curve over early time-drawdown data.

The effects of geohydrologic boundaries also can be analyzed with a time-departure curve. The type curve is matched to early time-drawdown data unaffected by the barrier boundary and the type-curve trace is extended just beyond later time-drawdown data. The type-curve trace beyond the early data indicates the trend the drawdowns would have taken if there was no barrier boundary present. The departure of the later time-drawdown data from this type-curve trace represents the effects of the image well associated with the barrier boundary. Values of departures at a number of times are noted and a time-departure curve is constructed on logarithmic paper. The proper type curve is matched to the time-departure curve, and match-point coordinates and values of  $T$  and  $S$  computed from early data are substituted into either the leaky artesian or non-leaky artesian formula to determine the distance from the observation well to the image well.

A minimum of three observation wells is required to determine the location and orientation of a barrier boundary. The distances to the image well associated with the barrier boundary from three observation wells are calculated and are scribed as arcs using the respective observation wells as centers. The intersection of these arcs locates the image well. The barrier boundary is oriented perpendicular to and crosses the midpoint of a line joining the pumped well and the image well.

The barrier boundaries determined from aquifer-test data represent the limits of a hypothetical aquifer system that is equivalent hydraulically to the real system. These effective barrier boundaries will not exactly coincide with nor completely describe actual barrier boundaries.

### Recharge Boundary

Recharge boundaries can also be analyzed by methods similar to those pertaining to a barrier-boundary problem. Consider an aquifer bounded on one side by a recharge boundary as shown in figure 11A. The cone of depression cannot spread beyond the stream. The condition is established that there shall be no drawdown along an effective line of recharge somewhere offshore. The imaginary hydraulic system of a well and its image counterpart in an infinite aquifer shown in figure 11B satisfies the foregoing boundary condition. An imaginary recharge well has been placed directly opposite and at the same distance from the stream as the real well. The recharge image well operates simultaneously and at the same rate as the real well. The resultant real cone of depression is the arithmetic sum-

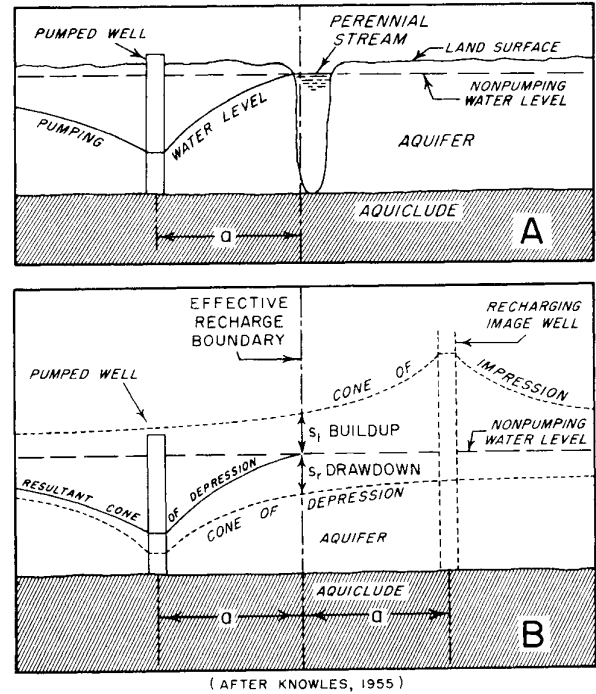


Figure 11. Diagrammatic representation of the image well theory as applied to a recharge boundary

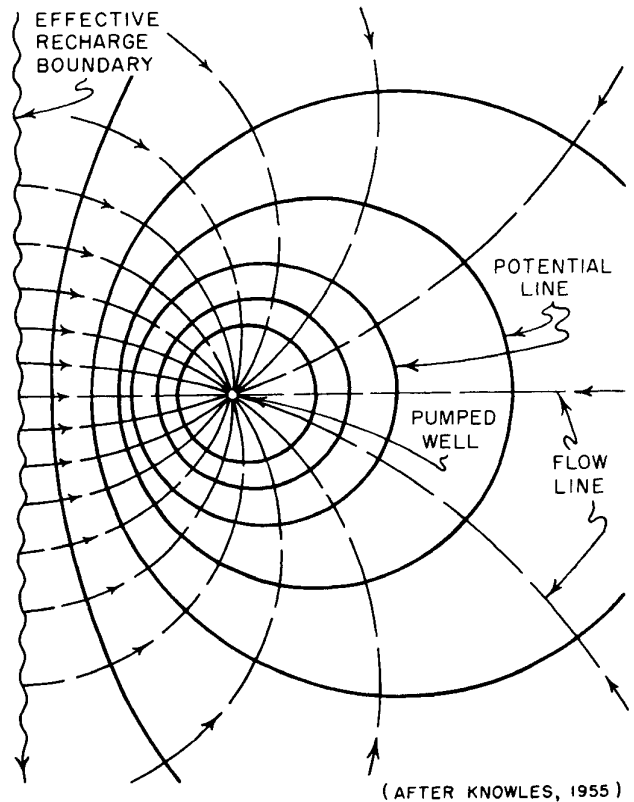


Figure 12. Generalized flow net showing flow lines and potential lines in the vicinity of a discharging well near a recharge boundary

tion of the components of the real well cone of depression and the image well cone of impression as shown in figure 11B. The resultant profile of the real cone of depression is steeper on the river side of the real well and flatter on the land side of the real well than it would be if no boundary was present. A generalized plan view of the flow net in the vicinity of a discharging well near a recharge boundary is shown in figure 12.

Under recharge-boundary conditions, water levels in wells will draw down at an initial rate under the influence of the pumped well only. When the cone of impression of the image well reaches the real well the time-rate of drawdown will change. The time-rate of drawdown will thereafter continually decrease and eventually equilibrium conditions will prevail, when recharge balances discharge. The image well associated with the recharge boundary can be located from data on the deflection of the time-drawdown curve under the influence of the recharging image well.

### Aquifer-Test Data

Values of  $s$  are plotted on logarithmic paper against values of  $t$ . The proper type curve is matched to the early portion of the time-drawdown field data curve which is unaffected by the recharge boundary. Hydraulic properties are calculated with either the leaky artesian or nonleaky artesian formula.

The type-curve trace is extended just beyond later time-drawdown data and the divergence of the type-curve trace and the latter part of the time-drawdown field data curve at a convenient time  $t_i$  is noted. The time  $t_p$  at which the type-curve trace intersects an  $s$  value equal to the divergence at  $t_i$  is also noted. The distance  $r_i$  is now computed with equation 42.

Sometimes the pumped and observation wells are so close to the recharge boundary that almost all time-drawdown data are influenced by recharge and it is impossible to isolate the effects of the image well. In these cases the time-drawdown graph cannot be used to locate the recharge boundary nor to compute hydraulic properties. Also, when the test site is very close to a recharge boundary, water levels stabilize rapidly and steady-state conditions prevail after a short pumping period.

It can be shown by the development of the nonleaky artesian formula that the drawdown at any point under steady-state conditions is described by the following equation (Rorabaugh, 1948):

$$s = 528Q \log (r_i/r_p) / T \quad (43)$$

where:

- $Q$  = discharge, in gpm
- $s$  = drawdown in observation well, in ft
- $r_i$  = distance from image well to observation point, in ft
- $r_p$  = distance from pumped well to observation point, in ft
- $T$  = coefficient of transmissibility, in gpd/ft

This equation was expressed in terms of the distance between the pumped well and the line of recharge by Rorabaugh (1948) as:

$$s = 528Q \log (\sqrt{4a^2 + r_p^2} - 4a r_p \cos \psi / r_p) / T \quad (44)$$

where:

- $a$  = distance from pumped well to recharge boundary, in ft
- $\psi$  = angle between a line connecting the pumped and image wells and a line connecting the pumped and observation wells

For the particular case where the observation well is on a line parallel to the recharge boundary the following equation (Rorabaugh, 1948) applies:

$$s = 528Q \log (\sqrt{4a^2 + r_p^2} / r_p) / T \quad (45)$$

For the particular case where the observation well is on a line perpendicular to the recharge boundary and on the river side, the following equation (Rorabaugh, 1948) applies:

$$s = 528Q \log [(2a - r_p) / r_p] / T \quad (46)$$

If the coefficient of transmissibility, the drawdown under equilibrium conditions, the pumping rate, and the distance from the observation well to the pumped well are known, the distance  $a$  may be computed by substituting data in one of equations 44 through 46. The distance-drawdown field data graph for observation wells parallel to the recharge boundary may often be used to determine the coefficient of transmissibility.

If the observation wells are not too distant from the pumped well, the observation wells will be approximately equidistant from the image well, and the gradient of the cone of depression parallel to the stream will not be distorted to any great degree. The effect of the recharge boundary on the drawdowns in the observation wells will be approximately equal for a given pumping period. Thus, the distance-drawdown field data graph for observation wells parallel to the recharge boundary reflects the actual gradient towards the pumped well and it can be used to determine the coefficient of transmissibility. Although the hydraulic gradient is nearly correct, the total values of drawdown in the observation wells are affected by the recharging image well. Because the drawdowns are affected by recharge, it follows that the storage coefficient cannot be computed from the distance-drawdown field data graph.

Values of drawdown in several observation wells parallel to the recharge boundary at the end of the test when water levels are stable and at unequal distances from the pumped well are plotted against the logarithms of  $r$  on semilogarithmic paper. This distance-drawdown field data graph will yield a straight-line graph. The slope of the straight line and the following equation are used to compute  $T$ :

$$T = 528Q / \Delta s \quad (47)$$

where:

- $T$  = coefficient of transmissibility, in gpd/ft
- $Q$  = discharge, in gpm
- $\Delta s$  = drawdown difference per log cycle, in ft

The computed value of  $T$  and other known data are substituted into one of equations 44 through 46, depending upon the position of the observation well, and the distance  $a$  is determined. The distance  $a$  can often be determined by a method outlined by Kazmann (1948).

After  $T$  and  $a$  are computed, the image well may be located and the coefficient of storage can often be estimated by the process of trial and error with the following equations:

$$s = s_p - s_i \quad (48)$$

$$s_p = 114.6QW(u_p)/T \quad (49)$$

$$s_i = 114.6QW(u_i)/T \quad (50)$$

$$u_p = 2693r_p^2S/Tt \quad (51)$$

$$u_i = 2693r_i^2S/Tt \quad (52)$$

where:

- $s$  = drawdown in observation well, in ft
- $s_p$  = drawdown due to pumped well, in ft
- $s_i$  = buildup due to image well, in ft
- $Q$  = discharge, in gpm
- $T$  = coefficient of transmissibility, in gpd/ft
- $S$  = coefficient of storage, fraction
- $r_p$  = distance from observation well to pumped well, in ft
- $r_i$  = distance from observation well to image well, in ft
- $t$  = time after pumping started, in min

Values of  $u_p$  and  $u_i$  are computed with equations 51 and 52 and corresponding values of  $W(u_p)$  and  $W(u_i)$  are obtained from appendix C.

Several values of  $S$  are assumed and values of  $s_p$  and  $s_i$  are computed. The  $S$  that results in values of  $s_p$  and  $s_i$  which satisfy equation 48 is selected as the coefficient of storage of the aquifer. There is the possibility that more than one value of  $S$  will satisfy equation 48. In this case the characteristics of the materials drained will dictate the correct  $S$ .

#### Percentage of Water Diverted From Source of Recharge

The percentage of pumped water being diverted from a source of recharge depends upon the hydraulic properties of the aquifer, the distance from the pumped well to the recharge boundary, and the pumping period. Theis (1941) derived the following equation for determining the percentage of the water pumped by a well that is obtained from a source of recharge:

$$P_r = 2/\pi \int_0^{\pi/2} e^{-f \sec^2 u} du \quad (53)$$

where:

- $u = \tan^{-1}(r/a)$
- $f = 2693a^2S/Tt$
- $P_r$  = percentage of pumped water being diverted from a source of recharge

$a$  = distance from pumped well to recharge boundary, in ft

$S$  = coefficient of storage, fraction

$T$  = coefficient of transmissibility, in gpd/ft

$t$  = time after pumping started, in min

$r_r$  = distance along recharge boundary measured from the perpendicular joining the real and image well, in ft

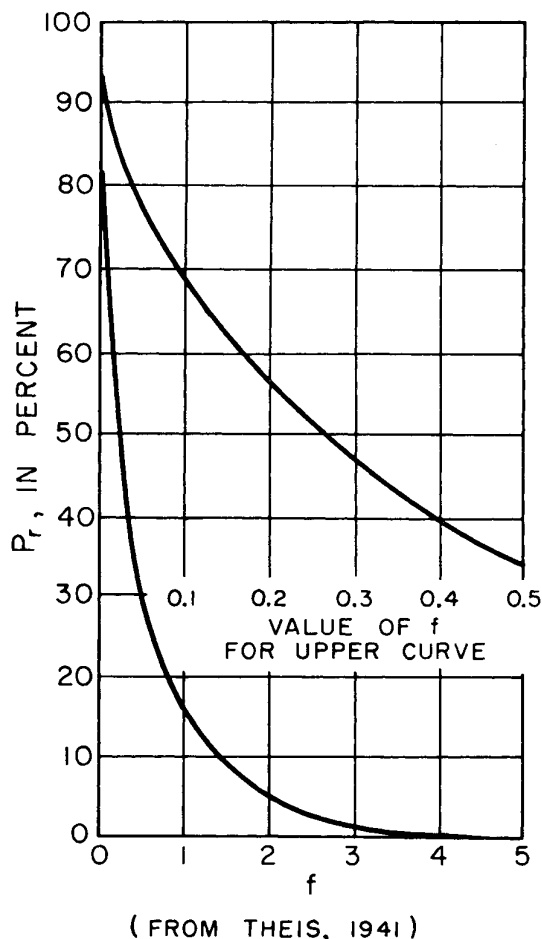


Figure 13. Graph for determination of percentage of pumped water being diverted from a source of recharge

Figure 13 gives values of  $P_r$  for various values of  $f$  and shows therefore the percentage of the pumped water diverted from a source of recharge. The quantity  $(100 - P_r)$  represents the percentage of the pumped water taken from storage within the aquifer.

#### Time Required to Reach Equilibrium

Considerable time elapses before a cone of depression stabilizes, water is no longer taken from storage within the aquifer, and a new state of approximate equilibrium is established. The time required to reach approximate equi-

brum may be computed with the following equation (see Foley, Walton, and Drescher, 1953):

$$t_e = a^2 S / [112 T \varepsilon \log (2ar)^2] \quad (54)$$

where:

- $t_e$  = time required to reach approximate equilibrium, in years
- $a$  = distance from pumped well to recharge boundary, in ft
- $r$  = distance from pumped well to observation point, in ft
- $S$  = coefficient of storage, fraction
- $T$  = coefficient of transmissibility, in gpd/ft
- $\varepsilon$  = deviation from absolute equilibrium (generally arbitrarily assumed to be 0.05)

### Multiple Boundary Systems

Aquifers are often delimited by two or more boundaries, and time-drawdown data deviate more than once under the influence of two or more image wells. Suppose that the cone of depression intercepts two barrier boundaries and that available drawdown data are affected by two discharging image wells. The proper type curve is matched to early time-drawdown data unaffected by the barrier boundary and  $T$  and  $S$  are computed. The type-curve trace is extended beyond early time-drawdown data. The type curve is then matched to later time-drawdown data affected by the closest barrier boundary. For a particular value of  $W(u)$  or  $W(u,r/B)$ , the  $s$  match-point coordinate for the second matched position of the type curve must be twice the  $s$  match-point coordinate for the first matched position of the type curve. The second type-curve trace is extended just beyond later time-drawdown data. The type curve is again matched to the time-drawdown data, this time over the late time-drawdown data affected by both barrier boundaries. For a particular value of  $W(u)$  or  $W(u,r/B)$  the  $s$  match-point coordinate for the third matched position of the type curve must be three times the  $s$  match-point coordinate for the first matched position of the type curve. The departure of type-curve traces 1 and 2,  $s_{i1}$ , at a convenient time  $t_{i1}$  is noted and the time  $t_{i2}$  at which the departure of type-curve traces 2 and 3 is a particular value,  $s_{i2}$ , is determined. The time  $t_{p1}$  at which the first type-curve trace intersects an  $s$  value equal to  $s_{i1}$  and the time  $t_{p2}$  at which the first type-curve trace intersects an  $s$  value equal to  $s_{i2}$  are also noted. Values of  $t_{i1}$ ,  $t_{i2}$ ,  $t_{p1}$ , and  $t_{p2}$  are substituted into the following equations for computation of the distances from the observation well to both image wells:

$$r_{i1} = r_p \sqrt{t_{i1}/t_{p1}} \quad (55)$$

$$r_{i2} = r_p \sqrt{t_{i2}/t_{p2}} \quad (56)$$

where:

- $r_{i1}$  = distance from observation well to closest image well, in ft
- $r_{i2}$  = distance from observation well to farthest image well, in ft
- $r_p$  = distance from observation well to pumped well, in ft

$t_{p1}$  or  $t_{p2}$  = time after pumping started for a particular value of  $s_{i1}$  or  $s_{i2}$  to be observed before either boundary becomes effective, in min

$t_{i1}$  = time after pumping started when the departure of type-curve traces 1 and 2 is equal to  $s_{i1}$ , in min

$t_{i2}$  = time after pumping started when the departure of type-curve traces 2 and 3 is equal to  $s_{i2}$ , in min

Multiple boundary conditions can also be analyzed with time-departure curves. Following procedures outlined earlier a time-departure curve is prepared by comparing the extension of the type-curve trace through early time-drawdown data and later time-drawdown data. Departures are plotted on logarithmic paper against values of time. The proper type curve is matched to time-departure curves and  $r_{i1}$  is determined with the nonleaky artesian or leaky artesian formula using values of  $T$  and  $S$  computed from early data unaffected by the boundaries. The latter part of the time-departure data will again deviate from the type-curve trace. As before, the departures are plotted on logarithmic paper against values of time to form a second time-departure curve. The proper type curve is matched to the second time-departure curve, and match-point coordinates and values of  $T$  and  $S$  computed from early data unaffected by the boundaries are substituted into the nonleaky artesian or leaky artesian formula for computation of  $r_{i2}$ . Any number of image wells can be located by repeating the processes outlined above.

### Primary and Secondary Image Wells

As stated earlier, aquifers are often delimited by two or more geohydrologic boundaries. Two converging boundaries delimit a wedge-shaped aquifer; two parallel boundaries form an infinite strip aquifer; two parallel boundaries intersected at right angles by a third boundary form a semi-infinite strip aquifer; and four boundaries intersecting at right angles form a rectangular aquifer. The image-well theory may be applied to such cases by taking into consideration successive reflections on the boundaries.

A number of image wells are associated with a pair of converging boundaries. A primary image well placed across each boundary will balance the effect of the pumped well at each boundary. However, each primary image well produces an unbalanced effect at the opposite boundary. Secondary image wells must be added at appropriate positions until the effects of the real and image wells are balanced at both boundaries.

Although image-well systems can be devised regardless of the wedge angle involved, simple solutions of closed image systems are preferred. The actual aquifer wedge angle  $\theta$  is approximated as equal to one of certain aliquot parts of  $360^\circ$ . These particular values of  $\theta$  were specified by Knowles (1955) as follows: "If the aquifer wedge boundaries are of like character,  $\theta$  must be an aliquot part of  $180^\circ$ . If the boundaries are not of like character,  $\theta$  must be an aliquot

part of 90°." Under the foregoing conditions and from the solution of the wedge problem as given by Carslaw and Jaeger (1959), it is evident that the exact number of image wells  $n_i$  depends upon the angle  $\theta$  included between the boundaries and is given by the expression,  $n_i = (360/\theta) - 1$ . The locus of image-well locations is a circle whose center is at the apex of the wedge and whose radius is equal to the distance from the pumped well to the wedge apex.

If the aquifer wedge boundaries are not of like character the character of each image well, recharge or discharge, can be ascertained by balancing the image-well system, considering each boundary separately (see Walton, 1953). A primary image well placed across a barrier boundary is discharging in character, and a primary image well placed across a recharge boundary is recharging in character. A secondary image well placed across a barrier boundary has the same character as its parent image well, and a secondary image well placed across a recharge boundary has the opposite character of its parent image well. Image-well systems for several wedge shaped aquifers are shown in figure 14.

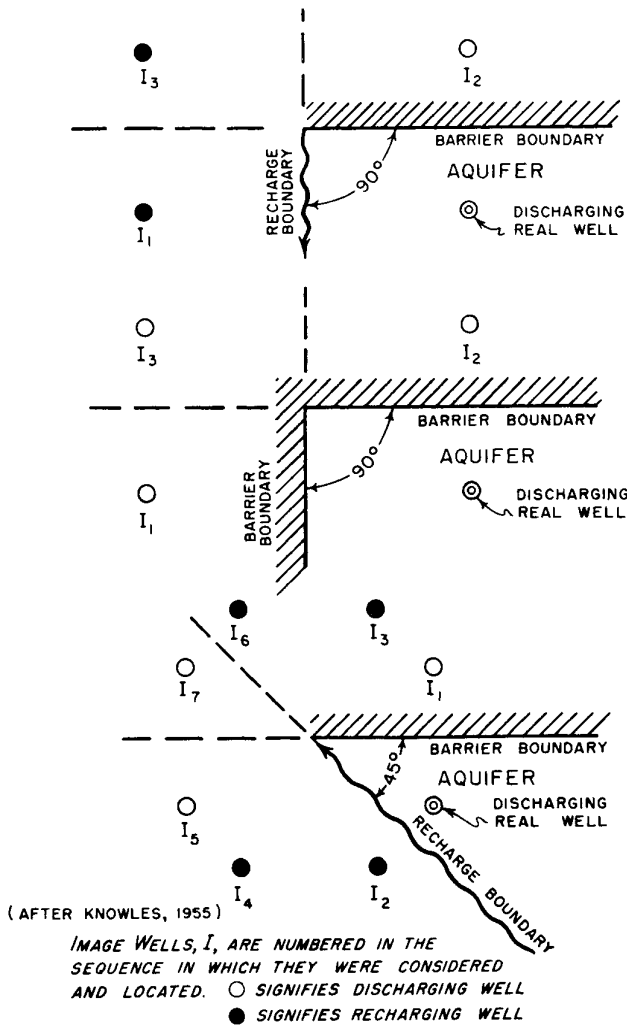


Figure 14. Plans of image-well systems for several wedge shaped aquifers

If the arrangement of two boundaries is such that they are parallel to each other, analysis by the image-well theory requires the use of an image-well system extending to infinity (Knowles, 1955). Each successively added secondary image well produces a residual effect at the opposite boundary. However, in practice it is only necessary to add pairs of image wells until the next pair has negligible influence on the sum of all image-well effects out to the point. Image-well systems for several parallel boundary situations are shown in figures 15 and 16.

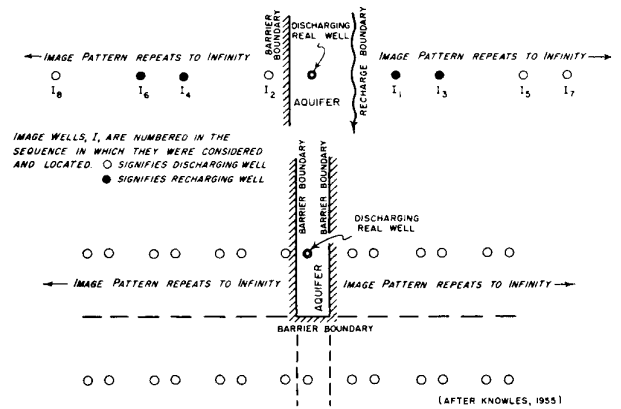


Figure 15. Plans of image-well systems for selected parallel boundary situations

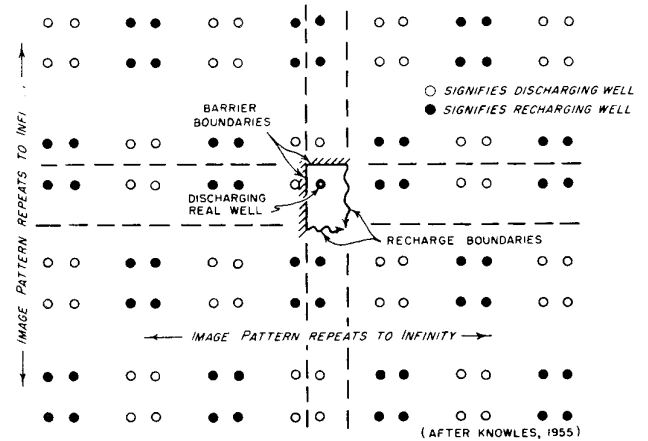


Figure 16. Plan of image-well system for a rectangular aquifer

## Recharge

The amount of recharge to an aquifer can often be estimated by flow-net analysis. Ground-water and hydrologic budgets also may be used to determine the annual rate of recharge to the ground-water reservoir.

## Flow-Net Analysis

Areas of influence of pumping are outlined on water-table or piezometric surface maps. A pumpage inventory is

made and hydrographs of wells are studied to determine the relation between water levels and pumpage. If water-level decline is directly proportional to the pumping rate and water levels stabilize after each increase in pumpage, recharge balances discharge. Under these conditions, recharge can be estimated with the following equation:

$$R = Q/A_e \quad (57)$$

where:

- $R$  = rate of recharge, in gpd/sq mi
- $Q$  = total pumpage within area of influence, in gpd
- $A_e$  = area of influence, in sq mi

If the vertical permeability of a confining bed is known, recharge by the vertical leakage of water through the confining bed can be estimated with the following form of Darcy's law:

$$Q_c = (P'/m') \Delta h A_c \quad (58)$$

where:

- $Q_c$  = leakage through confining bed, in gpd
- $P'$  = coefficient of vertical permeability of confining bed, in gpd/sq ft
- $m'$  = thickness of confining bed through which leakage occurs, in ft
- $A_c$  = area of confining bed through which leakage occurs, in sq ft
- $\Delta h$  = difference between the head in the aquifer and in the source bed above the confining bed, in ft

Recharge can also be estimated by studying the difference in quantity of water crossing successive water-table or piezometric surface contours between two limiting flow lines with the following equation:

$$R = [(Q_2 - Q_1) \pm \Delta h_i S A_i (2.1 \times 10^8)] / A_i \quad (59)$$

where:

- $R$  = rate of recharge, in gpd/sq mi
- $Q_2 - Q_1$  = difference in quantity of water crossing successive contour lines between limiting flow lines, in gpd
- $\Delta h_i$  = average rate of water-level decline or rise in area between limiting flow lines and successive contours, in fpd
- $A_i$  = area between limiting flow lines and successive contours, in sq mi
- $S$  = coefficient of storage, fraction

The + sign in equation 59 is used when there is a water-level rise and the — sign is used when there is a water-level decline.

$Q_1$  and  $Q_2$  are computed with the following form of Darcy's equation:

$$Q = TIL \quad (60)$$

where:

- $Q$  = quantity of water percolating through a given flow cross section, in gpd
- $T$  = coefficient of transmissibility, in gpd/ft
- $I$  = hydraulic gradient at flow cross section, in ft/mi
- $L$  = length of flow cross section, in mi

## Ground-Water and Hydrologic Budgets

The ground-water budget is a quantitative statement of the balance between water gains and losses of the ground-water reservoir, and a hydrologic budget is a quantitative statement of the balance between the total water gains and losses of a basin for a period of time. The budgets consider all waters, surface and subsurface, entering and leaving or stored within a basin. Water entering a basin is equated to water leaving a basin, plus or minus changes in basin storage.

In many parts of Illinois, the surface topographic boundaries of small drainage basins are reasonably congruous with ground-water divides, and there is no subsurface flow into or out of the basins except in the vicinity of stream-gaging stations. Water stored on the surface of many basins in ponds is very small, and discharge from wells is mostly for domestic and livestock use and is not significant.

Under these conditions, the ground-water and hydrologic budget may be stated as the following equations (Schicht and Walton, 1961):

$$P_g = R_g + ET_g + U \pm \Delta S_g \quad (61)$$

$$P = R_i + ET + U \pm \Delta S_s \pm \Delta S_g \quad (62)$$

where:

- $P$  = precipitation
- $R_i$  = streamflow
- $ET$  = evapotranspiration
- $U$  = subsurface underflow
- $\Delta S_s$  = change in soil moisture
- $\Delta S_g$  = change in ground-water storage
- $P_g$  = ground-water recharge
- $R_g$  = ground-water runoff
- $ET_g$  = ground-water evapotranspiration

Streamflow consists of surface runoff  $R_s$  and ground-water runoff  $R_g$ . Surface runoff is precipitation that finds its way into the stream channel without infiltrating into the soil. Ground-water runoff is precipitation that infiltrates into the soil or to the water table and then percolates into the stream channel. Surface runoff reaches streams rapidly and is discharged from basins within a few days. Ground water percolates slowly towards and reaches streams gradually. A few days after precipitation ceases, there is no surface runoff and streamflow is derived entirely from ground-water runoff. The time after the peak of the streamflow hydrograph at which surface runoff terminates is given approximately by the following equation (Linsley, Kohler, and Paulhus, 1958):

$$N = A_b^{0.2} \quad (63)$$

where:

- $A_b$  = drainage area of basin, in sq mi
- $N$  = time after the peak of the streamflow hydrograph when surface runoff ceases, in days

Principles for separating the streamflow hydrograph into its two components, surface and ground-water runoff, are not well developed. Ground-water runoff (base flow) several days after precipitation ceases is readily determined;

however, ground-water runoff under flood hydrographs is the subject of much discussion. Some simple base flow separation procedures are given by Linsley, Kohler, and Paulhus (1958).

Ground-water runoff into the stream channel ceases temporarily during periods of flood; however, ground water continues to percolate towards the stream from uplands creating ground-water storage in the lowlands adjacent to the stream channel. During periods when the stream stage rises above the water table some streamflow percolates into the ground creating bank storage. As soon as the stream stage starts to fall, ground-water runoff is considerably increased not only because of the accumulated bank storage but also because of the accumulated ground-water storage in the lowlands. When bank and ground-water storage is drained out, ground-water runoff will generally be greater than before precipitation occurred because, except during some periods in the summer and winter, precipitation infiltrating into the ground-water reservoir causes the water table to rise and the hydraulic gradient towards the stream to increase.

Ground-water runoff depends in part upon the position of the water table because associated with a particular mean ground-water stage there is a related hydraulic gradient and a consequent discharge of ground water into a stream (Schicht and Walton, 1961). The relationship between mean ground-water stage and ground-water runoff can be determined by plotting mean ground-water stages against streamflow on corresponding dates when streamflow consists entirely of ground-water runoff. Periods are selected assuming that surface runoff is complete within  $N$  days (see equation 63) after rainfall and that in the following protracted period of fair weather streamflow is all ground-water runoff.

In summer months evapotranspiration is very effective in reducing ground-water runoff. In Illinois, with the same ground-water stage, ground-water runoff is much less in August than in February. Separate rating curves of mean ground-water stage versus ground-water runoff must be prepared for dates April through October, when ground-water evapotranspiration is great, and for dates November through March, when ground-water evapotranspiration is very small.

Water is discharged from basins into the atmosphere through evapotranspiration, a term combining evaporation from land and water surfaces and transpiration from plants. Evapotranspiration may be subdivided into two parts according to the source of the water discharged into the atmosphere as follows: 1) surface evaporation and soil evapotranspiration  $ET_s$ , and 2) ground-water evapotranspiration  $ET_g$ . The part of evapotranspiration derived from the water table is ground-water evapotranspiration.

Ground water continuously percolates towards streams; however, the roots of plants and soil capillaries intercept and discharge into the atmosphere some of the water which otherwise would become ground-water runoff. Ground-

water evapotranspiration can be estimated from rating curves of mean ground-water stage versus ground-water runoff (Schicht and Walton, 1961). Ground-water runoff corresponding to a ground-water stage is read from rating curves prepared for dates April through October and for dates November through March. The difference in ground-water runoff between the two curves is the approximate ground-water evapotranspiration.

Subsurface underflow from basins can be estimated with a form of Darcy's law (equation 60) if the coefficient of transmissibility of the deposits and the hydraulic gradient of the water table are known.

The change in mean ground-water stage during an inventory period  $\Delta H$  multiplied by the gravity yield  $Y_g$  of the deposits within the zone of ground-water fluctuation is equal to the change in ground-water storage  $S_g$ . Stated as an equation:

$$\Delta S_g = \Delta H Y_g \quad (64)$$

Gravity yield may be defined (Rasmussen and Andreasen, 1959) as the ratio of the volume of water that deposits will yield by gravity drainage to the total volume of deposits drained during a given period of ground-water decline. The gravity yield of deposits is not immediate and as a result the gravity yield is not constant but increases at a diminishing rate with the time of drainage, gradually approaching the specific yield. The relationship between gravity yield and time of drainage becomes evident when values of  $Y_g$  are plotted against the average duration of ground-water decline preceding inventory periods (Schicht and Walton, 1961).

The hydrologic budget contains two factors, evapotranspiration and change in soil moisture, which are not always measured in the field. However, during the period of winter and early spring months (December through March) evapotranspiration and soil-moisture change are very small. Soil-moisture change can be eliminated and evapotranspiration can be estimated to average 0.3 inch per month in Illinois without introducing serious error in the hydrologic budget. Equation 62 may be rewritten for inventory periods during winter and early spring months when the water table is rising, as follows (Schicht and Walton, 1961):

$$Y_g = (P - R_i - ET - U) / \Delta H \quad (65)$$

The relationship between gravity yield and the time of drainage of deposits can be estimated with equation 65 and data for several inventory periods during winter and early spring months.

Ground-water runoff and evapotranspiration are determined from rating curves of mean ground-water stage versus runoff described earlier. Subsurface underflow is computed with equation 60. Changes in ground-water storage are estimated by substituting appropriate values of gravity yield based on the average period of ground-water decline preceding the inventory period in equation 64. Knowing ground-water runoff, evapotranspiration, underflow, and change in storage, ground-water recharge can then be determined by balancing equation 61.

## Part 2. Analysis of Yields of Wells and Aquifers

*This section describes methods used to evaluate practical sustained yields of wells and aquifers using the results of analyses presented in Part 1. Analysis of step-draw-down data and mechanical analysis of aquifers to determine the optimum well yields, spacing, and construction features are discussed.*

### Model Aquifers and Mathematical Models

Geohydrologic settings in many areas have heretofore been considered too complex to permit quantitative description with analytical expressions. In some cases, restrictions associated with complicated mathematics might be eliminated by devising approximate methods of analysis based on idealized mathematical models of aquifer situations (Walton and Neill, 1960). Appropriate assumptions often lead to a simplification of aquifer conditions to the point where mathematical solutions become practical.

Cursory consideration may suggest that simplified assumptions are so idealistic as to preclude a reasonably accurate solution. However, with sound professional judgment geohydrologic conditions can often be highly idealized with little sacrifice in accuracy of analysis. In addition, the adequacy and accuracy of basic data are seldom sufficient to warrant a rigorous theoretical and precise evaluation of the practical sustained yield of wells and aquifers. In most cases, the complexity of geologic conditions dictates that quantitative appraisals derived from any method of analysis can at best be considered only approximations.

In applying analytical methods to well and aquifer evaluation problems, the geohydrologic boundaries of the aquifer evident from areal studies must be idealized to fit comparatively elementary geometric forms such as wedges and infinite, or semi-infinite, rectilinear strips. Boundaries are assumed to be straight-line demarcations and are given mathematical expression by means of the image-well theory. The hydraulic properties of the aquifer and confining bed (if present) and recharge are considered mathematically by using appropriate ground-water formulas.

Actual ground-water conditions are simulated with model aquifers (Walton and Walker, 1961) which have straight-line boundaries, and an effective width, length, and thickness. The aquifer is sometimes overlain by a confining bed which has an effective thickness.

Mathematical models are based on the hydraulic properties of model aquifers, the image-well theory, and ground-water formulas. Problems associated with geohydrologic boundaries are simplified to consideration of an infinite aquifer in which real and image wells operate simultaneously. The effects of real and image wells are computed

with appropriate ground-water formulas. The gross hydraulic properties of the aquifer and confining bed (if present) are considered in evaluating the effects of boundaries; detailed hydraulic property variations are considered in estimating interference between wells and drawdowns in production wells.

Most geohydrologic boundaries are not clear-cut straight-line features but are irregular in shape and extent. However, it is generally permissible to treat boundaries as straight-line demarcations because irregularities are often small when compared with the areal extent of most aquifers. It should be recognized that idealized mathematical models describe the drawdown least accurately in the immediate vicinity of boundaries. The greater the distance to the boundary from the observation point, the smaller will be the error involved by the approximation.

Ideal boundary conditions and water-bearing characteristics are rarely if ever found in nature. Most aquifers are heterogeneous and anisotropic. The coefficient of transmissibility of deposits often changes markedly in short distances and stratification of deposits results in large differences between permeabilities measured parallel and across bedding. These recognized departures from ideal conditions do not necessarily dictate that mathematical models be rarely used. Such departures emphasize the need for sound professional judgment in designing mathematical models to fit actual conditions and in properly qualifying results according to the extent of departures.

It is recognized that analytical analysis provides only approximate answers, often on a bulk basis. Quantitative appraisal of geohydrologic systems having highly complex geometry and great variations in hydraulic properties may require the use of an electrical analog model (Stallman, 1960). Results obtained from analytical methods and analog models need to be compared to determine the limitations of analytical methods.

### Records of Past Pumpage and Water Levels

Records of past pumpage and water levels may be used to establish whether or not assumed mathematical models satisfy the geohydrologic limits of the aquifer. The water-level decline at several points is computed as a test, using

the hydraulic properties of the aquifer and confining bed (if present) and estimated past pumpage data, and taking into account known geohydrologic boundaries.

Production wells are grouped into centers of pumping and discharge from each pumping center is broken into step increments. Centers of pumping and geohydrologic boundaries are drawn to scale on a map and the image wells associated with the boundaries are located. The distances from observation points to the pumping centers and to the image wells are scaled from the map. The water-level decline at observation points resulting from each increment of pumpage at each pumping center is determined, using appropriate ground-water formulas to compute the effects of the real and image wells.

Sometimes the exact location of geohydrologic boundaries is unknown and the initial assumed conditions may prove to be in error in light of a comparison between computed and actual decline. In this event the mathematical model is modified and computations repeated until assumed conditions result in correct computed declines. A rule to be observed in the construction of mathematical models is that the assumed model be in accord with the geohydrology of the real aquifer and that the assumed model aquifer be geometrically similar to the physical flow system. If computed and actual decline agree, the mathematical model may be used to predict with reasonable accuracy the effects of future ground-water development and the practical sustained yield of an aquifer.

### Computation by Electronic Digital Computer

The time-consuming computations associated with mathematical models can in most instances be reduced to simple standardized procedures which can be inexpensively handled by means of digital computing machines (Walton and Neill, 1960).

A complete set of instructions for the University of Illinois electronic digital computer (Illiacc) has been devised for the solution of the nonleaky artesian formula which may be written as:

$$s = (114.6Q/T) \int_u^\infty e^{-u}/u \, du = (114.6Q/T) W(u)$$

where:

$$W(u) = (-\delta - \ln u) + [u - (u^2/2.2!)] + [(u^3/3.3!) - (u^4/4.4!)] \dots$$

$$u = 2693r^2S/Tt$$

$$\delta = 0.5772$$

$s$  = the drawdown or buildup at the observation point, in ft

$Q$  = the discharge or recharge rate of the real or image well, in gpm

$r$  = the distance from the real or image well to the observation point, in ft

$t$  = the time after pumping or recharging started, in min

$T$  = the coefficient of transmissibility, in gpd/ft

$S$  = the coefficient of storage, fraction

Data enter the Illiac in the form of a pattern of holes punched in paper tape. Arrangement of data on the input paper tape is important to repeated automatic solution of the nonleaky artesian formula. Many of the same data items may be used repeatedly in various combinations; consequently, the data input format and the instructions to the Illiac were designed to minimize repetitious labor in data tape preparation. An illustrative order of items on the data tape is shown in figure 17. The  $T$  and  $S$  portion is located at the leading end of the data tape since only one set of these values is required for a single mathematical model. Either all or portions of the remainder of the format may be repeated many times.

Number of values in T-table

$$T_1, T_2, T_3, \dots, T_n \quad 1 \leq n \leq 24$$

-T Last entry in table is a negative number

S = Coefficient of storage

Number of values in r-table

$$r_1, r_2, r_3, \dots, r_n \quad 1 \leq n \leq 325$$

$$(Q,t)_{11}, (Q,t)_{12}, \dots, (Q,t)_{1m_1} \quad 1 \leq m_1 \leq 46$$

-Q This entry in table must be a negative number

$$ID_{111}, ID_{112}, \dots, ID_{11k} \quad k = m_1$$

-ID This entry in ID set must be a negative number

+ID When this entry is positive, a new ID-table follows

$$ID_{211}, ID_{212}, \dots, ID_{21k}$$

-ID

-ID When this entry is negative, new Q,t and new ID follow

$$(Q,t)_{21}, (Q,t)_{22}, \dots, (Q,t)_{2m_2} \quad 1 \leq m_2 \leq 46$$

-Q

$$ID_{321}, ID_{322}, \dots, ID_{32k} \quad k = m_2$$

-ID

+ID When this entry is positive, a new ID-table follows

$$ID_{421}, ID_{422}, \dots, ID_{42k}$$

$$ID_{ij} 1 \dots ID_{ijk} \quad \begin{matrix} i = n \\ j = \text{no. of Q,t-tables} \end{matrix}$$

-ID

+ID When this entry is +, the format can be repeated in a similar manner beginning with the r-table. Computer stops when this entry is negative.

(FROM WALTON & NEILL, 1960)

Figure 17. Illustrative data input format for digital computer analysis of a mathematical model

Details of machine programming are beyond the scope of this report. An outline or a flow diagram, figure 18, and the data input format, figure 17, will be used as a basis for a brief discussion of steps in the solution of a mathematical

model. Each block in figure 18 may represent either an individual instruction to the computer or many individual instructions.

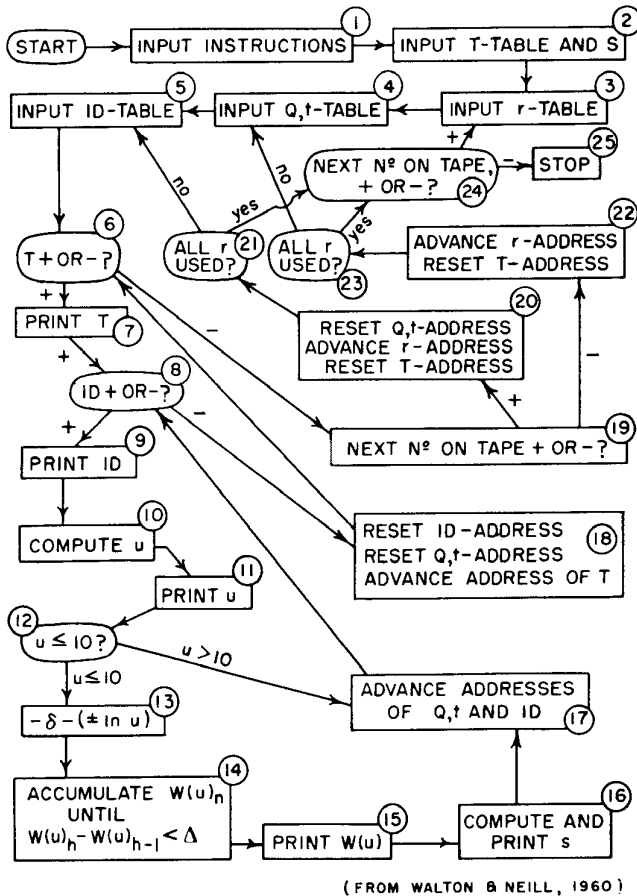


Figure 18. Abbreviated flow diagram for digital computer analysis of a mathematical model

The first step after starting the Illiac, block 1 of figure 18, involves arrangement of the complete program of instructions in designated locations in the memory. Block 2 inserts values of  $T$  and  $S$  as input data and blocks 3 and 4 insert values of  $r$  and tables of  $Q$  and  $t$ , respectively. Instruction blocks 3 and 4 are used several times during an analysis, with block 4 functioning more frequently than block 3.

Increments of drawdown and buildup for given values of  $Q$  and  $t$  and particular real and image wells are given identification numbers (ID numbers). Instructions given in blocks 5, 9, 17, and 18 insure proper identification of the many drawdowns and buildups. Block 5 functions more times than the other input blocks in providing sets of identification numbers for use during analysis. The printing of  $T$ , block 7, also provides identification and segregates groups of values in the output format.

The first five blocks of figure 18 provide the Illiac with a complete program of instructions and one set of data with identification numbers, which are required before the

machine can proceed to obey arithmetic-type instructions. During the computational phase, the programmer must arrange for arithmetic instructions to function in harmony with instructions involving movement of data in the computer, subsequent insertion of other sets of data from the input tape, and the output of results. The algebraic sign of a number is frequently used as a basis for synchronizing the operation of the different types of instructions. For example, quantities conveniently referred to as  $-T$ ,  $-Q$ , and  $ID$  are punched at the end of their respective tables (see figure 17) to enable the Illiac to make pertinent decisions in flow diagram blocks 6, 8, 19, and 24. An alternate cycle from block 12, when  $u$  is greater than 10, was also arranged because drawdowns associated with these values of  $u$  are too small to be of practical significance. The alternative saves computer time and omits several insignificant entries in the output record.

A table of values for  $W(u)$  and  $u$  has been published and could be stored in the Illiac. However, a table would use valuable memory space and it is quicker and easier for the Illiac to compute the required values of  $W(u)$  when needed than to locate them in a table stored in the computer memory. Instructions represented by block 14 are concerned with the solution of the exponential integral  $W(u)$  that is handled as a convergent series by accumulating pairs of terms enclosed by parentheses in the nonleaky artesian formula. The summation process continues until the increment becomes less than a preassigned value  $\Delta$ . Subsequently, the value of  $W(u)$  is printed and the computation for drawdown is completed in blocks 15 and 16, respectively.

At this point in the instruction program, the Illiac has completed a cycle for one drawdown or buildup. The machine will continue to operate as shown diagrammatically in figure 18 until all sets of input data have been read from the tape and used in computations.

A teletypewriter reads the output tape and prints values of  $T$ , identification numbers, values of  $u$  and  $W(u)$ , and drawdown or buildup. Data in the output format and a few computations made by conventional methods are used to spot check the performance of the Illiac.

## Well Characteristics

The drawdown  $s$  in a production well has all or some of the following components, depending upon geohydrologic and well conditions: the drawdown  $s_a$  (aquifer loss) due to laminar flow of water through the aquifer towards the well; plus the drawdown  $s_w$  (well loss) due to the turbulent flow of water through the screen or well face and inside the casing to the pump intake; plus the drawdown  $s_p$  due to the partial penetration of the pumped well; plus the drawdown  $s_d$  due to dewatering a portion of an aquifer; plus the drawdown  $s_b$  due to barrier boundaries of the aquifer; minus the buildup  $s_r$  due to recharge boundaries of the aquifer. Stated as an equation:

$$s = s_a + s_w + s_p + s_d + s_b - s_r \quad (66)$$

## Well Loss

The components of drawdown and buildup, except well loss and partial penetration loss, can be computed with the nonleaky artesian or leaky artesian formula. Well loss may be represented approximately by the following equation (Jacob, 1946b):

$$s_w = C Q^2 \quad (67)$$

where:

$s_w$  = well loss, in ft

$C$  = well-loss constant, in  $\text{sec}^2/\text{ft}^5$

$Q$  = discharge, in cubic feet per second (cfs)

Rorabaugh (1953) derived a similar equation and presents a more exact method for evaluation of well loss when a large range of pumping rates is encountered. In practice, however, equation 67 has been found to be adequate in most cases.

The value of  $C$  in equation 67 may be computed from the data collected during a "step-drawdown" test, in which the well is operated during successive periods at constant fractions of full capacity, by using the following equation (Jacob, 1946b):

$$C = \frac{(\Delta s^i / \Delta Q_i) - (\Delta s^{i-1} / \Delta Q_{i-1})}{\Delta Q_{i-1} + \Delta Q_i} \quad (68)$$

The  $\Delta s$  terms in equation 68 represent increments of drawdown produced by each increase ( $\Delta Q$ ) in the rate of pumping. The dimensions of  $\Delta s$  and  $\Delta Q$  are feet and cubic feet per second, respectively. Increments of drawdown are determined by taking in each case the difference between the observed water level and the extension of the preceding water-level curve. Steps of any length of time may be used providing the  $\Delta s$  values chosen are for the same length of time in each step. For steps 1 and 2 equation 68 may be rewritten as:

$$C = \frac{(\Delta s_2 / \Delta Q_2) - (\Delta s_1 / \Delta Q_1)}{\Delta Q_1 + \Delta Q_2} \quad (69)$$

For steps 2 and 3, equation 68 may be written as:

$$C = \frac{(\Delta s_3 / \Delta Q_3) - (\Delta s_2 / \Delta Q_2)}{\Delta Q_2 + \Delta Q_3} \quad (70)$$

Equation 68 assumes that the well is stable and that  $C$  does not change during the step-drawdown test. However, newly completed wells and old wells are sometimes unstable and the value of  $C$  is affected by changes in pumping rates. The value of  $C$  computed for steps 1 and 2 may be greater or less than that computed for steps 2 and 3 if the well is unstable. Sand and gravel often shift outside a well during step 3 under the influence of a high rate of pumping, resulting in either the development or clogging of the pores of the aquifer immediately behind the well screen. If the value of  $C$  for steps 2 and 3 is considerably less than that for steps 1 and 2, it is probable that development has occurred during the step-drawdown test. A large increase in  $C$  with higher

pumping rates indicates clogging of the well screen or well wall. If development during the pumping period is large  $\Delta s_2 / \Delta Q_2$  will be greater than  $\Delta s_3 / \Delta Q_3$  and solution of equation 70 will be impossible. Thus, it is possible to appraise the stability of a well with step-drawdown test data and equations 69 and 70.

Drilling processes often clog the voids or fracture openings of the well face and well wall or the openings of the well screen. Maximum yield per foot of drawdown cannot be obtained unless development is sufficient to remove these fine materials. The effectiveness of development can be appraised from the results of a step-drawdown test. The value of  $C$  of a properly developed and designed well is generally less than  $5 \text{ sec}^2/\text{ft}^5$ .

The capacities of wells often diminish with heavy pumping as screen slots or perforations and the voids of the aquifer in the immediate vicinity of the well bore become clogged. The step-drawdown test also can be used to appraise the degree of well deterioration. Values of  $C$  between 5 and  $10 \text{ sec}^2/\text{ft}^5$  indicate mild deterioration, and clogging is severe when  $C$  is greater than  $10 \text{ sec}^2/\text{ft}^5$ . It is difficult and sometimes impossible to restore the original capacity if the well-loss constant is greater than  $40 \text{ sec}^2/\text{ft}^5$ . Wells of diminished capacity can often be returned to near original capacity by one of several rehabilitation methods. The success of rehabilitation work can be appraised from the results of step-drawdown tests made prior to and after treatment.

## Collector Wells

The problem of estimating the sustained yields of collector wells is often encountered. The complex construction features of collector wells cannot be directly considered with existing ground-water formulas. However, drawdown in collector wells can be estimated by simulating the collector well with a vertical well having the same specific capacity as the collector well. The effective radius of a vertical well that simulates the collector well can often be determined with aquifer-test data.

Several Ranney collector wells have been constructed in Illinois. The Ranney collector well consists of a large diameter reinforced concrete caisson from which horizontal screen laterals are projected radially near the bottom. The standard caisson is generally 13 feet in diameter. The horizontal screen laterals are fabricated from heavy steel plate, perforated with longitudinal slots, and may be 8 to 24 inches in diameter and 100 to 450 feet in length depending upon geologic conditions and design of unit (Mikels and Klaer, 1956).

Because the flow pattern within the horizontal lateral system is complex, the sustained yield of the collector is usually determined by simulating the collector with a vertical well having the same specific capacity as the collector well. The effective radius of a vertical well that simulates a collector well in the case of a radial lateral pattern covering the entire circumference and having equal length laterals, is equal to 75 to 85 per cent of the individual lateral lengths

(Mikels and Klaer, 1956). Several effective radii of vertical wells that simulate collector wells having lateral patterns covering only part of the circumference and laterals of unequal length are given in table 3.

**Table 3. Effective radii of collector wells**

Vertical well effective radius (ft)	Collector well construction features
72	Five laterals projected in a fan-shaped pattern ranging in length from 60 to 120 feet and totaling 496 feet around 180 degrees of the circumference
60	Four laterals projected to lengths of about 100 feet each around 90 degrees of the circumference
74	Seven laterals 136 to 176 feet in length around 130 degrees of the circumference

*From Mikels and Klaer (1956)*

### **Well Design Criteria**

There are many criteria used in screen and artificial pack selection and to date there are no standardized well design criteria acceptable to all those concerned with water wells. The well design criteria presented in this report are somewhat of a compromise between the various criteria in the literature and are those adapted for conditions found in Illinois. The criteria are applicable to domestic, industrial, municipal, and irrigation wells. The objective is to design an efficient and economical well with a service life of at least 10 years for any aquifer and purpose.

### **Screened Wells**

In the unconsolidated deposits, a screen is required to hold back sediment and allow water to flow into the well without excessive head loss or the passage of fine materials during pumping. There are two types of screened wells: natural pack and artificial pack. Materials surrounding the well are developed in place in the case of the natural pack well; materials having a coarser uniform grain size than the natural formation are artificially placed around the well in the case of the artificial pack well. In the natural pack case, development removes the finer material from the aquifer so that only coarser material surrounds the screen. The materials around the well are made more uniform in grain size and the sand and gravel is graded in such a way that fine deposits from the aquifer cannot clog the natural pack.

Artificial pack wells are usually justified when the aquifer is homogeneous, has a uniformity coefficient less than 3.0, and has an effective grain size less than 0.01 inch (Ahrens, 1957). In addition, an artificial pack is sometimes needed to stabilize well-graded aquifers having a large percentage of fine materials in order to avoid excessive settlement of materials above the screen or to permit the use of larger screen slots.

The uniformity coefficient  $C_u$  is the ratio of the sieve

size that will retain 40 per cent of the aquifer materials to the effective size. The sieve size that retains 90 per cent of the aquifer materials is the effective size.

Careful selection of the artificial pack is important to prevent the clogging of the pack with fine materials from the aquifer. The proper grain size for an artificial pack is selected on the basis of the mechanical analysis of the aquifer. A criterion that has been successfully used in Illinois is that the ratio (P:A) of the 50-per-cent sizes of the pack and the aquifer be 5 (Smith, 1954).

Artificial packs should range in thickness from 6 to 9 inches. To avoid segregation or bridging during placement a uniform grain size pack should be used. The screen slot opening should be designed so that at least 90 per cent of the size fractions of the artificial pack are retained.

The design of a natural pack well is somewhat more involved, as the screen governs in large part the extent to which development is accomplished. One of the important factors in the design of natural pack well screens is the width of the screen openings, referred to as slot size. The optimum slot size is selected principally on the basis of the grain size distribution of the aquifer, but geohydrologic conditions also play an important role. Slot sizes are selected which will allow a definite proportion of fine materials to pass into the well. The fines are removed from the well with a bailer, and such methods as surging are used to draw the finer material out of the aquifer around the well and thereby provide improved permeability in the immediate vicinity of the screen.

With a uniformity coefficient greater than 6 (a heterogeneous aquifer) and in the case where the materials overlying the aquifer are fairly firm and will not easily cave, the sieve size that retains 30 per cent of the aquifer materials is generally selected as the slot size. With a uniformity coefficient greater than 6 and in the case where the materials overlying the aquifer are soft and will easily cave, the sieve size that retains 50 per cent of the aquifer materials is selected as the slot size.

With a uniformity coefficient as low as 3 (a homogeneous aquifer) and in the case where the materials overlying the aquifer are fairly firm and will not easily cave, the sieve size that retains 40 per cent of the aquifer materials is selected as the slot size. With a uniformity coefficient as low as 3 and in the case where the materials overlying the aquifer are soft and will easily cave, the sieve size that retains 60 per cent of the aquifer materials is selected as the slot size.

A well sometimes encounters several layers of sand and gravel having different grain sizes and gradations. If the 50-per-cent size of the materials in the coarsest aquifer is less than 4 times the 50-per-cent size of the materials in the finest aquifer, the slot size and pack, if needed, should be selected based on the mechanical analysis of the finest material (Ahrens, 1957). Otherwise, the slot size and pack should be tailored to individual layers.

The screen length is based on the effective open area of

a screen and an optimum screen entrance velocity. When a screen is placed in an aquifer, sediment will settle in around it and partially block the slot openings. The amount of blocking depends largely upon the shape and type of slot and the shape, size, and sorting of the aquifer or pack material. On the average about one-half the open area of the screen will be blocked by aquifer material. Thus, the effective open area averages about 50 per cent of the actual open area of a screen. Little or no increase in well efficiency results from actual open areas greater than 15 per cent of the total surface area of the screen (Corey, 1949).

To insure a long service life by avoiding migration of fine materials toward the screen and subsequent clogging of the well wall and screen openings, screen length is based on velocities between 2 and 12 feet per minute (fpm). In general, aquifers of low permeability are composed of finer grained material than aquifers of high permeability. The possibility of clogging openings depends in large part upon the grain size of the finer aquifer materials, and there is a relationship between optimum screen entrance velocities and the coefficient of permeability of the aquifer. A study was made of several actual case histories of well failures due to the partial clogging of the well walls and screen openings, resulting in values in table 4.

**Table 4. Optimum screen entrance velocities**

Coefficient of permeability (gpd/sq ft)	Optimum screen entrance velocities (fpm)
> 6000	12
6000	11
5000	10
4000	9
3000	8
2500	7
2000	6
1500	5
1000	4
500	3
< 500	2

The permeability of the aquifer is determined from aquifer tests. To prevent rapid clogging of screen and formation, the length of screen for a natural pack well is selected using table 4 and the following equation:

$$L_s = Q/7.48A_oV_c \quad (71)$$

where:

- $L_s$  = optimum length of screen, in ft
- $Q$  = discharge, in gpm
- $A_o$  = effective open area per foot of screen, in sq ft
- $V_c$  = optimum entrance velocity, in fpm

The same procedure is followed in selecting the optimum length of screen for an artificial pack well except that the average of the permeabilities of the aquifer and pack is used to determine the optimum screen entrance velocity.

Smith (1961) describes another method for determining optimum length of screens.

Well diameters are usually determined by the probable pump required; nominal diameters of screens and casings

are in most instances the same. The casing should be at least 2 inches larger than the nominal diameter of the pump bowl. The following are well diameters that have been used in Illinois (Smith, 1961):

Pumping rate (gpm)	Diameter of well (in.)
125	6
300	8
600	10
1200	12
2000	14
3000	16

The open area of a screen increases with the diameter of the screen; thus selection of well diameter may depend upon the desired open area rather than the probable pump required.

In order to install and maintain pumping equipment, the well should be straight and plumb. The alignment of a well should be kept within practical limits. The standard specifications for deep wells adopted by the American Water Works Association includes the following requirements:

"Plumbness and alignment shall be tested by lowering into the well to a depth at least as great as the lowest anticipated pump setting a section of pipe 40 feet long or a dummy of the same length. The outer diameter of the pump shall not be more than 1/2 inch smaller than the diameter of that part of the casing or hole being tested. If a dummy is used it shall consist of a rigid spindle with 3 rings, each ring being 12 inches wide. The rings shall be truly cylindrical and shall be spaced one at each end of the dummy and one ring in the center thereof. The central member of the dummy shall be rigid so that it will maintain the alignment of the axis of the rings.

"Should the dummy fail to move freely throughout the depth to be tested or should the well vary from the vertical in excess of 2/3 of the smallest inside diameter or beyond limitations of this test, the plumbness and alignment of the well shall be corrected by the contractor at his own expense."

Methods for checking the alignment and plumbness of wells are described in the January-February, 1960, edition of The Johnson National Drillers' Journal.

### Spacing of Wells

The problem of spacing production wells is frequently encountered. The farther apart wells are spaced the less their mutual interference but the greater the cost of connecting pipeline and electrical equipment. The spacing of wells is often dictated by practical considerations such as property boundaries and existing distribution pipe networks. The following discussion is concerned only with the influ-

ence of aquifer characteristics and economics on the spacing of production wells.

Theis (1957) derived the following equation for determining the optimum well spacing in the simple case of two wells pumping at the same rate from a thick and areally extensive aquifer:

$$r_s = 2.4 \times 10^8 c_p Q^2 / kT \quad (72)$$

where:

$r_s$  = optimum well spacing, in ft

$c_p$  = cost to raise a gallon of water 1 foot, consisting largely of power charges, but also properly including some additional charges on the equipment, in dollars

$k$  = capitalized cost for maintenance, depreciation, original cost of pipeline, etc., in dollars per year per foot of intervening distance

$Q$  = pumping rate of each well, in gpm

$T$  = coefficient of transmissibility, in gpd/ft

For small values of  $T$  and  $Q$ ,  $r_s$  from equation 72 is of no practical significance. Because the effects of partial penetration are appreciable within a distance of about twice the

saturated thickness of the aquifer,  $2m$ , from the production well, it is generally advisable to space wells at least a distance of  $2m$  apart in aquifers 100 or less feet thick. Experience has shown that in the case of a multiple well system consisting of more than 2 wells the proper spacing between wells is at least 250 feet.

Production wells should be spaced parallel to and as far away as possible from barrier boundaries and as near to the center of a buried valley as possible. Wells should be spaced on a line parallel to a recharge boundary and as close to the source of recharge as possible.

Theis (1941) derived the following equation to determine the permissible distance between production and disposal wells in an areally extensive isotropic aquifer:

$$r_d = 2Q_d / TI \quad (73)$$

where:

$r_d$  = permissible distance between production and disposal wells to prevent recirculation of water, in ft

$Q_d$  = Pumping and disposal rate, in gpd

$T$  = coefficient of transmissibility, in gpd/ft

$I$  = natural hydraulic gradient of water table or piezometric surface, in ft/ft

### Part 3. Illustrative Examples of Analyses

Practical applications of the formulas and methods described in Part 1 and Part 2 of this report are shown in the following examples. These illustrate analyses based on actual field data for most of the major analytical methods discussed.

#### Barometric Efficiency of a Well

Figure 19 shows the effect of atmospheric-pressure fluctuations (Roberts and Romine, 1947) on the water level in a well which is located in Champaign County near the village of Savoy in east-central Illinois. The well was drilled

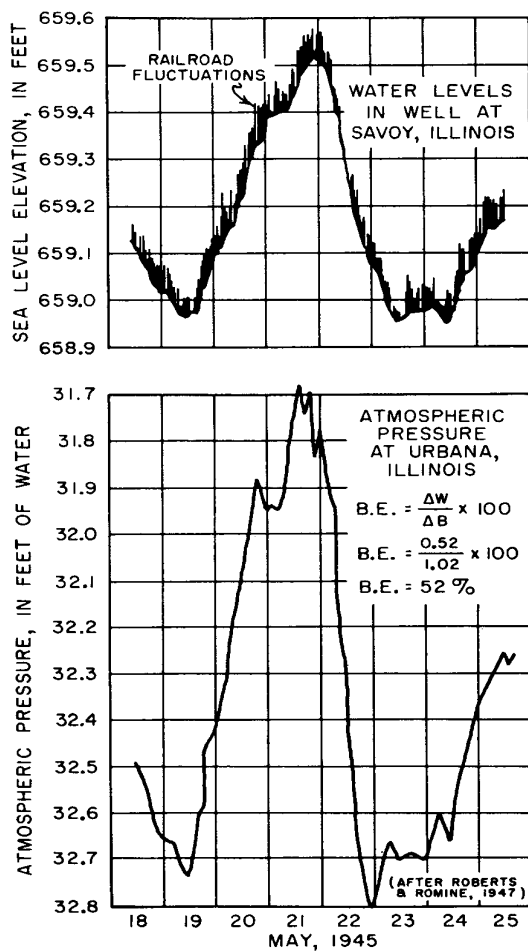


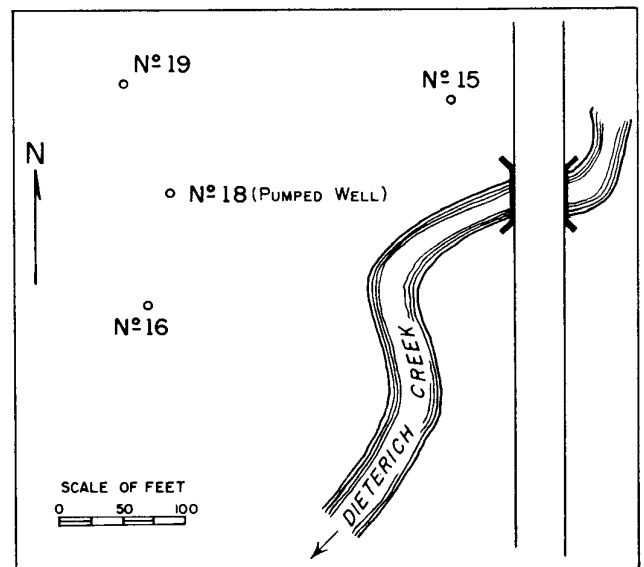
Figure 19. Effect of atmospheric pressure fluctuations on the water level in a well at Savoy

in 1944 to supply water for the construction of the University of Illinois airport, is 169 feet deep, and is cased with 8-inch I.D. pipe. Thirteen feet of 7.5-inch-diameter, wire-wound, 50-slot screen is exposed to the aquifer. The non-pumping level was about 70 feet below land surface in May 1945. The aquifer is 15 feet of glacial sand and gravel overlying shales of Pennsylvanian age. Till with a very low permeability and 154 feet thick overlies the aquifer.

The barometric efficiency of the well was computed to be about 52 per cent by substituting data on water-level and atmospheric-pressure changes in equation 3 as shown in figure 19.

#### Aquifer-Test Data Under Leaky Artesian Conditions

An aquifer test was made by G. E. Neher of the State Water Survey in cooperation with Marbry & Johnson, Inc., consulting engineers, and E. C. Baker & Sons, well contractor, on July 2 and 3, 1951. A group of wells (figure 20) located in Effingham County about 1 mile southwest of the corporate limits of the village of Dieterich in sec. 22, T7N, R7E was used. The generalized graphic logs of the



(FROM WALTON, 1960a)

Figure 20. Map showing location of wells used in test near Dieterich

wells are given in figure 21. The effects of pumping well 18 were measured in observation wells 15, 16, and 19. Pumping was started at 2:10 pm. on July 2 and was continued for a period of about 20 hours at a constant rate of 25 gpm until 10: 00 a.m. on July 3.

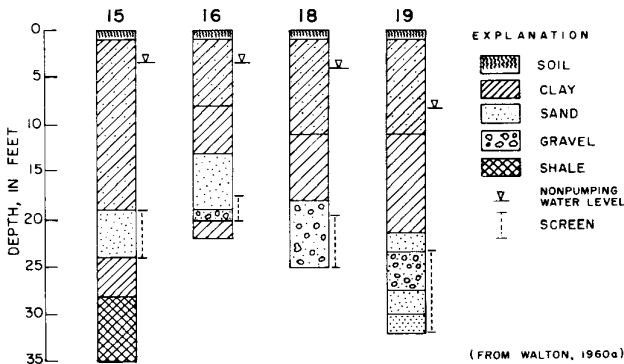


Figure 21. Generalized graphic logs of wells used in test near Dieterich

Drawdowns in the pumped well and observation wells were determined by comparing the extrapolated graphs of water levels measured before pumping started with graphs of water levels measured during the pumping period. Drawdowns were plotted against time on logarithmic paper. The

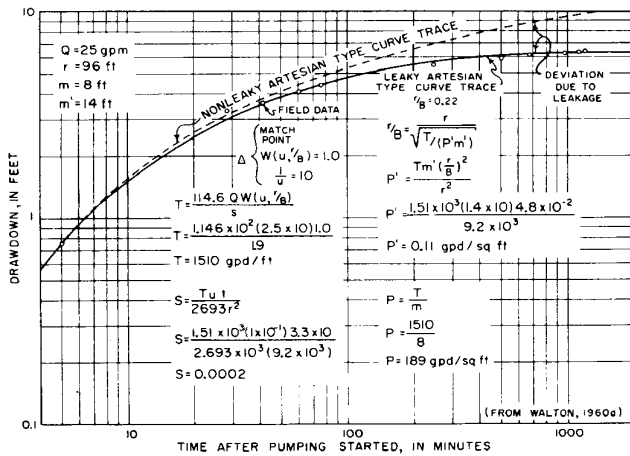


Figure 22. Time-drawdown graph for well 19 near Dieterich

Table 5. Time-drawdown data for well 19 near Dieterich

Time after pumping started (min)	Drawdown (ft)
5	0.76
28	3.30
41	3.59
60	4.08
75	4.39
244	5.47
493	5.96
669	6.11
958	6.27
1129	6.40
1185	6.42

$Q = 25$  gpm and  $r = 96$  ft

time-drawdown field data graph for observation well 19 is given, as an example, in figure 22. Time-drawdown data for observation well 19 is given in table 5.

The time-drawdown field data graph was superposed on the family of leaky artesian type curves. The time-drawdown field data curve closely follows but falls slightly below the  $r/B = 0.2$  type curve. By interpolation an  $r/B = 0.22$  type curve was selected as analogous to the time-drawdown field data curve. Match-point coordinates and an  $r/B$  value of 0.22 were substituted into equations 9, 10, and 11 to compute coefficients of transmissibility, vertical permeability, and storage. Computations for well 19 are given in figure 22.

Table 6. Distance-drawdown data for test near Dieterich

Well number	Distance from pumped well (ft)	Drawdown (ft)
15	234	3.25
16	92	6.70
19	94	6.42

$Q = 25$  gpm and  $t = 1185$  min

Drawdowns in observation wells 15, 16, and 19 (table 6) at the end of the test when steady-state conditions prevailed were plotted on logarithmic paper against the distances, from the respective observation wells to the pumped well, to describe a distance-drawdown field data curve. The steady-state type curve was matched to the distance-drawdown field data curve and match-point coordinates were substituted in equations 12 and 13 for computation of coefficients of transmissibility and vertical permeability as shown in figure 23.

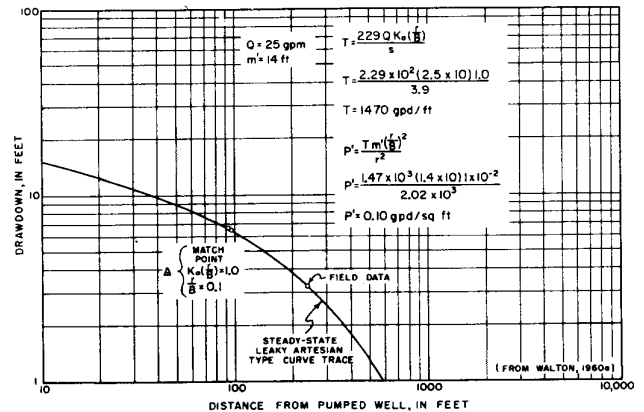


Figure 23. Distance-drawdown graph for test near Dieterich

The average values of  $T$ ,  $S$ , and  $P'$  computed by using time-drawdown and distance-drawdown data are 1500 gpd/ft, 0.0002, and 0.10 gpd/sq ft, respectively. As indicated by the distance-drawdown curve shown in figure 23, the 20-hour test sampled an area of the aquifer within a radius of roughly 2000 feet. The coefficients computed from the results of the test represent the average hydraulic

properties of the aquifer and confining bed within that cone of depression.

The test at Dieterich was chosen as an example to demonstrate analysis of data under leaky artesian conditions partly because, as shown in figure 20, the wells are near a possible source of recharge (Dieterich Creek). Two interpretations of the test data are therefore possible if the effects of partial penetration are excluded. The decrease in the time-rate of drawdown can be attributed either to the effects of leakage through the confining bed or to the effects of induced infiltration of surface water (recharge boundary).

Available geohydrologic data indicate that Dieterich Creek is not a recharge boundary. The stream bed rests on clayey materials and has not cut into the aquifer. In addition, the stream bed is silted and is relatively impermeable. The stream bed is only a few feet wide and streamflow (135 gpm at the time of the test) during the summer and fall months is low.

The results of the aquifer test lend support to this interpretation. If Dieterich Creek were a recharge boundary, the cone of depression would be distorted and distance-drawdown and time-drawdown data would yield differing results. However, values of  $T$  and  $P'$  computed from both time-drawdown and distance-drawdown data agree, indicating that Dieterich Creek is not a recharge boundary.

### Aquifer-Test Data Under Nonleaky Artesian Conditions

Representatives of Layne-Western Company conducted an aquifer test (see Bruin and Hudson, 1955) on July 2, 1953, on a village well at Gridley, McLean County, Illinois. Village officials, L. A. Miller & Associates as consulting engineers, and the State Water Survey observed the test. A group of wells (figure 24) located within the corporate limits of the village of Gridley in sec. 4, T26N, R3E was used. The generalized graphic logs of the wells are given in figure 25. The effects of pumping well 3 were measured in observation wells 1 and 2. Pumping was started at 9:45 a.m. on July 2, and was continued at a constant rate of 220 gpm for about 8 hours until 6:02 p.m.

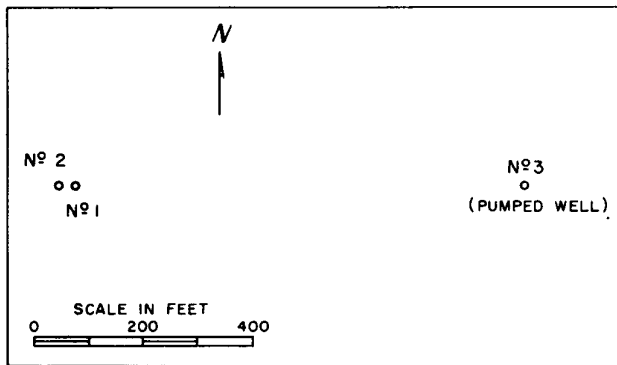


Figure 24. Map showing location of wells used in test at Gridley

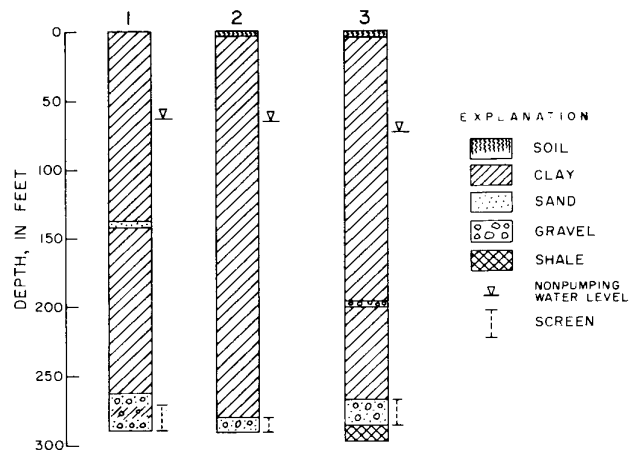


Figure 25. Generalized graphic logs of wells used in test at Gridley

Drawdowns in the pumped well and in the observation wells were plotted against time on semilogarithmic and logarithmic paper, respectively. The time-drawdown field data graph for the pumped well and for observation well 1 are given in figures 26 and 27, respectively. Time-drawdown data for the wells are given in tables 7 and 8.

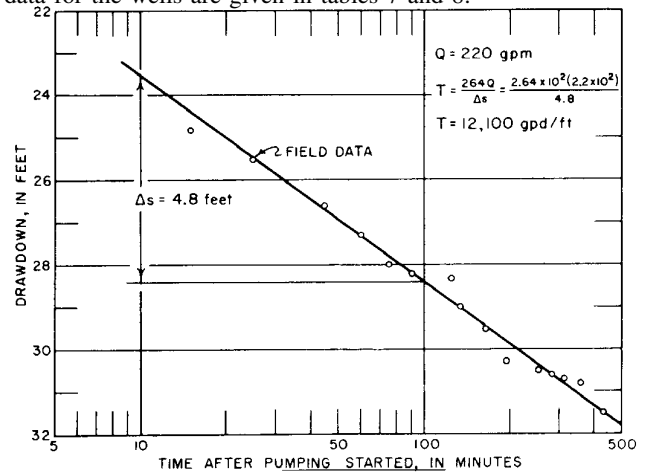


Figure 26. Time-drawdown graph for well 3 at Gridley

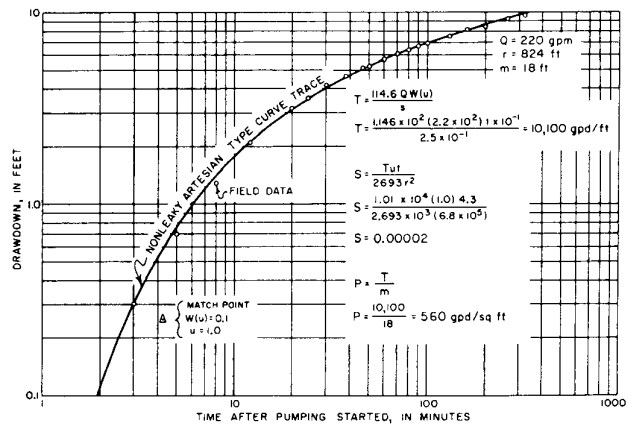


Figure 27. Time-drawdown graph for well 1 at Gridley

**Table 7. Time-drawdown data for well 1 at Gridley**

Time after pumping started (min)	Drawdown (ft)
3	0.3
5	0.7
8	1.3
12	2.1
20	3.2
24	3.6
30	4.1
38	4.7
47	5.1
50	5.3
60	5.7
70	6.1
80	6.3
90	6.7
100	7.0
130	7.5
160	8.3
200	8.5
260	9.2
320	9.7
380	10.2
500	10.9

$Q = 220$  gpm and  $r = 824$  ft

**Table 8. Time-drawdown data for well 3 at Gridley**

Time after pumping started (min)	Drawdown (ft)
15	24.8
25	25.5
45	26.6
60	27.3
76	28.0
90	28.2
132	29.0
166	29.5
195	30.3
256	30.5
282	30.6
314	30.7
360	30.8
430	31.5

$Q = 220$  gpm

The time-drawdown field data graph for well 1 was superposed on the nonleaky artesian type curve because leakage was not measurable during the test. Match-point coordinates and equations 14 and 15 were used to determine the hydraulic properties of the aquifer. Computations are given in figure 27.

A straight line was fitted to the time-drawdown field data graph for the pumped well as shown in figure 26. The slope of the line was substituted into equation 23 to calculate the coefficient of transmissibility. The coefficient of storage cannot be determined because the effective radius of the pumped well is not known and the total drawdown in the pumped well is affected by well loss.

The average values of  $T$  and  $S$  computed by using time-drawdown data are 11,000 gpd/ft and  $2.2 \times 10^{-5}$ , respectively.

**Aquifer-Test Data Under Water-Table Conditions**

An aquifer test was made by W. H. Walker of the State Water Survey in cooperation with the owner, the Caterpillar Tractor Co., and Layne-Western Co., well contractor, on December 22 and 23, 1958. A group of wells (figure 28) located about 3 miles north of Mossville, Peoria County, in sec. 15, T10N, R8E was used. The generalized graphic logs of the wells are given in figure 29. The effects of pumping well 4 were measured in observation wells 15 and 17. Pumping was started at 11:53 a.m. on December 22 and was continued for about 24 hours at a constant rate of 1100 gpm until 11:45 a.m. on December 23.

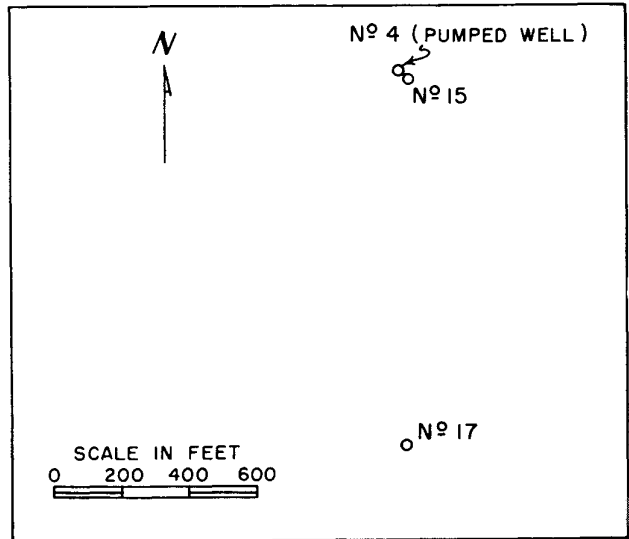


Figure 28. Map showing location of wells used in test near Mossville

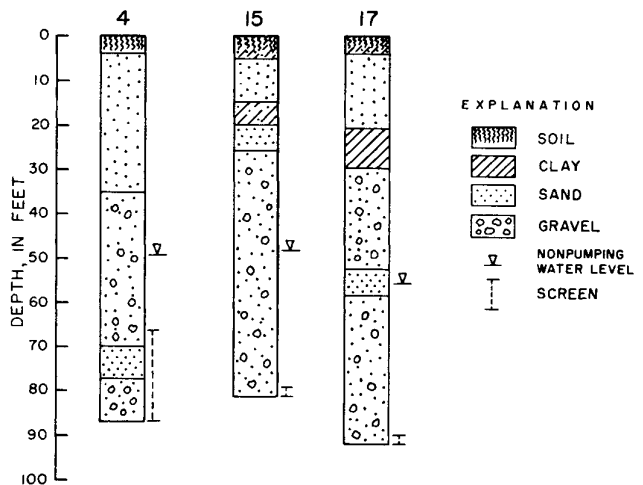


Figure 29. Generalized graphic logs of wells used in test near Mossville

Drawdowns in the pumped well and observation wells were determined by comparing the extrapolated graphs of water levels measured before pumping started with graphs of water levels measured during the pumping period. Draw-

downs in the observation wells were adjusted for the effects of dewatering and partial penetration with equations 17 and 19 and were plotted against time on logarithmic graph paper. The time-drawdown field data graph for well 15 is given as an example, in figure 30. Time-drawdown data for well 15 are also given in table 9.

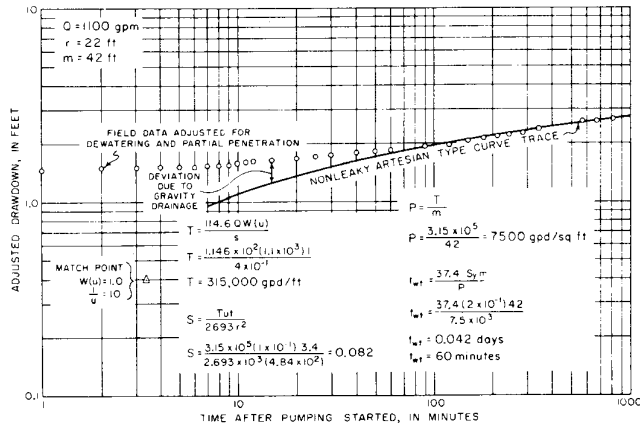


Figure 30. Time-drawdown graph for well 15 near Mossville

Table 9. Time-drawdown data for well 15 near Mossville

Time after pumping started (min)	Observed drawdown (ft)	Drawdown adjusted for dewatering and partial penetration (ft)
1	1.71	1.48
2	1.74	1.50
3	1.75	1.51
4	1.76	1.52
5	1.77	1.53
6	1.76	1.52
7	1.79	1.55
8	1.80	1.56
9	1.81	1.57
10	1.83	1.59
11	1.85	1.61
12	1.86	1.62
15	1.89	1.65
20	1.93	1.69
25	1.97	1.72
30	2.00	1.75
40	2.04	1.79
50	2.08	1.83
60	2.11	1.86
90	2.18	1.93
120	2.25	1.99
150	2.34	2.07
180	2.40	2.13
210	2.46	2.19
243	2.51	2.23
276	2.56	2.28
341	2.67	2.38
567	2.90	2.60
667	2.90	2.60
817	2.97	2.66
1147	3.23	2.91

$Q = 1100$  gpm and  $r = 22$  ft

The time-drawdown field data graph was superposed on the nonleaky artesian type curve. Emphasis was placed on late time-drawdown data, based on the assumption that

early time-drawdown data were influenced by the effects of gravity drainage to a much greater degree than later time-drawdown data. Match-point coordinates  $W(u)$ ,  $1/u$ ,  $s$ , and  $t$  were substituted on equations 14 and 15 to determine  $T$  and  $S$ . The coefficient of permeability was then computed. The value of  $t_{Dw}$  was estimated with equation 16 and the computed value of  $P$  and the value of  $t_{Dw}$  was compared with the region of early time-drawdown data ignored in matching curves. As shown in figure 30,  $t_{Dw}$  is about equal to the time the type curve and field data curve start to match, indicating that the solution is valid.

Table 10. Distance-drawdown data for test near Mossville

Well number	Distance from pumped well (ft)	Drawdown adjusted for dewatering and partial penetration (ft)
15	22	2.91
17	1125	0.32

$Q = 1100$  gpm and  $t = 1147$  min

Drawdowns (table 10) near the end of the test for a pumping period of 1147 minutes in the two observation wells were plotted on logarithmic paper against the squares of the distances from the respective observation wells to obtain a distance-drawdown field data curve. The nonleaky artesian type curve was matched to the distance-drawdown curve and match-point coordinates  $W(u)$ ,  $u$ ,  $s$ , and  $r^2$  were substituted into equations 14 and 15 to determine  $T$  and  $S$  as shown in figure 31. The average values of  $T$  and  $S$  computed from aquifer-test data are 340,000 gpd/ft and 0.09, respectively.

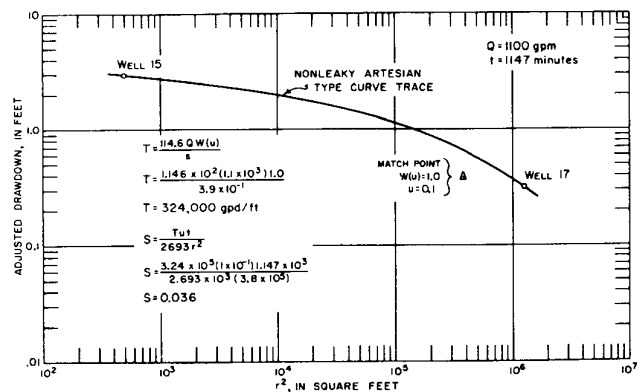


Figure 31. Distance-drawdown graph for test near Mossville

The results of the test indicate that the coefficient of storage is not constant but depends largely on the time of pumping and distance from the pumped well. The coefficient of storage appears to increase with time and to decrease with distance from the pumped well. The computed coefficients of storage are in the water-table range but are much less than the specific yield of the deposits which is estimated to be about 0.2. The coefficients of storage com-

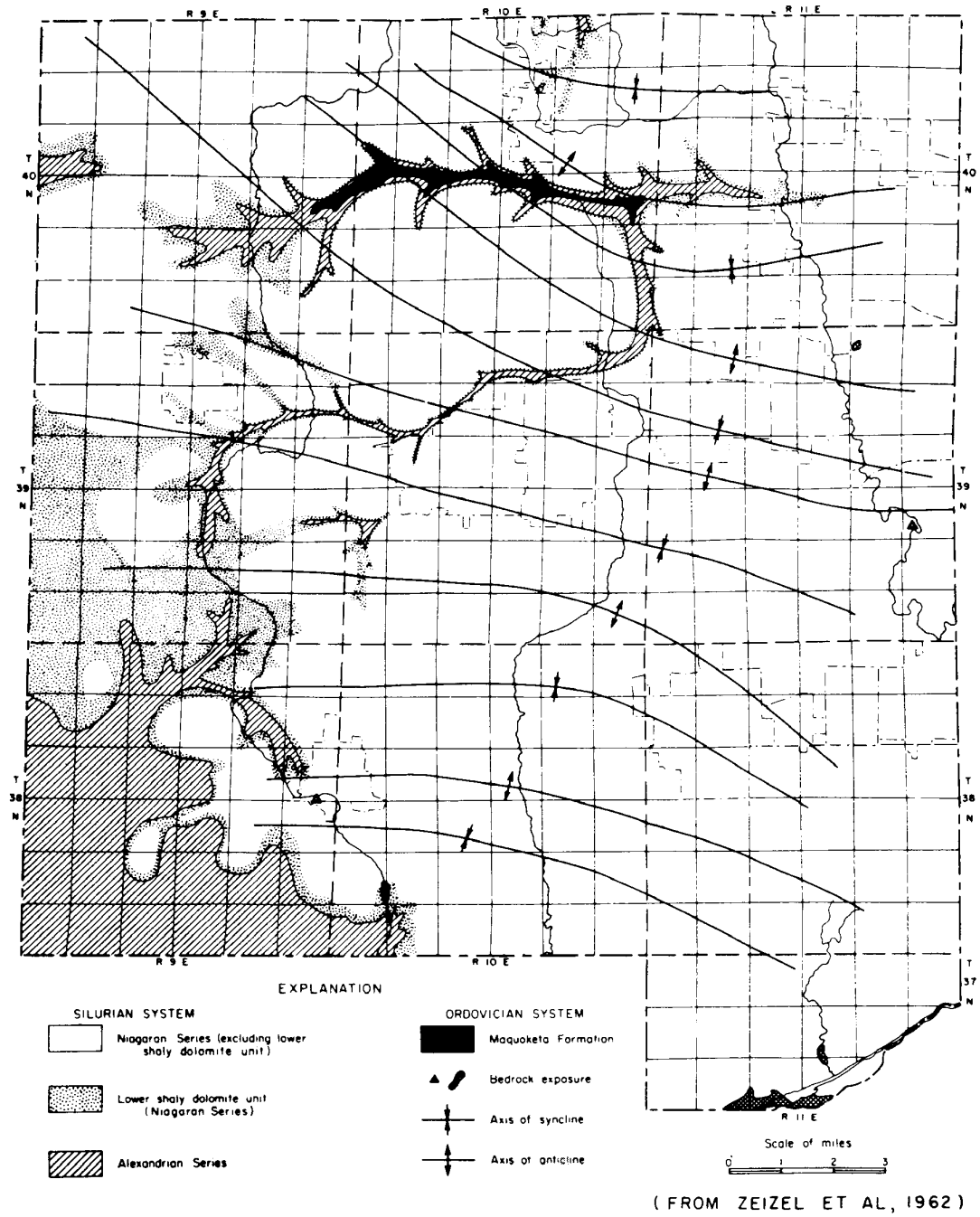


Figure 32. Areal geology of the bedrock surface in DuPage County



puted from test data apply to the part of the aquifer de-watered during the test.

Two interpretations of the aquifer-test data are possible: 1) placing emphasis on early time-drawdown data suggests that all later drawdown data are influenced by barrier boundaries; 2) disregarding the first hour of time-drawdown data and placing emphasis on later time-drawdown data suggests that barrier boundaries were not encountered during the test but that early data deviate from theory because of the effects of gravity drainage. If barrier boundaries were encountered during the test the cone of depression would be distorted. As a result, hydraulic properties determined from late distance-drawdown data would be unreasonable and could only by chance agree with hydraulic properties determined from late time-drawdown data. The fact that values of hydraulic properties computed with both time-drawdown and distance-drawdown data agree within reasonable limits lends support to the interpretation that the cone of depression did not encounter barrier boundaries and that early time-drawdown data were affected by slow gravity drainage.

### Specific-Capacity Data

#### Statistical Analysis

In DuPage County in northeastern Illinois rocks of Silurian age immediately underlie the glacial drift and in many areas yield large quantities of water to wells. In addition, dolomite beds in the Maquoketa Formation of Ordovician age encountered beneath rocks of Silurian age yield small to moderate quantities of ground water to wells.

Rocks of Silurian age are the Alexandrian Series overlain by the Niagaran Series (see Zeizel et al, 1962). Most of the bedrock surface beneath the glacial drift is formed by the Niagaran Series as shown in figure 32. The Alexandrian Series is the uppermost bedrock in small areas in the southwestern part of the county.

The thickness of the Silurian rocks increases from less than 50 feet in the western part of the county to more than 200 feet in portions of the southeastern part, as shown in figure 33. Where valleys occur in the bedrock, the Silurian rocks are thinned. In the bedrock valley in the north-central part of the county, Silurian rocks have been completely removed by erosion.

Many wells extend through Silurian strata and penetrate dolomite beds of the Maquoketa Formation. The thickness of the Maquoketa Formation ranges from 85 to 227 feet and averages about 175 feet in DuPage County.

Ground water in the dolomite aquifers of Silurian and Ordovician age occurs in joints, fissures, and solution cavities. The water-bearing openings are irregularly distributed both vertically and horizontally, and the yields of dolomite wells vary greatly from place to place.

The specific capacities of dolomite wells in the county have been studied (Zeizel et al, 1962) in detail, and this has shed much light on the water-yielding properties of the

individual units of the dolomite aquifers. Specific capacities of dolomite wells range from 0.6 to 530 gpm/ft and average 42 gpm/ft.

Many wells penetrate only rocks of the Niagaran (N) Series, some wells penetrate rocks of both the Niagaran and Alexandrian (A) Series, other wells penetrate rocks of the Niagaran and Alexandrian Series and the Maquoketa (M) Formation. The total depth of penetration of wells and the depth of penetration of the wells into each unit were determined from well logs and sample studies of drill cuttings.

In general, the specific capacity of a dolomite well increases with the depth of penetration and number of units penetrated, however, the upper part of the Silurian rocks is usually the most productive. Specific capacities were divided by the total depth of penetration of wells to obtain the specific capacities per foot of penetration.

Wells were segregated into three categories, N, N + A, and N + A + M, depending upon the units penetrated by wells. Specific capacities per foot of penetration for wells in each of the three categories were tabulated in order of magnitude, and frequencies were computed with equation 34.

Values of specific capacity per foot of penetration were then plotted against the percentage of wells on logarithmic probability paper as shown in figure 34.

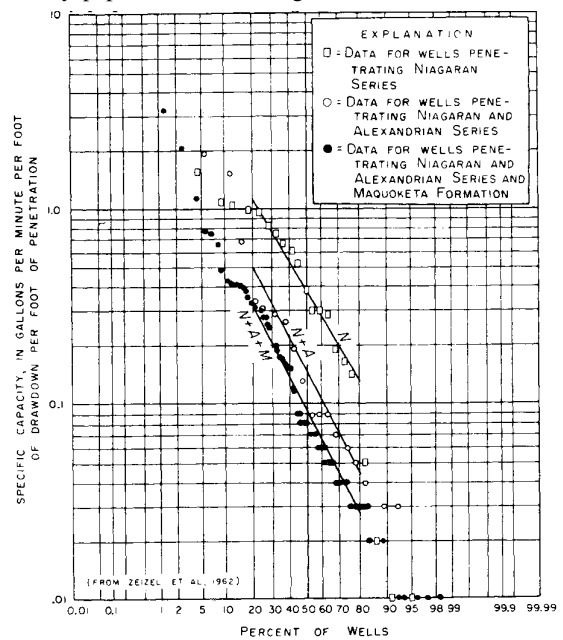


Figure 34. Specific capacity frequency graphs for dolomite wells in DuPage County

Specific capacities per foot of penetration decrease as the depth of penetration of wells and number of units penetrated increase, indicating that both the Niagaran and Alexandrian Series are more productive than the Maquoketa Formation and the Niagaran Series is more productive than the Alexandrian Series.

The dolomite unit-frequency graphs in figure 35 were

constructed with figure 34 by the process of subtraction taking into consideration uneven distribution of wells in the three categories. Based on the slopes of the dolomite unit-frequency graphs, the Maquoketa Formation is much

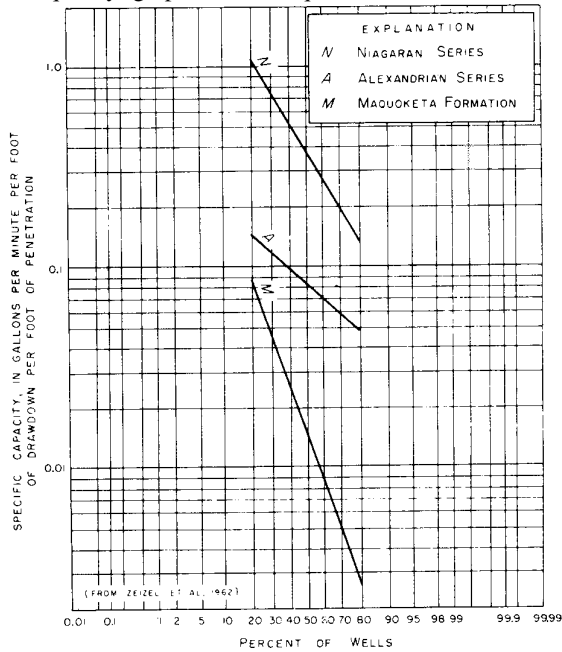


Figure 35. Specific capacity frequency graphs for the units penetrated by dolomite wells in DuPage County

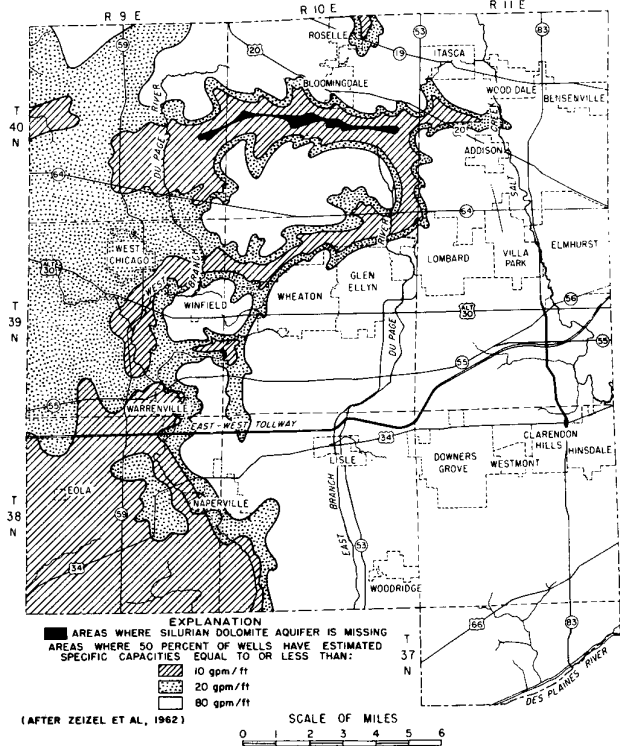


Figure 36. Estimated specific capacities of dolomite wells in DuPage County

less consistent in production than both the Niagaran and Alexandrian Series, and the productivity of the Alexandrian Series is more consistent than the productivity of the other dolomite units.

Because the productivity of the Silurian dolomite aquifer is inconsistent it is impossible to predict with a high degree of accuracy the specific capacity of a well before drilling at any location. Probable range of specific capacities of wells can be estimated based on the frequency graphs in figure 34 and the map in figure 33. Probable specific capacities of dolomite wells estimated by multiplying specific capacities per foot of drawdown by aquifer thicknesses are shown in figure 36. The map is based on specific capacities per foot of penetration measured in 50 per cent of existing wells and on the assumption that wells completely penetrate the Silurian rocks.

It is possible to drill what is essentially a dry hole at any location. However, based on existing data, the chances of obtaining a well with a specific capacity of more than 20 gpm/ft are good in most areas in the eastern two-thirds of the county. Wells with specific capacity less than 10 gpm/ft may be expected in areas in the southwestern part of the county and in the north-central part where the Niagaran Series is thin or missing.

Specific capacity frequency graphs for dolomite wells in Cook, DuPage, Kane, Lake, McHenry, and Will Counties in northeastern Illinois are given in figure 37. In northeastern Illinois the productivity of the Silurian rocks is highest in the eastern part of Will County and least in the western part of Will County. Specific capacities of wells in DuPage County are slightly less than specific capacities of wells in eastern Will County. The specific capacities in figure 37 are for a radius of 6 inches and a pumping period of 8 hours.

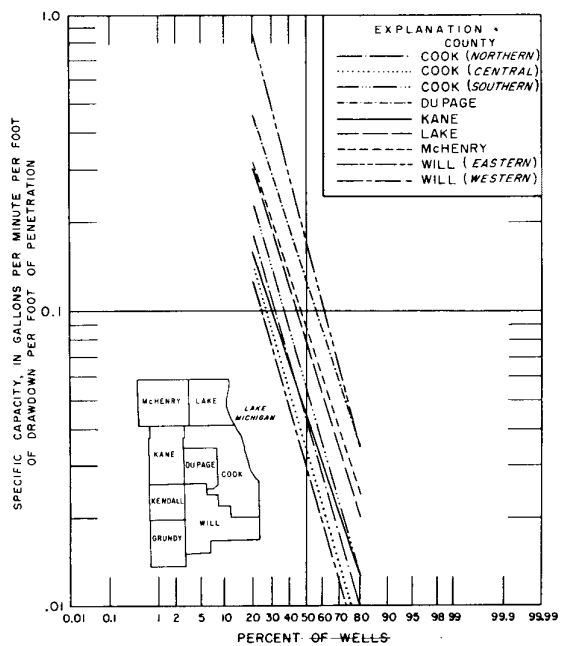


Figure 37. Specific capacity frequency graphs for dolomite wells in northeastern Illinois

## Yields of Deep Sandstone Wells And the Effects of Shooting

Most deep sandstone wells in northern Illinois tap several bedrock units and are multiunit wells. The Galena-Platteville Dolomite, Glenwood-St. Peter Sandstone, and Prairie du Chien Series of Ordovician age; and the Trempealeau Dolomite, Franconia Formation, Ironton-Galesville Sandstone, and Mt. Simon Sandstone of Cambrian age yield appreciable quantities of water to wells. During 1906-1960, well-production tests were made by the State Water Survey on more than 500 deep sandstone wells in northern Illinois. Specific-capacity data were studied by Walton and Csallany (1962) to determine the role of the individual bedrock units uncased in deep sandstone wells as contributors of water and to appraise the effects of shooting the deep sandstone wells.

Wells were grouped into categories according to the units uncased in the wells. The yields of the individual units were ascertained taking into consideration that the specific capacity of a multiunit well is the numerical sum of the specific capacities of the individual units.

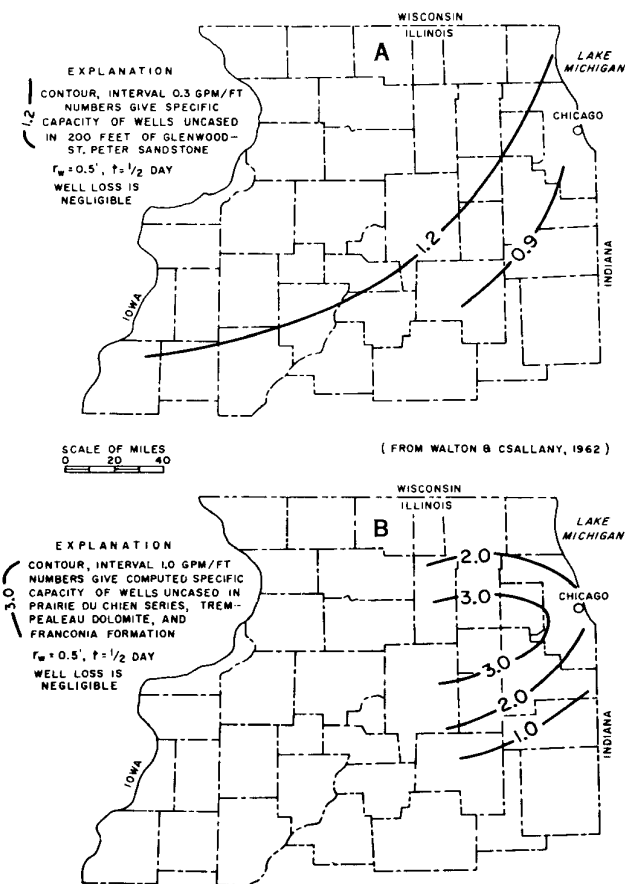


Figure 38. Specific capacities of wells uncased in the Glenwood-St. Peter Sandstone (A) and the Prairie du Chien Series, Trempealeau Dolomite, and Franconia Formation (B) in northeastern Illinois

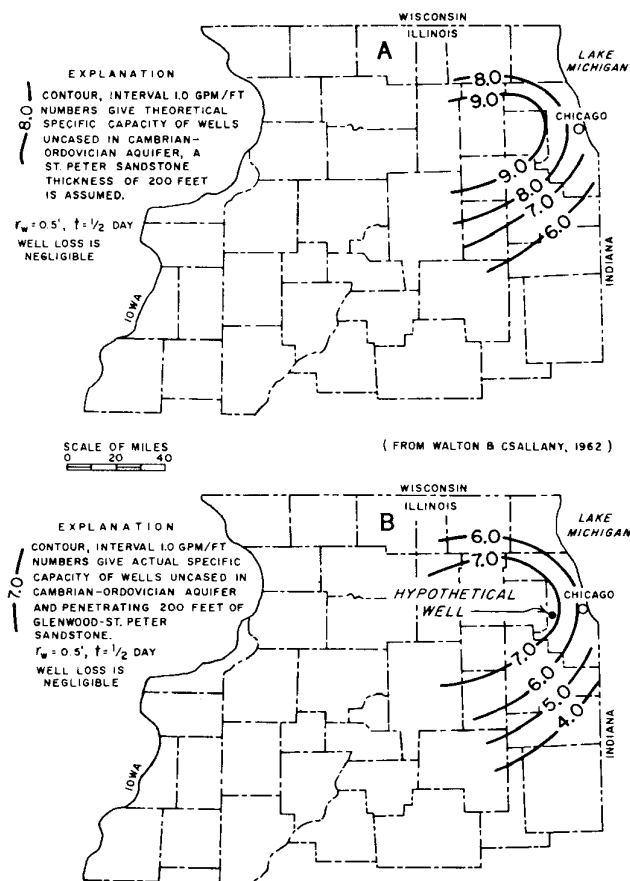


Figure 39. Specific capacities of wells uncased in the Cambrian-Ordovician Aquifer, theoretical (A) and actual (B) in northeastern Illinois

Regional variations in yields are shown for the Glenwood-St. Peter Sandstone and the Prairie du Chien Series, Trempealeau Dolomite, and Franconia Formation, figure 38; and for the Cambrian-Ordovician Aquifer, figure 39. Rocks consisting in downward order of the Galena-Platteville Dolomite, Glenwood-St. Peter Sandstone, and Prairie du Chien Series of Ordovician age; Trempealeau Dolomite, Franconia Formation, and Ironton-Galesville Sandstone of Cambrian age are collectively called the Cambrian-Ordovician Aquifer (Suter et al, 1959). The specific capacity of a well increases with the thickness of the Glenwood-St. Peter Sandstone but is not directly proportional to thickness as shown in figure 40A. The yields of wells per foot of penetration in the Mt. Simon Aquifer are fairly constant with depth throughout northern Illinois as shown in figure 40B. The yields of wells in the Ironton-Galesville Sandstone are fairly constant and average about 3.5 gpm/ft.

Explosives have been successfully used to develop newly constructed deep sandstone wells. Many wells are shot with nitroglycerine opposite several areas in the well bore. Shooting is normally accomplished with liquid or solidified nitro-

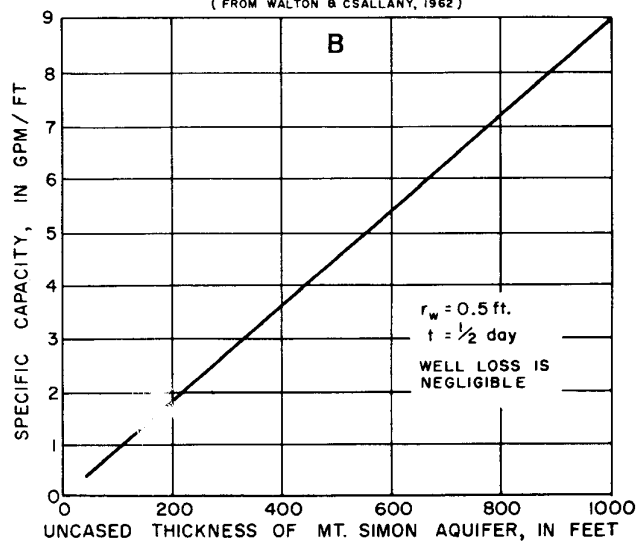
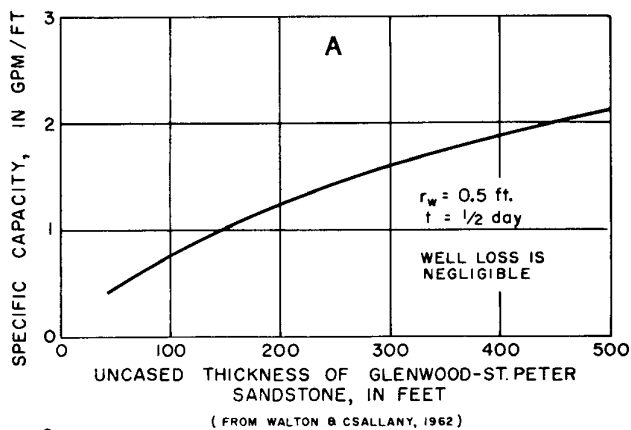


Figure 40. Relation between the specific capacity of a well and the uncased thickness of the Glenwood-St. Peter Sandstone (A) and the uncased thickness of the Mt. Simon Aquifer (B)

glycerine. Shots of approximately 100 to 600 pounds of 80 to 100 per cent nitroglycerine are usually exploded opposite the most permeable zones of a formation and are commonly spaced vertically 20 feet apart. Shots are often exploded opposite the lower 80 feet of the Ironton-Galesville Sandstone and occasionally opposite the middle 80 feet of the St. Peter Sandstone. The explosions loosen quantities of rock, varying from a few cubic feet to several hundred yards, that have to be bailed out of the wells.

Careful study (Walton and Csallany, 1962) of the effects of shooting suggests that in most cases the yields of deep sandstone wells are increased because 1) the hole is enlarged and 2) fine materials deposited during drilling on the well face and in the well wall are removed. Enlarging the effective diameter of the well bore by shooting results in an average increase in the specific capacity of a well of about 10 per cent. The yield of a newly completed well is on the average increased about 20 per cent by removing fine materials from the well face and well wall. Average

increases in the yields of newly completed wells uncased in the various units or aquifers are listed in table 11.

Table 11. Results of shooting deep sandstone wells in northern Illinois

Units or aquifers uncased in well	Average increase in specific capacity due to shooting (per cent)
Glenwood—St. Peter Sandstone	38
Cambrian—Ordovician Aquifer	22
Ironton—Galesville Sandstone	30
Cambrian—Ordovician and Mt. Simon Aquifers	25

From Walton and Csallany (1962)

Methods used to predict the yield of a hypothetical well in sec. 18, T38N, R12E, and the effects of shooting are described in detail below to demonstrate the usefulness of figures 38 through 41, and table 11. Suppose that the hypothetical well is 20 inches in diameter, drilled to the base of the Ironton-Galesville Sandstone, and is uncased in all units of the Cambrian-Ordovician Aquifer. The problem

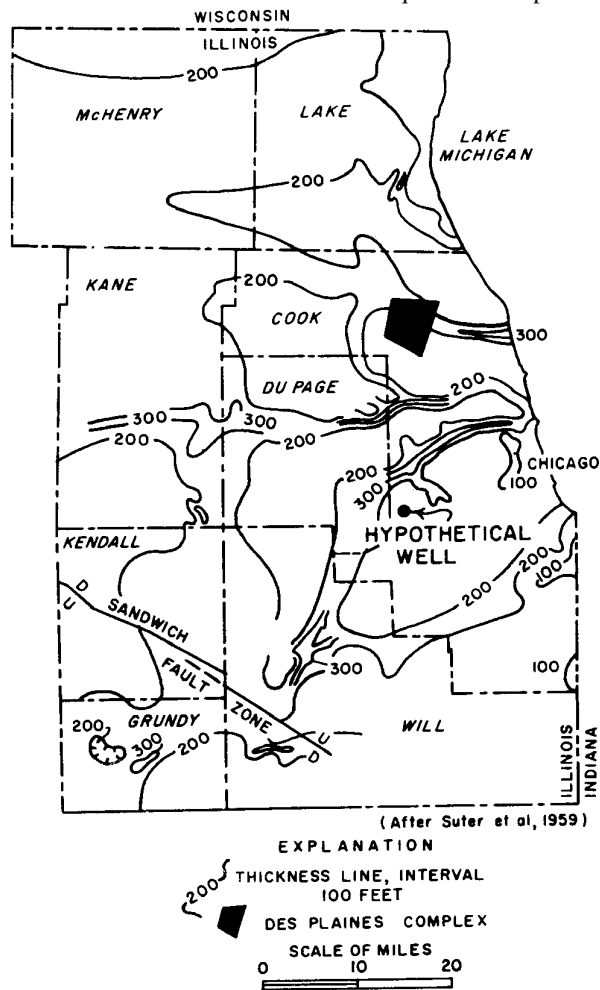


Figure 41. Thickness of the Glenwood-St. Peter Sandstone in northeastern Illinois

is to estimate the specific capacity of the hypothetical well for a pumping period of 7 hours and to estimate the effects of shooting the well. From figure 39B a specific capacity of about 7.1 gpm/ft is predicted. However, figure 39B assumes that the thickness of the Glenwood-St. Peter Sandstone is 200 feet, the diameter of the well is 12 inches, and the pumping period is 12 hours. Figure 41 indicates that the thickness of the Glenwood-St. Peter Sandstone is about 200 feet at the site of the hypothetical well. If the thickness were greater or less than 200 feet, figure 40A would have to be used to adjust the specific capacity obtained from figure 39B for the actual thickness of the Glenwood-St. Peter Sandstone at the well site. The specific capacity from figure 39B was adjusted to a diameter of 20 inches and a pumping period of 7 hours with equation 33. The adjusted specific capacity is about 7.8 gpm/ft.

Well loss has not been considered in the adjusted specific capacity because figure 39B assumes that the well loss is negligible. Suppose that the hypothetical well is pumped at a rate of 400 gpm. The total drawdown in the well is equal to the drawdown (aquifer loss) due to the laminar flow of water through the aquifer towards the well plus the drawdown (well loss) due to the turbulent flow of water as it enters the well itself and flows upward through the bore hole. The aquifer loss can be computed by dividing the assumed pumping rate, 400 gpm, by the adjusted specific capacity, 7.8 gpm/ft, and is about 51 feet. A reasonable estimate for the well-loss constant of a properly constructed deep sandstone well is 5 sec<sup>2</sup>/ft<sup>5</sup>. The well loss can be computed by substituting the estimated well-loss constant and the assumed pumping rate, expressed in cfs, into equation 67 and is about 4 feet. Taking into consideration well loss, a total drawdown of 55 feet is computed and a specific capacity of 7.3 gpm/ft (400 gpm/55 ft) is estimated for the hypothetical well.

The estimated specific capacity assumes that the efficiency

of the hypothetical well is average or about 80 per cent. Figure 39A shows that if the hypothetical well is 100 per cent efficient it would have a specific capacity of about 8.5 gpm/ft. Considering specific capacities based on both 80 and 100 per cent efficient wells, it is probable that the yield of the hypothetical well will be less than 8.5 gpm/ft and at least 7.0 gpm/ft. A specific capacity of about 7.5 gpm/ft is a reasonable estimate for the predicted yield of the hypothetical well in light of the data given in figure 39. The predicted specific capacity compares favorably with the actual yield, 7.7 gpm/ft, of an existing production well near the site of the hypothetical well (see figure 41).

The increase in specific capacity due to shooting the hypothetical well can be predicted with reasonable accuracy. Table 11 shows that the average per cent increase in specific capacity due to shooting the Cambrian-Ordovician Aquifer is about 22. The average increase due to shooting is based on records of wells shot only opposite the lower 80 feet of the Iron-ton-Galesville Sandstone with 100 to 600 pounds of 80 to 100 per cent nitroglycerine. Assuming that the hypothetical well is shot under the above conditions, an increase in specific capacity of about 1.7 gpm/ft (7.5 x 0.22) is predicted due to shooting. Thus, if the well were shot under average conditions it would have a specific capacity of about 9.2 gpm/ft (7.5 + 1.7). The predicted specific capacity agrees closely with the observed specific capacity, 9.1 gpm/ft, of a nearby existing production well after shooting.

Because the yields of some of the units commonly uncased in wells are inconsistent and vary from place to place, estimates based on the regional maps can be in error locally. The estimated probable yield of a well at a particular site should be compared with observed performance data for existing nearby production wells. With sound professional judgment based on both regional and local yields of wells, the yield of a proposed deep sandstone well can usually be predicted within a few per cent.

**Table 12. Results of acid treatment of dolomite wells in DuPage County**

Well owner	Depth of well (ft)	Diameter of well (in.)	Quantity of acid used (gal)	Period acid left in well (hr)	Date of acid treatment	Before acid treatment		After acid treatment		Per cent improvement in specific capacity
						Pumping rate (gpm)	Specific capacity (gpm/ft)	Pumping rate (gpm)	Specific capacity (gpm/ft)	
City of Naperville	178	24	—	336	12/43	250	4.2	1000	43.5	935
City of Naperville	190	24	3000	24	4/42	390	3.7	825	20.0	441
City of Naperville	202	24	1000	1/2	2/47	285	1.7	285	1.7	none
City of Naperville	202	24	3000	96	3/48	285	1.7	570	12.5	635
City of West Chicago	310	24	3000	---	4/56	375	3.3	800	10.0	203
Glen Oak Country Club	212	16	600	---	3/57	311	2.2	450	6.3	187
Village of Villa Park	235	12	1500	1	11/59	175	1.8	200	1.8	none
Village of Villa Park	285	8	1500	---	4/48	200	3.4	369	4.5	33
City of Elmhurst	290	8	3000	---	7/59	335	3.9	300	5.4	39
Village of Roselle	182	10	1000	24	3/55	140	2.3	170	7.7	235
Village of Itasca	181	20	1000	---	7/59	75	0.7	50	0.4	none
Village of Itasca	190	12	1000	20	4/59	156	1.2	250	3.8	216
Village of Itasca	190	12	2000	72	5/60	250	3.8	400	6.3	66

From Zeisel et al (1962)

## Effects of Acid Treatment

Acid treatment has been used successfully to develop newly constructed dolomite wells and to rehabilitate old dolomite wells in DuPage County (Zeizel et al, 1962). Several wells have been treated with inhibited 15 per cent hydrochloric acid in quantities ranging from 600 to 3000 gallons. Treatment was usually performed with the pump and discharge column removed from the well. Acid was introduced through a temporary line extending to a position near the bottom of the well. The solution was allowed to stand under pressure for periods ranging from 30 minutes to 4 days. The pump then was reinstalled and the spent acid was removed from the well during pumping periods ranging from 3 to 8 hours.

Well-production tests were made on a few wells before and after acid treatment. The results of the tests are summarized in table 12. There is an extremely wide range (0 to 935 per cent) in improvement. Most of the improvements over 100 per cent were recorded for rehabilitated wells; improvements generally less than 40 per cent were reported for newly constructed wells. In two of the cases where no improvement was observed the acid was allowed to stand for only an hour or less. The results of acid treatment of two wells are shown graphically in figure 42.

ability. This clogging is particularly noticeable in wells with pumping levels below the top of the aquifer. The yields of clogged wells can often be restored to their original value by acid treatment.

During the construction of many dolomite wells some very fine drill cuttings invariably infiltrate a short distance into the water-yielding openings of the aquifer and reduce the permeability of the well wall. A newly completed well is often less than 100 per cent efficient because of this partial clogging of openings. With acid treatment, the yield of a newly completed well can often be increased by removing the fine materials which have migrated into the formation.

The acid reacts with drill cuttings in openings and with the dolomite of the well wall. The effect of the reaction with the dolomite of the well wall is to increase the radius of the well bore. Large increases in the radius of a well bore result in comparatively small increases in specific capacity of the well because the specific capacity varies with the logarithm of  $1/r_w^2$ . Several thousand gallons of acid cannot dissolve in a day enough bulk dolomite to substantially increase the radius of the well bore. Thus, large increases in the yield of a dolomite well cannot be attributed to well bore enlargement. However, the acid will penetrate considerable distances along the fractures and will widen them and increase their permeability. In addition, the acid will dissolve drill cuttings in openings and increase the permeability of the well wall.

The effect of treatment will vary according to the permeability of the well wall before treatment. A tight dolomite with narrow openings will respond differently than one with openings of appreciable width. Furthermore, a formation that has been partially clogged during drilling will respond differently than one which has not been clogged.

According to Muskat (1937), acid treatment will be effective if the dolomite aquifer has extended fractures or the openings are partially clogged. Increases up to about 50 per cent for wells of initially moderate or high capacity may be explained by the assumption that the width of water-yielding openings of a small radial zone about the well bore have been increased and/or that drilling cuttings partially clogging the well wall have been removed. Moderate increases, 50 to 500 per cent, may be explained by the assumption that there are extended fractures in the dolomite which are penetrated and widened by the acid and/or that mild clogging is the principal factor governing the initial yield of the well. Wells of initially low capacity often react best to acid treatment. Increases larger than 500 per cent can only be explained by the assumption that there are extended fractures in the dolomite which are penetrated and widened by the acid and/or that there was initially a condition of almost complete clogging of the well wall.

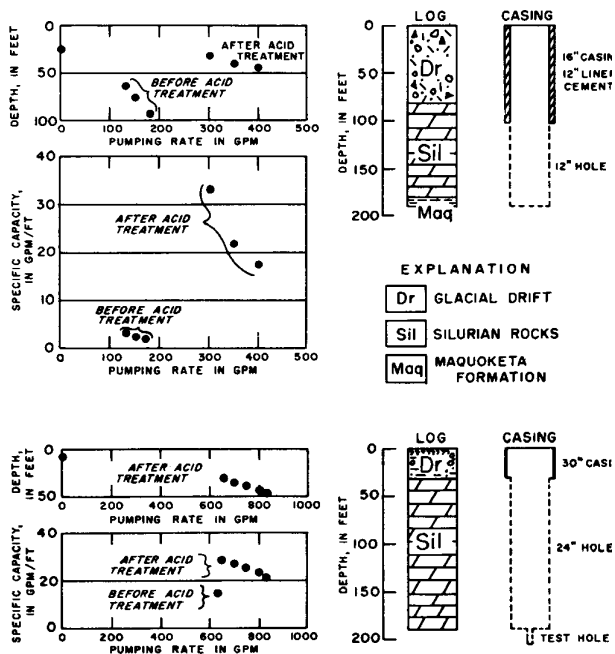


Figure 42. Step-drawdown test data showing the results of acid treatment of dolomite wells in DuPage County

When wells are operated at high pumping rates the pressure of the water in the dolomite aquifer is greatly reduced, carbon dioxide is liberated, and the water is unable to hold in solution its load of mineral salts. Consequently, calcium carbonate is precipitated in the openings of the well face and well wall, greatly reducing their perme-

## Flow-Net Studies

The results of two flow-net studies made in northeastern Illinois are presented in detail to illustrate the applicability of equations 35 and 38.

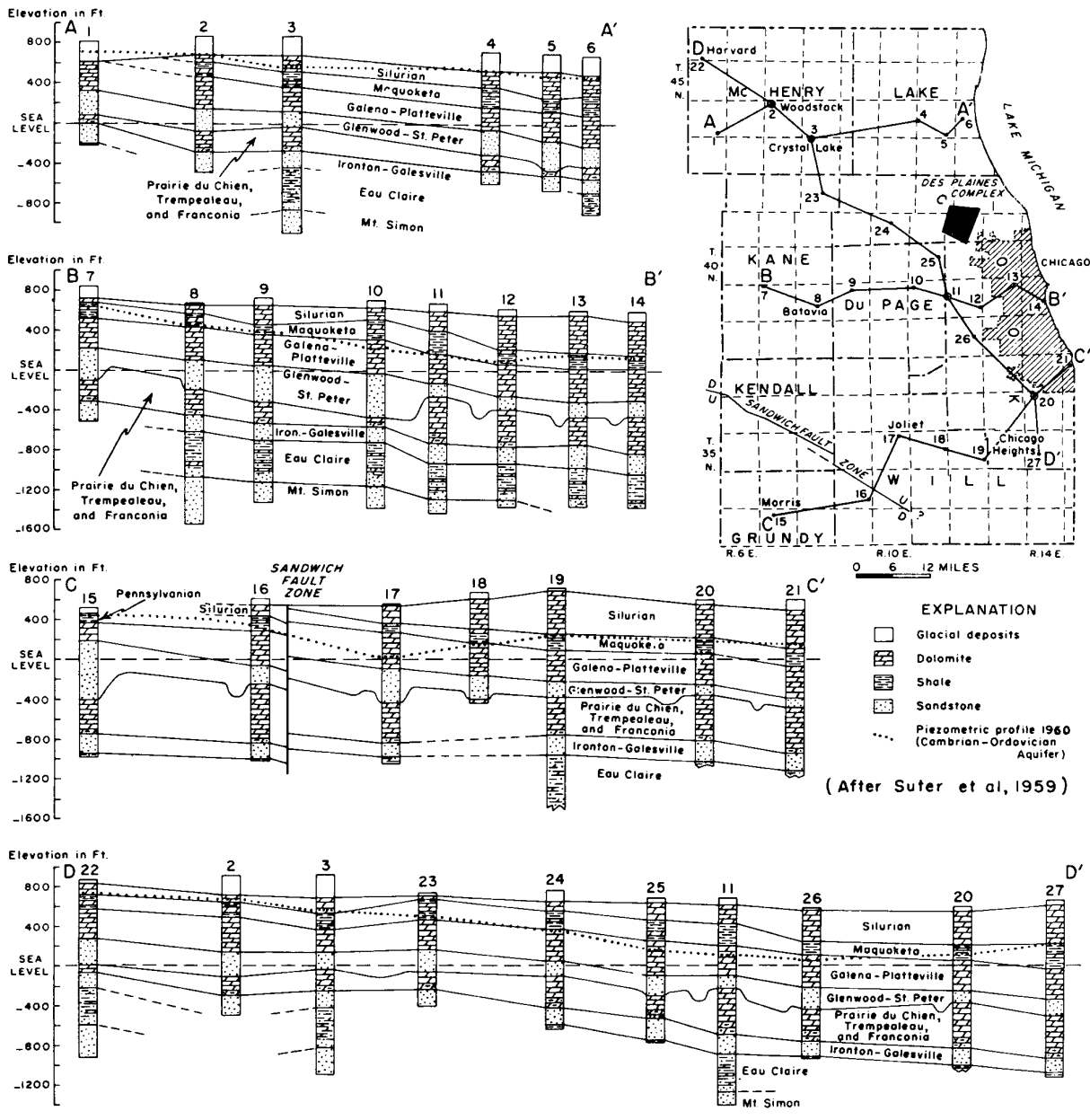


Figure 43. Cross sections of the structure and stratigraphy of the bedrock and piezometric profiles of the Cambrian-Ordovician Aquifer in northeastern Illinois

### Coefficient of Transmissibility

The piezometric surface of the Cambrian-Ordovician Aquifer in the vicinity of the city of Joliet in northeastern Illinois was studied to check the accuracy of the coefficients of transmissibility computed from the results of aquifer tests. The sequence, structure, and general characteristics of rocks in northeastern Illinois are shown in figure 43. The Cambrian-Ordovician Aquifer is underlain by shale beds of the Eau Claire Formation which have a very low permeability, and is overlain in large parts of northeastern Illinois by the Maquoketa Formation which confines the water in the aquifer under leaky artesian conditions.

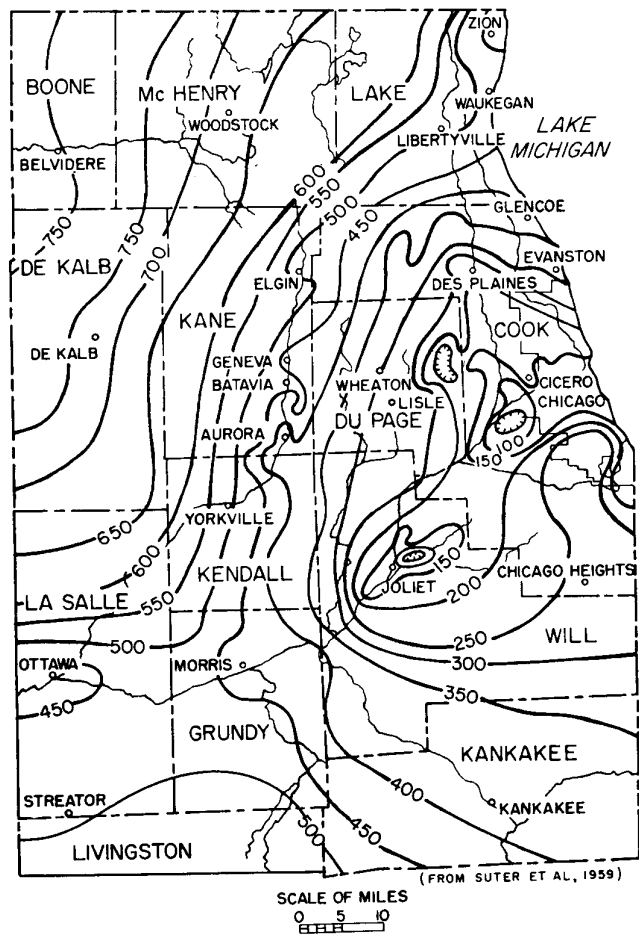


Figure 44. Piezometric surface of Cambrian-Ordovician Aquifer in northeastern Illinois in 1958

The piezometric surface of the Cambrian-Ordovician Aquifer in 1958 is shown in figure 44. The area bounded by isopiestic lines having elevations of 200 and 150 feet in the vicinity of Joliet was selected for flow-net analysis. The quantity of water  $Q$  moving toward Joliet midway between the 200-foot and 150-foot isopiestic lines is equal to the total pumpage from the Cambrian-Ordovician Aquifer in the Joliet area minus the amount of water taken from stor-

age within the area enclosed by the 150-foot isopiestic line. Because the coefficient of storage of the Cambrian-Ordovician Aquifer and the area enclosed by the 150-foot isopiestic line are very small, the amount of water taken from storage is negligible; therefore,  $Q$  is essentially equal to the total pumpage. Total pumpage from the Cambrian-Ordovician Aquifer in the Joliet area in 1958 was 11.6 mgd according to Suter et al (1959). The hydraulic gradient  $I$  and the length of cross section  $L$  midway between the 200-foot and 150-foot isopiestic lines, were estimated with figure 44 and equations 36 and 37. The average coefficient of transmissibility of the part of the Cambrian-Ordovician Aquifer within the Joliet cone of depression was computed, using the data mentioned above and equation 35, and is 16,600 gpd/ft. The value of  $T$  from flow-net analysis compares favorably with the coefficients of transmissibility computed from the results of the aquifer tests in the Joliet area given in table 13.

Table 13. Coefficients of transmissibility computed from aquifer-test data for the Joliet area

Well owner	Depth of well (ft)	Date of test	Pumping rate (gpm)	Coefficient of transmissibility (gpd/ft)
Village of Elwood	1645	1941	1345	16,200
Kankakee Ordnance Works	1649	1953	1253	17,400
Kankakee Ordnance Works	1569	1953	1220	17,000
City of Joliet	1620	1944	753	14,300
City of Joliet	1544	1946	600	16,200
City of Joliet	1608	1946	1290	17,100
Illinois State Penitentiary 1	1600	1948	650	19,100
Diagnostic Depot 3	1600	1948	642	19,300
City of Lockport	1572	1954	700	13,000
Village of Rockdale	1586	1946	293	16,500
Village of Romeoville	1537	1952	1016	16,000

From Suter et al (1959)

### Coefficient of Vertical Permeability

The Maquoketa Formation overlying the Cambrian-Ordovician Aquifer consists mostly of shale, dolomitic shale, and argillaceous dolomite and has a maximum thickness of about 250 feet in northeastern Illinois. The Cambrian-Ordovician Aquifer receives water from overlying glacial deposits largely in areas west of the border of the Maquoketa Formation shown in figure 45 where the Galena-Platteville Dolomite, the uppermost unit of the aquifer, is directly overlain by glacial deposits (Suter et al, 1959). Recharge of the glacial deposits in turn is derived from precipitation that falls locally. The piezometric surface map for the Cambrian-Ordovician Aquifer in the year 1864 (see figure 46A) indicates that, under natural conditions, water entering or recharging the aquifer was discharged by vertical leakage upward through the Maquoketa Formation and by leakage into the Illinois River Valley, in areas to the east and south.

The changes in artesian pressure produced by pumping since the days of early settlement have been pronounced and widespread. Pumpage from deep wells has increased from 200,000 gpd in 1864 to about 78 mgd in 1958. Figure

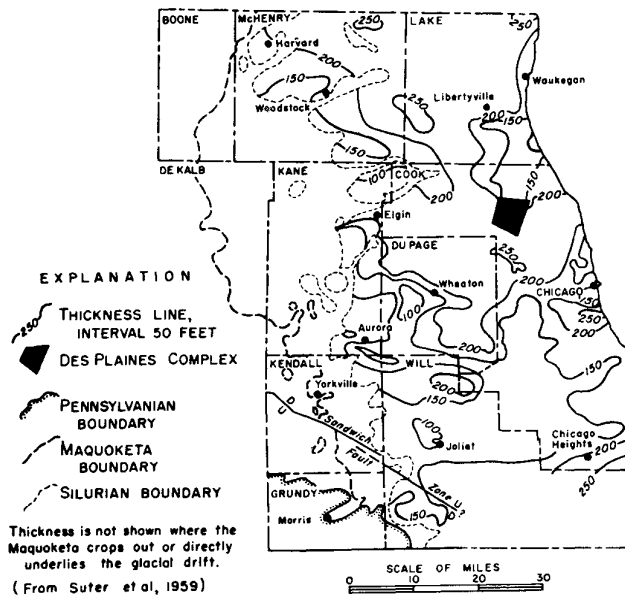


Figure 45. Thickness of the Maquoketa Formation in northeastern Illinois

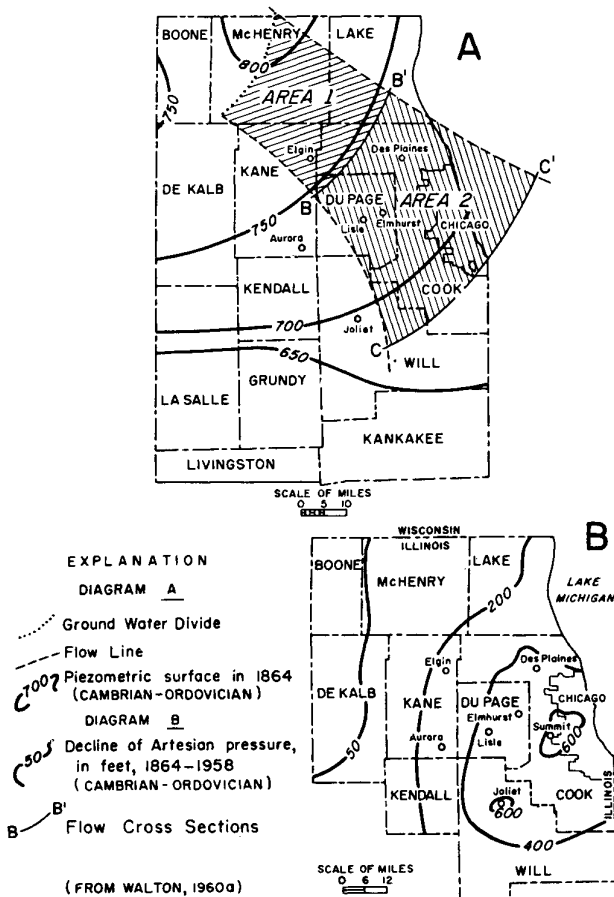


Figure 46. Piezometric surface of Cambrian-Ordovician Aquifer in northeastern Illinois, about 1864 (A); and decline in artesian pressure in Cambrian-Ordovician Aquifer, 1864-1958 (B)

46B shows the decline of artesian pressure in the Cambrian-Ordovician Aquifer from 1864 to 1958 as the result of heavy pumping. The greatest declines, more than 600 feet, have occurred in areas of heavy pumpage west of Chicago, at Summit and Joliet. In 1958, the piezometric surface of the Cambrian-Ordovician Aquifer was several hundred feet below the water table in most of northeastern Illinois, and downward movement of water through the Maquoketa Formation was appreciable under the influence of large differentials in head between shallow deposits and the Cambrian-Ordovician Aquifer (Walton, 1960a). The coefficient of vertical permeability of the Maquoketa Formation was computed by flow-net analysis.

Flow-lines were drawn from the ground-water divide in McHenry County toward the northern and southern boundaries of Cook County at right angles to the estimated piezometric surface contours for 1864 in figure 46A. The part of the aquifer (area 1) which is enclosed by the flow lines, the ground-water divide, and section B—B', was considered. In 1864, the piezometric surface was below the water table and downward leakage through the Maquoketa Formation into the aquifer was occurring in area 1. Leakage was equal to the quantity of water percolating through section B—B'. At section B—B' the hydraulic gradient of the piezometric surface was about 2 feet per mile and the distance between limiting flow lines was about 25 miles. Based on data given by Suter et al (1959) the average coefficient of transmissibility of the aquifer at section B—B' is about 19,000 gpd/ft. Using equation 60 and the data mentioned above, the quantity of water moving southeastward through the aquifer at section B—B' was computed to be about 1 mgd. Leakage downward through the Maquoketa Formation in area 1 was therefore about 1 mgd in 1864. As measured from figure 46A, area 1 is about 750 square miles. The average  $\Delta h$  over area 1 was determined to be about 85 feet by comparing estimated elevations of the water table and the piezometric surface contours in figure 46A. The average thickness of the Maquoketa Formation over area 1 from figure 45 is about 175 feet. Substitution of these data in equation 38 indicates that the average coefficient of vertical permeability of the Maquoketa Formation in area 1 is about 0.0001 gpd/sq ft (Walton, 1960a).

In 1864 the piezometric surface was above the water table southeast of section B—B', and the quantity of water entering the aquifer in area 1 was discharged by leakage up through the Maquoketa Formation in the areas between the limiting flow lines southeast of section B—B' in northeastern Illinois and northwestern Indiana. The average coefficient of vertical permeability of the Maquoketa Formation in area 2 was estimated to be about 0.00007 gpd/sq ft following procedures outlined for analysis of conditions in area 1.

Computations indicate that the average coefficient of vertical permeability of the Maquoketa Formation increases to the north and west. Available geologic information supports this conclusion. The lower unit of the Maquoketa

Formation, probably the least permeable of the three units, thins to the west. In addition, the Maquoketa Formation is the uppermost bedrock formation below the glacial deposits in a large part of area 1 and locally may be completely removed by erosion. Based on flow-net analysis and geologic data, the average coefficient of permeability of the Maquoketa Formation in northeastern Illinois is estimated to be about 0.00005 gpd/sq ft.

## Aquifer-Test Data Under Boundary Conditions

### Barrier Boundaries

An aquifer test was made by W. H. Walker of the State Water Survey in cooperation with Klingner & Associates, consulting engineers, and Layne-Western Co., well contractor, June 2, 1960. A group of wells (figure 47) located about 1½ miles north of the corporate limits of the village of St. David in sec. 10, T6N, R4E, in Fulton County was used. The generalized graphic logs of the wells are given in figure 48. The effects of pumping well 3—60 were measured in observation wells 1—60 and 2—60. Pumping was started at 10:00 a.m. and was continued for 6 hours at a constant rate of 62 gpm until 4:00 p.m.

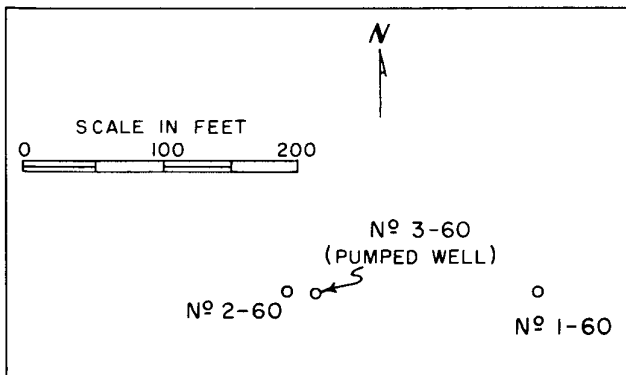


Figure 47. Map showing location of wells used in test near St. David

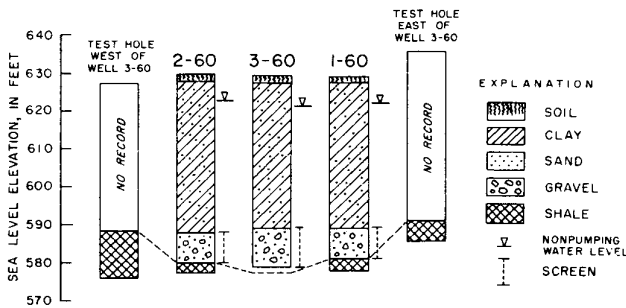


Figure 48. Generalized graphic logs of wells used in test near St. David

Drawdowns in the observation wells were plotted against time on logarithmic paper. The time-drawdown graphs for wells 1—60 and 2—60 are given in figures 49 and 50. Time-drawdown data for wells 1—60 and 2—60 are given in table 14.

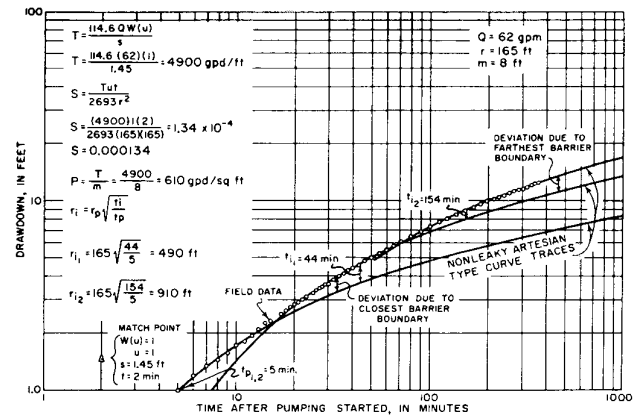


Figure 49. Time-drawdown graph for well 1-60 near St. David

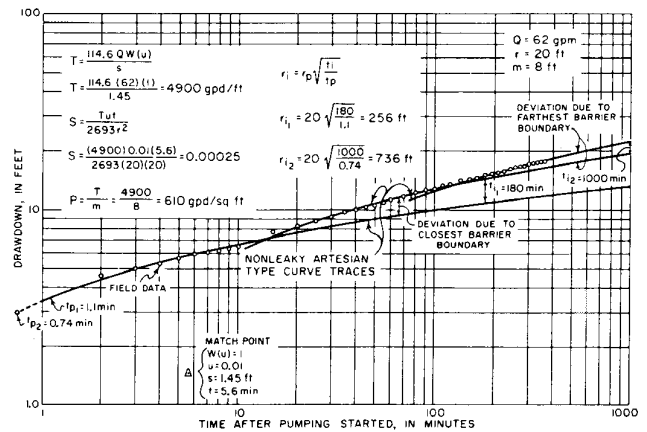


Figure 50. Time-drawdown graph for well 2-60 near St. David

Table 14. Time-drawdown data for test at St. David

Well 1-60		Well 2-60	
Time after pumping started (min)	Drawdown (ft)	Time after pumping started (min)	Drawdown (ft)
5	1.00	2	4.60
6	1.19	3	4.97
7	1.25	4	5.32
8	1.43	5	5.65
9	1.58	6	5.91
10	1.72	7	6.08
12	1.94	8	6.20
15	2.32	9	6.33
18	2.64	10	6.50
20	2.85	15	7.62
25	3.26	20	8.21
30	3.61	25	8.75
40	4.42	30	9.23
50	5.00	40	10.02
60	5.51	50	10.55
71	6.12	60	11.25
80	6.50	70	11.74
90	6.91	80	12.21
100	7.28	90	12.54
152	8.91	100	12.80
195	9.90	150	14.35
254	11.15	195	15.38
300	11.64	255	16.57
360	12.60	300	17.14
		360	17.78

Q = 62 gpm and r = 165 ft

Q = 62 gpm and r = 20 ft

The nonleaky artesian type curve was matched to early time-drawdown data and values of  $T$  and  $S$  were calculated using equations 14 and 15. After about 12 minutes of pumping the time-rate of drawdown in the observation wells increased and field data deviate upward from type-curve traces, indicating the presence of a barrier boundary. The nonleaky artesian type curve was again matched to later time-drawdown data affected by the barrier boundary. The correctness of the new match position was judged by noting that, in the second match position, the  $s$  value opposite a  $W(u)$  value of 1.0 is twice the  $s$  value opposite a  $W(u)$  value of 1.0 in the first match position. The divergence of the two type-curve traces at a time  $t_{i1}$  was determined. The time  $t_{p1}$  at which the first type-curve trace intersects an  $s$  value equal to the divergence at  $t_{i1}$  was noted. The distances from the observation wells to the image wells associated with the barrier boundary were then computed with equation 55.

After about 70 to 100 minutes of pumping the time-rate of drawdown in the observation wells again increased, and field data deviate upward from the second type-curve trace indicating the presence of a second barrier boundary. The nonleaky artesian type curve was matched to late time-drawdown data affected by both barrier boundaries. The correctness of the third match position was judged by noting that in the third match position the  $s$  value opposite a  $W(u)$  value of 1.0 is three times the  $s$  value opposite a  $W(u)$  value of 1.0 in the first match position. The divergence of the second and third type-curve traces at a time  $t_{i2}$  was determined. The time  $t_{p2}$  at which the first type-curve trace intersects an  $s$  value equal to the divergence at  $t_{i2}$  was noted. The distance from the observation wells to the image well associated with the second barrier boundary were then computed with equation 56.

The distances from each observation well to the image wells were scribed as arcs from the respective observation wells. Theoretically the arcs should intersect at common points, but the real aquifer is not a vertically bounded aquifer as assumed in the derivation of the image-well theory and as a result the arcs and their intersections are dispersed. In addition, only two observation wells are available so that the exact locations of the image wells, and therefore the barrier boundaries, cannot be determined with test data alone.

As indicated in figure 48, the aquifer occurs as a fill in a buried valley in shale bedrock. Based on aquifer-test data and geologic data, the boundaries were located at positions east and west of the pumped well. It should be pointed out that the boundaries determined with aquifer-test data occur at distances at which the change in thickness and hydraulic properties are great enough to constitute barrier boundaries. The boundaries represent a rectangular section which is equivalent hydraulically to the real aquifer.

The average values of  $T$  and  $S$  computed from time-drawdown data are 4900 gpd/ft and 0.0002, respectively. Based on an average saturated thickness of 8 feet, the co-

efficient of permeability is about 610 gpd/sq ft. Available data indicate that the aquifer is a thin strip of sand, and gravel approximately 600 feet wide which trends northeast to southwest through the test site area.

### Recharge Boundary

An aquifer test (Mikels, 1952) was made by Ranney Method Water Supplies, Inc., on November 19-22, 1952. A group of wells (figure 51) located along the shore of Lake Michigan within the city limits of Zion in sec. 26, T46N, R12E in Lake County was used. The generalized graphic logs of the wells are given in figure 52. The effects of pumping well A-P were measured in observation wells A-S-1, A-S-2, A-N-1, A-E-1, A-E-2, and A-E-3. The lake stage was also measured throughout the test. Pumping was started at 11:12 a.m. on November 19 and was continued for about 72 hours at a rate of 99 gpm until 11:30 a.m. on November 22. A power failure resulted in a short shutdown from 10:30 p.m. on November 19 to 12:15 a.m. on November 20. The hydrographs of water levels in observation wells and changes in the lake stage are shown in figure 53. The maximum drawdown in the pumped well was 12.8 feet.

Drawdowns in the observation wells for a pumping period of 53 hours, before the large change in lake stage occurred, were determined by comparing the extrapolated graphs of water levels measured before pumping started with graphs

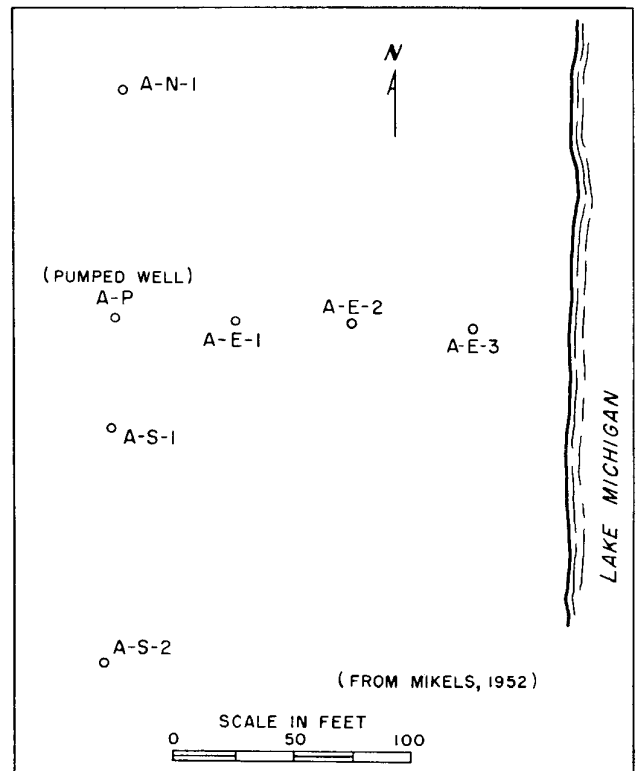


Figure 51. Map showing location of wells used in test at Zion

of water levels after 53 hours of pumping. Drawdown data are given in table 15. Figure 53 shows that the lake stage was about the same prior to the test as it was after 53 hours of pumping; therefore, water-level adjustments for change in lake stage are unnecessary. Drawdowns in the observation wells adjusted for the effects of dewatering were plotted on semilogarithmic paper against the distances from the respective observation wells to the pumped well as shown in figure 54.

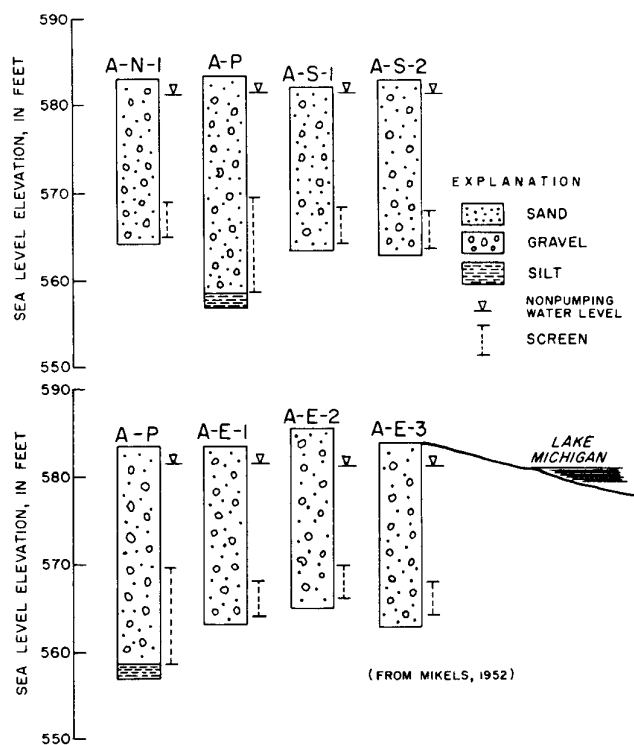


Figure 52. Generalized graphic logs of wells used in test at Zion

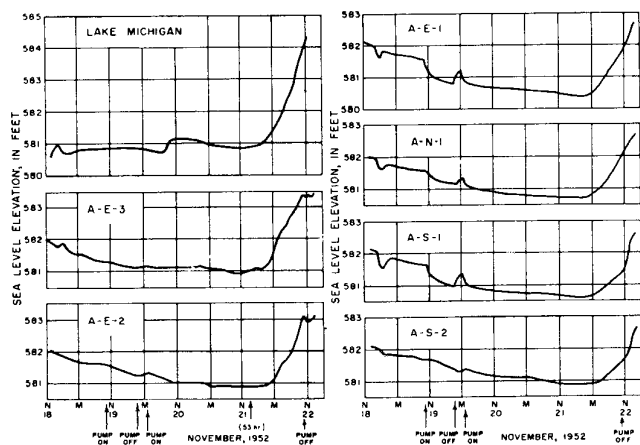


Figure 53. Lake stage and water levels in wells during test at Zion

Table 15. Distance-drawdown data for test at Zion

Well number	Distance from pumped well (ft)	Drawdown adjusted for dewatering (ft)
A-S-1	48	0.87
A-N-1	96	0.59
A-S-2	141	0.43
A-E-1	51	0.87
A-E-2	100	0.44
A-E-3	151	0.20

$Q = 99$  gpm and  $t = 3180$  min

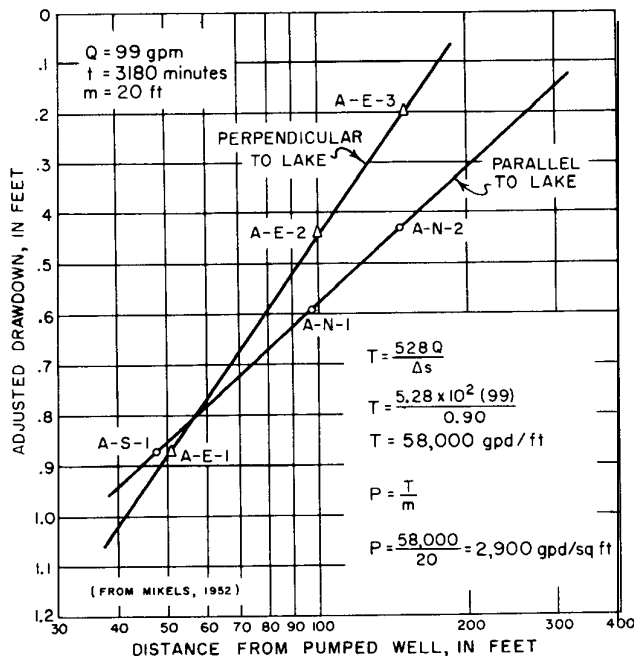


Figure 54. Distance-drawdown graphs for test at Zion

A straight line was drawn through the data for the observation wells parallel to the lake, and the slope of the line was substituted into equation 47 for computation of  $T$ . The coefficient of transmissibility was found to be 58,000 gpd/ft and the coefficient of permeability about 2900 gpd/sq ft.

Evidence of a hydraulic interconnection between the aquifer and the lake is shown by the similarity between lake and observation well hydrographs and by a comparison of slopes or hydraulic gradients of lines of wells perpendicular and parallel to the lake. As shown in figure 54, the slope of the line of wells perpendicular to the lake is much steeper than the slope of the line of wells parallel to the lake, indicating that the cone of depression was distorted by the presence of the lake and that water from the lake was diverted into the cone of depression by induced infiltration.

The time-rate of drawdown in the observation wells decreased a short time after pumping started; after a pumping period of 53 hours, water levels stabilized and near equilibrium conditions prevailed. Equation 16 indicates that the effects of gravity drainage were negligible after about 1 hour of pumping; therefore, most of the leveling off of water levels is due to the source of recharge.

Data in table 15, the computed value of  $T$ , and equations

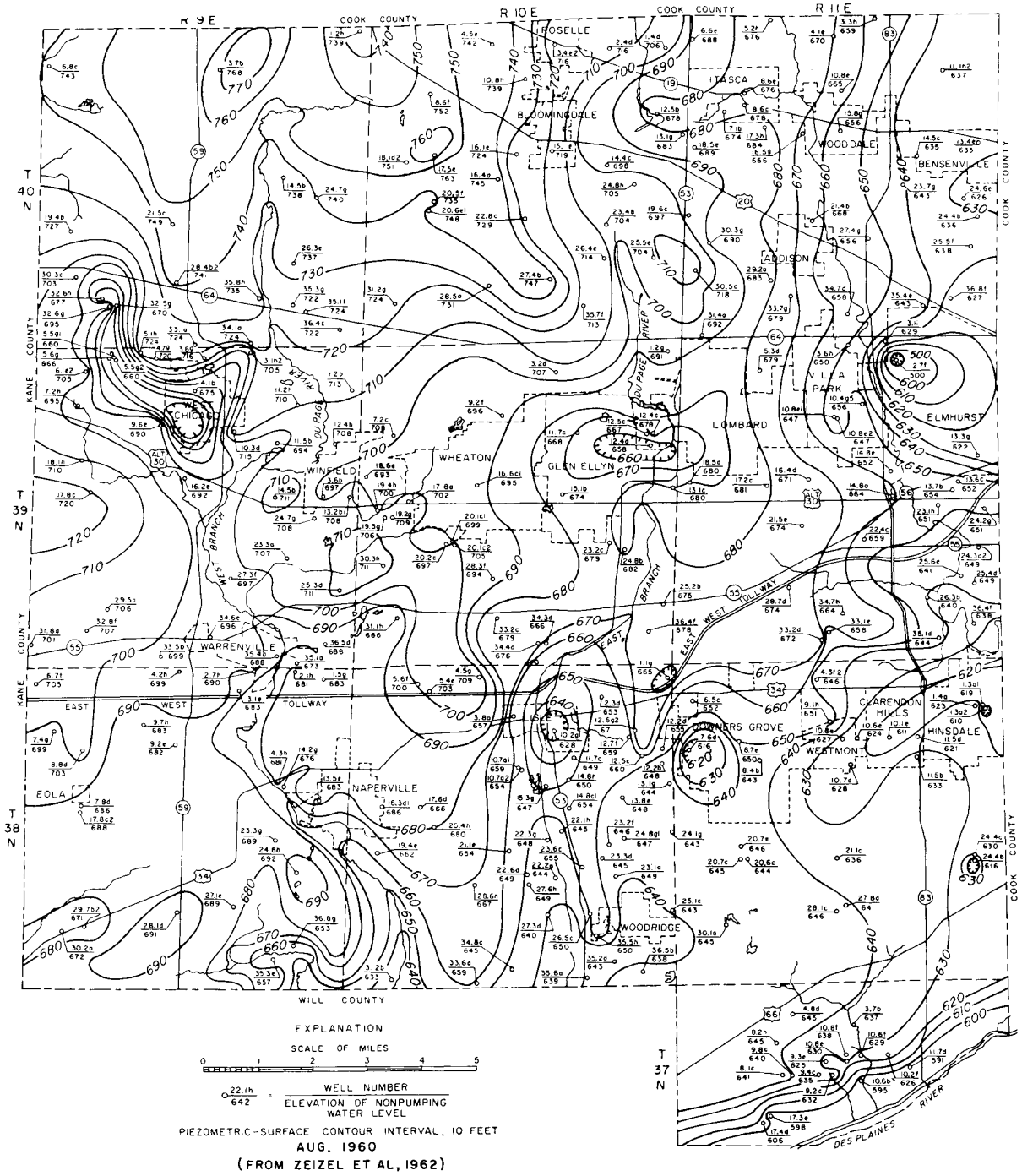


Figure 55. Piezometric surface of the Silurian dolomite aquifer in DuPage County

45 and 46 were used to determine the distance to the effective line of recharge. The distance  $a$  was computed to be 206 feet. The image well associated with the recharge boundary was located on a line perpendicular to the lake shore and at a distance of 412 feet from the pumped well.

Distances from the observation wells to the image well were measured. Knowing  $T$ ,  $a$ , and the distances from the observation wells to the image well, the coefficient of storage was computed with equations 48 through 52 by the process of trial and error. The average coefficient of storage is 0.01.

## Recharge Rates

### Area of Influence of Pumping

A study (Zeizel et al, 1962) was made to determine the rate of recharge to the Silurian dolomite aquifer in DuPage County. Recharge to the dolomite aquifer is derived from vertical leakage of water through overlying glacial drift and layers of dolomite to permeable zones within the dolomite.

A shaly dolomite unit which greatly retards the vertical movement of ground water occurs near the base of the Niagaran Series, the upper unit of the Silurian rocks. The shaly dolomite unit averages about 19 feet in thickness in DuPage County except where thinned or removed by erosion. Most high capacity dolomite wells in the county penetrate both the Niagaran and Alexandrian Series, and although most of the water is obtained from the part of the Niagaran Series above the shaly dolomite unit, large quantities of water are also derived from the Alexandrian Series below the shaly dolomite unit in many areas.

The rate of recharge to the dolomite aquifer in four areas in the county was estimated with the piezometric surface map in figure 55. Flow lines were drawn at right angles to piezometric surface contours, and the areas of influence of production wells in 1) the Wheaton-Glen Ellyn-Lombard area, 2) Downers Grove-Westmont-Clarendon Hills-Hinsdale area, 3) Argonne National Laboratory area, and 4) West Chicago area were outlined as shown in figure 56. Total ground-water pumpage from the Silurian dolomite aquifer within the four areas of influence in 1960 are given in table 16. Comparisons of pumpage and water-level graphs for wells in the areas of influence indicate that water-level declines are directly proportional to pumping rates and that water levels stabilize shortly after pumping rate changes; therefore, recharge balances discharge. Recharge rates in table 16 were computed by substituting data on pumpage and areas of influence into equation 57.

The glacial drift deposits are on a gross basis very similar in character in the four areas of influence and average vertical hydraulic gradients do not differ appreciably from area to area. Thus, the low recharge rate in the West Chicago area cannot be explained by differences in character of the glacial drift deposits or average hydraulic gradients. In the Wheaton-Glen Ellyn-Lombard and Downers Grove-

Westmont-Clarendon Hills-Hinsdale areas most of the water pumped is obtained from the thick Niagaran rocks above the shaly dolomite unit. The Niagaran rocks are thin in the West Chicago area and most of the water pumped is obtained from the Alexandrian rocks below the shaly dolomite unit. The dense, shaly dolomite and shale of the basal beds of the Niagaran Series may have restricted development of a weathered zone of solutionally-enlarged openings in the upper part of the dolomite and thereby restricted development of the permeability necessary for recharge to the underlying Alexandrian aquifer. Thus, the shaly dolomite unit retards leakage and exerts an important influence on recharge to the Silurian dolomite aquifer in DuPage County (Zeizel et al, 1962).

Areas in the county where recharge is probably low, and about the same as in the West Chicago area, were delineated by assuming that recharge is limited east of the Niagaran-Alexandrian contact where rocks of the Niagaran Series overlying the shaly dolomite unit are less than 50 feet

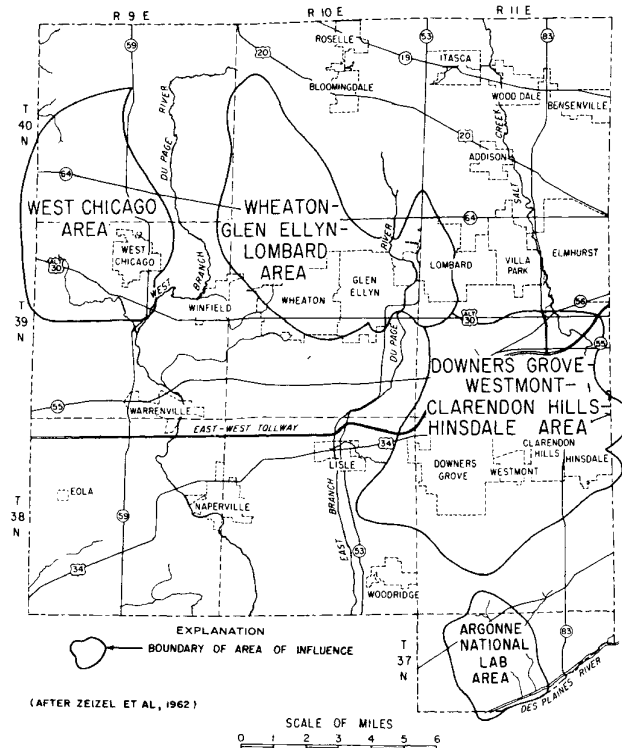


Figure 56. Areas influenced by withdrawals from wells in the Silurian dolomite aquifer in selected parts of DuPage County

Table 16. Recharge rates for the Silurian dolomite aquifer in DuPage County

Area of influence	1960 pumpage (mgd)	Area (sq mi)	Recharge rate (gpd/sq mi)
Wheaton-Glen Ellyn-Lombard	4.5	32.5	138,000
Downers Grove-Westmont-Clarendon Hills-Hinsdale	6.3	46.2	136,000
West Chicago	1.8	28.0	64,000
Argonne National Laboratory	1.2	7.6	158,000

thick or in areas where the Silurian rocks are missing. Areas where recharge is about the same as in the Wheaton-Glen Ellyn - Lombard, Downers Grove - Westmont - Clarendon Hills-Hinsdale, and Argonne areas were delineated by assuming recharge is high 1) west of the Niagaran-Alexandrian contact where rocks of the Alexandrian Series are more than 25 feet thick and 2) east of the Niagaran-Alexandrian contact where rocks of the Niagaran Series overlying the shaly dolomite unit are more than 25 feet thick.

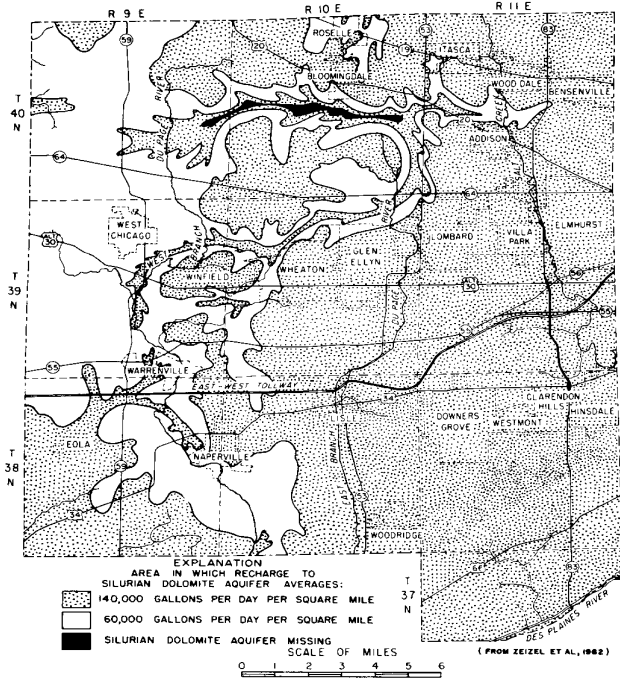


Figure 57. Estimated recharge rates for the Silurian dolomite aquifer in DuPage County

A map showing estimated recharge rates for the Silurian dolomite aquifer is shown in figure 57. It is probable that recharge averages about 60,000 gpd/sq mi in parts of the western one-third of the county and averages about 140,000 gpd/sq mi in large areas of the eastern two-thirds of the county.

### Flow-Net Analysis

Equation 59 was used to determine the rate of recharge to the Cambrian-Ordovician Aquifer in parts of northeastern Illinois west of Joliet. Limiting flow lines were drawn on the piezometric surface map in figure 58 from recharge areas west of the border of the Maquoketa Formation through DeKalb, Kendall, LaSalle, and Grundy Counties to the Joliet cone of depression. The quantities of water moving through the sections of the aquifer A—A' and B—B' west of the border of the Maquoketa Formation were computed with equation 60. Based on data given by Suter et al (1959), the average coefficient of transmissibility of the aquifer at sections A—A' and B—B' are 22,000 and 19,800 gpd/ft, respectively. From figure 58, the average hydraulic gradients and widths of flow cross sections are as given in table 17.

The difference between the quantity of water moving through sections A—A' and B—B', 5,270,000 gpd, is equal to the amount of recharge to the aquifer plus the amount of water taken from storage within the aquifer in the area between the flow cross sections.

Data given by Suter et al (1959) and Sasman et al (1961) indicate that the average water-level decline in the area between flow cross sections A—A' and B—B' was about 0.005 fpd during 1958. Based on data given by Suter, the average coefficient of storage in the area between flow

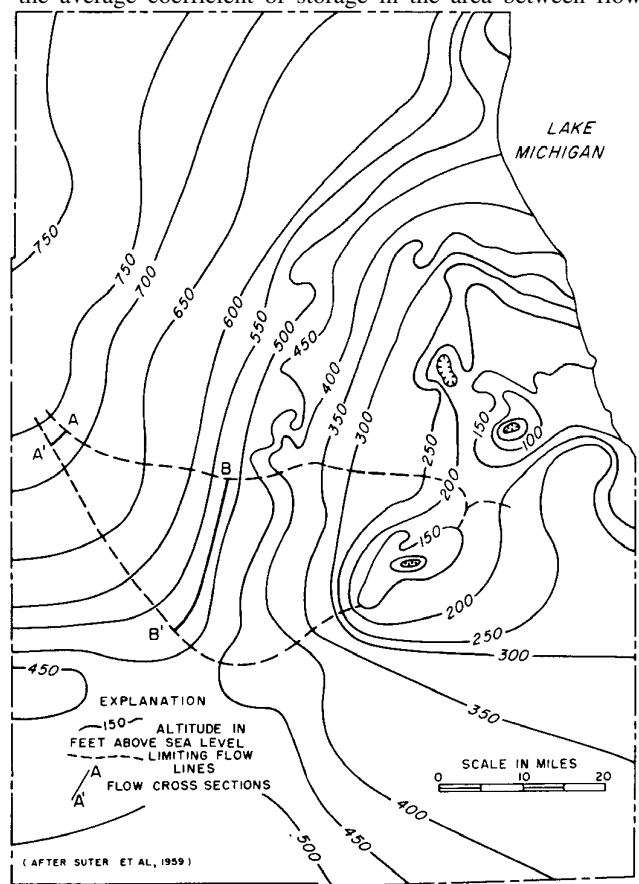


Figure 58. Flow-net analysis of the piezometric surface of the Cambrian-Ordovician Aquifer in northeastern Illinois in 1958

Table 17. Results of flow-net analysis for area west of Joliet

Flow cross section	Coefficient of transmissibility (gpd/ft)	Hydraulic gradient (ft/mi)	Length of flow cross section (mi)	Discharge through flow cross section (gpd)
A—A'	22,000	8.77	2.6	500,000
B—B'	19,800	13.16	20.4	5,320,000

cross sections A—A' and B—B' is 0.00035. As measured from figure 58, the area between flow cross sections A—A' and B—B' is about 250 square miles. Recharge to the area between flow cross sections A—A' and B—B' was computed to be about 21,000 gpd/sq mi by substituting the above data and table 17 data in equation 59.

### Leakage Through Confining Beds

Even though the coefficient of vertical permeability is very low, leakage in 1958 through the Maquoketa Formation in northeastern Illinois was appreciable. The area of the confining bed within the part of Illinois shown in figure 45 through which leakage occurred (4000 square miles) was large, and the average head differential between the piezometric surface of the Cambrian-Ordovician Aquifer and the water table (300 feet) was great. Computations made with equation 58 using the data given above, and assuming an average  $m'$  of 200 feet and a  $P'$  of 0.00005 gpd/sq ft, indicate that leakage was about 8.4 mgd or about 11 per cent of the water pumped from deep sandstone wells in 1958.

### Ground- Water and Hydrologic Budgets

Ground-water recharge to part of the Panther Creek drainage basin during years of above (1951), near (1952) and below (1956) normal precipitation was appraised using ground-water and hydrologic budgets (Schicht and Walton, 1961). Panther Creek drainage basin covers 95 square miles and is in north-central Illinois about 30 miles east of Peoria and about 20 miles north of Bloomington. The basin is above a stream-gaging station about 4 miles northwest of the city of El Paso and is in T26N to T28N and R1E to R3E. The topography consists mostly of gently undulating uplands whose relief seldom exceeds 20 feet per mile. Deposits of glacial drift averaging about 100 feet thick cover the bedrock and constitute the main features of the present land surface. The glacial deposits are immediately underlain by relatively impermeable bedrock formations consisting predominately of shale. The mean annual temperature is 51F and normal annual precipitation is 33.6 inches.

During this investigation ground-water levels were measured continuously in 5 observation wells equipped with recording gages. The record of streamflow was determined by a recording gage on Panther Creek at the lower end of the basin. Precipitation was measured by a network of precipitation gages whose density averaged 10.6 square miles per gage. Mean daily ground-water stage, streamflow, and precipitation were plotted as yearly hydrographs. As examples, graphs for the year 1952 are shown in figures 59, 60, and 61.

Rating curves were prepared to determine the relationship between mean ground-water stage and ground-water runoff. Dates were selected based on equation 63 when streamflow consisted entirely of ground-water runoff. Mean ground-water stages were plotted against ground-water

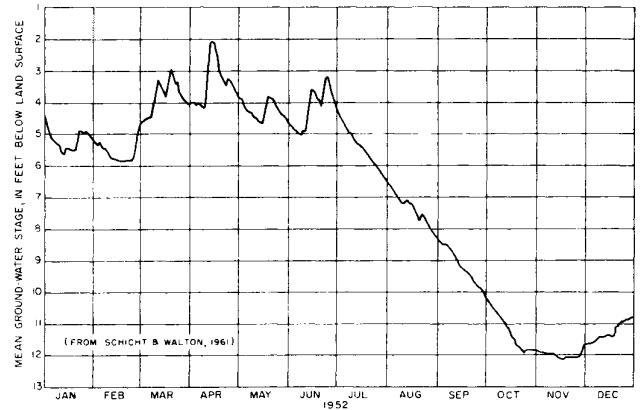


Figure 59. Mean daily ground-water stage in Panther Creek basin, 1952

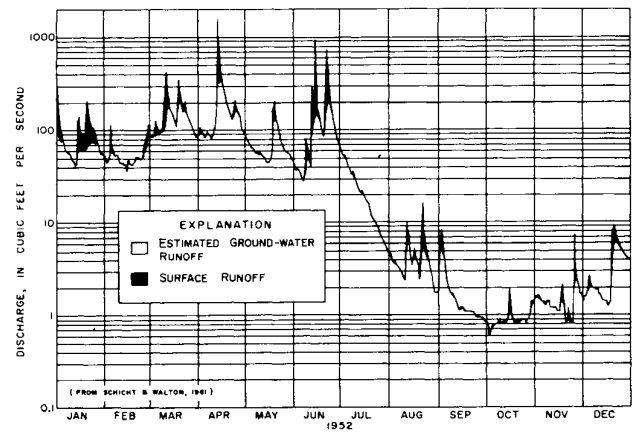


Figure 60. Mean daily streamflow in Panther Creek basin, 1952

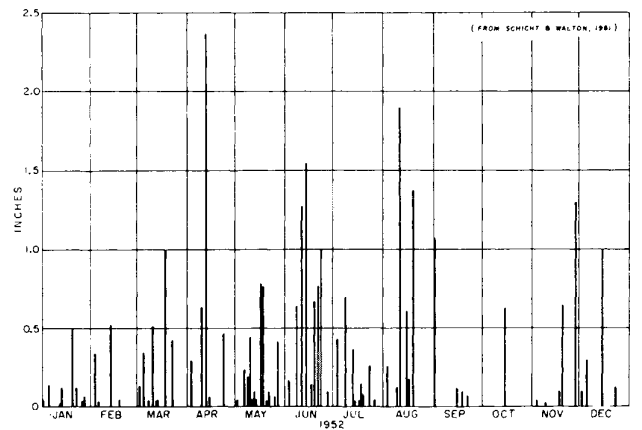


Figure 61. Mean daily precipitation in Panther Creek basin, 1952

runoff on corresponding dates as shown in figure 62. In figure 62, closed circles represent sets of data for dates, November to April, when evapotranspiration is at a minimum; open circles represent sets of data for dates, April through October, when evapotranspiration is appreciable.

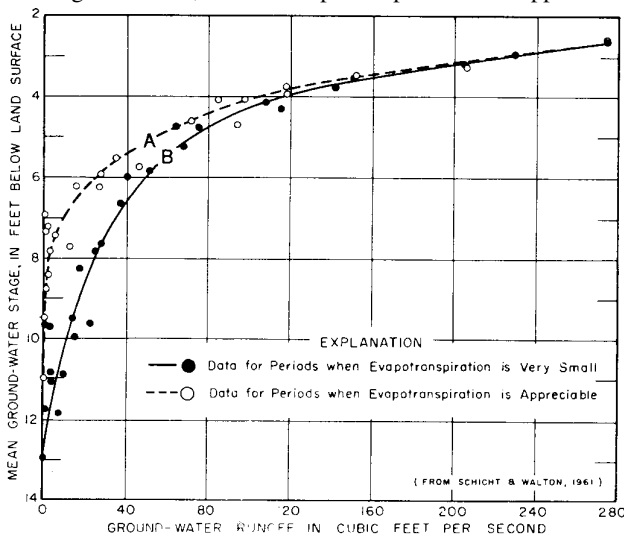


Figure 62. Rating curves of mean ground-water stage versus ground-water runoff for gaging station in Panther Creek basin

Ground-water runoff corresponding to each mean ground-water stage during the study periods was read directly from the rating curves. Curve A was used with data for dates April through October, and curve B was used with data for the rest of the year. Daily ground-water runoff was plotted on streamflow hydrographs and lines were drawn connecting points to describe ground-water runoff hydrographs as illustrated in figure 60. Monthly and annual ground-water runoff, surface runoff, and streamflow during 1951, 1952, and 1956, expressed in inches of water over the basin, are given in table 18.

Table 18. Monthly and annual streamflow, ground-water runoff, and surface runoff in inches, 1951, 1952, and 1956, Panther Creek basin

Month	1951		1952		1956				
	$R_s$	$R_g$	$R$	$R_s$	$R_g$	$R$			
Jan	0.61	0.16	0.77	0.39	0.77	1.16	neg*	0.01	0.01
Feb	2.85	0.15	3.00	0.08	0.57	0.65	0.14	0.08	0.22
Mar	0.97	0.30	1.27	0.43	1.57	2.00	0.01	0.04	0.05
Apr	1.08	1.44	2.52	0.65	1.94	2.59	0.03	0.03	0.06
May	0.12	0.82	0.94	0.06	0.82	0.88	0.34	0.08	0.42
June	1.80	0.56	2.36	1.03	1.10	2.13	0.04	0.07	0.11
July	3.63	1.13	4.76	neg	0.27	0.27	0.04	0.03	0.07
Aug	0.16	0.22	0.38	0.01	0.04	0.05	0.01	0.01	0.02
Sept	0.03	0.10	0.13	neg	0.02	0.02	neg	neg	neg
Oct	0.07	0.22	0.29	neg	0.01	0.01	neg	neg	neg
Nov	0.97	0.55	1.52	neg	0.02	0.02	neg	0.01	0.01
Dec	0.05	0.35	0.42	0.01	0.03	0.04	neg	0.01	0.01
Annual	12.34	6.00	18.34	2.66	7.16	9.82	0.61	0.37	0.98

\*negligible

$R_s$  = surface runoff;  $R_g$  = ground-water runoff;  $R$  = streamflow

From Schicht and Walton (1961)

Mean daily ground-water evapotranspiration, April through October, was estimated with figure 62 by noting the difference between curves A and B for each mean daily ground-water stage. Monthly and annual ground-water evapotranspiration for 1951, 1952, and 1956 are given in table 19.

Table 19. Monthly and annual ground-water evapotranspiration in inches, 1951, 1952, and 1956, Panther Creek basin

Month	$ET_g$		
	1951	1952	1956
Jan	neg*	neg	neg
Feb	neg	neg	neg
Mar	neg	neg	neg
Apr	0.08	0.13	0.06
May	0.27	0.43	0.11
June	0.18	0.18	0.12
July	0.05	0.47	0.13
Aug	0.34	0.33	0.14
Sept	0.23	0.28	0.12
Oct	0.04	0.19	0.06
Nov	neg	neg	neg
Dec	neg	neg	neg
Annual	1.19	2.01	0.74

\*negligible

From Schicht and Walton (1961)

The width of the lowlands adjacent to Panther Creek through which underflow occurs is about 500 feet. The thickness of the glacial drift is estimated to be less than 25 feet and the hydraulic gradient of the water table in the vicinity of the stream-gaging station is less than 50 feet per mile. The coefficient of transmissibility of the glacial deposits is in the magnitude of 500 gpd/ft. By substituting the above data in equation 60, underflow was computed to be about 0.01 cfs and is so small that it was omitted from budget computations.

Computations of gravity yield  $Y_g$  were made using equation 65 and data for nine inventory periods during winter and early spring months. Data and computations for one inventory period, January 1 to March 31, 1951, are given as an example in table 20.

Table 20. Results of gravity yield analysis for Panther Creek basin

Inventory period 1951	$P$ (in.)	$R$ (in.)	$ET$ (in.)	$\Delta H$ (ft)	Average time of drainage preceding inventory period (days)
Jan 1—Mar 31	6.93	5.04	0.90	4.7	23
$Y_g = \frac{P - R - ET}{12 \Delta H} 100$					
$Y_g = \frac{6.93 - 5.04 - 0.90}{12 \times 4.7} 100 = 1.8 \text{ per cent}$					

Values of  $Y_g$  were plotted against the average time of drainage preceding the inventory periods as shown in figure 63. Monthly and annual increases or decreases in ground-

water storage during 1951, 1952, and 1956 were estimated by multiplying mean ground-water stage changes by appropriate values of  $Y_g$  given in figure 63. Data on changes in ground-water storage appear in table 21.

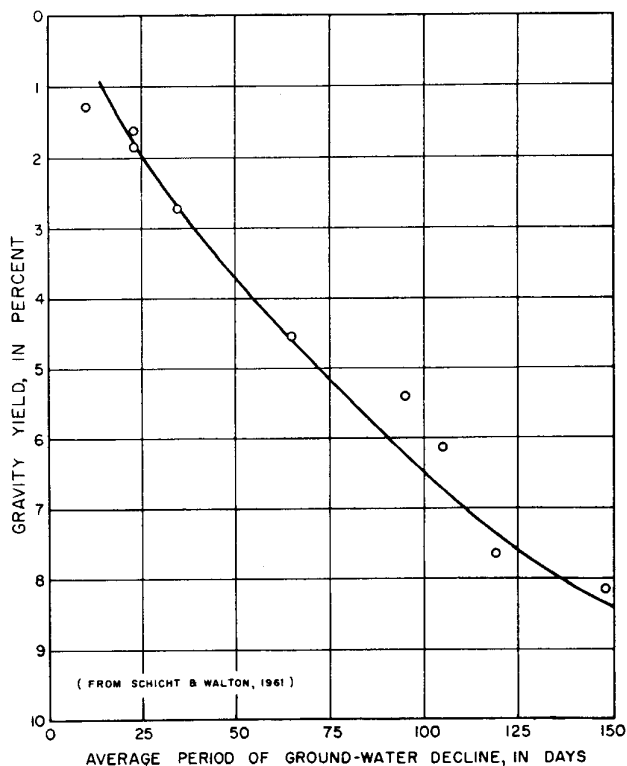


Figure 63. Graph showing relation of gravity yield and average period of drainage for Panther Creek basin

Table 21. Monthly and annual ground-water recharge and changes in storage in inches, 1951, 1952, and 1956, Panther Creek basin

Month	1951		1952		1956	
	$P_g$	$\Delta S_g$	$P_g$	$\Delta S_g$	$P_g$	$\Delta S_g$
Jan	0.44	0.28	0.69	-0.08	neg	-0.01
Feb	0.20	0.05	0.57	neg*	0.29	0.21
Mar	1.16	0.86	1.71	0.14	neg	-0.04
Apr	2.20	0.68	1.92	-0.15	0.11	0.02
May	0.89	-0.20	1.11	-0.14	0.20	0.01
June	0.79	0.05	1.36	0.08	0.09	-0.10
July	1.03	-0.15	0.15	-0.59	0.06	-0.10
Aug	0.41	-0.15	0.18	-0.19	0.06	-0.09
Sept	0.12	-0.21	0.03	-0.27	0.02	-0.10
Oct	0.03	-0.23	0.02	-0.18	0.02	-0.04
Nov	0.88	0.33	0.02	neg	0.01	neg
Dec	0.23	-0.12	0.27	0.24	0.01	neg
Annual	8.38	1.19	8.03	-1.14	0.87	-0.24

\*negligible

From Schicht and Walton (1961)

Monthly and annual ground-water recharge estimated by balancing equation 61 are given in table 21. Ground-water recharge during the three years ranged from 8.38 inches in 1951 to 0.87 inch in 1956. Ground-water recharge was 19 per cent of precipitation during a year of above

normal precipitation, 4.5 per cent of precipitation during a year of below normal precipitation, and 25 per cent of precipitation during a year of near normal precipitation. Data in table 21 show the pronounced adverse effects of extended dry periods on ground-water recharge. Even during a year of near normal precipitation very little ground-water recharge occurs during the 6 months July through November.

### Model Aquifer and Mathematical Model for Arcola Area

Applicability of model aquifers and mathematical models may be demonstrated by a case history (Walker and Walton, 1961) of ground-water development at the village of Arcola in east-central Illinois.

The village of Arcola is located in the southern part of Douglas County, 23 miles south of the city of Champaign and 45 miles east-southeast of the city of Decatur. The municipal water supply is obtained from wells in the unconsolidated deposits within and near the city corporate limits.

Based on geologic studies made by the Illinois State Geological Survey, the unconsolidated glacial deposits in the Arcola area are mainly Wisconsinan and Illinoian in age and range in thickness from 80 to 125 feet, as shown in figure 64. These deposits consist primarily of ice-laid till with some permeable water-laid silt and sand-and-gravel outwash. The thicker sections of glacial materials are contained in a valley cut into the bedrock which consists mainly of shale. The thicker and more permeable outwash materials, hereafter referred to as the aquifer, are generally found in the lower part of the drift and are Illinoian in age.

The thick upper unit of the Wisconsinan glacial till, which occurs from the surface to an average depth of 60 feet, contains a high percentage of silt and clay. The lower Wisconsinan unit and the Illinoian deposits immediately overlying the aquifer, hereafter referred to as the confining bed, contain sand lenses within sandy till. The aquifer contains a large amount of fine sand and silt and its permeability is not great.

The geologic cross section and the aquifer-thickness map shown in figure 64 were drawn from the few available drillers' logs of wells and test holes. As is often the case, data are not sufficient for a rigorous description of the areal extent of the aquifer. Analysis of existing geologic information suggests that the aquifer occurs as a thin and narrow strip of permeable sand and gravel exceeding 20 feet in thickness in many places and trending from northeast to southwest through Arcola. The more permeable part of the aquifer suitable for development by wells ranges in width from about 800 to less than 200 feet. Water occurs under leaky artesian conditions and recharge is derived from the vertical leakage of water through the confining bed into the aquifer.

During the period 1940 to 1955, five aquifer tests were made at Arcola to determine the hydraulic properties of the aquifer. Based on aquifer-test data, the coefficient of permeability of the aquifer ranges from 280 to 660 gpd/sq ft

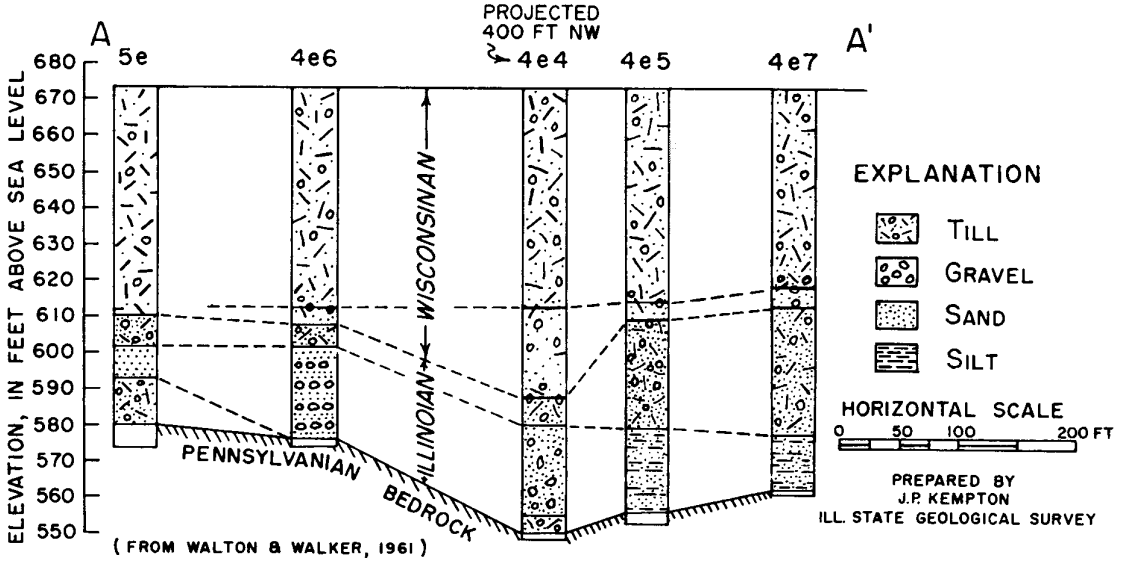
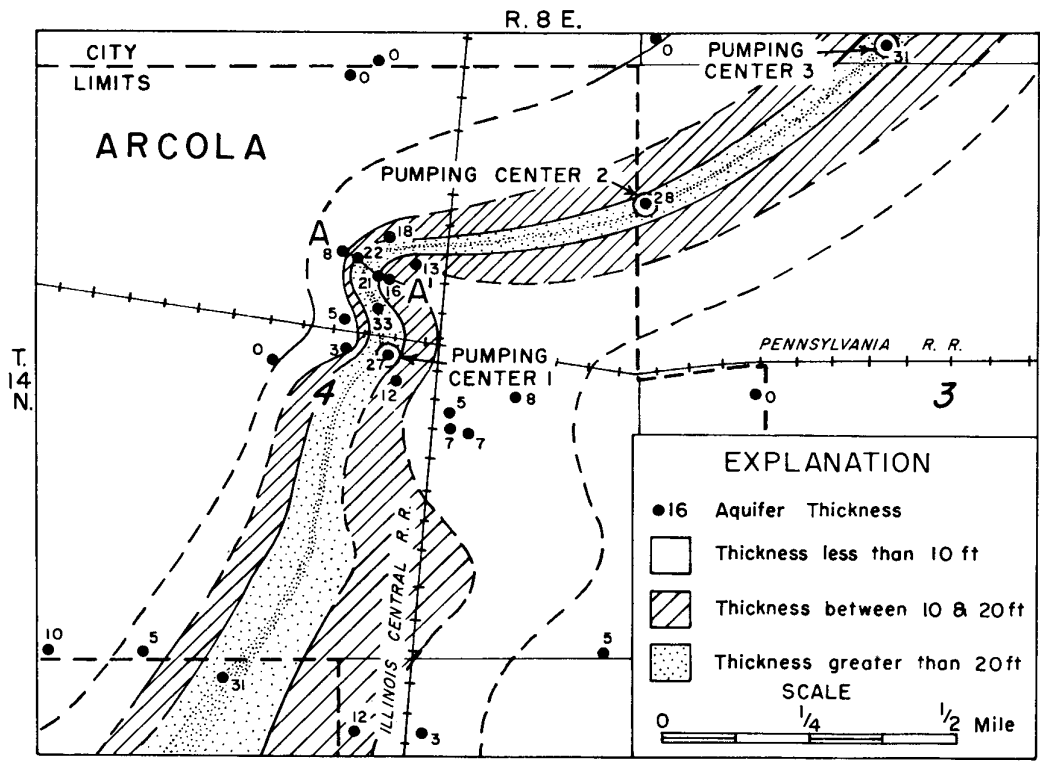


Figure 64. Map and geologic cross section showing thickness and areal extent of uifer at Arcola

and the coefficient of transmissibility ranges from 2200 to 18,000 gpd/ft. The smaller values of  $T$  and  $P$  reflect thinner and less permeable deposits near the edge of the aquifer, whereas the larger values reflect much thicker and more permeable deposits near the center of the aquifer. The average coefficient of storage of the aquifer is 0.001.

The municipal water supply has been obtained from the three pumping centers shown in figure 64. Average daily ground-water withdrawal increased from 20,000 gallons in 1891 to 146,000 gallons in 1959.

Past records of water-level decline and pumpage and analytical methods were used to determine the practical sustained yield of the aquifer. The practical sustained yield is here defined as the maximum amount of water that can be continuously withdrawn from existing wells without eventually lowering water levels below tops of screens in existing production wells.

An idealized model aquifer (Walton and Walker, 1961) that duplicates geohydrologic conditions in the Arcola area was created. Major factors considered in creating the model aquifer were: 1) the external barrier boundaries (bedrock walls) are tapered and irregular in shape; 2) the bedrock walls are not entirely impervious and some subsurface flow will occur from the bedrock into the aquifer, and thus the effective boundaries are not likely to coincide exactly with physical boundaries; 3) the hydraulic properties vary from place to place and are highly variable in the proximity of boundaries but are fairly uniform on a gross basis; and 4) the vertical permeability and thickness of the confining bed varies from place to place but are fairly uniform on a gross basis. With these factors taken into account, the results of geologic and hydrologic studies indicate that it is possible to simulate complex aquifer conditions with an infinite strip of sand and gravel which is 400 feet wide, 20 feet thick, bounded on the sides and bottom by impermeable material, and overlain by a confining bed 70 feet thick. The model aquifer and its orientation with respect to Arcola are shown in figure 65A. The average coefficients of transmissibility and storage of the model aquifer are 10,000 gpd/ft and 0.001, respectively.

Most drawdown data collected during the aquifer tests at Arcola are affected by barrier boundaries and it is impossible to isolate the effects of the leakage through the confining bed. Although the coefficient of vertical permeability of the confining bed cannot be determined from aquifer-test data, it can be estimated with the model aquifer.

The water-level decline in an observation well near pumping center 1 was computed using a mathematical model based on the model aquifer, calculated hydraulic properties of the aquifer, the image-well theory, the steady-state leaky artesian formula described by Jacob (1946a), estimated pumpage data, and several assumed values of the coefficient of vertical permeability. The coefficient of vertical permeability that resulted in a computed decline equal to the actual observed decline was assigned to the confining bed.

The pumping center, the observation well, and image

wells associated with the boundaries of the model aquifer were drawn to scale on a map as shown in figure 65B. The boundaries are parallel, therefore an image-well system extending to infinity is required. However, in practice it is only necessary to add pairs of image wells until the effect of the next pair has no measurable influence. Semilogarithmic distance-drawdown graphs were constructed based on calculated hydraulic properties of the model aquifer, assumed coefficients of vertical permeability of the confining bed, and past ground-water withdrawals. The distances  $r_e$  from the pumped well beyond which drawdown is not measurable were determined from the distance-drawdown graphs. Image wells at greater distances than  $r_e$  were not considered. The map showing the location of the pumping center, observation well, and image wells and the distance-drawdown graph constitute the mathematical model for the Arcola area.

The distances between the observation well, the pumping center, and the image wells were scaled from the mathematical model. The water-level decline in the observation well was computed with data on past pumpage by using the distance-drawdown graph to compute the effects of the real and image wells.

The observed decline in the observation well for a pumping rate of 115,000 gpd is 42 feet. A water-level decline of 42 feet was computed with a mathematical model based on a coefficient of vertical permeability of 0.04 gpd/sq ft. Therefore, a coefficient of vertical permeability of 0.04 gpd/sq ft was assigned to the confining bed overlying the model aquifer.

To test the mathematical model, the drawdowns recorded at pumping centers 2 and 3 caused by pumping center 1 were compared with drawdowns computed with the mathematical model. Actual declines at pumping centers 2 and 3 of 30 to 17 feet, respectively, are within a few per cent of the computed declines, 32 and 19 feet, respectively. The close agreement between computed and actual declines indicates that the model aquifer and mathematical model closely describe the geohydrologic conditions at Arcola. It is reasonable to assume that the model aquifer and mathematical model may be used to predict with reasonable accuracy the effects of future ground-water development and the practical sustained yield of the aquifer.

The mathematical model described here is based on a particular combination of aquifer boundaries and properties. There are probably other mathematical models involving several slightly different combinations of parameters which would also duplicate aquifer conditions.

In 1959 the multiple-well system at Arcola consisted of three wells ranging in depth from 106 to 122 feet and spaced 2500 feet apart in the more permeable parts of the aquifer as shown in figure 64. Available drawdowns in the wells, assuming pumping levels above the screens, range from 66 to 75 feet. Computations made with the mathematical model indicate that the practical sustained yield of the existing 3-well system is about 137 gpm or

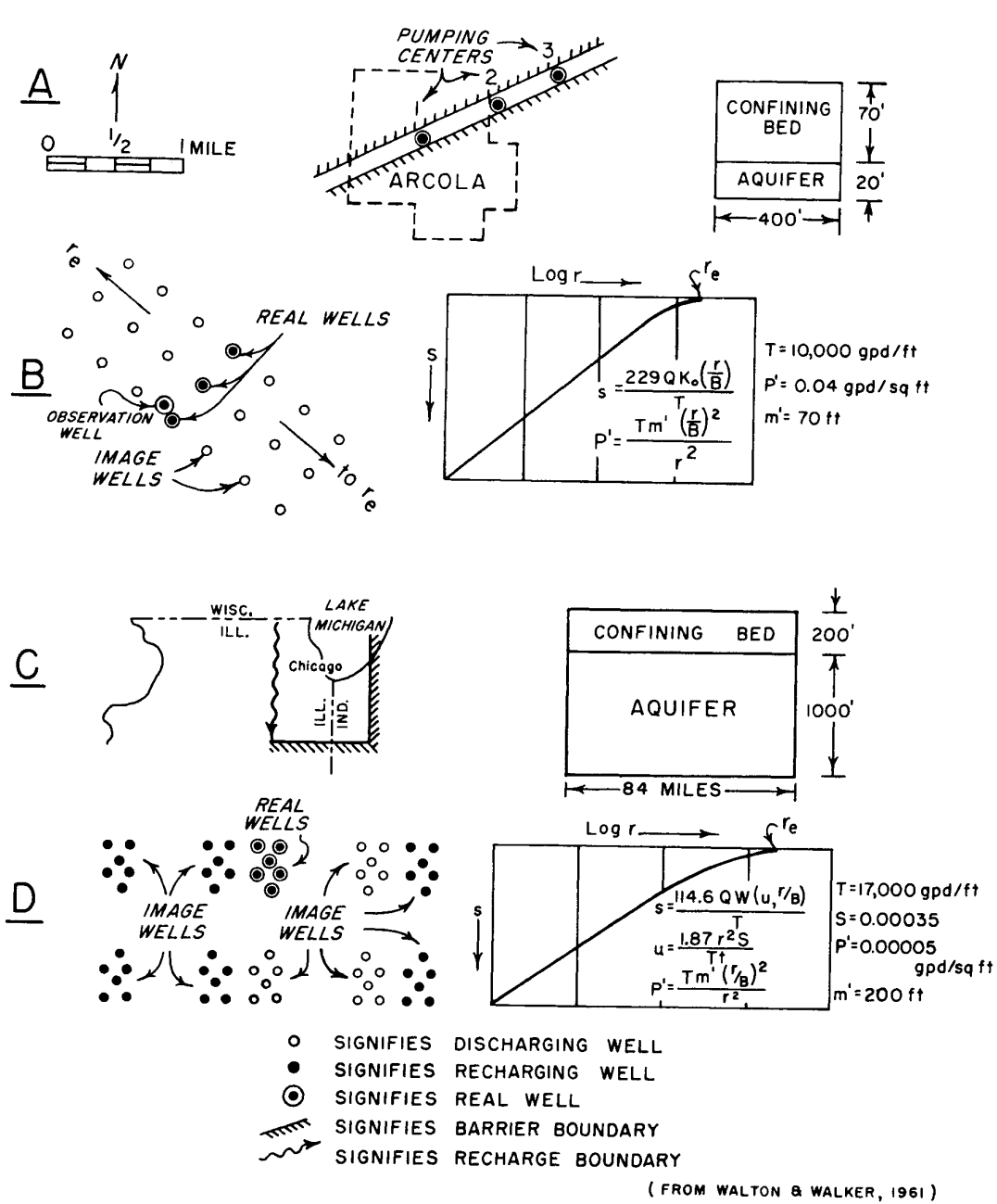


Figure 65. Model aquifers and mathematical models for Arcola area (A and B) and Chicago region (C and D)

200,000 gpd (Walker and Walton, 1961). A water supply equal to the practical sustained yield can be obtained by pumping production wells 1 and 3 at 57 gpm and production well 2 at 25 gpm. Partial penetration, well loss, and variations in hydraulic properties were considered in computations of drawdowns due to pumping the production wells themselves.

The rate of ground-water withdrawal increased from 115,000 gpd in 1957 to 146,000 gpd in 1959. If pumpage continues to increase in the future at this rate, it is estimated that the practical sustained yield of the existing 3-well system will be exceeded in 1963.

The Arcola case history is suggestive of how analytical methods can be utilized to evaluate wells and aquifers so that available ground-water resources can be properly managed. By checking computed performance of wells and aquifers with records of past pumpage and water levels, the hydrologist is assured of reasonably accurate solutions.

## Evaluation of Several Aquifers in Illinois

To date the principles outlined above have been applied to aquifer conditions in five areas in Illinois in addition to the Arcola area. The practical sustained yield of well fields and aquifers in the Chicago region in northeastern Illinois and in the Taylorville, Tallula, Assumption, and Pekin areas in central Illinois have been evaluated (Walton and Walker, 1961). Model aquifers and mathematical models for these areas are illustrated.

### Chicago Region

The Cambrian-Ordovician Aquifer is the most highly developed aquifer for large ground-water supplies in the Chicago region. The Cambrian-Ordovician Aquifer is encountered at an average depth of about 500 feet below the land surface at Chicago; it has an average thickness of 1000 feet and is composed chiefly of sandstones and dolomites. The Maquoketa Formation consisting largely of shale overlies the Cambrian-Ordovician Aquifer and confines the water in the deep aquifer under leaky artesian conditions. The Cambrian-Ordovician Aquifer receives water from overlying glacial deposits in areas averaging 47 miles west of Chicago where the Maquoketa Formation is absent.

Based on the results of 63 aquifer tests and other studies, the coefficients of transmissibility and storage of the Cambrian-Ordovician Aquifer and the coefficient of vertical permeability of the Maquoketa Formation are fairly uniform throughout large areas in northeastern Illinois and average 17,000 gpd/ft, 0.00035, and 0.00005 gpd/sq ft, respectively (Suter et al, 1959; and Walton, 1960a). The coefficient of transmissibility decreases rapidly south and east of Chicago.

The results of geologic and hydrologic studies indicate that it is possible to simulate the Cambrian-Ordovician Aquifer with an idealized model aquifer as shown in figure

65C. The model aquifer is a semi-infinite rectilinear strip of sandstones and dolomites 84 miles wide and 1000 feet thick. The model aquifer is bounded by a recharge boundary 47 miles west of Chicago and by two intersecting barrier boundaries 37 miles east and 60 miles south of Chicago, and is overlain by a confining bed consisting mostly of shale averaging 200 feet thick. The mathematical model for the Cambrian-Ordovician Aquifer is shown in figure 65D.

Pumpage of ground water from the Cambrian-Ordovician Aquifer increased gradually from 200,000 gpd in 1864 to 50 mgd in 1959 (Walton et al, 1960). Pumpage is concentrated in six centers as shown in figure 65D, the Chicago, Joliet, Elmhurst, Des Plaines, Aurora, and Elgin areas. As a result of heavy pumping, artesian pressure in deep sandstone wells declined more than 600 feet at Chicago between 1864 and 1958.

Studies made with the mathematical model show that the practical sustained yield of the Cambrian-Ordovician Aquifer is about 46 mgd (Suter et al, 1959) and is largely limited by the rate at which water can move eastward through the aquifer from recharge areas. The practical sustained yield of the aquifer is here defined as the maximum amount of water that can be continuously withdrawn with the present distribution of pumping centers without eventually dewatering the most productive and basal water-yielding formation of the Cambrian-Ordovician Aquifer. The practical sustained yield of the aquifer was exceeded in 1959, and in a sense ground-water users in the Chicago region started to mine water and to borrow water from future generations.

Declines in nonpumping water levels that may be expected between 1958 and 1980 at pumping centers were computed by using the mathematical model and assuming that the distribution of pumpage remains the same as it was in 1958 and pumpage increases in the future as it has in the past. Computed declines ranged from 300 feet in the Chicago area to 190 feet at Elgin and averaged 250 feet (Suter et al, 1959).

### Taylorville Area

Municipal and industrial water supplies at Taylorville are obtained from wells in glacial deposits chiefly Illinoian in age that range in thickness from 50 to 180 feet (Walker and Walton, 1961). The glacial deposits occur in a buried valley cut into relatively impermeable bedrock of Pennsylvanian age and are a complex of ice-laid till, water-laid silt sand-and-gravel outwash, and wind-deposited silt and fin sand (loess). The bedrock valley trending northeast to southwest through Taylorville was at one time in the past filled with glacial till. The outwash sand and gravel aquifer which yields water in large quantities to wells occurs as a fill in a narrow valley cut into the upper part of the till deposits. The outwash deposits range in width from one-half to one mile and range in thickness from a few feet to 113 feet.

Water occurs in the aquifer under water-table conditions

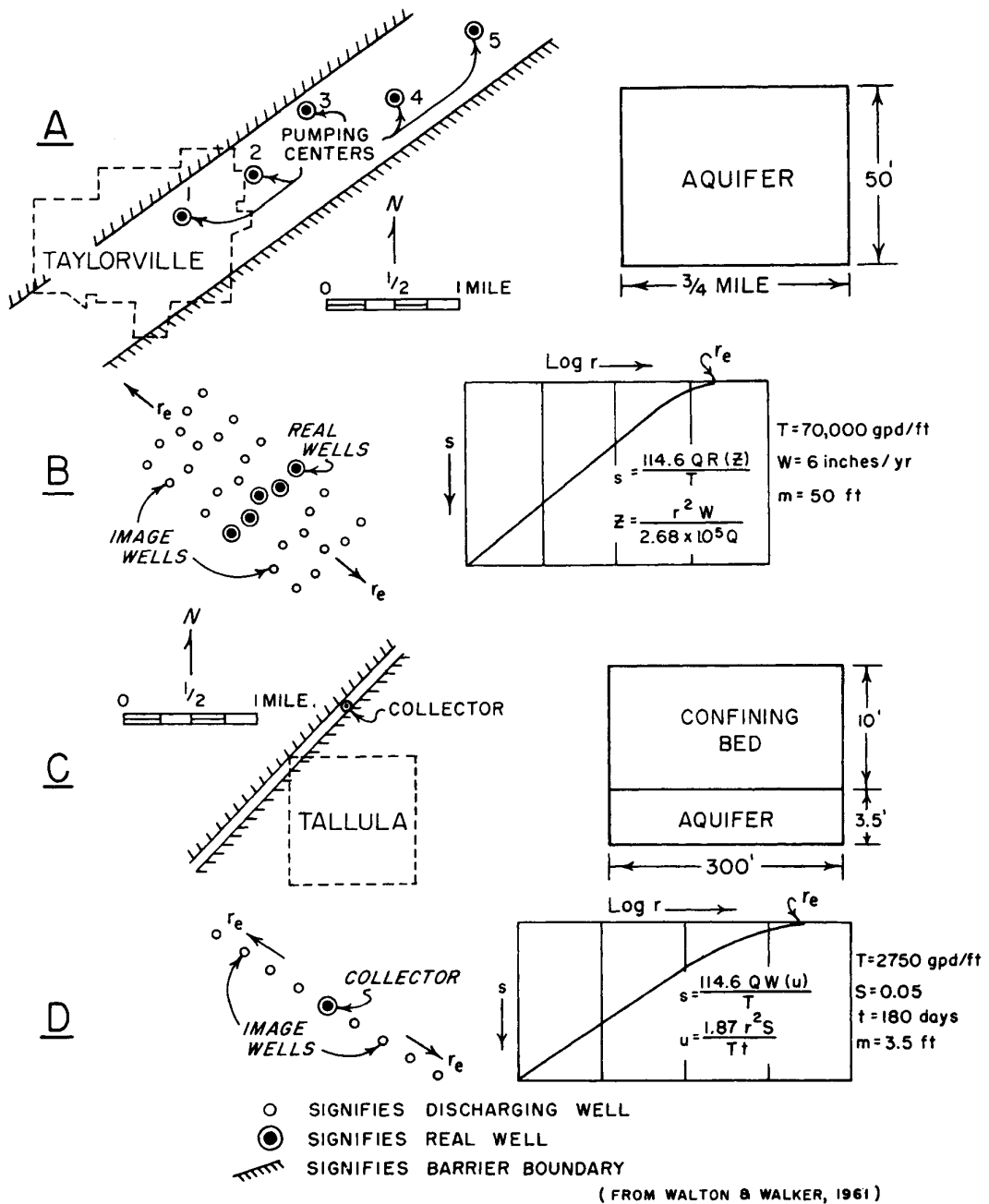


Figure 66. Model aquifers and mathematical models for Taylorville (A and B) and Tallula (C and D) areas

and the source of recharge is precipitation. The recharge area of the aquifer is bounded approximately by ground-water divides and the edges of the aquifer. It is estimated that an average of 6 inches or 17 per cent of mean annual precipitation reaches the water table in the 6.3-square-mile recharge area.

The hydraulic properties of the aquifer are known from the results of seven aquifer tests. Analysis of data indicates that the coefficient of transmissibility ranges from 34,000 to 130,000 gpd/ft and the coefficient of permeability ranges from 600 to 2200 gpd/sq ft. The coefficient of storage of the aquifer averages 0.15.

Total ground-water withdrawals from municipal and industrial wells at Taylorville increased progressively from about 28,000 gpd in 1890 to a maximum of about 3 mgd in 1953. Pumpage decreased rapidly from 3 mgd in 1953 to 1.75 mgd in 1957. In 1959 total ground-water withdrawal was 1.77 mgd. Heavy pumpage, concentrated in five well fields as shown in Figure 66A, caused water levels to decline about 40 feet between 1888 and 1956. Many of the production wells are located in the thinner and less permeable parts of the aquifer.

The idealized model aquifer for the Taylorville area shown in figure 66A is an infinite rectilinear strip of sand and gravel three-fourths mile wide and 50 feet thick which is bounded on the sides and bottom by impermeable material. The average coefficients of transmissibility and storage of the model aquifer are 70,000 gpd/ft and 0.20, respectively. The mathematical model for the model aquifer is shown in figure 66B.

Studies made with the mathematical model indicate that, with the present distribution of pumpage and available drawdowns ranging from 40 to 80 feet, the practical sustained yield of the aquifer is 745 gpm or 1.07 mgd. About 970 gpm or 1.4 mgd can be obtained without excessive drawdown from four wells screened in the thicker and more permeable sections of aquifer within a 3-mile radius of Taylorville.

Pumpage in 1959 exceeded the practical sustained yield of the aquifer. Computed future water-level declines for 1959 to 1965 indicated that by 1961 pumping levels in many production wells would recede to positions below tops of screens, and that by 1965 pumping levels would decline to critical stages several feet below tops of screens.

### **Tallula Area**

The municipal water supply for the village of Tallula is obtained from a collector well on the flood plain of a small creek (Walker and Walton, 1961). The collector well penetrates a thin sand and gravel aquifer that ranges from 2.5 to 4.5 feet thick and is encountered at an average depth of 16 feet below land surface. The aquifer is not very permeable and consists of stratified beds of sand, gravel, and silt in various mixtures. A confining bed averaging 10 feet thick and consisting of alluvial clay, silt, and fine sand

overlies the aquifer. The sand and gravel aquifer is inferred to be from 150 to 370 feet wide and is contained in a narrow valley cut into relatively impermeable bedrock of Pennsylvanian age.

Recharge is derived chiefly from precipitation by the vertical leakage of water through the confining bed. Because of the small area and silted condition of the bed of the creek, low streamflow, and the presence of silty materials beneath the streambed, very little recharge occurs by the induced infiltration of surface water especially during summer, fall, and winter months. Large amounts of water enter the aquifer through a recharge well connected to a lagoon and located 60 feet from the end of one of the laterals in the collector well.

The coefficients of transmissibility and permeability of the aquifer determined from the results of two pumping tests are 2750 gpd/ft and 790 gpd/sq ft, respectively. Under natural conditions, leaky artesian conditions exist; however, under heavy pumping conditions and during prolonged dry periods, the confining bed is partially drained.

Pumpage from the collector well increased from 9000 gpd in 1955 to 29,000 gpd in 1959. As the result of pumping at a rate of 37,000 gpd during summer months in 1959, water levels declined below the top of the upper lateral in the collector well.

The idealized model aquifer for the Tallula area, as shown in figure 66C, is a semi-infinite rectilinear strip of sand and gravel 300 feet wide and 3.5 feet thick which is bounded on the sides and bottom by impermeable material and is overlain by a confining bed 10 feet thick. The mathematical model for the model aquifer is shown in figure 66D.

The practical sustained yield of the collector well is much greater during years of near or above normal precipitation when the lagoon is frequently replenished and artificial recharge is continuous than it is during dry periods when little artificial recharge can be expected. Computations made by simulating the collector well with a vertical well having a radius of 66 feet and using the mathematical model indicate that the practical sustained yield of the collector well is 11 gpm or 16,000 gpd during extended dry periods and 20 gpm or 25,000 gpd during years of normal precipitation.

### **Assumption Area**

A new well field was recently developed 2½ miles southeast of the city of Assumption to supplement the municipal water supply. Geologic studies suggest that the aquifer is mainly poorly sorted sand ranging from 5 to 13 feet thick. The aquifer is greatly limited in areal extent to a rectilinear area 600 feet wide by 2200 feet long. Clayey materials (confining bed) with an average saturated thickness of 8 feet overlie the aquifer, and water occurs under leaky artesian conditions. Recharge is received chiefly from precipitation by the vertical leakage of water through the confining bed.

Based on the results of two aquifer tests, the coefficients of transmissibility and permeability of the aquifer are 4900

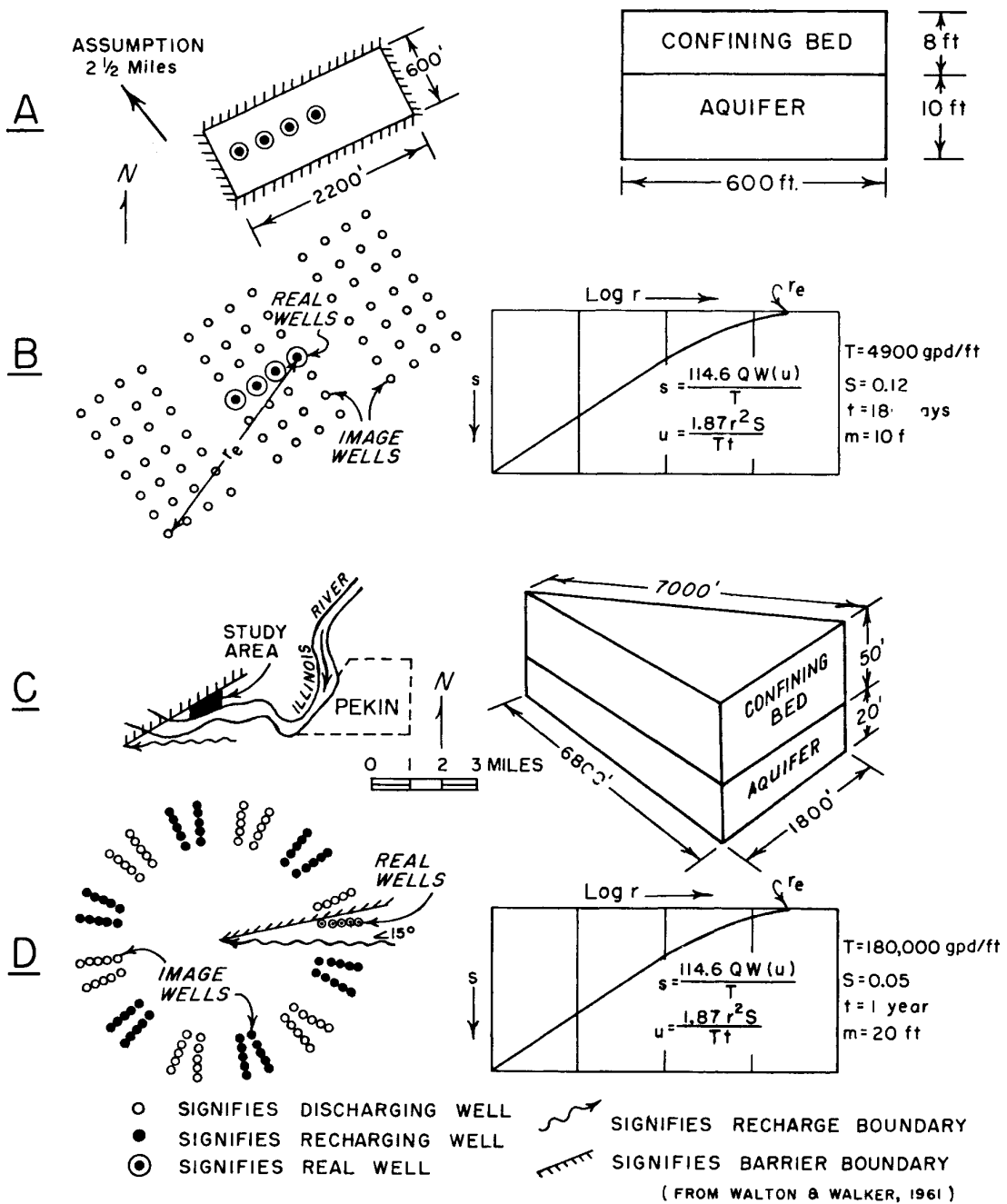


Figure 67. Model aquifers and mathematical models for Assumption (A and B) and Pekin (C and D) areas

gpd/ft and 410 gpd/sq ft, respectively (Walton and Walker, 1961). The coefficient of vertical permeability of the confining bed is 0.19 gpd/sq ft.

The idealized model aquifer for the Assumption area, shown in figure 67A, is a box of sand 600 feet wide, 2200 feet long, and 10 feet thick. The model aquifer is bounded on the sides and bottom by impermeable material and is overlain by a confining bed with an average saturated thickness of 8 feet. The mathematical model for the model aquifer is shown in figure 67B.

The response of the aquifer to long-term pumping was studied by means of the mathematical model. Computations based on an average available drawdown of 12 feet indicate that the practical sustained yield of a 4-well system, consisting of wells 6 inches in diameter, 24 feet deep, with 5 feet of screen, and spaced 300 feet apart, is about 38 gpm or 55,000 gpd. Gravity drainage of the confining bed and part of the aquifer during extended dry periods was taken into account in estimating the practical sustained yield of the aquifer.

### Pekin Area

In 1960 an intensive geohydrologic study was made by an industry to determine the feasibility of developing a large ground-water supply from unconsolidated deposits in an area along the Illinois River, about 3 miles southwest of the city of Pekin. The study included a test drilling program and a controlled aquifer test. The data thus obtained together with information from other sources led to an evaluation of the practical sustained yield of the aquifer in the study area, and to the design of a multiple-well system capable of meeting the demand of the industry.

The unconsolidated deposits in the study area consist of recent silty alluvial materials and glacial outwash of Wisconsinan age. These deposits are contained in a buried valley cut into the underlying bedrock of Pennsylvanian age. The permeable outwash forming the aquifer ranges in thickness from less than 5 feet to more than 33 feet and consists of stratified beds of gravel and sand. Logs of wells and test holes show that the boundary marking the limits of the aquifer trends northeast to southwest through the study area. In the proposed well field area the aquifer averages 20 feet thick and is overlain with fine-grained alluvial materials with an average saturated thickness of 50 feet. The Illinois River, which trends east to west through the study area, has been dredged into the alluvial materials but not into the aquifer.

Computations made with aquifer-test data show that the coefficients of transmissibility and permeability of the aquifer are 180,000 gpd/ft and 9000 gpd/sq ft, respectively (Walton and Walker, 1961). During the aquifer test, leaky artesian conditions occurred a short time after pumping started, and gravity drainage of the alluvial materials was appreciable during the latter part of the test period especially in the immediate vicinity of the pumped well. Test data

were adversely affected by a barrier boundary (the edge of the aquifer); however, the effects of recharge from the Illinois River caused water levels to stabilize rapidly indicating a fair connection between the aquifer and the river.

A model aquifer which simulates the actual geohydrologic conditions present in the study area is shown in figure 67C. The mathematical model for the model aquifer is shown in figure 67D. Computations made with the mathematical model indicate that 4000 gpm or 5.76 mgd can be obtained with maximum drawdowns above the top of the aquifer from 5 wells spaced about 325 feet apart.

### Well Loss

#### Sand and Gravel Well

A step-drawdown test (Bruin and Hudson, 1955) was conducted by E. G. Jones and Jack Bruin of the State Water Survey on an irrigation well owned by J. R. Thomason. The well was constructed by the Thorpe Concrete Well Co. and was completed on November 4, 1953. The well is located approximately 1300 feet east and 1450 feet north of the southwest corner of sec. 29, T4N, R9W, near Granite City. The driller's log of the well is given in table 22. The bottom 60 feet of the well is screened with porous concrete screen and the upper 46 feet is cased with concrete casing. The casing and screen have an inside diameter of 30 inches and an outside diameter of 40 inches.

Table 22. Log of well near Granite City

Material	Depth (ft)	
	from	to
Sandy clay	0	23
Yellow medium coarse sand	23	28
Fine gray sand	28	44
Medium fine gray sand	44	52
Sand	52	60
Coarse, clean sand	60	84
Medium coarse sand	84	100
Coarse sand and boulders	100	106

The test was started at 9:45 a.m. on April 27, 1954, and was continued for about 4 hours until 1:40 p.m. The well was pumped at three rates, 1000, 1280, and 1400 gpm. Test data are given in table 23.

The test data were plotted on semilogarithmic paper with the pumping levels on the arithmetic axis and the time after pumping started on the logarithmic axis as shown in figure 68. It can be noted that the time-drawdown curve at 1000 gpm has a slope of 0.21 feet per log cycle. Equation 23 indicates that the slope of the semilogarithmic time-drawdown curve is directly proportional to  $Q$ . The slope at 1280 gpm was estimated to be about 0.269 feet per log cycle by multiplying the slope at 1000 gpm by the ratio of 1280:1000. By similar procedure the slope at 1400 gpm was computed to be 0.294 feet per log cycle. These slopes were used to extrapolate water-level trends beyond periods

of pumping as shown by the dashed lines in figure 68. These extrapolations were used to obtain increments of drawdown produced by each increase in the rate of pumping. Increments of drawdown were determined for a pumping period of 1 hour and are given in table 24.

**Table 23. Data for step-drawdown test near Granite City**

Time	Feet to water	Pumping rate (gpm)
9:13 a.m.	23.95	
9:23	23.95	0
9:45	started pumping	
9:50	29.13	1000
9:55	29.23	1000
10:00	29.30	1000
10:10	29.30	1000
10:15	29.32	1000
10:20	29.37	1000
10:30	29.35	1000
10:35	29.36	1000
10:52	29.40	1000
11:00	29.39	1000
11:25	29.43	1000
11:30	30.97	1280
11:50	31.01	1280
12:00	31.02	1280
12:15 p.m.	31.04	1280
12:30	31.08	1280
12:45	31.08	1280
12:50	31.90	1400
1:00	31.95	1400
1:15	31.90	1400
1:30	31.90	1400
1:40	31.93	1400

From Bruin and Hudson (1955)

**Table 24. Drawdowns and pumping rates for well 1 near Granite City**

Step	Q (gpm)	ΔQ (gpm)	ΔQ (cfs)	Δs (ft)
1	1000	1000	2.22	5.43
2	1280	280	0.62	1.59
3	1400	120	0.27	0.72

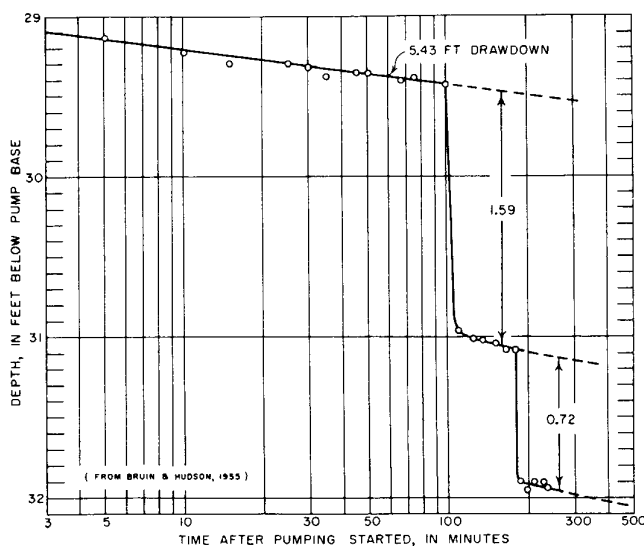


**Figure 68. Time-drawdown graph for well near Granite City**

Data in table 24 were substituted into equations 69 and 70 for computations of  $C$  as shown below:

For steps 1 and 2

$$C = \frac{(1.59/0.62) - (5.43/2.22)}{2.22 + 0.62}$$

$$C = 0.04 \text{ sec}^2/\text{ft}^5$$

For steps 2 and 3

$$C = \frac{(0.77/0.27) - (1.59/0.62)}{0.62 + 0.27}$$

$$C = 0.28 \text{ sec}^2/\text{ft}^5$$

The value of  $C$  for steps 2 and 3 is greater than the value of  $C$  for steps 1 and 2. However, both values of  $C$  are very low and it is probable that the values of  $C$  differ in this case not because the well is unstable but because of slight inaccuracies in measured drawdowns and pumping rates. The average value of  $C$  is about  $0.16 \text{ sec}^2/\text{ft}^5$ .

The well loss at the 1400 gpm pumping rate was computed to be about 1.0 foot with equation 67 as shown below:

$$s_w = 0.16 (1440/449)^2$$

The total drawdown in the well at 1400 gpm was 7.74 feet. Thus, well loss amounted to about 13 per cent of the total drawdown in the production well for a pumping rate of 1400 gpm.

### Bedrock Wells

A step-drawdown test was made by Sandor Csallany of the State Water Survey in cooperation with Marbry & Johnson, Inc., consulting engineers, and E. C. Baker & Sons, well contractor, on a sandstone well owned by the village of Iuka. The well is located about 600 feet west and 1300 feet south of the northeast corner of sec. 18, T2N, R4E, in Marion County. The log and construction features of the pumped well and three observation wells are shown in figure 69. The locations of the wells are shown in figure 70. Two major water-yielding zones are encountered in wells 1, 2, and 3 between the depths of 20 and 31 feet and 40 and 85 feet.

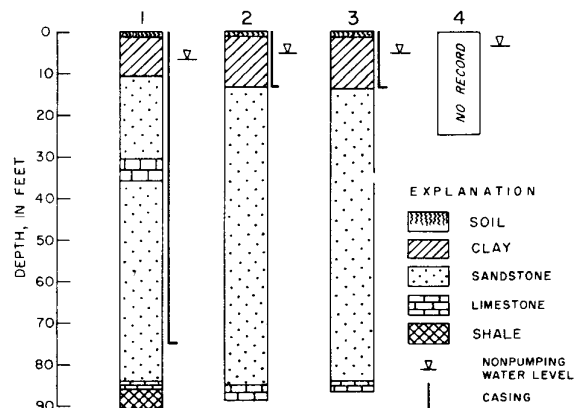


**Figure 69. Generalized graphic logs of wells used in test at Iuka**



observation well increased about in proportion to the pumping rate. When the pumping level declined below the upper water-yielding zone there was free flow from the upper water-yielding openings. Thus, the maximum contribution from the upper zone was attained during the second step. As shown by the time-drawdown graph for well 4, discharge from the upper zone was not appreciably increased, indicating that most of the increase in discharge during step 2 was obtained from the lower zone.

The pumping level in well 3 declined below the top of the lower zone during the third step with a pumping rate of 12.7 gpm. The specific capacity of the well for a pumping rate of 12.7 gpm and a pumping period of 1 hour is 0.17 gpm/ft and is less than the specific capacity for pumping rates of 5.4 and 9.3 gpm. Water levels in the shallow observation well were not affected by the increase in pumping rate, whereas the time-rate of drawdown in the deep observation well increased about in proportion to the pumping rate. The specific capacity during the third step is less than the specific capacity during the second step because there was free flow from some of the openings in the lower zone and the openings in the basal part of the lower zone were called upon for much of the increase in pumpage.

From the above discussion, it is obvious that erroneously optimistic predicted yields of the production well under higher rates of pumping would occur if the specific capacities for steps 1 or 2 were used in computations.

Experience has shown that the constant-rate method of well testing when applied to wells tapping bedrock aquifers, especially dolomite aquifers, has sometimes resulted in erroneously optimistic predicted yields of wells under higher rates of pumping. The value of  $C$  increases with higher pumping rates as the pumping level recedes below producing zones. The step-drawdown test provides data that can be analyzed to obtain more accurate predictions of yields under various pumping-rate conditions.

Drawdown at the end of each pumping period is plotted against the corresponding pumping rate and a curve is drawn through the points. The drawdown in the well caused by a planned rate of discharge may be read directly from the curve or approximated for higher pumping rates by projecting the curve.

Step-drawdown tests were made on several deep sandstone wells in northeastern Illinois. Data collected during these tests were substituted into equations 69 and 70 to determine well-loss constants. Computed values of  $C$  (Walton and Csallany, 1962) range from 4 to 15  $\text{sec}^2/\text{ft}^5$ .

Step-drawdown tests were made on several dolomite wells in DuPage County. Analysis of available data (Zeizel et al, 1962) indicates that the well-loss constant is a function of 1) the specific capacity and therefore the hydraulic properties of the Silurian dolomite aquifer, and 2) the position of the pumping level in relation to the top of the Silurian dolomite aquifer. High values of  $C$  are computed for wells having low specific capacities and low values of  $C$  are computed for wells having high specific capacities. Apparently

turbulence and therefore well loss increases as the coefficient of transmissibility of the aquifer decreases. It is probable that the size and/or number of openings in the dolomite decrease with the coefficient of transmissibility.

The well-loss constant increases greatly when water levels are lowered below the top of the Silurian dolomite aquifer. As the pumping level declines below the top of the aquifer, maximum contribution from openings in the upper part of the dolomite above the pumping level is attained and future increases in pumping are obtained from the openings below the pumping level. A greater burden is placed upon lower openings and well loss is greatly increased.

Graphs, figures 73 and 74, were prepared showing the relation between specific capacity and  $C$  for the two cases, when the pumping level is above the top of the aquifer and when the pumping level is below the top of the aquifer.

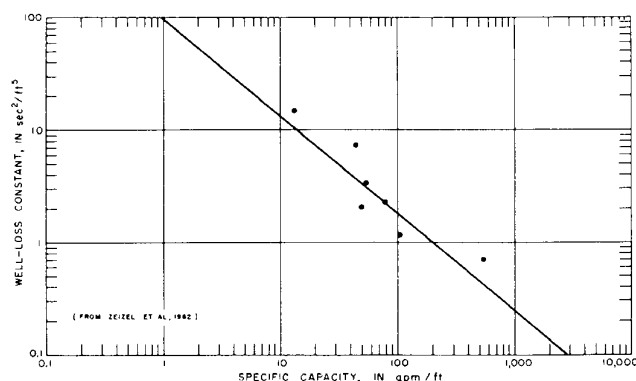


Figure 73. Well-loss constant versus specific capacity, pumping levels are above the top of the Silurian dolomite aquifer in DuPage County

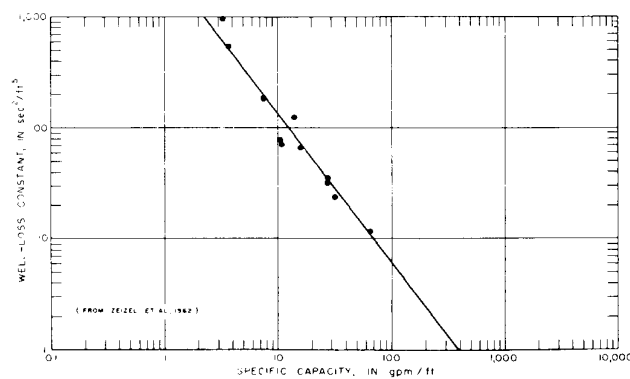


Figure 74. Well-loss constant versus specific capacity, pumping levels are below top of the Silurian dolomite aquifer in DuPage County

### Collector Well Data

The collector well at Tallula consists of a 6-foot-diameter caisson from which two horizontal 8-inch-diameter vitrified perforated clay pipe laterals are projected near the bottom. The concrete caisson extends from 9.5 feet above to 26 feet below land surface. One horizontal lateral (upper lateral)

projects from the caisson at a depth of 18 feet below land surface and is 478 feet long. The other horizontal lateral (lower lateral) projects from the caisson at a depth of 21 feet below land surface and is 310 feet long. The laterals were placed in a trench excavated through the sand and gravel aquifer that averages 3.5 feet thick and occurs as a strip 150 to 370 feet wide encountered at an average depth of 16 feet below land surface. After the laterals were placed, the trench was backfilled with gravel to a depth of 15 feet below land surface and with clay and top soil to the original land surface.

On April 28, 1955, a well-production test was made using the collector well. A drawdown of 1.52 feet was computed for a pumping period of 41 minutes and a pumping rate of 35 gpm. The coefficients of transmissibility and storage of the aquifer are 2750 gpd/ft and 0.002, respectively. Computations made with the data mentioned above and the nonleaky artesian formula indicate that the collector well is equivalent to a vertical well with a radius of about 66 feet.

### Design of Sand and Gravel Well

The results of studies on the mechanical analyses of samples of two aquifers in Illinois will demonstrate some of the principles involved in the design of sand and gravel wells.

Suppose that it is desired to estimate the optimum yield and to design an 8-inch-diameter well with a continuous slot screen 30 feet long. The coefficients of transmissibility, permeability, and storage of the aquifer are 15,000 gpd/ft, 500 gpd/sq ft, and 0.0003, respectively, and there is 125 feet of available drawdown. The grain size distribution curves for the samples of the aquifer are given in figure 75. The sieve analyses are for actual samples taken from a test well penetrating a deeply buried sand and gravel aquifer and owned by the city of Woodstock.

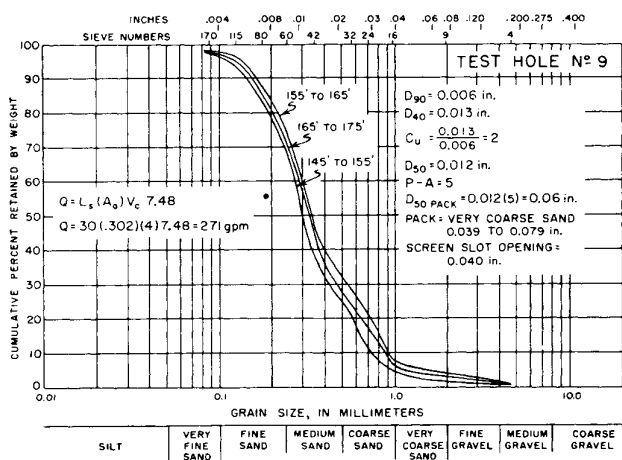


Figure 75. Mechanical analyses of samples of an aquifer at Woodstock

The 50-per-cent size of the coarsest sample is less than 4 times the 50-per-cent size of the finest sample, therefore, the slot size and pack are not tailored to individual samples but are based on the finest sample. The curves in figure 75 show that the effective grain size of the materials of the finest sample is 0.006 inch and the uniformity coefficient is about 2. An artificial pack well is indicated because the effective grain size is less than 0.01 inch and the uniformity coefficient is less than 3. The 50-per-cent size of the materials of the finest sample is 0.012 inch; thus, with a pack to aquifer ratio of 5, a very coarse sand pack with particles ranging in diameter from about 0.04 to 0.08 inch is indicated. To retain 90 per cent of the size fractions of the pack, a slot size of 0.04 inch is required. An artificial pack thickness of 6 inches is adequate.

The permeability of the pack is estimated to be about 1500 gpd/sq ft, and from table 4 optimum screen entrance velocities of 5 and 3 fpm are indicated for the pack and aquifer, respectively. The average of the velocities for the pack and aquifer, 4 fpm, is selected for use in determining the optimum yield of the well.

The actual open area of an 8-inch-diameter, 40-slot, continuous-slot screen is 0.604 sq ft for each foot of screen. The effective open area is estimated to be about 50 per cent of the actual open area, or 0.302 sq ft for each foot of screen. Substitution of data on the length of screen, effective open area, and optimum screen entrance velocity into equation 71 results in the conclusion that the optimum yield of the well is about 271 gpm. Computations are shown in figure 75.

Computations made with the nonleaky artesian formula, the given hydraulic properties, and available drawdown, indicate that the aquifer would yield more than 600 gpm to an 8-inch well. However, pumping the well at continuous rates exceeding 271 gpm would probably result in a short service life.

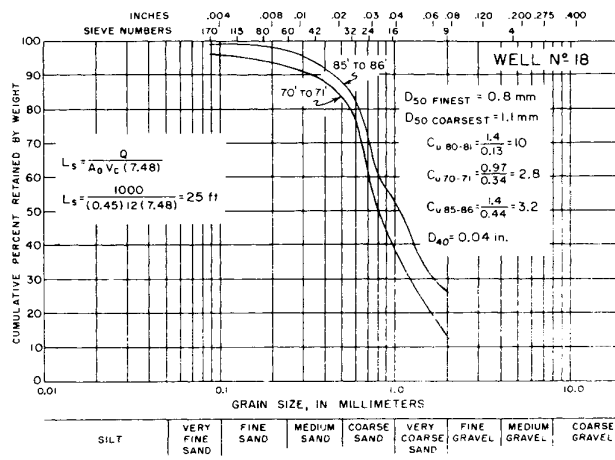


Figure 76. Mechanical analyses of samples of an aquifer near Mossville

For a demonstration of the design of a natural pack well, consider the grain size distribution curves in figure 76. The sieve analyses are for samples taken from a test well owned by the Caterpillar Tractor Company and located near Mossville. The coefficients of transmissibility, permeability, and storage of the sand and gravel aquifer are 340,000 gpd/ft, 8100 gpd/sq ft, and 0.09, respectively. The saturated thickness of the aquifer is 42 feet.

The 50-per-cent size of the materials in the finest sample is less than 4 times the 50-per-cent size of the materials in the coarsest sample; therefore, the slot size is not tailored to individual samples but is based on the mechanical analysis of the finest sample. The effective grain sizes of both samples are greater than 0.01 inch and the average uniformity coefficient is 3. A natural pack well is therefore indicated. The materials overlying the aquifer will not easily cave so the sieve size (0.04 inch) that retains 40 per cent of the aquifer materials is selected as the proper slot size.

Suppose a pumping rate of 1000 gpm is desired. The

proper length of the screen can be estimated with equation 71. The optimum screen entrance velocity, from table 4, is equal to 12 fpm, and the proper diameter of the screen considering pump requirements is estimated to be 12 inches. The effective open area of a continuous-slot, 40-slot, 12-inch-diameter screen is about 0.45 sq ft for each foot of screen. Substitution of the above data in equation 71 indicates that the screen should be about 25 feet long. Computations are given in figure 76.

Alternate designs are possible if the well diameter is not limited by pump requirements. Computations indicate that a 24-inch-diameter, 40-slot, continuous-slot screen that is 15 feet long will also yield 1000 gpm with a long service life.

A shorter 8-inch screen can be used if an artificial pack well is constructed instead of a natural pack. Analysis of figure 76 indicates that a 100-slot, continuous-slot screen that is 22 feet long will also yield 1000 gpm with a long service life.

## **Conclusions**

It is often possible to evaluate well and aquifers with analytical methods by devising approximate methods of analysis based on idealized models of aquifer situations. Comparisons of computed and actual water-level declines in areas where case histories of ground-water development are available indicate that aquifer behavior actually does coincide rather closely with what may be predicted theoretically with model aquifers and mathematical models.

It is apparent that quantitative answers depend primarily upon the accurate description of geologic and hydrologic controls. In the future, as the techniques of ground-water resource evaluation are refined, a need for more precise, quantitative data concerning requisite geologic information will develop.

Formulas and methods given in this report should not be used without due regard to basic assumptions. Diverse results and vexations will arise if attempts are made to force the application of formulas to aquifer situations differing greatly from ideal conditions.

## **Acknowledgments**

Many former and present members of the State Water Survey and State Geological Survey participated in aquifer tests, wrote earlier special reports which have been used as reference material, or aided the writer indirectly in preparing this report. Grateful acknowledgment is made, therefore, to the following engineers and geologists: W. H. Walker, G. B. Maxey, Max Suter, R. E. Bergstrom, R. J. Schicht, J. E. Hackett, R. T. Sasman, A. T. Zeizel, T. A. Prickett, G. H. Emrich, R. R. Russell, J. W. Foster, H. G. Rose, Jack Bruin, H. E. Hudson, Jr., W. J. Roberts, R. E. Aten, G. E. Neher, J. P. Dorr, and O. E. Michels.

Acknowledgment is made to consulting engineers, well drillers, and municipal officials who were most cooperative and helpful in making data available on aquifer tests, pumpage, and water levels.

H. F. Smith, Head of the Engineering Section, State Water Survey, encouraged the preparation of this report. J. W. Brother prepared the illustrations.

## Selected References

- Ahrens, T. P. 1957. Well design criteria. *Water Well Jour.*, Sept. and Nov.
- American Water Works Association. 1958. AWWA standard for deep wells. New York.
- Anon. 1941. The principles and practical methods of developing water wells. Edward E. Johnson, Inc., St. Paul, Minn., Bull. 1033.
- Anon. 1955. The corrosion and incrustation of well screens. Edward E. Johnson, Inc., St. Paul, Minn., Bull. 834.
- Babbitt, H. E., and D. H. Caldwell. 1948. The free surface around, and interference between gravity wells. *Univ. of Illinois Bull.* 45.
- Bakhtmeteff, B. A., and N. V. Feodoroff. 1937. Flow through granular media. *Jour. Applied Mechanics* v. 25.
- Banks, H. O. 1953. Utilization of underground storage reservoirs. *Trans. Am. Soc. Civil Engrs.* v. 118.
- Barksdale, H. C., and G. D. Debuchanne. 1946. Artificial recharge of productive ground-water aquifers in New Jersey. *Economic Geol.* v. 41.
- Bennett, R. R., and R. R. Meyer. 1952. Geology and ground-water resources of the Baltimore area. Maryland Dept. Geology, Mines and Water Res. Bull. 4.
- Bennison, E. W. 1947. Ground-water. Edward E. Johnson, Inc., St. Paul, Minn.
- Bennison, E. W. 1953. Fundamentals of water well operation and maintenance. *Jour. Am. Water Works Assoc.* v. 45.
- Boulton, N. S. 1951. The flow pattern near a gravity well in a uniform water-bearing medium. *Jour. (British) Inst. Civil Engrs.* v. 36.
- Boulton, N. S. 1954a. The drawdown of the water table under non-steady conditions near a pumped well in an unconfined formation. *Proc. (British) Inst. Civil Engrs.* v. 3, pt. 3.
- Boulton, N. S. 1954b. Unsteady radial flow to a pumped well allowing for delayed yield from storage. *International Assoc. Sci. Hydrology. General Assembly of Rome*, v. 2, publ. 37.
- Brashears, M. L., Jr. 1953. Recharging ground-water reservoirs with wells and basins. *Mining Eng.* v. 5.
- Brown, R. H. 1953. Selected procedures for analyzing aquifer test data. *Jour. Am. Water Works Assoc.* v. 45.
- Bruin, J., and H. E. Hudson, Jr. 1955. Selected methods for pumping test analysis. *Illinois State Water Survey Rept. of Invest.* 25.
- Butler, S. S. 1957. *Engineering Hydrology*, Prentice-Hall, Englewood Cliffs, N. J.
- Carlsaw, H. S., and J. C. Jaeger. 1959. *Conduction of heat in solids*. Oxford University Press, New York.
- Chamberlin, T. C. 1885. The requisite and qualifying conditions of artesian wells. *U.S. Geol. Survey 5th Ann. Rept.*
- Clark, W. E. 1956. Forecasting the dry-weather flow of Pond Creek, Oklahoma; a progress report. *Trans. Am. Geophys. Union* v. 24.
- Conkling, H. 1946. Utilization of ground-water storage in stream-system developments. *Trans. Am. Soc. Civil Engrs.* v. 111.
- Cooper, H. H., Jr., and C. E. Jacob. 1946. A generalized graphical method for evaluating formation constants and summarizing well-field history. *Trans. Am. Geophys. Union* v. 27 (4).
- Corey, G. L. 1949. Hydraulic properties of well screens. Thesis, Colorado Agr. and Mech. College, Fort Collins.
- Cross, W. P. 1949. The relation of geology to dry-weather stream flow in Ohio. *Trans. Am. Geophys. Union* v. 30.
- de Glee, G. J. 1930. Over grondwaterstromingen bij wateronttrekking door middel van putten. J. Waltman Jr., Delft.
- DeWitt, M. M. 1947. How to acidize water wells. *The American City* v. 62 (10).
- Dupuit, Jules. 1863. *Etudes théoriques et pratiques sur la mouvement des eaux dans les canaux découverts et à travers les terrains perméables*, 2nd ed. Dunod, Paris.
- Fair, G. M., and L. P. Hatch. 1933. Fundamental factors governing the streamline flow of water through sand. *Jour. Am. Water Works Assoc.* v. 25.
- Ferris, J. G. 1948. Ground-water hydraulics as a geophysical aid. *Mich. Dept. Conserv., Geol. Survey Div. Tech. Rept.* 1.
- Ferris, J. G. 1950a. A quantitative method for determining ground-water characteristics for drainage design. *Agr. Eng.* v. 31 (6).
- Ferris, J. G. 1950b. Water spreading and recharge wells. *Proc. Indiana Water Conserv. Conf., Ind. Dept. Conserv., Div. Water Resources.*
- Ferris, J. G. 1951. Cyclic fluctuations of water level as a basis for determining aquifer transmissibility. *International Assoc. Sci. Hydrology, General Assembly of Brussels*, v. 2, publ. 33.
- Ferris, J. G. 1959. Ground water, chap. 7. In C. O. Wisler and E. F. Brater, ed., *Hydrology*, John Wiley & Sons, New York.
- Ferris, J. G., and others. 1959. Ground-water resources of southeastern Oakland County, Michigan. *Mich. Dept. Conserv., Geol. Survey Div. Progress Rept.* 16.
- Foley, F. C., W. C. Walton, and W. J. Drescher. 1953. Ground-water conditions in the Milwaukee-Waukesha area, Wisconsin. *U.S. Geol. Survey Water Supply Paper* 1229.
- Forchheimer, Philipp. 1901. *Wasserbewegung durch Boden*. Zietschr. Ver. Deutscher Ing., v. 45., Berlin.
- Forchheimer, Philipp. 1930. *Hydraulik*. Teubner, 3rd ed., Leipzig and Berlin.
- Gardner, W., T. R. Collier, and D. Farr. 1934. Ground-water; pt. 1, Fundamental principles governing its physical control. *Utah Agr. Exp. Sta. Tech. Bull.* 252.
- Graton, L. C., and H. J. Fraser. 1935. Systematic packing of spheres with particular relation to porosity and permeability. *Jour. Geol.* v. 43.
- Grundy, F. 1951. The ground-water depletion curve, its construction and uses. *International Assoc. Sci. Hydrology, General Assembly of Brussels*, v. 2, publ. 33.
- Guyton, W. F. 1941. Applications of coefficients of transmissibility and storage to regional problems in the Houston district, Texas. *Trans. Am. Geophys. Union 22nd Ann. Meeting*, pt. 3.
- Guyton, W. F. 1946. Artificial recharge of glacial sand and gravel with filtered river water at Louisville, Kentucky. *Economic Geol.* v. 41.
- Hall, H. P. 1954. A historical review of investigations of seepage toward wells. *Boston Soc. Civil Eng. Jour.* v. 41 (3).
- Hansen, V. E. 1952. Complicated well problems solved by the membrane analogy. *Trans. Am. Geophys. Union* v. 33 (6).
- Hantush, M. S. 1949. Plane potential flow of ground water with linear leakage. Ph.D. thesis, Univ. Utah.
- Hantush, M. S., and C. E. Jacob. 1954. Plane potential flow of ground water with linear leakage. *Trans. Am. Geophys. Union* v. 35 (6).
- Hantush, M. S., and C. E. Jacob. 1955a. Non-steady radial flow in an infinite leaky aquifer. *Trans. Am. Geophys. Union* v. 36 (1).
- Hantush, M. S., and C. E. Jacob. 1955b. Non-steady Green's functions for an infinite strip of leaky aquifers. *Trans. Am. Geophys. Union* v. 36 (1).
- Hantush, M. S., and C. E. Jacob. 1955c. Steady three-dimensional flow to a well in a two-layer aquifer. *Trans. Am. Geophys. Union* v. 36 (2).
- Hantush, M. S. 1956. Analysis of data from pumping tests in leaky aquifers. *Trans. Am. Geophys. Union* v. 37 (6).
- Hantush, M. S. 1957a. Non-steady flow to a well partially penetrating an infinite leaky aquifer. *Proc. Iraqi Sci. Soc.* v. 1.

- Hantush, M. S. 1957b. Preliminary quantitative study of the Roswell ground-water reservoir, New Mexico. New Mexico Inst. Mining and Tech., Res. and Development Div., Campus Sta., Socorro, N. Mex.
- Hantush, M. S. 1959a. Analysis of data from pumping wells near a river. *Jour. Geophys. Res.* v. 64 ( 11 ).
- Hantush, M. S. 1959b. Non-steady flow to flowing wells in leaky aquifers. *Jour. Geophys. Res.* v. 64 ( 8 ).
- Hantush, M. S. 1960. Modification of the theory of leaky aquifers. *Jour. Geophys. Res.* v. 65 ( 11 ).
- Hantush, M. S. 1961. Drawdown around a partially penetrating well. *Jour. of Hydraulics Div., Proc. Am. Soc. Civil Engrs.* v. 87 (Hy 4) July.
- Houk, I. E. 1921. Rainfall and runoff in Miami Valley. Miami Conservancy Dist. Tech. Repts., pt. 8, Dayton, Ohio.
- Hubbert, M. K. 1940. The theory of ground-water motion. *Jour. Geol.* v. 48 (8).
- Ingersoll, L. R., O. J. Zobel, and A. C. Ingersoll. 1948. Heat conduction with engineering and geological applications. McGraw-Hill Book Co., New York.
- Jacob, C. E. 1940. On the flow of water in an elastic artesian aquifer. *Trans. Am. Geophys. Union* pt. 2.
- Jacob, C. E. 1941. Notes on the elasticity of the Lloyd sand on Long Island, New York. *Trans. Am. Geophys. Union* pt. 3.
- Jacob, C. E. 1943. Correlation of ground-water levels and precipitation on Long Island, New York. *Trans. Am. Geophys. Union* pt. 1.
- Jacob, C. E. 1944. Notes on determining permeability by pumping tests under water-table conditions. U.S. Geol. Survey mimeo. rept.
- Jacob, C. E. 1945a. Partial penetration of pumping well, adjustments for. U.S. Geol. Survey Water Resources Bull., Aug.
- Jacob, C. E. 1945b. Correlation of ground-water levels and precipitation on Long Island, New York. New York Dept. Conserv. Water Power and Control Comm. Bull. GW-14.
- Jacob, C. E. 1946a. Radial flow in a leaky artesian aquifer. *Trans. Am. Geophys. Union* v. 27 (2) .
- Jacob, C. E. 1946b. Drawdown test to determine effective radius of artesian well. *Proc. Am. Soc. Civil Engrs.* v. 72 ( 5 ) .
- Jacob, C. E. 1950. Flow of ground water, chap. 5. In *Engineering Hydraulics*, John Wiley & Sons, New York.
- Jacob, C. E., and S. W. Lohman. 1952. Nonsteady flow to a well of a constant drawdown in an extensive aquifer. *Trans. Am. Geophys. Union* v. 33 (4).
- Jones, P. H., and T. B. Buford. 1951. Electric logging applied to ground-water exploration. *Geophysics* v. 16.
- Kano, T. 1939. Frictional loss of head in the wall of a well. *Japan Jour. Astron. and Geophys.* v. 17 ( 1 ) .
- Kazmann, R. G. 1946. Notes on determining the effective distance to a line of recharge. *Trans. Am. Geophys. Union* v. 27 (6).
- Kazmann, R. G. 1947. River infiltration as a source of ground-water supply. *Proc. Am. Soc. Civil Engrs.* v. 73 (6), pt. 1.
- Kazmann, R. G. 1948. The induced infiltration of river water to wells. *Trans. Am. Geophys. Union* v. 29 ( 1 ).
- Kimball, B. F. 1946. Assignment of frequencies to a completely ordered set of sample data. *Trans. Am. Geophys. Union* v. 27.
- Kirkham, Don. 1959. Exact theory of flow into a partially penetrating well. *Jour. Geophys. Res.* v. 64.
- Kleber, J. P. 1950. Well cleaning with Calgon. *Jour. Am. Water Works Assoc.* v. 42.
- Knowles, D. B. 1955. Ground-water hydraulics. U.S. Geol. Survey Ground Water Notes, Hydraulics, No. 28, open-file rept.
- Kozeny, J. 1933. Theorie und Berechnung der Brunnen. *Wasserkraft und Wasserwirtschaft* v. 28.
- Krul, W. F. J. M., and F. A. Lieftrinck. 1946. Recent ground-water investigations in the Netherlands. Elsevier Pub. Co., New York and Amsterdam.
- Langbein, W. B., and W. G. Hoyt. 1959. Water facts for the nation's future. The Ronald Press Co., New York.
- Lee, C. H. 1912. An intensive study of the water resources of a part of Owens Valley, California. U.S. Geol. Survey Water Supply Paper 294.
- Leggette, R. M. 1955. Modern methods of developing ground-water supplies. *Proc. Am. Soc. Civil Engrs.* v. 81, Separate No. 627.
- Linsley, R. K., Jr., Max A. Kohler, and J. L. Paulhus. 1958. *Hydrology for engineers*. McGraw-Hill Book Co., New York.
- McGuinness, C. L. 1946. Recharge and depletion of ground-water supplies. *Proc. Am. Soc. Civil Engrs.* v. 72.
- Meinzer, O. E. 1923. The occurrence of ground water in the United States. U.S. Geol. Survey Water Supply Paper 489.
- Meinzer, O. E., and H. A. Hard. 1925. The artesian water supply of the Dakota sandstone in North Dakota, with special reference to the Edgeley quadrangle. U.S. Geol. Survey Water Supply Paper 520.
- Meinzer, O. E., and N. D. Stearns. 1929. A study of ground water in the Pomperaug basin, Connecticut. U.S. Geol. Survey Water Supply Paper 597-B.
- Meinzer, O. E. 1932. Outline of methods for estimating ground-water supplies. U.S. Geol. Survey Water Supply Paper 638-C.
- Meinzer, O. E. 1942. *Hydrology*. McGraw-Hill Book Co., New York.
- Merriam, C. F. 1948. Ground-water records in river-flow forecasting. *Trans. Am. Geophys. Union* v. 29.
- Mikels, F. C. 1952. Report on hydrogeological survey for city of Zion, Illinois. Ranney Method Water Supplies, Inc., Columbus, Ohio.
- Mikels, F. C., and F. H. Klaer, Jr. 1956. Application of ground-water hydraulics to the development of water supplies by induced infiltration. *International Assoc. Sci. Hydrology, Symposia Darcy, Dijon*, publ. 41.
- Mitchelson, A. T., and D. C. Muckel. 1937. Spreading water for storage underground. U.S. Dept. Agr. Tech. Bull. 578, Washington, D. C.
- Moulder, E. A. 1951. Locus circles for a hydrogeologic boundary and its corresponding image well. *Water Res. Bull.*, Aug.
- Muskat, Morris. 1937. The flow of homogeneous fluids through porous media. McGraw-Hill Book Co., New York.
- Muskat, Morris. 1946. The flow of homogeneous fluids through porous media. J. W. Edwards, Inc., Ann Arbor, Mich.
- Parker, G. G., and others. 1955. Water resources of southeastern Florida with special reference to the geology and ground water of the Miami area. U.S. Geol. Survey Water Supply Paper 1255.
- Peterson, J. S., Carl Rohwer, and M. L. Albertson. 1955. Effect of well screens on flow into wells. *Trans. Am. Soc. Civil Engrs.* v. 120.
- Piper, A. M. 1944. A graphic procedure in the geochemical interpretation of water analysis. *Trans. Am. Geophys. Union*, 25th Ann. Meeting, pt. 6.
- Pirson, S. J. 1958. *Oil reservoir engineering*. McGraw-Hill Book Co., New York.
- Poiseville, J. L. M. 1846. Experimental investigations on the flow of liquids in tubes of very small diameters. *Royal Acad. Sci. Inst., France, Math. Phys. Sci. Mem.*
- Rasmussen, W. C., and G. E. Andreasen. 1959. Hydrologic budget of the Beaverdam Creek basin, Maryland. U.S. Geol. Survey Water Supply Paper 1472.
- Remson, I., and S. M. Lang. 1955. A pumping-test method for the determination of specific yield. *Trans. Am. Geophys. Union* v. 36 (1).
- Roberts, W. J., and H. E. Romine. 1947. Effect of train loading on the water level in a deep glacial-drift well in central Illinois. *Trans. Am. Geophys. Union* v. 28 ( 6 ).
- Robinson, T. W. 1939. Earth-tides shown by fluctuations of water levels in wells in New Mexico and Iowa. *Trans. Am. Geophys. Union* pt. 4.
- Rorabaugh, M. I. 1948. Ground-water resources of the northeastern part of the Louisville area, Kentucky. City of Louisville, Louisville Water Company.
- Rorabaugh, M. I. 1951. Stream-bed percolation in development of water supplies. *International Assoc. Sci. Hydrology, General Assembly of Brussels*, v. 2, publ. 33.
- Rorabaugh, M. I. 1953. Graphical and theoretical analysis of step drawdown test of artesian well. *Proc. Am. Soc. Civil Engrs.* v. 79, Separate No. 362.
- Rouse, Hunter. 1949. *Engineering hydraulics*. John Wiley & Sons, New York.
- Sasman, R. T., T. A. Prickett, and R. R. Russell. 1961. Water-level decline and pumpage during 1960 in deep wells in the Chicago region, Illinois. *Illinois State Water Survey Circ.* 83.
- Scheidegger, A. E. 1957. *The physics of flow through porous media*. Univ. Toronto Press, Toronto.

- Schicht, R. J., and W. C. Walton. 1961. Hydrologic budgets for three small watersheds in Illinois. Illinois State Water Survey Rept. of Invest. 40.
- Shaw, F. S., and R. V. Southwell. 1941. Relaxation methods applied to engineering problems, pt. 7; Problems relating to the percolation of fluids through porous materials. Proc. Royal Soc. London, A, v. 178.
- Slichter, C. S. 1898. Theoretical investigations of the motion of ground waters. U.S. Geol. Survey 19th Ann. Rept., pt. 2.
- Smith, H. F. 1954. Gravel packing water wells. Illinois State Water Survey Circ. 44.
- Smith, H. F. 1961. Modern water well design and construction procedures. Illinois State Water Survey mimeo. rept.
- Stallman, R. W. 1952. Nonequilibrium type curves modified for two-well systems. U.S. Geol. Survey Ground Water Notes, Hydraulics, No. 3, open-file rept.
- Stallman, R. W. 1956. Numerical analysis of regional water levels to define aquifer hydrology. Trans. Am. Geophys. Union v. 37.
- Stallman, R. W. 1956. Use of numerical methods for analyzing data on ground-water levels. International Assoc. Sci. Hydrology, Symposia Darcy. Dijon, publ. 41.
- Stallman, R. W. 1960. From geologic data to aquifer analog models. Geol. Times v. 5(7).
- Steggewentz, J. H. 1939. Calculating the yield of a well, taking into account of replenishment of the ground water above. Water and Water Eng. v. 41.
- Stringfield, V. T. 1951. Geologic and hydrologic factors affecting perennial yield of aquifers. Jour. Am. Water Works Assoc. v. 43.
- Stuart, W. T., C. V. Theis, and G. M. Stanley. 1948. Ground-water problems of the Iron River district, Michigan. Mich. Dept. Conserv., Geol. Survey Div. Tech. Rept. 2.
- Stuart, W. T. 1955. Pumping test evaluates water problem at Eureka. Nevada. Mining Eng., Feb.
- Suter, Max, R. E. Bergstrom, H. F. Smith, G. H. Emrich, W. C. Walton, and T. E. Larson. 1959. Preliminary report on ground-water resources of the Chicago region, Illinois. State Water Survey and Geol. Survey Cooperative Ground-Water Rept. 1.
- Suter, Max, and R. H. Harneson. 1960. Artificial ground-water recharge at Peoria, Illinois. Illinois State Water Survey Bull. 48.
- Theis, C. V. 1932. Equation for lines of flow in vicinity of discharging artesian well. Trans. Am. Geophys. Union.
- Theis, C. V. 1935. The relation between the lowering of piezometric surface and the rate and duration of discharge of a well using ground-water storage. Trans. Am. Geophys. Union 16th Ann. Meeting, pt. 2.
- Theis, C. V. 1938. The significance and nature of the cone of depression in ground-water bodies. Economic Geol. v. 33(8).
- Theis, C. V. 1940. The source of water derived from wells, essential factors controlling the response of an aquifer to development. Civil Eng., May.
- Theis, C. V. 1941. The effect of a well on the flow of a nearby stream. Trans. Am. Geophys. Union pt. 3.
- Theis, C. V. 1954. Computation of drawdowns at equilibrium caused by wells drawing water from an aquifer fed by a finite straight line source. U.S. Geol. Survey Ground Water Note, Hydraulics, No. 19.
- Theis, C. V. 1957. The spacing of pumped wells. U.S. Geol. Survey Ground Water Branch, Ground Water Notes, Hydraulics, No. 31, open-file rept.
- Thomas, H. E. 1951. The conservation of ground water. McGraw-Hill Book Co., New York.
- Todd, D. K. 1955a. Flow in porous media studied in Hele-Shaw Channel. Civil Eng. v. 25.
- Todd, D. K. 1955b. Investigating ground water by applied geophysics. Proc. Am. Soc. Civil Engrs. v. 81, Separate No. 625.
- Todd, D. K. 1959. Ground-water hydrology. John Wiley & Sons, New York.
- Tolman, C. F. 1937. Ground water. McGraw-Hill Book Co., New York.
- Turneure, F. E., and H. L. Russell. 1924. Public water supplies. John Wiley & Sons, New York.
- Ubell, K. 1956. Unsteady flow of ground water caused by well drawdown. International Assoc. Sci. Hydrology, Symposia Darcy, Dijon, publ. 41.
- Veatch, A. C. 1906. Fluctuation of the water level in wells, with special reference to Long Island, New York. U.S. Geol. Survey Water Supply Paper 155.
- Vorhis, R. C. 1953. Milwaukee hydroseismograms and their interpretation. U.S. Geol. Survey Water Res. Bull., May.
- Walker, W. H., and W. C. Walton. 1961. Ground-water development in three areas of central Illinois. Illinois State Water Survey Rept. of Invest. 41.
- Walton, W. C., and W. J. Drescher. 1952. Composite type curve for analyzing ground-water pumping test data. U.S. Geol. Survey Ground Water Note, Hydraulics Section, No. 2.
- Walton, W. C. 1953. The hydraulic properties of a dolomite aquifer underlying the village of Ada, Ohio. Ohio Div. of Water Tech. Rept. 1.
- Walton, W. C. 1955. Ground-water hydraulics as an aid to geologic interpretation. Ohio Jour. Sci. v. 55 (1).
- Walton, W. C. 1959. Efficiency of wells. Illinois State Water Survey mimeo. rept.
- Walton, W. C., and J. W. Stewart. 1959. Aquifer test in the Snake River basalt. Jour. of Irrigation and Drainage Div., Proc. Am. Soc. Civil Engrs. v. 85, pt. 1.
- Walton, W. C. 1960a. Leaky artesian aquifer conditions in Illinois. Illinois State Water Survey Rept. of Invest. 39.
- Walton, W. C. 1960b. Application and limitation of methods used to analyze pumping test data. Water Well Jour., Feb. and March.
- Walton, W. C., R. T. Sasman, and R. R. Russell. 1960. Water level decline and pumpage during 1959 in deep wells in the Chicago region, Illinois. Illinois State Water Survey Circ. 79.
- Walton, W. C., and G. D. Scudder. 1960. Ground-water resources of the valley-train deposits in the Fairborn area, Ohio. Ohio Div. of Water Tech. Rept. 3.
- Walton, W. C., and J. C. Neill. 1960. Analyzing ground-water problems with mathematical model aquifers and a digital computer. International Assoc. Sci. Hydrology, General Assembly of Helsinki, v. 2, publ. 52.
- Walton, W. C., and W. H. Walker. 1961. Evaluating wells and aquifers by analytical methods. Jour. Geophys. Res. v. 66(10).
- Walton, W. C., and Sandor Csallany. 1962. Yields of deep sandstone wells in northern Illinois. Illinois State Water Survey Rept. of Invest. 43.
- Warren, M. A. 1952. Graphical short cuts in applying the non-equilibrium formula to ground-water problems. U.S. Geol. Survey Water Res. Bull., Aug.
- Wenzel, L. K. 1936. The Thiem method for determining permeability of water-bearing materials and its application to the determination of specific yield, results of investigations in the Platte River Valley, Nebraska. U.S. Geol. Survey Water Supply Paper 679-A.
- Wenzel, L. K. 1942. Methods of determining permeability of water-bearing materials, with special reference to discharging-well methods. U.S. Geol. Survey Water Supply Paper 887.
- Wenzel, L. K., and H. H. Sand. 1942. Water supply of the Dakota sandstone in the Ellentown-Jamestown area, North Dakota. U.S. Geol. Survey Water Supply Paper 889-A.
- Wenzel, L. K., and A. L. Greenlee. 1943. A method for determining transmissibility and storage coefficients by tests of multiple well-systems. Trans. Am. Geophys. Union 24th Ann. Meeting, pt. 2.
- White, W. N. 1932. A method of estimating ground-water supplies based on discharge by plants and evaporation from soil, results of investigations in Escalante Valley, Utah. U.S. Geol. Survey Water Supply Paper 659-A.
- Woollard, G. P., and G. G. Hanson. 1954. Geophysical methods applied to geologic problems in Wisconsin. Wis. Geol. Survey Bull. 78, Madison.
- Wyckoff, R. D., H. G. Botset, and Morris Muskat. 1932. Flow of liquids through porous media under the action of gravity. Physics v. 3 (2), Aug.
- Zeisel, A. J., W. C. Walton, R. T. Sasman, and T. A. Prickett. In press 1962. Ground-water resources of DuPage County, Illinois. Illinois State Water Survey and Geol. Survey Cooperative Ground-Water Rept. 2.

APPENDIX A  
VALUES OF W (u, r/B)

$\frac{r}{B}$ u	0	0.001	0.002	0.003	0.004	0.005	0.006	0.007	0.008	0.009	0.01
0	00	14.0474	12.6611	11.8502	11.2748	10.8286	10.4640	10.1557	9.8887	9.6532	9.4425
.000001	13.2383	13.0031	12.4417	11.8153	11.2711	10.8283	10.4640	10.1557	9.8887		
.000002	12.5451	12.4240	12.1013	11.6716	11.2259	10.8174	10.4619	10.1554	9.8886	9.6532	
.000003	12.1397	12.0581	11.8322	11.5098	11.1462	10.7849	10.4509	10.1523	9.8879	9.6530	9.4425
.000004	11.8520	11.7905	11.6168	11.3597	11.0555	10.7374	10.4291	10.1436	9.8849	9.6521	9.4422
.000005	11.6289	11.5795	11.4384	11.2248	10.9642	10.6822	10.3993	10.1290	9.8786	9.6496	9.4413
.000006	11.4465	11.4053	11.2866	11.1040	10.8764	10.6240	10.3640	10.1094	9.8686	9.6450	9.4394
.000007	11.2924	11.2570	11.1545	10.9951	10.7933	10.5652	10.3255	10.0862	9.8555	9.6382	9.4361
.000008	11.1589	11.1279	11.0377	10.8962	10.7151	10.5072	10.2854	10.0602	9.8398	9.6292	9.4313
.000009	11.0411	11.0135	10.9330	10.8059	10.6416	10.4508	10.2446	10.0324	9.8219	9.6182	9.4251
.00001	10.9357	10.9109	10.8382	10.7228	10.5725	10.3963	10.2038	10.0034	9.8024	9.6059	9.4176
.00002	10.2426	10.2301	10.1932	10.1332	10.0522	9.9530	9.8386	9.7126	9.5781	9.4383	9.2961
.00003	9.8371	9.8288	9.8041	9.7635	9.7081	9.6392	9.5583	9.4671	9.3674	9.2611	9.1499
.00004	9.5495	9.5432	9.5246	9.4940	9.4520	9.3992	9.3366	9.2653	9.1863	9.1009	9.0102
.00005	9.3263	9.3213	9.3064	9.2818	9.2480	9.2052	9.1542	9.0957	9.0304	8.9591	8.8827
.00006	9.1440	9.1398	9.1274	9.1069	9.0785	9.0426	8.9996	8.9500	8.8943	8.8332	8.7673
.00007	8.9899	8.9863	8.9756	8.9580	8.9336	8.9027	8.8654	8.8224	8.7739	8.7204	8.6625
.00008	8.8563	8.8532	8.8439	8.8284	8.8070	8.7798	8.7470	8.7090	8.6661	8.6186	8.5669
.00009	8.7386	8.7358	8.7275	8.7138	8.6947	8.6703	8.6411	8.6071	8.5686	8.5258	8.4792
.0001	8.6332	8.6308	8.6233	8.6109	8.5937	8.5717	8.5453	8.5145	8.4796	8.4407	C.3983
.0002	7.9402	7.9390	7.9352	7.9290	7.9203	7.9092	7.8958	7.8800	7.8619	7.8416	7.8192
.0003	7.5348	7.5340	7.5315	7.5274	7.5216	7.5141	7.5051	7.4945	7.4823	7.4686	7.4534
.0004	7.2472	7.2466	7.2447	7.2416	7.2373	7.2317	7.2249	7.2169	7.2078	7.1974	7.1859
.0005	7.0242	7.0237	7.0222	7.0197	7.0163	7.0118	7.0063	6.9999	6.9926	6.9843	6.9750
.0006	6.8420	6.8416	6.8403	6.8383	6.8353	6.8316	6.8271	6.8218	6.8156	6.8086	6.8009
.0007	6.6879	6.6876	6.6865	6.6848	6.6823	6.6790	6.6752	6.6706	6.6653	6.6594	6.6527
.0008	6.5545	6.5542	6.5532	6.5517	6.5495	6.5467	6.5433	6.5393	6.5347	6.5295	6.5237
.0009	6.4368	6.4365	6.4357	6.4344	6.4324	6.4299	6.4269	6.4233	6.4192	6.4146	6.4094
.001	6.3315	6.3313	6.3305	6.3293	6.3276	6.3253	6.3226	6.3194	6.3157	6.3115	6.3069
.002	5.6394	5.6393	5.6389	5.6383	5.6374	5.6363	5.6350	5.6334	5.6315	5.6294	5.6271
.003	5.2349	5.2348	5.2346	5.2342	5.2336	5.2329	5.2320	5.2310	5.2297	5.2283	5.2267
.004	4.9482	4.9482	4.9480	4.9477	4.9472	4.9467	4.9460	4.9453	4.9443	4.9433	4.9421
.005	4.7261	4.7260	4.7259	4.7256	4.7253	4.7249	4.7244	4.7237	4.7230	4.7222	4.7212
.006	4.5448	4.5448	4.5447	4.5444	4.5441	4.5438	4.5433	4.5428	4.5422	4.5415	4.5407
.007	4.3916	4.3916	4.3915	4.3913	4.3910	4.3908	4.3904	4.3899	4.3894	4.3888	4.3882
.008	4.2591	4.2590	4.2590	4.2588	4.2586	4.2583	4.2580	4.2576	4.2572	4.2567	4.2561
.009	4.1423	4.1423	4.1422	4.1420	4.1418	4.1416	4.1413	4.1410	4.1406	4.1401	4.1396
.01	4.0379	4.0379	4.0378	4.0377	4.0375	4.0373	4.0371	4.0368	4.0364	4.0360	4.0356
.02	3.3547	3.3547	3.3547	3.3546	3.3545	3.3544	3.3543	3.3542	3.3540	3.3538	3.3536
.03	2.9591	2.9591	2.9591	2.9590	2.9590	2.9589	2.9589	2.9588	2.9587	2.9585	2.9584
.04	2.6813	2.6812	2.6812	2.6812	2.6812	2.6811	2.6810	2.6810	2.6809	2.6808	2.6807
.05	2.4679	2.4679	2.4679	2.4679	2.4678	2.4678	2.4678	2.4677	2.4676	2.4676	2.4675
.06	2.2953	2.2953	2.2953	2.2953	2.2952	2.2952	2.2952	2.2952	2.2951	2.2950	2.2950
.07	2.1508	2.1508	2.1508	2.1508	2.1508	2.1508	2.1508	2.1507	2.1507	2.1506	2.1506
.08	2.0269	2.0269	2.0269	2.0269	2.0269	2.0269	2.0269	2.0268	2.0268	2.0268	2.0267
.09	1.9187	1.9187	1.9187	1.9187	1.9187	1.9187	1.9187	1.9186	1.9186	1.9186	1.9185
.1	1.8229	1.8229	1.8229	1.8229	1.8229	1.8229	1.8229	1.8228	1.8228	1.8228	1.8227
.2	1.2227	1.2226	1.2226	1.2226	1.2226	1.2226	1.2226	1.2226	1.2226	1.2226	1.2226
.3	0.9057	0.9057	0.9057	0.9057	0.9057	0.9057	0.9057	0.9057	0.9056	0.9056	0.9056
.4	7024	7024	7024	7024	7024	7024	7024	7024	7024	7024	7024
.5	5598	5598	5598	5598	5598	5598	5598	5598	5598	5598	5598
.6	4544	4544	4544	4544	4544	4544	4544	4544	4544	4544	4544
.7	3738	3738	3738	3738	3738	3738	3738	3738	3738	3738	3738
.8	3106	3106	3106	3106	3106	3106	3106	3106	3106	3106	3106
.9	2602	2602	2602	2602	2602	2602	2602	2602	2602	2602	2602
1.0	0.2194	0.2194	0.2194	0.2194	0.2194	0.2194	0.2194	0.2194	0.2194	0.2194	0.2194
2.0	489	489	489	489	489	489	489	489	489	489	489
3.0	130	130	130	130	130	130	130	130	130	130	130
4.0	38	38	38	38	38	38	38	38	38	38	38
5.0	11	11	11	11	11	11	11	11	11	11	11
6.0	4	4	4	4	4	4	4	4	4	4	4
7.0	1	1	1	1	1	1	1	1	1	1	1
8.0	0	0	0	0	0	0	0	0	0	0	0

(FROM HANTUSH, 1956)

APPENDIX A (CONTINUED)

VALUES OF W (u, r/B)

$\frac{r}{B}$ u	0.01	0.015	0.02	0.025	0.03	0.035	0.04	0.045	0.05	0.055	0.06	0.065	0.07	0.075	0.08	0.085	0.09	0.095	0.10
0	9.4425	8.6319	8.0569	7.6111	7.2471	6.9394	6.6731	6.4383	6.2285	6.0388	5.8658	5.7067	5.5596	5.4228	5.2950	5.1750	5.0620	4.9553	4.8541
.000001																			
.000002																			
.000003	9.4425																		
.000004	9.4422																		
.000005	9.4413																		
.000006	9.4394																		
.000007	9.4361	8.6319																	
.000008	9.4313	8.6318																	
.000009	9.4251	8.6316																	
.00001	9.4176	8.6313	8.0569																
.00002	9.2961	8.6152	8.0558	7.6111	7.2471														
.00003	9.1499	8.5737	8.0483	7.6101	7.2470														
.00004	9.0102	8.5168	8.0320	7.6069	7.2465	6.9394	6.6731												
.00005	8.8827	8.4533	8.0080	7.6000	7.2450	6.9391	6.6730												
.00006	8.7673	8.3880	7.9786	7.5894	7.2419	6.9384	6.6729	6.4383											
.00007	8.6625	8.3233	7.9456	7.5754	7.2371	6.9370	6.6726	6.4382	6.2285										
.00008	8.5669	8.2603	7.9105	7.5589	7.2305	6.9347	6.6719	6.4361	6.2284										
.00009	8.4792	8.1996	7.8743	7.5402	7.2222	6.9316	6.6709	6.4378	6.2283										
.0001	8.3983	8.1414	7.8375	7.5199	7.2122	6.9273	6.6693	6.4372	6.2282	6.0388	5.8658	5.7067	5.5596	5.4228	5.2950				
.0002	7.8192	7.6780	7.4972	7.2898	7.0685	6.8439	6.6242	6.4143	6.2173	6.0338	5.8637	5.7059	5.5593	5.4227	5.2949	5.1750	5.0620	4.9553	
.0003	7.4534	7.3562	7.2281	7.0759	6.9068	6.7276	6.5444	6.3623	6.1848	6.0145	5.8527	5.6999	5.5562	5.4212	5.2942	5.1747	5.0619	4.9552	4.8541
.0004	7.1859	7.1119	7.0128	6.8929	6.7567	6.6088	6.4538	6.2955	6.1373	5.9818	5.8309	5.6860	5.5476	5.4160	5.2912	5.1730	5.0610	4.9547	4.8539
.0005	6.9750	6.9152	6.8346	6.7357	6.6219	6.4964	6.3626	6.2236	6.0821	5.9406	5.8011	5.6648	5.5330	5.4062	5.2848	5.1689	5.0585	4.9532	4.8530
.0006	6.8009	6.7508	6.6828	6.5988	6.5011	6.3923	6.2748	6.1512	6.0239	5.8948	5.7658	5.6383	5.5134	5.3921	5.2749	5.1621	5.0539	4.9502	4.8510
.0007	6.6527	6.6096	6.5508	6.4777	6.3923	6.2962	6.1917	6.0807	5.9652	5.8468	5.7274	5.6081	5.4902	5.3745	5.2618	5.1526	5.0471	4.9454	4.8478
.0008	6.5237	6.4858	6.4340	6.3695	6.2935	6.2076	6.1136	6.0129	5.9073	5.7982	5.6873	5.5755	5.4642	5.3542	5.2461	5.1406	5.0381	4.9388	4.8430
.0009	6.4094	6.3757	6.3294	6.2716	6.2032	6.1256	6.0401	5.9481	5.8509	5.7500	5.6465	5.5416	5.4364	5.3317	5.2282	5.1266	5.0272	4.9306	4.8368
.001	6.3069	6.2765	6.2347	6.1823	6.1202	6.0494	5.9711	5.8864	5.7965	5.7026	5.6058	5.5071	5.4075	5.3078	5.2087	5.1109	5.0133	4.9208	4.8292
.007	5.6271	5.6118	5.5907	5.5638	5.5314	5.4939	5.4516	5.4047	5.3538	5.2991	5.2411	5.1803	5.1170	5.0517	4.9848	4.9166	4.8475	4.7778	4.7079
.003	5.2267	5.2166	5.2025	5.1845	5.1627	5.1373	5.1064	5.0762	5.0408	5.0025	4.9615	4.9180	4.8722	4.8243	4.7746	4.7234	4.6707	4.6169	4.5622
.004	4.9421	4.9345	4.9240	4.9105	4.8941	4.8749	4.8530	4.8286	4.8016	4.7722	4.7406	4.7068	4.6710	4.6335	4.5942	4.5533	4.5111	4.4676	4.4230
.005	4.7212	4.7152	4.7068	4.6960	4.6829	4.6675	4.6499	4.6302	4.6084	4.5846	4.5590	4.5314	4.5022	4.4713	4.4389	4.4050	4.3699	4.3335	4.2960
.006	4.5407	4.5357	4.5287	4.5197	4.5088	4.4960	4.4814	4.4649	4.4467	4.4267	4.4051	4.3819	4.3573	4.3311	4.3036	4.2747	4.2446	4.2134	4.1812
.007	4.3882	4.3839	4.3779	4.3702	4.3609	4.3500	4.3374	4.3233	4.3077	4.2905	4.2719	4.2518	4.2305	4.2078	4.1839	4.1588	4.1326	4.1053	4.0771
.008	4.2561	4.2524	4.2471	4.2404	4.2323	4.2228	4.2118	4.1994	4.1857	4.1707	4.1544	4.1368	4.1180	4.0980	4.0769	4.0547	4.0315	4.0073	3.9822
.009	4.1396	4.1363	4.1317	4.1258	4.1186	4.1101	4.1004	4.0894	4.0772	4.0638	4.0493	4.0336	4.0169	3.9991	3.9802	3.9603	3.9395	3.9178	3.8952
.01	4.0356	4.0326	4.0285	4.0231	4.0167	4.0091	4.0003	3.9905	3.9795	3.9675	3.9544	3.9403	3.9252	3.9091	3.8920	3.8741	3.8552	3.8356	3.8150
.02	3.3536	3.3521	3.3502	3.3476	3.3444	3.3408	3.3365	3.3317	3.3264	3.3205	3.3141	3.3071	3.2997	3.2917	3.2832	3.2742	3.2647	3.2547	3.2442
.03	2.9584	2.9575	2.9562	2.9545	2.9523	2.9501	2.9474	2.9444	2.9409	2.9370	2.9329	2.9284	2.9235	2.9183	2.9127	2.9069	2.9007	2.8941	2.8873
.04	2.6807	2.6800	2.6791	2.6779	2.6765	2.6747	2.6727	2.6705	2.6680	2.6652	2.6622	2.6589	2.6553	2.6515	2.6475	2.6432	2.6386	2.6338	2.6288
.05	2.4675	2.4670	2.4662	2.4653	2.4642	2.4628	2.4613	2.4595	2.4576	2.4554	2.4531	2.4505	2.4478	2.4448	2.4416	2.4383	2.4347	2.4310	2.4271
.06	2.2950	2.2945	2.2940	2.2932	2.2923	2.2912	2.2900	2.2885	2.2870	2.2852	2.2833	2.2812	2.2790	2.2766	2.2740	2.2713	2.2684	2.2654	2.2622
.07	2.1506	2.1502	2.1497	2.1491	2.1483	2.1474	2.1464	2.1452	2.1439	2.1424	2.1408	2.1391	2.1372	2.1352	2.1331	2.1308	2.1284	2.1258	2.1232
.08	2.0267	2.0264	2.0260	2.0255	2.0248	2.0240	2.0231	2.0221	2.0210	2.0198	2.0184	2.0169	2.0153	2.0136	2.0118	2.0099	2.0078	2.0054	2.0034
.09	1.9163	1.9183	1.9179	1.9174	1.9169	1.9162	1.9154	1.9146	1.9136	1.9125	1.9114	1.9101	1.9087	1.9072	1.9056	1.9040	1.9022	1.9003	1.8983
.1	1.8227	1.8225	1.8222	1.8218	1.8213	1.8207	1.8200	1.8193	1.8184	1.8175	1.8164	1.8153	1.8141	1.8128	1.8114	1.8099	1.8084	1.8067	1.8050
.2	1.2226	1.2225	1.2224	1.2222	1.2220	1.2218	1.2215	1.2212	1.2209	1.2205	1.2201	1.2198	1.2192	1.2186	1.2181	1.2175	1.2168	1.2162	1.2155
.3	0.9056	0.9056	0.9055	0.9054	0.9053	0.9052	0.9050	0.9049	0.9047	0.9045	0.9043	0.9040	0.9038	0.9035	0.9032	0.9029	0.9025	0.9022	0.9018
.4	7024	7023	7023	7022	7022	7021	7020	7019	7018	7016	7015	7014	7012	7010	7008	7006	7004	7002	7000
.5	5598	5597	5597	5597	5596	5596	5595	5594	5594	5593	5592	5591	5590	5588	5587	5586	5584	5583	5581
.6	4544	4544	4543	4543	4543	4542	4542	4542	4541	4540	4540	4539	4538	4537	4536	4535	4534	4533	4532
.7	3738	3738	3737	3737	3737	3737	3736	3736	3735	3735	3734	3734	3733	3733	3732	3732	3731	3730	3729
.8	3106	3106	3106	3106	3106	3105	3105	3105	3104	3104	3104	3103	3103	3102	3102	3101	3101	3100	3100
.9	2602	2602	2602	2602	2601	2601	2601	2601	2601	2600	2600	2600	2599	2599	2599	2598	2598	2597	2597
1.0	0.2194	0.2194	0.2194	0.2194	0.2193	0.2193	0.2193	0.2193	0.2193	0.2193	0.2192	0.2192	0.2192	0.2191	0.2191	0.2191	0.2191	0.2190	0.2190
2.0	489	489	489	489	429	489	489	489	489	489	489	489	489	489	489	489	489	488	488
3.0	130	130	130	130	130	130	130	130	130	130	130	130	130	130	130	130	130	130	130
4.0	38	38	38	38	38	38	38	38	38	38	38	38	38	38	38	38	38	38	38
5.0	11	11	11	11	11	11	11	11	11	11	11	11	11	11	11	11	11	11	11
6.0	4	4	4	4	4	4	4	4	4	4	4	4	4	4	4	4	4	4	4
7.0	1	1	1	1	1	1	1	1	1	1	1	1	1	1	1	1	1	1	1
8.0	0	0	0	0	0	0	0	0	0	0	0	0	0	0	0	0	0	0	0

APPENDIX A (CONTINUED)  
VALUES OF  $W(u, r/B)$

$\frac{r}{B}$ u	0.1	0.15	0.2	0.25	0.3	0.35	0.4	0.45	0.5	0.55	0.6	0.65	0.7	0.75	0.8	0.85	0.9	0.95	1.0
0	4.8541	4.0601	3.5054	3.0850	2.7449	2.4654	2.2291	2.0258	1.8488	1.6981	1.5550	1.4317	1.3210	1.2212	1.1307	1.0485	0.9735	0.9049	0.8420
.0001																			
.0002																			
.0003	4.8541																		
.0004	4.8539																		
.0005	4.8530																		
.0006	4.8510	4.0601																	
.0007	4.8478	4.0600																	
.0008	4.8430	4.0599																	
.0009	4.8368	4.0598																	
.001	4.8292	4.0595	3.5054																
.002	4.7079	4.0435	3.5043	3.0830	2.7449														
.003	4.5622	4.0092	3.4969	3.0821	2.7448														
.004	4.4230	3.9551	3.4806	3.0788	2.7444														
.005	4.2960	3.8821	3.4567	3.0719	2.7428	2.4654	2.2291												
.006						2.4651	2.2290												
.006	4.1812	3.8284	3.4274	3.0614	2.7398	2.4644	2.2289	2.0258											
.007	4.0771	3.7529	3.3947	3.0476	2.7350	2.4630	2.2286	2.0257											
.008	3.9822	3.6903	3.3598	3.0311	2.7284	2.4608	2.2279	2.0256	1.8488										
.009	3.8952	3.6302	3.3239	3.0126	2.7202	2.4576	2.2269	2.0253	1.8487										
.01	3.8150	3.5725	3.2875	2.9925	2.7104	2.4534	2.2253	2.0248	1.8486	1.6931	1.5550	1.4317	1.3210	1.2212	1.1307	1.0485			
.02	3.2442	3.1158	2.9521	2.7658	2.5688	2.3713	2.1809	2.0023	1.8379	1.6883	1.5530	1.4309	1.3207	1.2210	1.1306	1.0484	0.9735	0.9049	
.03	2.8873	2.8017	2.6896	2.5571	2.4110	2.2578	2.1031	1.9515	1.8062	1.6695	1.5423	1.4251	1.3177	1.2195	1.1299	1.0481	9733	9048	0.8420
.04	2.6288	2.5655	2.4816	2.3802	2.2661	2.1431	2.0155	1.8869	1.7603	1.6379	1.5213	1.4117	1.3094	1.2146	1.1270	1.0465	9724	9044	8418
.05	2.4271	2.3776	2.3110	2.2299	2.1371	2.0356	1.9283	1.8181	1.7075	1.5985	1.4927	1.3914	1.2955	1.2052	1.1210	1.0426	9700	9029	8409
.06	2.2622	2.2218	2.1673	2.1002	2.0227	1.9369	1.8452	1.7497	1.6524	1.5551	1.4593	1.3663	1.2770	1.1919	1.1116	1.0362	9657	9001	8391
.07	2.1232	2.0894	2.0435	1.9867	1.9206	1.8469	1.7673	1.6835	1.5975	1.5101	1.4232	1.3380	1.2551	1.1754	1.0993	1.0272	9593	8956	8360
.08	2.0034	1.9745	1.9351	1.8861	1.8290	1.7646	1.6947	1.6206	1.5436	1.4650	1.3860	1.3078	1.2310	1.1564	1.0847	1.0161	9510	8895	8316
.09	1.8983	1.8732	1.8389	1.7961	1.7460	1.6892	1.6272	1.5609	1.4918	1.4206	1.3486	1.2766	1.2054	1.1358	1.0682	1.0032	9411	8819	8759
1	1.8050	1.7829	1.7527	1.7149	1.6704	1.6198	1.5644	1.5048	1.4422	1.3774	1.3115	1.2451	1.1791	1.1140	1.0505	0.9890	0.9297	0.8730	0.8190
2	1.2155	1.2066	1.1944	1.1789	1.1602	1.1387	1.1145	1.0879	1.0592	1.0286	0.9964	0.9629	0.9284	0.8932	0.8575	0.8216	0.7857	0.7501	0.7148
3	0.9018	0.8969	0.8902	0.8817	0.8713	0.8593	0.8457	0.8306	0.8142	0.7964	0.7775	0.7577	0.7362	0.7154	0.6932	0.6706	0.6476	0.6244	0.6010
4	0.7000	0.6969	0.6927	0.6874	0.6809	0.6733	0.6647	0.6551	0.6446	0.6332	0.6209	0.6080	0.5943	0.5800	0.5653	0.5501	0.5345	0.5186	0.5024
5	0.5581	0.5561	0.5532	0.5496	0.5453	0.5402	0.5344	0.5278	0.5206	0.5128	0.5044	0.4955	0.4860	0.4760	0.4658	0.4550	0.4440	0.4326	0.4210
6	0.4532	0.4518	0.4498	0.4472	0.4441	0.4405	0.4364	0.4317	0.4266	0.4210	0.4150	0.4086	0.4018	0.3946	0.3871	0.3793	0.3712	0.3629	0.3543
7	0.3729	0.3719	0.3704	0.3685	0.3663	0.3636	0.3606	0.3572	0.3534	0.3493	0.3449	0.3401	0.3351	0.329	0.3242	0.3183	0.3123	0.3060	0.2996
8	0.3100	0.3092	0.3081	0.3067	0.3050	0.3030	0.3008	0.2982	0.2953	0.2922	0.2889	0.2853	0.2815	0.277	0.2732	0.2687	0.2641	0.2592	0.2543
9	0.2597	0.2591	0.2583	0.2572	0.2559	0.2544	0.2527	0.2507	0.2485	0.2461	0.2436	0.2408	0.2378	0.234	0.2314	0.2280	0.2244	0.2207	0.2168
1.0	0.2190	0.2186	0.2179	0.2171	0.2161	0.2149	0.2135	0.2120	0.2103	0.2085	0.2065	0.2043	0.2020	0.1995	0.1970	0.1943	0.1914	0.1885	0.1855
2.0	0.488	0.488	0.487	0.486	0.485	0.484	0.482	0.480	0.477	0.475	0.473	0.470	0.467	0.463	0.460	0.456	0.452	0.446	0.444
3.0	0.130	0.130	0.130	0.130	0.130	0.130	0.129	0.129	0.128	0.128	0.127	0.127	0.126	0.125	0.125	0.124	0.123	0.123	0.122
4.0	0.38	0.38	0.38	0.38	0.38	0.38	0.38	0.38	0.37	0.37	0.37	0.37	0.37	0.37	0.37	0.36	0.36	0.36	0.36
5.0	0.11	0.11	0.11	0.11	0.11	0.11	0.11	0.11	0.11	0.11	0.11	0.11	0.11	0.11	0.11	0.11	0.11	0.11	0.11
6.0	0.4	0.4	0.4	0.4	0.4	0.4	0.4	0.4	0.4	0.4	0.4	0.4	0.4	0.4	0.4	0.4	0.4	0.4	0.4
7.0	0.1	0.1	0.1	0.1	0.1	0.1	0.1	0.1	0.1	0.1	0.1	0.1	0.1	0.1	0.1	0.1	0.1	0.1	0.1
8.0	0	0	0	0	0	0	0	0	0	0	0	0	0	0	0	0	0	0	0

$\frac{r}{B}$ u	1.0	1.5	2.0	2.5	3.0	3.5	4.0	4.5	5.0	6.0	7.0	8.0	9.0
0	0.8420	0.4276	0.2278	0.1247	0.0695	0.0392	0.0223	0.0128	0.0074	0.0025	0.0008	0.0003	0.0001
.01													
.02													
.03	0.8420												
.04	8418												
.05	8409												
.06	8391												
.07	8360	0.4276											
.08	8316	4275											
.09	8259	4274											
.1	0.8190	0.4271	0.2278										
.2	7148	4135	0.2268	0.1247	0.0695								
.3	6010	3812	0.2211	0.1240	0.0694								
.4	5024	3411	0.2096	0.1217	0.0691	0.0392							
.5	4210	3007	0.1944	0.1174	0.0681	0.390	0.0223						
.6	3543	2630	0.1774	0.1112	0.0664	0.386	0.222	0.0128					
.7	2996	2292	0.1602	0.1040	0.0639	0.379	0.221	0.127					
.8	2543	1994	0.1436	0.0961	0.0607	0.368	0.218	0.127	0.0074				
.9	2168	1734	0.1281	0.0881	0.0572	0.354	0.213	0.125	0.73				
1.0	0.1855	0.1509	0.1139	0.0803	0.0534	0.0338	0.0207	0.0123	0.0073	0.0025			
2.0	0.444	0.394	0.335	0.271	0.210	0.156	0.112	0.077	0.051	0.021	0.0008	0.0003	
3.0	0.122	0.112	0.100	0.086	0.071	0.057	0.045	0.034	0.025	0.012	0.006	0.003	0.0001
4.0	0.36	0.34	0.31	0.27	0.24	0.20	0.16	0.13	0.10	0.06	0.03	0.02	0.0001
5.0	0.11	0.10	0.10	0.09	0.08	0.07	0.06	0.05	0.04	0.02	0.01	0.01	0
6.0	0.4	0.3	0.3	0.3	0.3	0.2	0.2	0.2	0.2	0.1	0.1	0	
7.0	0.1	0.1	0.1	0.1	0.1	0.1	0.1	0.1	0.1	0.1	0	0	
8.0	0	0	0	0	0	0	0	0	0	0	0	0	

APPENDIX B  
VALUES OF  $K_0 \left(\frac{r}{B}\right)$

$N / \frac{r}{B}$	$N \times 10^{-3}$	$N \times 10^{-2}$	$N \times 10^{-1}$	N
1.0	7.0237	4.7212	2.4271	0.4210
1.1	6.9284	4.6260	2.3333	.3656
1.2	6.8414	4.5390	2.2479	.3185
1.3	6.7613	4.4590	2.1695	.2782
1.4	6.6872	4.3849	2.0972	.2437
1.5	6.6182	4.3159	2.0300	.2138
1.6	6.5537	4.2514	1.9674	.1880
1.7	6.4931	4.1908	1.9088	.1655
1.8	6.4359	4.1337	1.8537	.1459
1.9	6.3818	4.0797	1.8018	.1288
2.0	6.3305	4.0285	1.7527	.1139
2.1	6.2818	3.9797	1.7062	.1008
2.2	6.2352	3.9332	1.6620	.0893
2.3	6.1908	3.8888	1.6199	.0791
2.4	6.1482	3.8463	1.5798	.0702
2.5	6.1074	3.8056	1.5415	.0623
2.6	6.0682	3.7664	1.5048	.0554
2.7	6.0304	3.7287	1.4697	.0493
2.8	5.9941	3.6924	1.4360	.0438
2.9	5.9590	3.6574	1.4036	.0390
3.0	5.9251	3.6235	1.3725	.0347
3.1	5.8923	3.5908	1.3425	.0310
3.2	5.8606	3.5591	1.3136	.0276
3.3	5.8298	3.5284	1.2857	.0246
3.4	5.7999	3.4986	1.2587	.0220
3.5	5.7709	3.4697	1.2327	.0196
3.6	5.7428	3.4416	1.2075	.0175
3.7	5.7154	3.4143	1.1832	.0156
3.8	5.6887	3.3877	1.1596	.0140
3.9	5.6627	3.3618	1.1367	.0125
4.0	5.6374	3.3365	1.1145	.0112
4.1	5.6127	3.3119	1.0930	.0100
4.2	5.5886	3.2879	1.0721	.0089
4.3	5.5651	3.2645	1.0518	.0080
4.4	5.5421	3.2415	1.0321	.0071
4.5	5.5196	3.2192	1.0129	.0064
4.6	5.4977	3.1973	0.9943	.0057
4.7	5.4762	3.1758	.9761	.0051
4.8	5.4551	3.1549	.9584	.0046
4.9	5.4345	3.1343	.9412	.0041
5.0	5.4143	3.1142	.9244	.0037
5.1	5.3945	3.0945	.9081	
5.2	5.3751	3.0752	.8921	
5.3	5.3560	3.0562	.8766	
5.4	5.3373	3.0376	.8614	
5.5	5.3190	3.0195	.8466	
5.6	5.3010	3.0015	.8321	
5.7	5.2833	2.9839	.8180	
5.8	5.2659	2.9666	.8042	
5.9	5.2488	2.9496	.7907	

(AFTER HANTUSH, 1956)

APPENDIX B (CONTINUED)

VALUES OF  $K_0(r/B)$

$N/\frac{r}{B}$	$N \times 10^{-3}$	$N \times 10^{-2}$	$N \times 10^{-1}$	N
6.0	5.2320	2.9329	.7775	.0012
6.1	5.2155	2.9165	.7646	
6.2	5.1992	2.9003	.7520	
6.3	5.1832	2.8844	.7397	
6.4	5.1675	2.8688	.7277	
6.5	5.1520	2.8534	.7159	
6.6	5.1367	2.8382	.7043	
6.7	5.1216	2.8233	.6930	
6.8	5.1068	2.8086	.6820	
6.9	5.0922	2.7941	.6711	
7.0	5.0779	2.7798	.6605	.0004
7.1	5.0637	2.7657	.6501	
7.2	5.0497	2.7519	.6399	
7.3	5.0359	2.7382	.6300	
7.4	5.0223	2.7247	.6202	
7.5	5.0089	2.7114	.6106	
7.6	4.9956	2.6983	.6012	
7.7	4.9876	2.6853	.5920	
7.8	4.9697	2.6726	.5829	
7.9	4.4569	2.6599	.5740	
8.0	4.9443	2.6475	.5653	
8.1	4.9319	2.6352	.5568	
8.2	4.9197	2.6231	.5484	
8.3	4.9075	2.6111	.5402	
8.4	4.8956	2.5992	.5321	
8.5	4.8837	2.5875	.5242	
8.6	4.8720	2.5759	.5165	
8.7	4.8605	2.5645	.5088	
8.8	4.8491	2.5532	.5013	
8.9	4.8378	2.5421	.4940	
9.0	4.8266	2.5310	.4867	
9.1	4.8155	2.5201	.4796	
9.2	4.8046	2.5093	.4727	
9.3	4.7938	2.4986	.4658	
9.4	4.7831	2.4881	.4591	
9.5	4.7725	2.4776	.4524	
9.6	4.7621	2.4673	.4459	
9.7	4.7517	2.4571	.4396	
9.8	4.7414	2.4470	.4333	
9.9	4.7313	2.4370	.4271	

APPENDIX C  
VALUES OF W(u)

$N$	$M$	$NX10^{-10}$	$NX10^{-9}$	$NX10^{-8}$	$NX10^{-7}$	$NX10^{-6}$	$NX10^{-5}$	$NX10^{-4}$	$NX10^{-3}$	$NX10^{-2}$	$NX10^{-1}$	$NX10^0$	$NX10^1$	$NX10^2$	$NX10^3$	$N$	
1.0		33.9616	31.6590	29.3564	27.0538	24.7512	22.4486	20.1460	17.8435	15.5409	13.2383	10.9357	8.6332	6.3315	4.0379	1.8229	0.2194
1.1		33.8662	31.5637	29.2611	26.9585	24.6559	22.3533	20.0507	17.7482	15.4456	13.1430	10.8404	8.5379	6.2363	3.9436	1.7371	0.1860
1.2		33.7792	31.4767	29.1741	26.8715	24.5689	22.2663	19.9637	17.6611	15.3586	13.0560	10.7534	8.4509	6.1494	3.8570	1.6505	0.1584
1.3		33.6992	31.3966	29.0940	26.7914	24.4889	22.1863	19.8837	17.5811	15.2785	12.9759	10.6734	8.3709	6.0695	3.7785	1.5889	0.1355
1.4		33.6252	31.3225	29.0199	26.7173	24.4147	22.1122	19.8096	17.5070	15.2044	12.9018	10.5903	8.2968	5.9955	3.7054	1.5241	0.1162
1.5		33.5561	31.2535	28.9509	26.6483	24.3458	22.0432	19.7406	17.4300	15.1354	12.8328	10.5303	8.2278	5.9266	3.6374	1.4645	0.1000
1.6		33.4916	31.1890	28.8864	26.5838	24.2812	21.9786	19.6760	17.3735	15.0709	12.7683	10.4657	8.1634	5.8621	3.5739	1.4092	0.0861
1.7		33.4309	31.1283	28.8258	26.5232	24.2206	21.9180	19.6154	17.3128	15.0103	12.7077	10.4051	8.1027	5.8016	3.5143	1.3578	0.0745
1.8		33.3738	31.0712	28.7656	26.4660	24.1634	21.8608	19.5583	17.2557	14.9531	12.6505	10.3479	8.0455	5.7446	3.4581	1.3098	0.0647
1.9		33.3197	31.0171	28.7145	26.4119	24.1094	21.8068	19.5042	17.2016	14.8990	12.5964	10.2939	7.9915	5.6906	3.4050	1.2649	0.05620
2.0		33.2684	30.9658	28.6632	26.3607	24.0581	21.7555	19.4529	17.1503	14.8477	12.5451	10.2426	7.9402	5.6394	3.3547	1.2227	0.04890
2.1		33.2196	30.9170	28.6145	26.3119	24.0093	21.7067	19.4041	17.1015	14.7989	12.4964	10.1938	7.8914	5.5907	3.3069	1.1829	0.04261
2.2		33.1731	30.8705	28.5679	26.2653	23.9628	21.6602	19.3576	17.0550	14.7524	12.4498	10.1473	7.8449	5.5434	3.2614	1.1454	0.03719
2.3		33.1286	30.8261	28.5235	26.2209	23.9183	21.6157	19.3131	17.0106	14.7080	12.4054	10.1028	7.8004	5.4999	3.2179	1.1099	0.03250
2.4		33.0861	30.7835	28.4809	26.1783	23.8758	21.5732	19.2706	16.9680	14.6654	12.3628	10.0603	7.7579	5.4575	3.1763	1.0762	0.02844
2.5		33.0453	30.7427	28.4401	26.1375	23.8349	21.5323	19.2298	16.9272	14.6246	12.3220	10.0194	7.7172	5.4167	3.1365	1.0443	0.02491
2.6		33.0060	30.7035	28.4009	26.0983	23.7957	21.4931	19.1905	16.8880	14.5844	12.2825	9.9802	7.6779	5.3776	3.0983	1.0139	0.02185
2.7		32.9683	30.6657	28.3631	26.0606	23.7580	21.4554	19.1528	16.8502	14.5476	12.2450	9.9425	7.6401	5.3400	3.0615	9849	0.01918
2.8		32.9319	30.6294	28.3268	26.0242	23.7216	21.4190	19.1164	16.8138	14.5113	12.2087	9.9061	7.6038	5.3037	3.0261	9573	0.01686
2.9		32.8968	30.5943	28.2917	25.9891	23.6865	21.3839	19.0813	16.7788	14.4762	12.1736	9.8710	7.5687	5.2687	2.9920	9309	0.01482
3.0		32.8629	30.5604	28.2578	25.9552	23.6526	21.3500	19.0474	16.7449	14.4423	12.1397	9.8371	7.5348	5.2349	2.9591	9057	0.01305
3.1		32.8302	30.5276	28.2250	25.9224	23.6198	21.3172	19.0146	16.7129	14.4095	12.1069	9.8043	7.5020	5.2022	2.9273	8815	0.01149
3.2		32.7984	30.4958	28.1932	25.8907	23.5881	21.2855	18.9829	16.6803	14.3777	12.0751	9.7726	7.4703	5.1706	2.8965	8583	0.01013
3.3		32.7676	30.4651	28.1625	25.8599	23.5573	21.2547	18.9521	16.6495	14.3470	12.0444	9.7418	7.4395	5.1399	2.8668	8361	0.00895
3.4		32.7378	30.4352	28.1326	25.8300	23.5274	21.2249	18.9223	16.6197	14.3171	12.0145	9.7120	7.4097	5.1102	2.8379	8147	0.007891
3.5		32.7088	30.4062	28.1036	25.8010	23.4985	21.1959	18.8933	16.5907	14.2881	11.9855	9.6830	7.3807	5.0813	2.8099	7942	0.006970
3.6		31.6806	30.3780	28.0755	25.7729	23.4703	21.1677	18.8651	16.5625	14.2599	11.9571	9.6548	7.3526	5.0532	2.7827	7745	0.006160
3.7		32.6532	30.3506	28.0481	25.7455	23.4429	21.1403	18.8377	16.5351	14.2325	11.9300	9.6274	7.3252	5.0259	2.7563	7554	0.005448
3.8		32.6266	30.3240	28.0214	25.7188	23.4162	21.1136	18.8110	16.5085	14.2059	11.9033	9.6007	7.2985	4.9993	2.7306	7371	0.004820
3.9		32.6006	30.2980	27.9954	25.6928	23.3902	21.0877	18.7851	16.4825	14.1799	11.8773	9.5748	7.2725	4.9735	2.7056	7194	0.004277
4.0		32.5753	30.2727	27.9701	25.665	23.3649	21.0623	18.7598	16.4572	14.1546	11.8520	9.5495	7.2472	4.9482	2.6813	7024	0.003779
4.1		32.5506	30.2480	27.9454	25.6428	23.3402	21.0376	18.7351	16.4325	14.1299	11.8273	9.5248	7.2225	4.9236	2.6576	6859	0.003349
4.2		32.5265	30.2239	27.9213	25.6187	23.3161	21.0136	18.7110	16.4084	14.1058	11.8032	9.5007	7.1985	4.8997	2.6344	6700	0.002996
4.3		32.5029	30.2004	27.8978	25.5952	23.2926	20.9900	18.6874	16.3848	14.0823	11.7797	9.4771	7.1749	4.8762	2.6119	6546	0.002633
4.4		32.4800	30.1771	27.8748	25.5722	23.2696	20.9670	18.6644	16.3619	14.0593	11.7567	9.4541	7.1520	4.8533	2.5899	6397	0.002336
4.5		32.4575	30.1549	27.8523	25.5497	23.2471	20.9446	18.6420	16.3394	14.0368	11.7342	9.4317	7.1295	4.8310	2.5684	6253	0.002073
4.6		32.4355	30.1329	27.8303	25.5277	23.2252	20.9226	18.6200	16.3174	14.0148	11.7122	9.4097	7.1075	4.8091	2.5474	6114	0.001841
4.7		32.4140	30.1114	27.8088	25.5062	23.2037	20.9011	18.5985	16.2959	13.9933	11.6907	9.3882	7.0860	4.7877	2.5268	5979	0.001635
4.8		32.3929	30.0901	27.7878	25.4852	23.1826	20.8800	18.5774	16.2748	13.9723	11.6697	9.3671	7.0650	4.7667	2.5068	5848	0.001453
4.9		32.3723	30.0697	27.7672	25.4646	23.1620	20.8604	18.5568	16.2542	13.9510	11.6491	9.3465	7.0444	4.7462	2.4871	5721	0.001291
5.0		32.3521	30.0495	27.7470	25.4444	23.1418	20.8392	18.5366	16.2340	13.9314	11.6289	9.3263	7.0242	4.7261	2.4679	5598	0.001148
5.1		32.3323	30.0297	27.7271	25.4246	23.1220	20.8194	18.5168	16.2142	13.9116	11.6091	9.3065	7.0044	4.7064	2.4491	5478	0.001021
5.2		32.3120	30.0103	27.7077	25.4051	23.1026	20.8000	18.4974	16.1948	13.8922	11.5896	9.2871	6.9850	4.6871	2.4306	5362	0.0009086
5.3		32.2939	29.9913	27.6887	25.3865	23.0835	20.7809	18.4783	16.1758	13.8732	11.5706	9.2681	6.9659	4.6681	2.4126	5250	0.0008066
5.4		32.2752	29.9726	27.6700	25.3674	23.0648	20.7624	18.4596	16.1571	13.8545	11.5519	9.2494	6.9473	4.6495	2.3948	5144	0.0007106
5.5		32.2568	29.9542	27.6516	25.3491	23.0465	20.7439	18.4413	16.1387	13.8361	11.5336	9.2310	6.9289	4.6313	2.3775	5034	0.0006409
5.6		32.2388	29.9362	27.6336	25.3310	23.0285	20.7259	18.4233	16.1207	13.8181	11.5155	9.2130	6.9109	4.6134	2.3600	4930	0.0005708
5.7		32.2211	29.9185	27.6159	25.3133	23.0103	20.7082	18.4056	16.1030	13.8004	11.4978	9.1953	6.8932	4.5958	2.3437	4830	0.0005085
5.8		32.2037	29.9011	27.5985	25.2959	22.9931	20.6908	18.3882	16.0856	13.7830	11.4804	9.1779	6.8758	4.5785	2.3273	4732	0.0004532
5.9		32.1866	29.8840	27.5814	25.2789	22.9763	20.6737	18.3711	16.0685	13.7659	11.4633	9.1608	6.8588	4.5615	2.3111	4637	0.0004039
6.0		32.1698	29.8672	27.5646	25.2620	22.9595	20.6569	18.3543	16.0517	13.7491	11.4465	9.1440	6.8420	4.5448	2.2953	4544	0.0003601
6.1		32.1533	29.8507	27.5481	25.2455	22.9429	20.6403	18.3378	16.0352	13.7326	11.4300	9.1275	6.8254	4.5283	2.2797	4454	0.0003211
6.2		32.1370	29.8344	27.5318	25.2293	22.9267	20.6241	18.3215	16.0189	13.7163	11.4138	9.1112	6.8092	4.5122	2.2645	4366	0.0002864
6.3		32.1210	29.8184	27.5158	25.2133	22.9107	20.6081	18.3055	16.0029	13.7003	11.3978	9.0952	6.7932	4.4963	2.2494	4280	0.0002555
6.4		32.1053	29.8027	27.5001	25.1975	22.8949	20.5923	18.2898	15.9872	13.6846	11.3820	9.0795	6.7775	4.4806	2.2346	4197	0.0002279
6.5		32.0898	29.7872	27.4846	25.1820	22.8794	20.5768	18.2742	15.9717	13.6691	11.3665	9.0640	6.7620	4.4652	2.2201	4115	0.0002034
6.6		32.0745	29.7719	27.4693	25.1667	22.8641	20.5616	18.2590	15.9564	13.6538	11.3512	9.0487	6.7467	4.4501	2.2058	4036	0.0001816
6.7		32.0595	29.7569	27.4543	25.1517	22.8491	20.5465	18.2439	15.9414	13.6389	11.3362	9.0337	6.7317	4.4351	2.1917	3959	0.0001621
6.8		32.0446	29.7421	27.4395	25.1360	22.8343	20.5317	18.2291	15.9265	13.6240	11.3214	9.0189	6.7169	4.4204	2.1770	3883	0.0001448
6.9		32.0300	29														

APPENDIX D  
VALUES OF  $G(\lambda, \frac{r_w}{B})$

$\frac{r_w}{B}$	0	$1 \times 10^{-5}$	$2 \times 10^{-5}$	$4 \times 10^{-5}$	$6 \times 10^{-5}$	$8 \times 10^{-5}$	$10^{-4}$	$2 \times 10^{-4}$	$4 \times 10^{-4}$	$6 \times 10^{-4}$	$8 \times 10^{-4}$	$10^{-3}$	$2 \times 10^{-3}$	$4 \times 10^{-3}$	$6 \times 10^{-3}$	$8 \times 10^{-3}$	$10^{-2}$
$1 \times 10^{-7}$	0.346																0.346
2	0.311												0.311	0.311	0.311	0.312	0.312
3	0.294												0.294	0.294	0.294	0.295	0.295
4	0.283												0.283	0.283	0.283	0.284	0.285
5	0.274												0.274	0.274	0.275	0.275	0.276
6	0.268												0.268	0.268	0.268	0.269	0.271
7	0.263												0.263	0.263	0.263	0.264	0.266
8	0.258												0.258	0.258	0.259	0.260	0.261
9	0.254												0.254	0.255	0.256	0.257	0.258
$1 \times 10^{-6}$	0.251												0.251	0.252	0.252	0.254	0.255
2	0.232												0.232	0.233	0.234	0.236	0.239
3	0.222												0.222	0.223	0.225	0.227	0.231
4	0.215												0.215	0.216	0.219	0.222	0.226
5	0.210												0.210	0.212	0.215	0.218	0.222
6	0.206												0.206	0.208	0.211	0.215	0.220
7	0.203												0.203	0.205	0.209	0.213	0.219
8	0.201												0.201	0.203	0.207	0.212	0.218
9	0.198												0.198	0.201	0.205	0.210	0.217
$1 \times 10^{-5}$	0.196											0.196	0.197	0.200	0.204	0.209	0.216
2	0.185											0.185	0.185	0.190	0.197	0.205	0.213
3	0.178											0.178	0.179	0.186	0.194	0.203	0.212
4	0.173											0.173	0.176	0.183	0.193	0.202	
5	0.170											0.170	0.173	0.181	0.192		
6	0.168											0.168	0.171	0.180	0.192		
7	0.166											0.166	0.167	0.170	0.179		
8	0.164											0.164	0.165	0.169	0.179		
9	0.163											0.163	0.164	0.168	0.179		
$1 \times 10^{-4}$	0.161							0.161	0.162	0.162	0.162	0.162	0.167	0.178			
2	0.152						0.152	0.153	0.153	0.154	0.155	0.155	0.163	0.177			
3	0.148						0.148	0.148	0.149	0.150	0.152	0.152	0.162				
4	0.145						0.145	0.145	0.146	0.147	0.150	0.150	0.162				
5	0.143						0.143	0.143	0.144	0.145	0.148	0.148	0.161				
6	0.141						0.141	0.142	0.143	0.144	0.147	0.147	0.160				
7	0.140						0.140	0.140	0.141	0.143	0.146	0.146	0.160				
8	0.138						0.138	0.139	0.141	0.143	0.145	0.145	0.160				
9	0.137						0.137	0.138	0.140	0.142	0.144	0.144	0.160				
$1 \times 10^{-3}$	0.136						0.136	0.137	0.138	0.139	0.141	0.144	0.159				
2	0.130						0.130	0.131	0.133	0.135	0.139	0.143	0.159				
3	0.127						0.127	0.127	0.130	0.134	0.138	0.142	0.158				
4	0.124						0.124	0.125	0.129	0.134							
5	0.123						0.123	0.124	0.128	0.133							
6	0.121						0.121	0.123	0.128								
7	0.120						0.120	0.122	0.127								
8	0.119						0.119	0.121	0.127								
9	0.118						0.118	0.121	0.127								
$1 \times 10^{-2}$	0.118						0.118	0.127									
2	0.114						0.114	0.126									
3	0.111						0.111	0.112									
4	0.109				0.109	0.111	0.110	0.111									
5	0.108				0.108	0.109	0.110	0.110									
6	0.107			0.107	0.108	0.109	0.110										
7	0.106			0.106	0.107	0.108	0.109										
8	0.105			0.105	0.106	0.108	0.109										
9	0.104		0.104	0.105	0.106	0.107	0.108										
$1 \times 10^{-1}$	0.104		0.104	0.104	0.105	0.106	0.108										
2	0.100	0.100	0.101	0.102	0.103	0.105	0.107										
3	0.0982	0.0982	0.0986	0.100	0.103												
4	0.0968	0.0968	0.0974	0.0994	0.102												
5	0.0958	0.0958	0.0966	0.0989													
6	0.0950	0.0951	0.0959	0.0986													
7	0.0943	0.0944	0.0954	0.0984													
8	0.0937	0.0939	0.0949	0.0982													
9	0.0932	0.0934	0.0946	0.0981													
$1 \times 10^0$	0.0927	0.0930	0.0943	0.0980													
2	0.0899	0.0906	0.0927	0.0977													
3	0.0883	0.0893	0.0920	0.0976													
4	0.0872	0.0885	0.0917														
5	0.0864	0.0880	0.0916														
6	0.0857	0.0876	0.0915														
7	0.0851	0.0873	0.0915														
8	0.0846	0.0870	0.0915														
9	0.0842	0.0869	0.0914														
$1 \times 10^1$	0.0838	0.0867	0.0914														
2	0.0814	0.0862															
3	0.0861	0.0860															
4	0.0792																
5	0.0785																
6	0.0779																
7	0.0774																
8	0.0770																
9	0.0767																
10	0.0764	0.0860	0.0914	0.0976	0.102	0.105	0.107	0.116	0.126	0.133	0.138	0.142	0.158	0.177	0.191	0.202	0.212

(FROM HANTUSH, 1959)

APPENDIX E  
VALUES OF  $D(u)_q$

$u$	$u^2$	$D(u)_q$
0.0500	0.0025	10.32
0.0600	0.0036	8.468
0.0700	0.0049	7.109
0.0800	0.0064	6.130
0.0900	0.0081	5.331
0.1000	0.010	4.714
0.1140	0.013	4.008
0.1265	0.016	3.532
0.1414	0.020	3.079
0.1581	0.025	2.657
0.1732	0.030	2.354
0.1871	0.035	2.109
0.2000	0.040	1.943
0.2236	0.050	1.658
0.2449	0.060	1.441
0.2646	0.070	1.282
0.3000	0.090	1.049
0.3317	0.110	0.8810
0.3605	0.130	0.7598
0.4000	0.160	0.6284
0.4359	0.190	0.5324
0.4796	0.230	0.4384
0.5291	0.280	0.3517
0.5745	0.330	0.2895
0.6164	0.380	0.2434
0.6633	0.440	0.2008
0.7071	0.500	0.1837
0.7616	0.580	0.1345
0.8124	0.660	0.1094
0.8718	0.760	0.0864
0.9486	0.900	0.0623
1.0000	1.000	0.0507

( FROM KNOWLES, 1955 )

## APPENDIX F

### Selected Conversion Factors and Constants

1 millidarcy = 0.0182 gpd/sq ft (for water at 68F)  
 1 darcy = 18.24 gpd/sq ft (for water at 68F)  
 1 inch of mercury = 1.13 feet of water  
 1 cfs = 449 gpm  
 $1 \text{ sec}^2/\text{ft}^5 = 2.02 \times 10^5 \text{ (ft/gpm}^2\text{)}$   
 $1 \text{ gpd} = 6.95 \times 10^{-4} \text{ gpm}$   
 1 mgd = 695 gpm  
 1 mgd = 1.54 cfs  
 $1 \text{ cfs} = 6.46 \times 10^5 \text{ gpd}$   
 $1 \text{ sq mi} = 2.79 \times 10^7 \text{ sq ft}$   
 1 inch of water over 1 sq mi =  $1.74 \times 10^7$  gals  
 1 inch of water over 1 sq mi per year =  $4.77 \times 10^4$  gpd  
 1 acre = 43,560 sq ft  
 1 sq mi = 640 acres  
 1 cu ft = 7.48 gals  
 $1 \text{ gal} = 1.34 \times 10^{-1} \text{ cu ft}$   
 1 ft water = 0.4335 lb/sq in.  
 $1 \text{ day} = 1.44 \times 10^3 \text{ min}$   
 specific weight of water = 62.4 lb/cu ft  
 reciprocal of bulk modulus of  
     elasticity of water =  $3.3 \times 10^{-6} \text{ sq in./lb}$   
 $1 \text{ ft per mi} = 1.89 \times 10^{-4} \text{ ft per ft}$   
 $1 \text{ gal lift 1 foot} = 3.15 \times 10^{-6} \text{ kwh}$

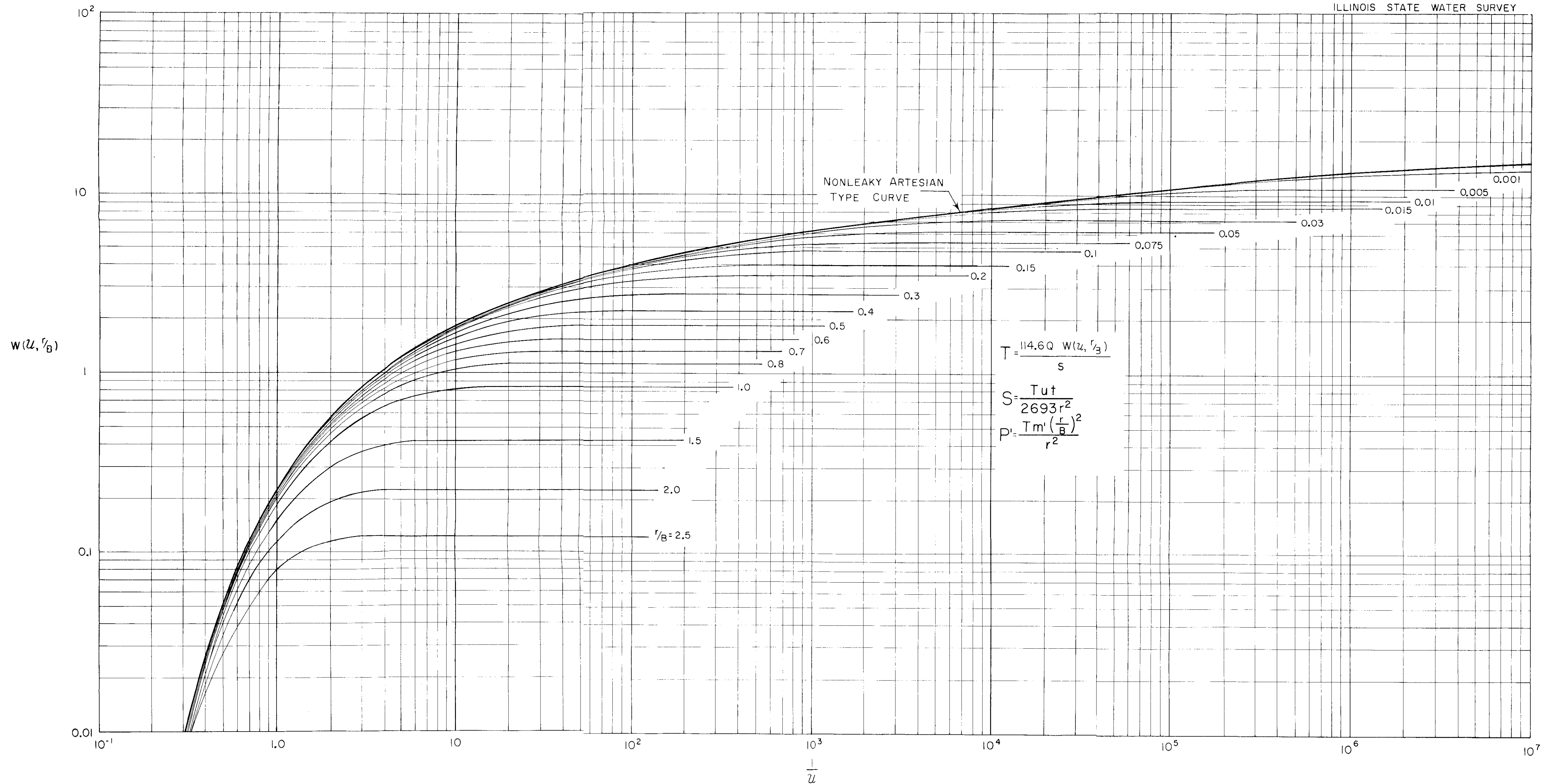


PLATE 1. NONSTEADY STATE LEAKY ARTESIAN TYPE CURVES

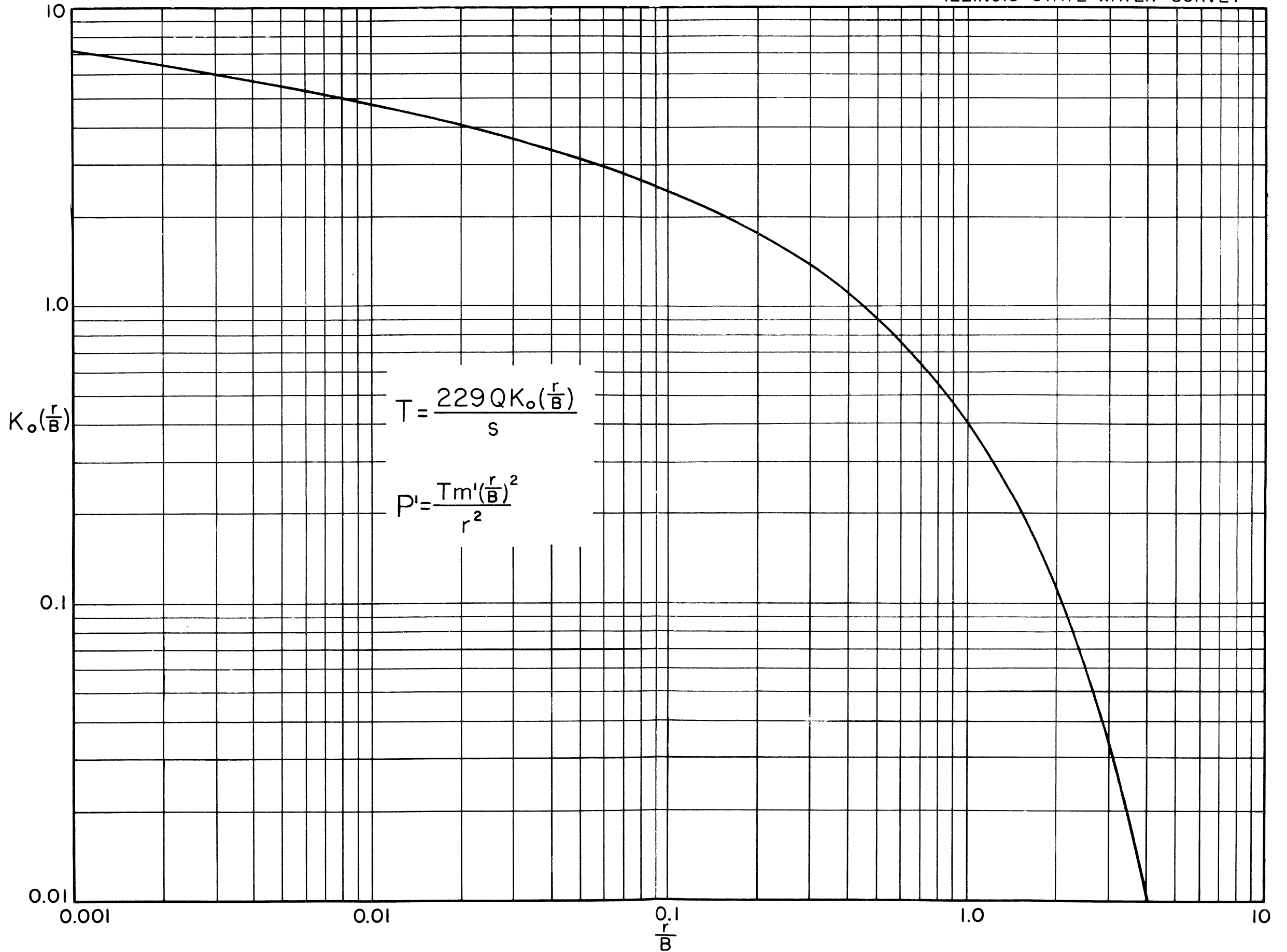


PLATE 2. STEADY STATE LEAKY ARTESIAN TYPE CURVE

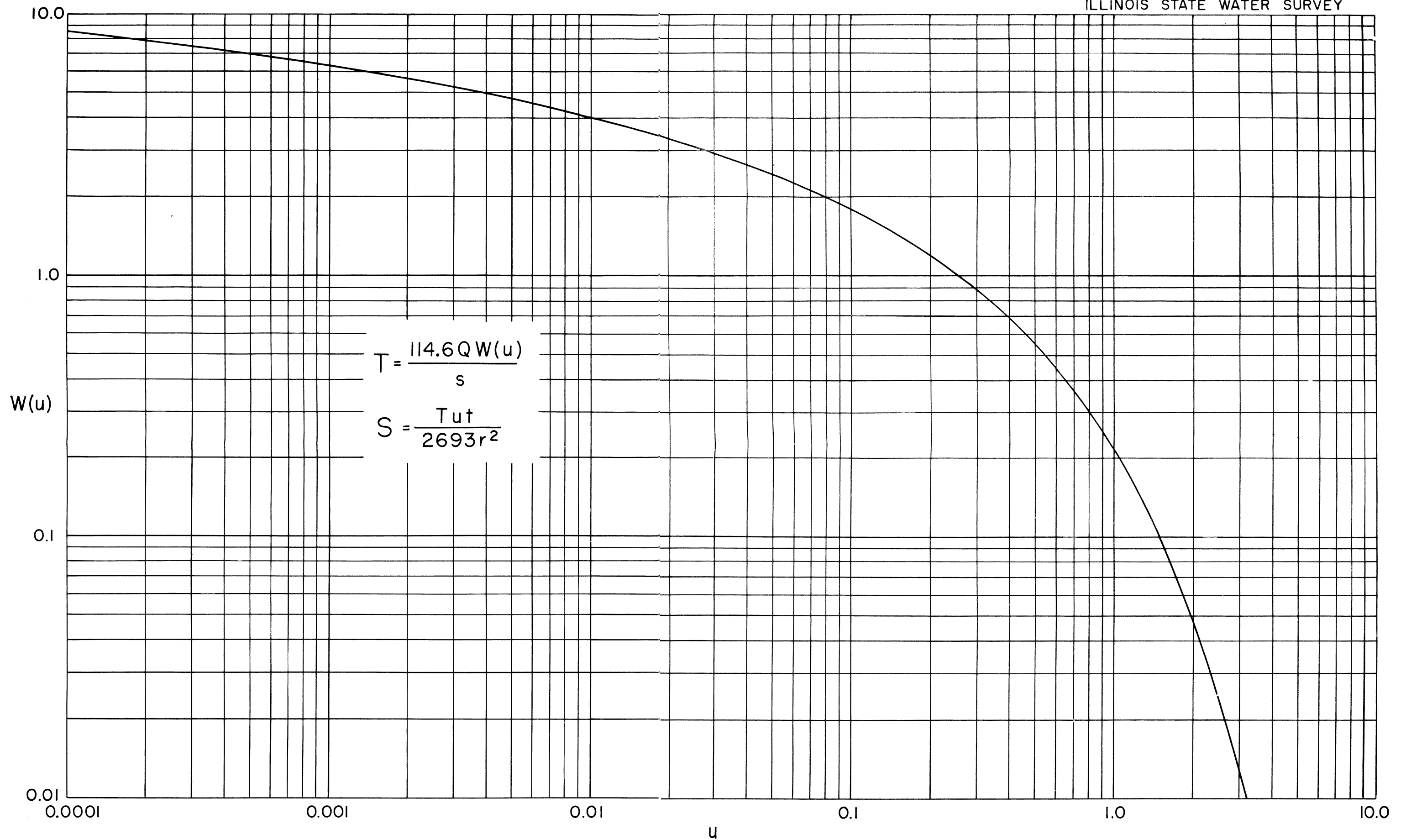


PLATE 3. NONLEAKY ARTESIAN TYPE CURVE

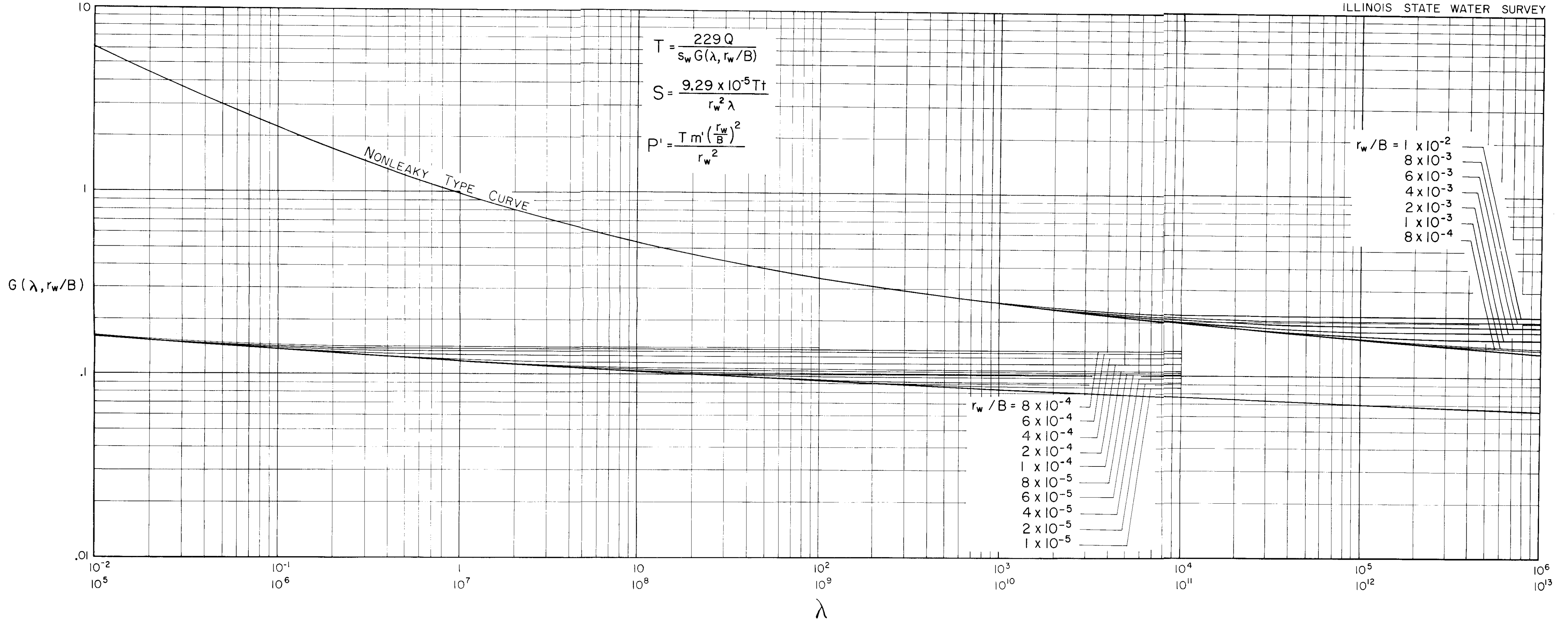


PLATE 4. NONSTEADY STATE LEAKY ARTESIAN, CONSTANT DRAWDOWN, VARIABLE DISCHARGE TYPE CURVES